Università degli Studi di Palermo

D067 - TECHNOLOGIES AND SCIENCES FOR HUMAN HEALTH

Chemical and Pharmaceutical Biological Sciences and Technologies

"Extracellular vesicles from a renewable natural source: development of new biomaterials"

PhD Student: Dr. Sabrina Picciotto

Coordinator: Prof. Vincenzo Cavalieri

Tutors

Dr. Antonella Bongiovanni

Prof. Giulio Ghersi

Cycle XXXV
2023

INDEX

Abstract

Extracellular vesicles (EVs) are cell-derived, membranous nanoparticles that mediate intercellular communication by transferring bioactive compounds such as proteins and RNAs.

The discovery of EVs as natural nanotechnologies and means of communication between cells and even species has aroused great interest in the field of drug delivery. The EVs possess intrinsically several attributes that make them a good vehicle for the release of drugs in specific target organs and tissues. Indeed these particles: i) are well tolerated in the body, ii) have long circulating half-life, iii) are internalized by recipient cells and iv) are able of crossing the blood brain barrier. Pristine and engineered mammalian cell-derived EVs have recently contributing to the expanding research field known as "cell-free therapy". Although the promising progresses, translational applications are currently obstructed by the challenges in the production manufacturing and bioengineering at scale of EVs. This PhD project has been supported by the European project H2020-VES4US, whose main purpose has been to develop a radically new platform for the production and functionalization of extracellular vesicles obtained from a renewable biological source, which will allow their application in a variety of fields, from nanomedicine to cosmetics or nutraceuticals. In this multidisciplinary and international scenario, the results of this PhD project supported the development of innovative bioprocesses inherent the separation and characterization of EVs from microalgae and their subsequent functionalization, in order to further exploit them for pharmaceutical, cosmetic and cosmeceutical application.

List of Papers

The work developed during this PhD *Thesis* collects the following scientific manuscripts already published and under preparation for submission in international journals:

Giorgia Adamo,* Pamela Santonicola,*, **Sabrina Picciotto**,*, Paola Gargano, Aldo Nicosia, Daniele Paolo Romancino, Angela Paterna, Estella Rao, Samuele Raccosta, Rosina Noto, Paolo Colombo, Mingxing Wei, Mauro Manno, Elia Di Schiavi, and Antonella Bongiovanni. Harnessing Nature's nanoSecrets: Preclinical Evaluation of the Bioactivity of Microalgal-derived Extracellular Vesicles. bioRxiv 2023.04.04.535547; doi: https://doi.org/10.1101/2023.04.04.535547. **Co-first Author. Manuscript submitted to ACS Nano**

Giorgia Adamo*, **Sabrina Picciotto**, Angela Paterna, Paola Gargano, Estella Rao, Samuele Raccosta, Monica Salamone, Daniele Paolo Romancino, Mauro Manno, and Antonella Bongiovanni. Functional enzymatic assays to predict the functional of extracellular vesicle and to validate integrity and quality batch reproducibility. **Co-Author. Manuscript submitted**

C. Paganini, U. Capasso Palmiero, **S. Picciotto**, A. Molinelli, I. Porello, G. Adamo, M. Manno, A. Bongiovanni, P. Arosio. High-Yield Separation of Extracellular Vesicles Using Programmable Zwitterionic Coacervates. Small 2022, 2204736. https://doi.org/10.1002/smll.202204736. **Co-Author. Impact Factor: 15.153**

Paterna A, Rao E, Adamo G, Raccosta S, **Picciotto S**, Romancino D, Noto R, Touzet N, Bongiovanni A, Manno M. Isolation of Extracellular Vesicles From Microalgae: A Renewable and Scalable Bioprocess. Front Bioeng Biotechnol. 2022 Mar 14;10:836747. doi: 10.3389/fbioe.2022.836747. PMID: 35360396; PMCID: PMC8963918. **Co-Author. Impact Factor: 6.064**

Picciotto S, Santonicola P, Paterna A, Rao E, Raccosta S, Romancino DP, Noto R, Touzet N, Manno M, Di Schiavi E, Bongiovanni A, Adamo G. Extracellular Vesicles From Microalgae: Uptake Studies in Human Cells and Caenorhabditis elegans. Front

Bioeng Biotechnol. 2022 Mar 24;10:830189. doi: 10.3389/fbioe.2022.830189. PMID: 35402397; PMCID: PMC8987914. **First-Author. Impact Factor: 6.064**

Adamo G, Fierli D, Romancino DP, **Picciotto S**, Barone ME, Aranyos A, Božič D, Morsbach S, Raccosta S, Stanly C, Paganini C, Gai M, Cusimano A, Martorana V, Noto R, Carrotta R, Librizzi F, Randazzo L, Parkes R, Capasso Palmiero U, Rao E, Paterna A, Santonicola P, Iglič A, Corcuera L, Kisslinger A, Di Schiavi E, Liguori GL, Landfester K, Kralj-Iglič V, Arosio P, Pocsfalvi G, Touzet N, Manno M, Bongiovanni A. Nanoalgosomes: Introducing extracellular vesicles produced by microalgae. J Extracell Vesicles. 2021 Apr;10(6):e12081. doi: 10.1002/jev2.12081. Epub 2021 Apr 27. PMID: 33936568; PMCID: PMC8077145. **Co-first Author. Impact Factor: 25.84**

Picciotto S, Barone ME, Fierli D, Aranyos A, Adamo G, BoŽič D, Romancino DP, Stanly C, Parkes R, Morsbach S, Raccosta S, Paganini C, Cusimano A, Martorana V, Noto R, Carrotta R, Librizzi F, Capasso Palmiero U, Santonicola P, Iglič A, Gai M, Corcuera L, Kisslinger A, Di Schiavi E, Landfester K, Liguori GL, Kralj-Iglič V, Arosio P, Pocsfalvi G, Manno M, Touzet N, Bongiovanni A. Isolation of extracellular vesicles from microalgae: towards the production of sustainable and natural nanocarriers of bioactive compounds. Biomater Sci. 2021 Apr 21;9(8):2917-2930. doi: 10.1039/d0bm01696a. Epub 2021 Feb 23. PMID: 33620041. **First-Author. Impact Factor: 7.59**

Mario Allegra, Antonella Bongiovanni, Giuseppe Città, Antonella Cusimano, Valentina Dal Grande, Manuel Gentile, Annamaria Kisslinger, Dario La Guardia, Giovanna Liguori, Fabrizio Lo Presti, Salvatore Perna, **Sabrina Picciotto**, Simona Ottaviano, Carla Sala & Alessandro Signa (2021). The Role of Metaphor in Serious Games Design: the BubbleMumble Case Study. In: de Rosa, F., Marfisi Schottman, I., Baalsrud Hauge, J., Bellotti, F., Dondio, P., Romero, M. (eds) Games and Learning Alliance. GALA 2021. Lecture Notes in Computer Science, vol 13134. Springer, Cham. https://doi.org/10.1007/978-3-030-92182-8_19. **Co-Author. Chapter Book**

Sabrina Picciotto; Daniele P. Romancino Valentina Buffa Antonella Cusimano Antonella Bongiovanni Giorgia Adamo. "Chapter Four – Post-translational lipidation in extracellular vesicles: chemical mechanisms, biological functions and applications". Advances in Biomembranes and Lipid Self-Assembly, Volume 32 ISSN 2451-9634. **First-Author. Chapter Book**

Chapter 1

General Introduction

1.1 Nanotechnology and Nanomedicine: The Applications of Nanoparticles in Drug Delivery Systems

Nanotechnology is the engineering and manufacturing of materials at the atomic and molecular scale. The National Nanotechnology Initiative defines nanomaterials as structures roughly in the 1-100 nm size regime in at least one dimension[1]. Nanomaterials have influenced the frontiers of nanomedicine starting from biosensors, microfluidics, drug delivery, and microarray tests to tissue engineering[2]. Nanomedicine, focuses on the use of nanoscience knowledge and techniques in medical biology and alternative drug delivery for improving the effectiveness of disease treatment by reducing harmful side effects to normal tissues[3]. The engineered drug delivery systems are either targeted to a particular location or are intended for the controlled release of therapeutic agents at a particular site[4,5]. Nanoparticles have the potential advantages of modifying the solubility of the drug and the diffusion in the plasma membrane, thus overcoming the limit of bio-accessibility after intake [2]. Nanoparticles also have also advantages for the control of drug release profile, diffusivity, bioavailability and immunogenicity[6]. The priority of the biotech and pharma industrial sectors is to find effective and safe molecular delivery vehicles as 40% of new drugs fail to complete the clinical validation due to poor delivery[8]. In this context, Extracellular Vesicles (EVs) are a very recent addition to the nanotechnology vehicle toolbox and are considered one of the most promising bio-nanovehicles for the delivery of bioactive compounds[11].

1.2 Extracellular Vesicles - Cell-Derived nanovehicle toolbox

1.2.1 Composition and Functionality of Extracellular Vesicles

Extracellular vesicles (EVs) are groups of small naturally occurring particles that were previously overlooked in the study of cellular secretions[12]. There are three main categories of EVs based on their formation, size, and composition: exosomes, microvesicles, and apoptotic bodies[13]. Exosomes are small (30-100 nm) nanovesicles formed by reverse budding of multivesicular bodies and released when they fuse with the cytoplasmic membrane (Fig. 1). Microvesicles are larger (100-1000 nm) and produced during cytoplasmic membrane shedding (Fig. 1). Apoptotic bodies are generated from outward membrane blebbing during cell apoptosis and are 500-2000 nm in size (Fig. 1)[14]. As of now, there is a lack of subtype-specific markers and overlap in vesicle sizes. As a result, it is challenging to separate and differentiate between different types of vesicles[15]. For this reason the scientific community agreed on the nomenclature referring to small EVs (sEVs) for EVs below 150 nm in diameter and

large EVs (lEVs) for EVs of >150 nm. [13]The content of EVs includes in their lumen various types of RNA (such as mRNA, miRNA, and lncRNA), lipids, and proteins; EV membrane contains receptors, ligands, and specific markers (Fig. 1)[13,14]. Initially, EVs were seen as "garbage bags" with a main function of discarding cellular waste. However, recent studies have shown that they can transfer biological information between cells and alter the recipient cells' phenotype. Cells package distinct biomolecules into EVs through sorting mechanisms and release them continuously or after stimulation[16,17]. EVs can be internalized by target recipient cells, leading to the transfer of mRNAs and miRNAs, resulting in the production or silencing of target proteins, including membrane proteins. They can be extracted from bodily fluids like blood, urine, cerebrospinal fluid, and saliva[18]. The contents of EVs reflect the status of the donor cell and can be used in diagnostics and to monitor treatment efficacy[19,20]. Indeed, EVs play a role in normal physiological processes, they are also associated with pathological processes like autoimmune diseases and cancer[21,22]. With their crucial role in intercellular communication, EVs play a significant role in both health and disease and their potential as a drug delivery platform is being explored[23,24].
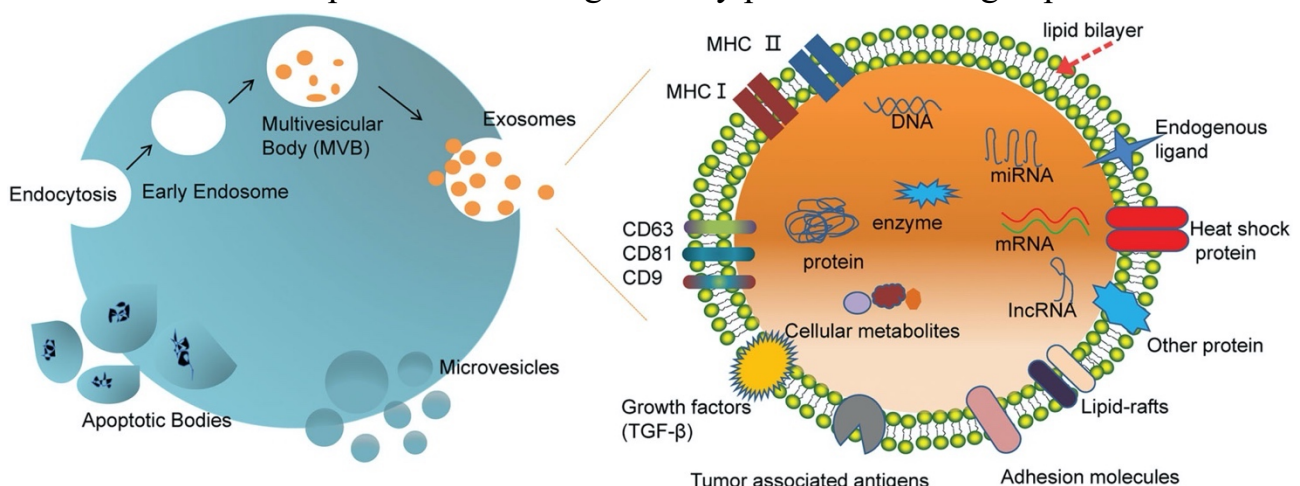
Figure 1. Summary: The biogenesis of three types of extracellular vesicles (exosomes, microvesicles, and apoptotic bodies) and the components of exosomes are depicted in a scheme. Exosomes are vesicles secreted by cells and have a size of approximately 100 nm. They contain a range of cellular components, such as mRNAs, miRNAs, proteins, enzymes, lipids, carbohydrates, etc. The surface of exosomes is adorned with various membrane proteins that carry out various physiological functions[25].

1.2.2 Isolation and characterization of EVs

Several techniques are available for isolating and characterizing EVs, and each has unique factors that may affect yields[13]. The International Society for Extracellular Vesicles (ISEV) has released multiple papers emphasizing the importance of

standardizing sample collection, EV separation and characterization methods, providing detailed information that should be recorded and published[26,27,28]. The newly established EV-TRACK database, created by an international consortium of 92 researchers from 12 countries, aims to standardize EV isolation and characterization methods. The database evaluates and scores the experimental parameters of 1226 EV-related articles using the EV-METRIC score[29]. The choice of an EV isolation method depends on the sample source. Separating EVs from cell culture typically involves centrifugation to remove dead cells and debris, followed by ultracentrifugation to collect EVs[13]. However, new techniques that include column enrichment or precipitation are continuously emerging. Ultracentrifugation is still widely used and considered the most popular primary isolation method. For complex biological fluid samples, it is recommended to use multiple methods to remove specific components before ultracentrifugation or alternative isolation methods such ultracentrifugation-based, size-based, immunoaffinity capture-based, precipitation, and microfluidics[13,30] (Fig. 2). The best method depends on the purpose of research, as each has its own pros and cons. Once separated, EV populations require characterization for their intended downstream applications. There is a range of techniques available for this purpose such as transmission electron microscopy (TEM), scanning electron microscopy (SEM), atomic force microscopy (AFM), nanoparticle tracking analysis (NTA), dynamic light scattering (DLS), resistive pulse sensing, enzyme-linked immunosorbent assay (ELISA), flow cytometry, fluorescence-activated cell sorting (FACS), microfluidics and electrochemical biosensors, have been developed for research and clinical purposes to assess EVs purity and quantify EV cargo[31,32] (Fig. 2).
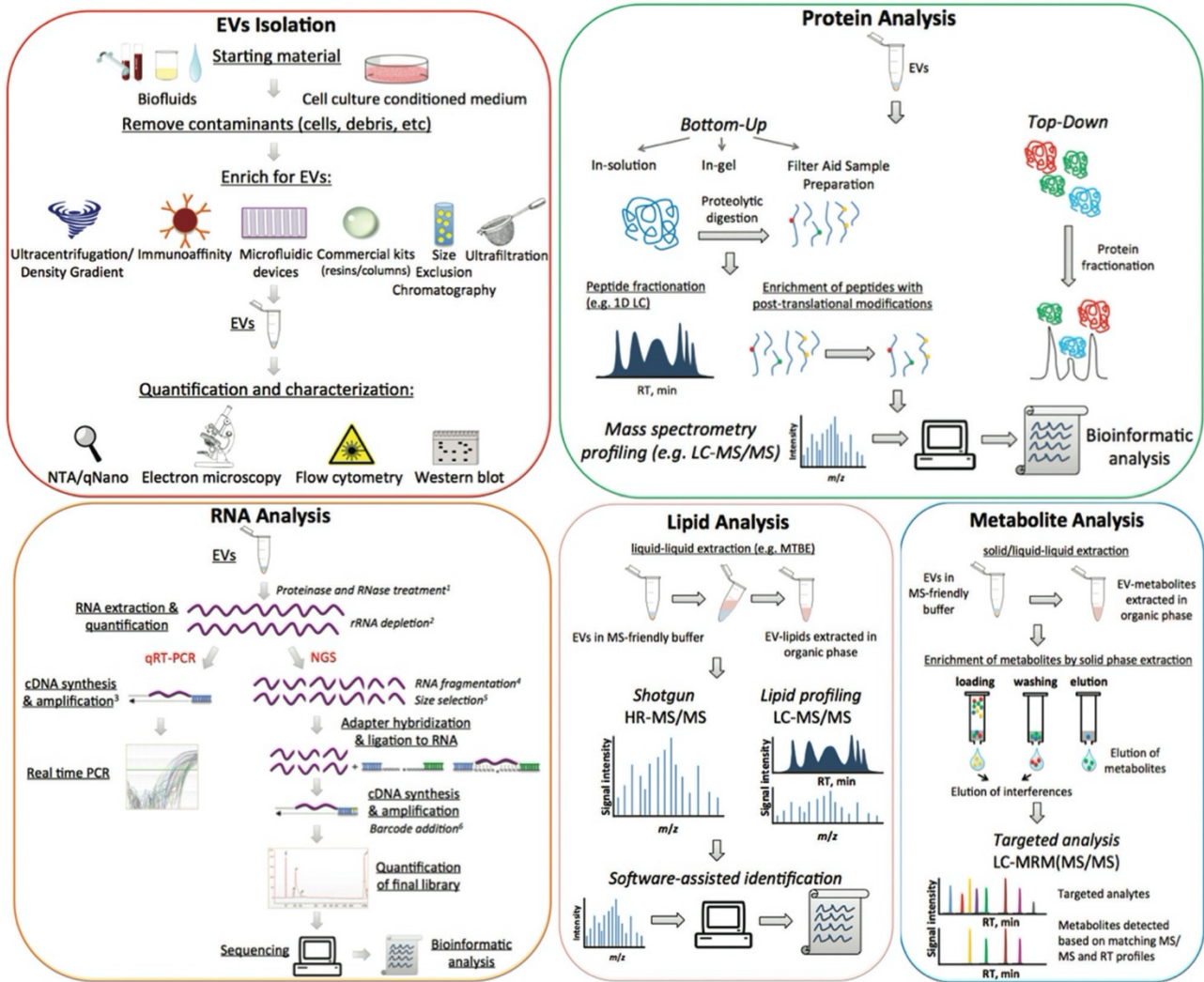
Figure 2. Scheme for EV isolation, quantification, and characterization, including analysis of EV molecular content.[30].

1.3 Utilizing Extracellular Vesicles for Nanomedical Purposes

1.3.1 EV-based Therapeutics: A Promising Advancement in Drug Delivery Systems

EVs have a competitive advantage as a drug delivery system over synthetic reagents due to their reduced immunogenicity and toxicity[33]. Liposomes, which are synthetic lipid nanoparticles, are commonly used for delivering nucleic acids and small molecules[34]. The first liposomal anticancer drug, DoxilVR, was approved by the FDA in 1995[35]. Despite the appearance of similar drugs, toxicity remains a problem that delays clinical applications[36]. Synthetic lipid nanoparticles tend to induce a toxic immune response, accumulate in the liver, and perform poorly in comparison to expectations[37,38].

Furthermore, EV therapy is recently considered an advancement from stem cell therapy for in vivo regeneration[12]. It is now believed that the benefits of stem cells come from

the paracrine factors in EVs. Research has shown that administering pristine EVs alone can provide similar benefits and new therapeutic opportunities[39,40]. EVs from sources like MSCs have shown potential in animal models for various diseases and can be used to deliver drugs and vaccines[41]. Early clinical studies show EVs to be safe and effective as a therapy for cancer and graft-versus-host disease, and outer membrane vesicles from Neisseria meningitides (the EV-based product Bexsero®) has received a marketing authorization as a vaccine for meningitis[42,43]. EV-based therapies, as a cell-free therapy, avoid the problems associated with cell-therapy, such as necrosis or abnormal differentiation[44]. The small size of EVs also has therapeutic benefits like reducing phagocytosis, improving injection, and extravaation through tumor blood vessels[45]. Although synthetic vectors have similar size benefits, EVs have unique therapeutic advantages like biocompatibility, stability, communication, and the ability to interact with cells. Some studies show that EVs have selective fusion, tissue specificity, and the ability to cross the blood-brain barrier[46]. EVs have a competitive advantage as drug delivery system due to their innate biocompatibility and limited immunogenicity compared to synthetic drug delivery agents like lipid nanoparticles[44,47]. For instance, siRNA-loaded exosomes were shown to inhibit pancreatic cancer in mice better than siRNA-loaded lipid nanoparticles without eliciting an immune response. Although EVs may accumulate in the liver and other organs, they are still considered to have limited immunogenicity and cytotoxicity compared to other delivery systems like adenoviruses, lentiviruses, retroviruses, and lipid transfection reagents[48]. Therapeutic EVs can also be modified through molecular engineering techniques, leading to different biological functions (Fig. 3). EVs can be loaded either exogenously by incorporating cargo on isolated EVs or endogenously by introducing cargo into the producer cell. The cargo can be therapeutic RNA molecules, proteins, or surface molecules like biologically active proteins or neutralizing molecules[49,50,51]. Surface ligands can target EVs to specific recipient cell types, enabling crossing of physiological barriers, like the blood-brain barrier. Additions to the EV surface can facilitate fusion with the recipient cell's plasma membrane or cytoplasmic release of cargo after endosomal uptake[52]. The method of administration of EVs affects their biodistribution, a factor to consider when developing therapeutic applications (Fig. 3). In recent decades, biological medications like monoclonal antibodies and cell therapies such as CAR T cells have made significant progress in managing disease. Currently, there are fewer than 100 studies, mostly proof-of-concept, related to EV-based drug delivery systems and therefore, there is exciting potential to explore new functionalization technologies and achieve effective therapeutic outcomes from EVs treatments[53].
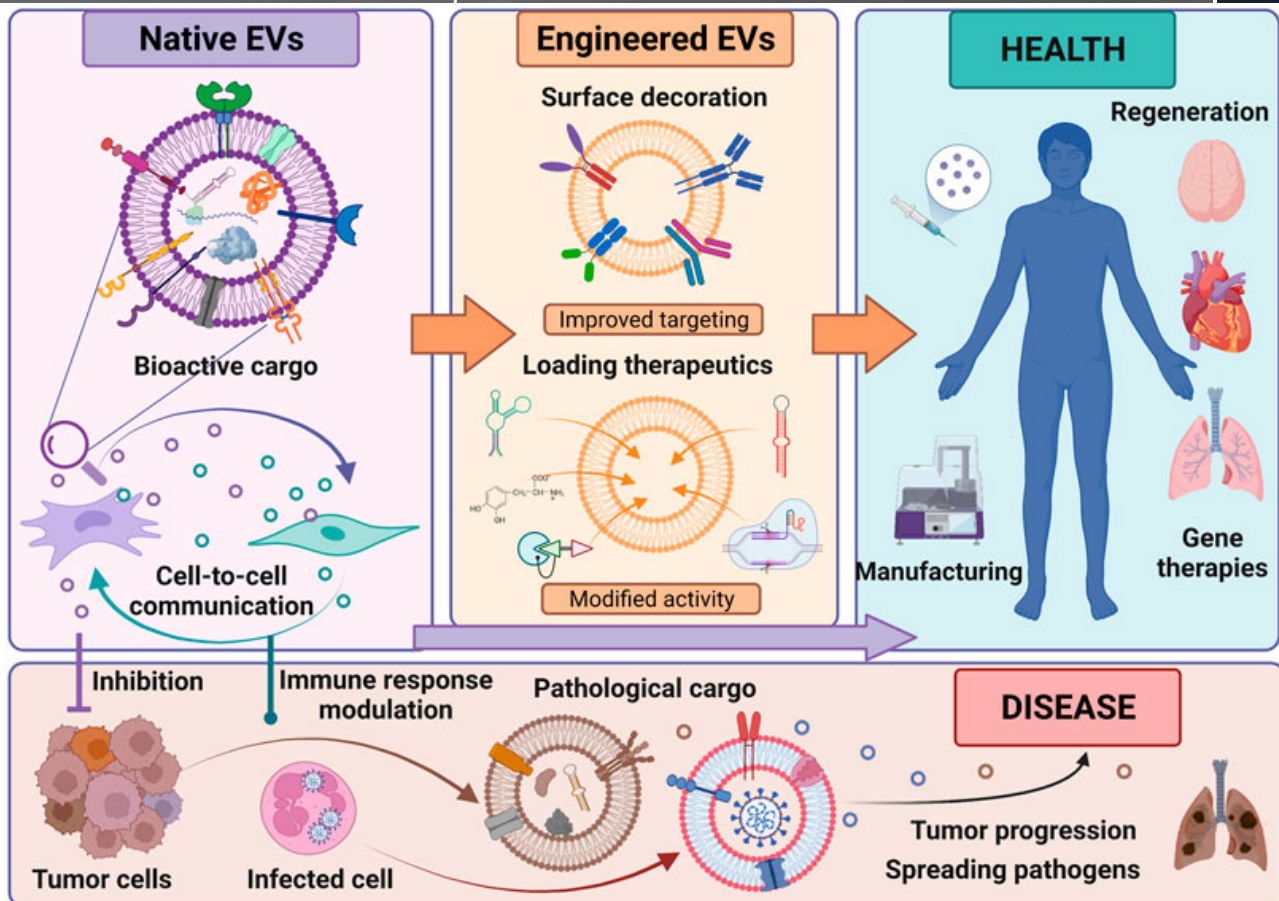
Figure 3. Extracellular vesicles (EVs) play a role in both health and disease, with their bioactive cargo of proteins, lipids, and nucleic acids impacting target cells. Bioengineering of EVs can improve their functionality and specificity by modifying their surface or loading therapeutic cargo. Native and engineered EVs can be utilized as cell-free therapeutics for promoting health. However, EVs produced under pathological conditions by cancer or infected cells can contribute to the spread and progression of disease[54].

1.3.2 EV-based drug delivery vehicles

EVs are being studied as a way to deliver various cargo, including drugs and small molecules with poor pharmaceutical properties[46,55]. Proteins and RNA, such as siRNAs and miRNAs, can also be delivered, despite their low cellular uptake, poor pharmacokinetics, off-target toxicity, or stability problems, as they have been shown to be effective once they reach their mRNA targets[56]. Studies have been conducted to explore ways of delivering therapeutic cargo to native EVs (Fig. 4). The incubation of EVs with curcumin led to a more bioavailable and anti-inflammatory drug in a mouse model of inflammation[57]. Also, the incubation of EVs with the immunosuppressive miR-150 produced a functional association between the miRNA and EVs[58]. The use of EVs as a delivery system for various small molecules, including curcumin, doxorubicin, and paclitaxel, has been studied[59]. Preclinical animal trials suggest that

the EV-delivered small molecule treatment is more potent with improved pharmacokinetic profiles, including better delivery to the brain and tumors and efficient retention of cargo in tumor cells, compared to other delivery methods such as liposomes and synthetic nanoparticles[60]. Therefore, clinical trials are underway to test the use of EVs loaded with curcumin or chemotherapeutic drugs[57,61]. Recently, an improvement in loading RNA into extracellular vesicles (EVs) has been demonstrated using hydrophobic modified siRNA (hsiRNA) for Huntingtin mRNA silencing, which was efficient *in vitro* and *in vivo*[62]. Another study showed that using an anchor peptide (CP05) for targeting CD63 on EVs could effectively load functional cargos and restore dystrophin and improve phenotype in dystrophin-deficient mice[63]. Exogenous loading methods into EVs include electroporation, permeabilization, sonication, extrusion, and commercial cationic liposomes, however the results can vary greatly and it's difficult to determine the loading efficiency[64,65]. Electroporation has shown poor loading efficiency due to formation of siRNA aggregates but many studies have also reported successful loading[66]. A study using fibroblast-EVs electroporated with siRNA and shRNA targeting oncogenic KRAS (iExosomes) showed suppression of cancer growth and increased survival in mouse models of pancreatic ductal adenocarcinoma[67,68]. A clinical-grade production of MSC-derived iExosomes showed increased survival of mice with PDAC and were stable after 5 months of storage at -80°C[69]. A clinical trial is ongoing to explore the potential of EVs as a delivery vehicle for RNA species. Endogenous loading refers to the expression of cargo (such as small RNA, small molecules, mRNA/protein, etc.) within the producer cell which is then sorted into extracellular vesicles (EVs). This allows the utilization of the cell's machinery for sorting the cargo into EVs[70,71,72,73]. Engineered EVs can be modified to possess desired traits, such as increased targeting properties, through techniques such as transfection of the parental cell with a plasmid encoding Lamp2b fused with RVG[74,75]. Clinical trials are underway to assess the use of MSC-derived EVs loaded with miR-124 for treatment of acute ischemic stroke[76,77]. Other engineering techniques include displaying RNA aptamers, anti-EGFR nanobodies, or reporter moieties on EVs for targeted cancer therapy. A recent study used optogenetically engineered EVs to deliver proteins through the late-domain pathway[68]. A subtype of EVs called ARMMs (ARRDC1-mediated microvesicles) has been found to deliver NOTCH receptors and trigger NOTCH-specific gene expression, as well as transport other macromolecules[78,79,80]. The delivery of p53 protein and its mRNA, as well as CRISPR-Cas9/guide RNA complex, has been demonstrated using ARRDC1 chimeric proteins[79]. To increase EV production, engineered cells called EXOtic devices overexpress three genes, leading to a 15-fold increase in EV yield. The devices are transfected with a mRNA packaging plasmid, an mRNA of interest, a cytosolic delivery helper, and a

targeting plasmid, and have shown effectiveness in reducing neurotoxicity and neuroinflammation in Parkinson's disease models.

Hybrid EVs are emerging as a potential delivery strategy, with the fusion of EVs and synthetic liposomes modifying the exosomal surface to enhance stability, reduce immunogenicity, and extend half-life[74]. Another approach, EPNs (enveloped protein nanocages), uses membrane binding and self-assembly proteins for biogenesis and efficient delivery into target cells. The development of therapeutic EVs is based on a growing understanding of EV biology, including biogenesis, protein and RNA sorting, and the use of protein engineering, RNA posttranscriptional modifications, and RNA binding proteins for controlled RNA packing[81,82].
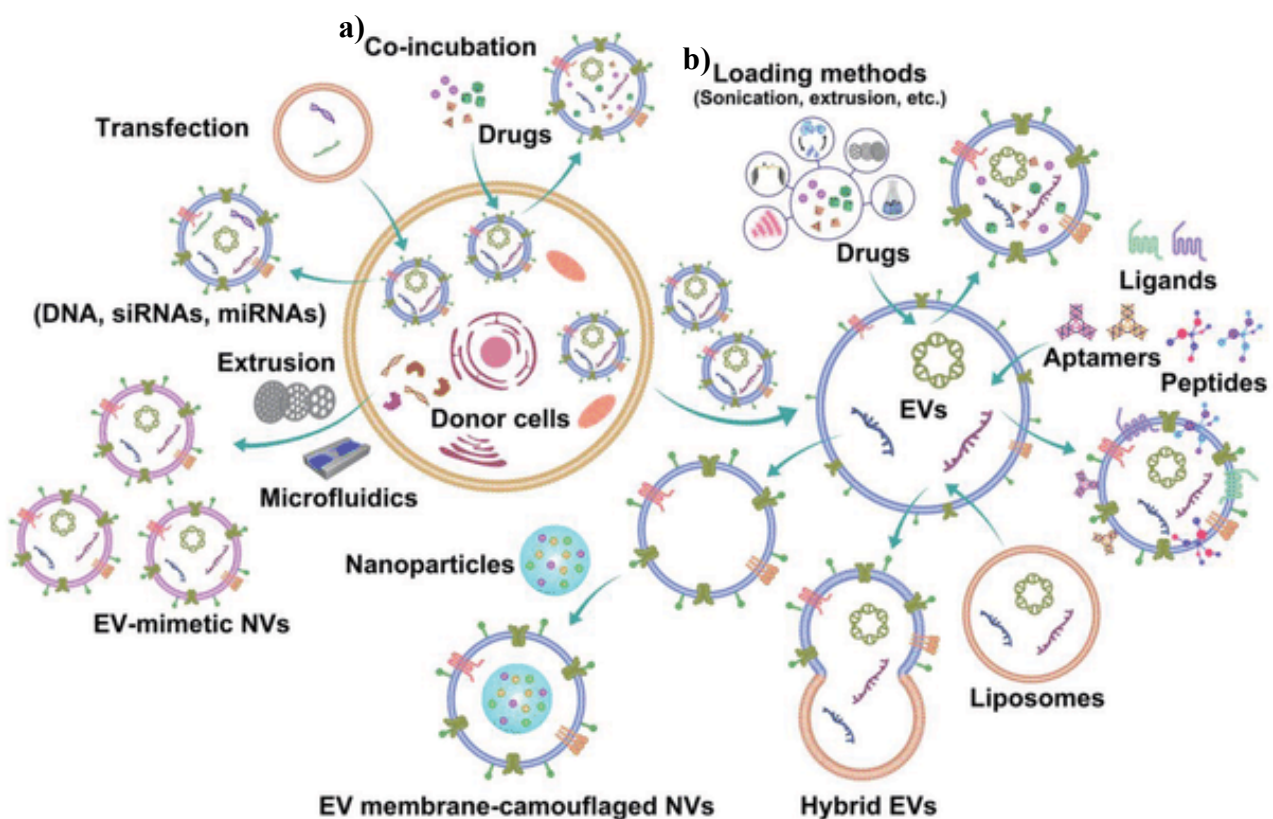
Figure 4. a) Strategies for **engineering donor cells** for EV production include co-incubation and gene transfection to introduce cargo and extrusion and microfluidic techniques to fabricate EV-mimetic nanovesicles (NVs). b) Strategies for **EV engineering** (**exogenous loading**) include sonication, electroporation, freeze-thaw, extrusion, and saponin permeabilization to introduce cargo, ligand-displaying to anchor targeting agents, mixing nanomaterials like liposomes and micelles with EV membranes to create hybrid EVs, and a bioinspired synthetic approach[83].

1.4 Challenges in the field of EV therapies

Over the past decade, extensive research in the field of EVs has enhanced our knowledge of their biogenesis, molecular content, and biological functions. However,

challenges remain before EVs can be used as therapies[84,85]. Selecting and characterizing the appropriate cell source for EV production is crucial for the intended therapeutic application. The manufacturing of EV-based therapeutics and cosmetic formulations is mainly based on human mesenchymal stem cells (MSC), whose large-scale production is neither sustainable, controllable nor economically viable[86]. The challenge is to ensure EV mass production for market roll-out when drug candidates reach the commercial clearance. Other important concerns are the still inefficient EV payload uptake and the need to commerce tropism and biodistribution while commercial adverse effects[87]. This has led the research community to explore alternative approaches to source EVs from other biological origins, such as bovine milk, bacteria and several edible plants including tomato and lemon[88,89]. However, the quest for the ideal EV source is still open as these alternatives still fail to meet the characteristics of safety, scalability, sustainability, quality and cost-effectiveness that are required by customers, especially when looking at the industrial phase. Currently, various manufacturing bioprocesses are being developed to isolate EVs, but finding the optimal method for producer cell expansion (i.e., MSCs) and scalable and clinical-grade EV isolation is still ongoing. Stability and storage must be improved for EVs to be used as off-the-shelf therapies. Additionally, the potency of isolated EVs must be assessed in standardized potency assays, which are currently lacking. EVs must also be characterized in relevant preclinical models to assess their safety, toxicity, pharmacokinetic, and pharmacodynamic profiles for accurate clinical dose predictions[84,85].

1.5 Microalgae as renewable and natural source

Microalgae are photosynthetic organisms, economically valuable biomass resources that are widely applied in food, pharmaceuticals and environmental remediation[90]. Several species of microalgae are rich in active components such as polysaccharides, pigments, proteins, vitamins, polyunsaturated fatty acids, antioxidants, which are beneficial in treating tumours, inflammation and cardiovascular disease[91,92,93]. Given these peculiar features, microalgae are increasingly considered worldwide as potential sources of food supplements and pharmaceutical compounds. Microalgae metabolites (lipid peroxidase, mycosporine-like amino acids (MAAs), carotenoid pigments (e.g. fucoxanthin), phytosterols (e.g. campesterol), vitamins (e.g. pro-vitamin), sulphated polysaccharides or flavonoids (e.g. catechin) have been shown to exhibit antioxidant-like activity[94]. Has been reported that flavonoids such as kaempferol and quercetin, typical of some species of microalgae, can play an important role in brain function with positive effects on neuronal activity[95]. Polyunsaturated fatty acids, such as

eicosapentaenoic acid (EPA) and docosahexaenoic acid (DHA) are the most valuable long chain polyunsaturated fatty acids (LC-PUFA) present in microalgae in relatively high proportions[96]. The beneficial role of these omega-3 fatty acids has been reported against atherosclerosis, hypertension or inflammation[97]. In fact, they appear to be the most 17 commercialized biomolecules of microalgae. In addition, another important property that has aroused interest is the use of microalgae by antimicrobial action. Compounds such as cyanovirin, oleic acid, linoleic acid, palmitoleic acid, β-carotene, fucoxanthin or phycocyanin produced by different species of microalgae, have antioxidant or anti-inflammatory properties as well as antimicrobial activity, for example against *Staphylococcus aureus* and Methicillin-Resistant *Staphylococcus aureu*[98]. For this reason, already many species of microalgae have been subjected to increasingly frequent checks to detect new antibacterial drugs. The diversity of microalgae is immense, of the estimated millions of extant species, some 30,000 have been described, but only a dozen are grown on a large scale for biotechnological applications[99]. Considering the remarkable biodiversity of microalgae and the improvement in culture, screening, extraction and purification techniques, it is likely that these microorganisms will represent an important source of new products in the future as part of blue technology. Until now, bioactive compounds from cyanobacteria have been more investigated than those from eukaryotic microalgae, probably caused to their simpler culture methods, and have been the subject of several recent papers[100,101,102,103]. The current global challenges such as climate change, pandemic, increasing population and depletion of fossil fuels have driven research to search for new sustainable sources for food, feed, high-end chemicals, and energy production. Microalgae has gained significant relevance as an excellent renewable cell factory in developing products because of their unique bioactive components and the possibility to grow them at industrial-scale via economically and environmental sustainable processes[104].

1.6 References

1. Farokhzad OC, Langer R. Impact of nanotechnology on drug delivery. ACS Nano. 2009 Jan 27;3(1):16-20. Doi: 10.1021/nn900002m.

2. Patra JK, Das G, Fraceto LF, Campos EVR, Rodriguez-Torres MDP, Acosta-Torres LS, Diaz-Torres LA, Grillo R, Swamy MK, Sharma S, Habtemariam S, Shin HS. Nano based drug delivery systems: recent developments and future prospects. J Nanobiotechnology. 2018 Sep 19;16(1):71. Doi: 10.1186/s12951-018-0392-8.

3. Haba Y, Kojima C, Harada A, Ura T, Horinaka H, Kono K. Preparation of poly (ethylene glycol)-modified poly (amido amine) dendrimers encapsulating gold nanoparticles and their heat-generating ability. Langmuir. 2007;23:5243–5246. Doi: 10.1021/la0700826.

4. Jahangirian H, Lemraski EG, Webster TJ, Rafiee-Moghaddam R, Abdollahi Y. A review of drug delivery systems based on nanotechnology and green chemistry: green nanomedicine. Int J Nanomed. 2017;12:2957. Doi: 10.2147/IJN.S127683.

5. Lam PL, Wong WY, Bian Z, Chui CH, Gambari R. Recent advances in green nanoparticulate systems for drug delivery: efficient delivery and safety concern. Nanomedicine. 2017;12:357–385. Doi: 10.2217/nnm-2016-0305.

6. Liu J, Liu Z, Pang Y, Zhou H. The interaction between nanoparticles and immune system: application in the treatment of inflammatory diseases. J Nanobiotechnology. 2022 Mar 12;20(1):127. Doi: 10.1186/s12951-022-01343-7.

7. Mitchell MJ, Billingsley MM, Haley RM, Wechsler ME, Peppas NA, Langer R. Engineering precision nanoparticles for drug delivery. Nat Rev Drug Discov. 2021 Feb;20(2):101-124. Doi: 10.1038/s41573-020-0090-8.

8. Sun D, Gao W, Hu H, Zhou S. Why 90% of clinical drug development fails and how to improve it? Acta Pharm Sin B. 2022 Jul;12(7):3049-3062. Doi: 10.1016/j.apsb.2022.02.002.

9. Qin S, Tang X, Chen Y, Chen K, Fan N, Xiao W, Zheng Q, Li G, Teng Y, Wu M, Song X. mRNA-based therapeutics: powerful and versatile tools to combat diseases. Signal Transduct Target Ther. 2022 May 21;7(1):166. Doi: 10.1038/s41392-022-01007-w.

10. Rohner E, Yang R, Foo KS, Goedel A, Chien KR. Unlocking the promise of mRNA therapeutics. Nat Biotechnol. 2022 Nov;40(11):1586-1600. Doi: 10.1038/s41587-022-01491-z.

11. Elsharkasy OM, Nordin JZ, Hagey DW, de Jong OG, Schiffelers RM, Andaloussi SE, Vader P. Extracellular vesicles as drug delivery systems: Why and how? Adv Drug Deliv Rev. 2020;159:332-343. Doi: 10.1016/j.addr.2020.04.004.

12. Armstrong JP, Holme MN, Stevens MM. Re-Engineering Extracellular Vesicles as Smart Nanoscale Therapeutics. ACS Nano. 2017 Jan 24;11(1):69-83. Doi: 10.1021/acsnano.6b07607.

13. Théry C, Witwer KW, et. Al., Minimal information for studies of extracellular vesicles 2018 (MISEV2018): a position statement of the International Society for Extracellular Vesicles and update of the MISEV2014 guidelines. J Extracell Vesicles. 2018 Nov 23;7(1):1535750. Doi: 10.1080/20013078.2018.1535750.

14. Théry C, Zitvogel L, Amigorena S. Exosomes: composition, biogenesis and function. Nat Rev Immunol. 2002 Aug;2(8):569-79. Doi: 10.1038/nri855.

15. Gyorgy B, Szabo RG, Pasztoi M, Pal Z, Misjak P, Aradi B, Laszlo V, Pallinger E, Pap E, Kittel A, Nagy G, et al. Membrane Vesicles, Current State-of-the-Art: Emerging Role of Extracellular Vesicles. Cell Mol Life Sci. 2011; 68:2667-2688.

16. EL Andaloussi S, Mäger I, Breakefield XO, Wood MJ. Extracellular vesicles: biology and emerging therapeutic opportunities. Nat Rev Drug Discov. 2013 May;12(5):347-57. Doi: 10.1038/nrd3978.

17. Raposo G, Nijman HW, Stoorvogel W, Liejendekker R, Harding CV, Melief CJ, Geuze HJ. B lymphocytes secrete antigen-presenting vesicles. J Exp Med. 1996 Mar 1;183(3):1161-72. Doi: 10.1084/jem.183.3.1161.

18. Vu LT, Gong J, Pham TT, Kim Y, Le MTN. microRNA exchange via extracellular vesicles in cancer. Cell Prolif. 2020 Nov;53(11):e12877. Doi: 10.1111/cpr.12877.

19. Zeng Y, Qiu Y, Jiang W, Shen J, Yao X, He X, Li L, Fu B, Liu X. Biological Features of Extracellular Vesicles and Challenges. Front Cell Dev Biol. 2022 Jun 24;10:816698. Doi: 10.3389/fcell.2022.816698.

20. Ciferri MC, Quarto R, Tasso R. Extracellular Vesicles as Biomarkers and Therapeutic Tools: From Pre-Clinical to Clinical Applications. Biology (Basel). 2021 Apr 23;10(5):359. Doi: 10.3390/biology10050359.

21. Turpin D, Truchetet ME, Faustin B, Augusto JF, Contin-Bordes C, Brisson A, Blanco P, Duffau P. Role of extracellular vesicles in autoimmune diseases. Autoimmun Rev. 2016 Feb;15(2):174-83. Doi: 10.1016/j.autrev.2015.11.004.

22. Yuana Y, Sturk A, Nieuwland R. Extracellular vesicles in physiological and pathological conditions. Blood Rev. 2013 Jan;27(1):31-9. Doi: 10.1016/j.blre.2012.12.002.

23. Pitt JM, Kroemer G, Zitvogel L. Extracellular vesicles: masters of intercellular communication and potential clinical interventions. J Clin Invest. 2016 Apr 1;126(4):1139-43. Doi: 10.1172/JCI87316.

24. Zappulli V, Friis KP, Fitzpatrick Z, Maguire CA, Breakefield XO. Extracellular vesicles and intercellular communication within the nervous system. J Clin Invest. 2016 Apr 1;126(4):1198-207. Doi: 10.1172/JCI81134.

25. Meng W, He C, Hao Y, Wang L, Li L, Zhu G. Prospects and challenges of extracellular vesicle-based drug delivery system: considering cell source. Drug Deliv. 2020 Dec;27(1):585-598. Doi: 10.1080/10717544.2020.1748758.

26. Witwer KW, Buzás EI, Bemis LT, Bora A, Lässer C, Lötvall J, Nolte-'t Hoen EN, Piper MG, Sivaraman S, Skog J, Théry C, Wauben MH, Hochberg F. Standardization of sample collection, isolation and analysis methods in extracellular vesicle research. J Extracell Vesicles. 2013 May 27;2. doi: 10.3402/jev.v2i0.20360.

27. Lötvall J, Hill AF, Hochberg F, Buzás EI, Di Vizio D, Gardiner C, Gho YS, Kurochkin IV, Mathivanan S, Quesenberry P, Sahoo S, Tahara H, Wauben MH, Witwer KW, Théry C. Minimal experimental requirements for definition of extracellular vesicles and their functions: a position statement from the International Society for Extracellular Vesicles. J Extracell Vesicles. 2014 Dec 22;3:26913. doi: 10.3402/jev.v3.26913.

28. Mateescu B, Kowal EJ, van Balkom BW, Bartel S, Bhattacharyya SN, Buzás EI, Buck AH, de Candia P, Chow FW, Das S, Driedonks TA, Fernández-Messina L, Haderk F, Hill AF, Jones JC, Van Keuren-Jensen KR, Lai CP, Lässer C, Liegro ID, Lunavat TR, Lorenowicz MJ, Maas SL, Mäger I, Mittelbrunn M, Momma S, Mukherjee K, Nawaz M, Pegtel DM, Pfaffl MW, Schiffelers RM, Tahara H, Théry C, Tosar JP, Wauben MH, Witwer KW, Nolte-'t Hoen EN. Obstacles and opportunities in the functional analysis of extracellular vesicle RNA - an ISEV position paper. J Extracell Vesicles. 2017 Mar 7;6(1):1286095. doi: 10.1080/20013078.2017.1286095.

29. EV-TRACK Consortium; Van Deun J, Mestdagh P, Agostinis P, Akay Ö, Anand S, Anckaert J, Martinez ZA, Baetens T, Beghein E, Bertier L, Berx G, Boere J, Boukouris S, Bremer M, Buschmann D, Byrd JB, Casert C, Cheng L, Cmoch A, Daveloose D, De Smedt E, Demirsoy S, Depoorter V, Dhondt B, Driedonks TA, Dudek A, Elsharawy A, Floris I, Foers AD, Gärtner K, Garg AD, Geeurickx E, Gettemans J, Ghazavi F, Giebel B, Kormelink TG, Hancock G, Helsmoortel H, Hill AF, Hyenne V, Kalra H, Kim D, Kowal J, Kraemer S, Leidinger P, Leonelli C, Liang Y, Lippens L, Liu S, Lo Cicero A, Martin S, Mathivanan S, Mathiyalagan P, Matusek T, Milani G, Monguió-Tortajada M, Mus LM, Muth DC, Németh A, Nolte-'t Hoen EN, O'Driscoll L, Palmulli R, Pfaffl MW, Primdal-Bengtson B, Romano E, Rousseau Q, Sahoo S, Sampaio N, Samuel M, Scicluna B, Soen B, Steels A, Swinnen JV, Takatalo M, Thaminy S, Théry C, Tulkens J, Van

Audenhove I, van der Grein S, Van Goethem A, van Herwijnen MJ, Van Niel G, Van Roy N, Van Vliet AR, Vandamme N, Vanhauwaert S, Vergauwen G, Verweij F, Wallaert A, Wauben M, Witwer KW, Zonneveld MI, De Wever O, Vandesompele J, Hendrix A. EV-TRACK: transparent reporting and centralizing knowledge in extracellular vesicle research. Nat Methods. 2017 Feb 28;14(3):228-232. doi: 10.1038/nmeth.4185.

30. Ramirez MI, Amorim MG, Gadelha C, Milic I, Welsh JA, Freitas VM, Nawaz M, Akbar N, Couch Y, Makin L, Cooke F, Vettore AL, Batista PX, Freezor R, Pezuk JA, Rosa-Fernandes L, Carreira ACO, Devitt A, Jacobs L, Silva IT, Coakley G, Nunes DN, Carter D, Palmisano G, Dias-Neto E. Technical challenges of working with extracellular vesicles. Nanoscale. 2018 Jan 18;10(3):881-906. Doi: 10.1039/c7nr08360b.

31. Dragovic RA, Gardiner C, Brooks AS, Tannetta DS, Ferguson DJ, Hole P, Carr B, Redman CW, Harris AL, Dobson PJ, Harrison P, Sargent IL. Sizing and phenotyping of cellular vesicles using Nanoparticle Tracking Analysis. Nanomedicine. 2011 Dec;7(6):780-8. Doi: 10.1016/j.nano.2011.04.003.

32. Zivko C, Fuhrmann G, Luciani P. Liver-derived extracellular vesicles: A cell by cell overview to isolation and characterization practices. Biochim Biophys Acta Gen Subj. 2021 Apr;1865(4):129559. Doi: 10.1016/j.bbagen.2020.129559.

33. Armstrong JPK, Stevens MM. Strategic design of extracellular vesicle drug delivery systems. Adv Drug Deliv Rev. 2018 May;130:12-16. Doi: 10.1016/j.addr.2018.06.017. Epub 2018 Jun 28.

34. Tenchov R, Bird R, Curtze AE, Zhou Q. Lipid Nanoparticles─From Liposomes to mRNA Vaccine Delivery, a Landscape of Research Diversity and Advancement. ACS Nano. 2021 Nov 23;15(11):16982-17015. Doi: 10.1021/acsnano.1c04996.

35. Barenholz Y. Doxil®--the first FDA-approved nano-drug: lessons learned. J Control Release. 2012 Jun 10;160(2):117-34. Doi: 10.1016/j.jconrel.2012.03.020.

36. Palazzolo S, Bayda S, Hadla M, Caligiuri I, Corona G, Toffoli G, Rizzolio F. The Clinical Translation of Organic Nanomaterials for Cancer Therapy: A Focus on Polymeric Nanoparticles, Micelles, Liposomes and Exosomes. Curr Med Chem. 2018;25(34):4224-4268. Doi: 10.2174/0929867324666170830113755.

37. De Jong WH, Borm PJ. Drug delivery and nanoparticles:applications and hazards. Int J Nanomedicine. 2008;3(2):133-49. Doi: 10.2147/ijn.s596.

38. Zolnik BS, González-Fernández A, Sadrieh N, Dobrovolskaia MA. Nanoparticles and the immune system. Endocrinology. 2010 Feb;151(2):458-65. Doi: 10.1210/en.2009-1082.

39. Hur YH, Cerione RA, Antonyak MA. Extracellular vesicles and their roles in stem cell biology. Stem Cells. 2020 Apr;38(4):469-476. Doi: 10.1002/stem.3140.

40. Harrell CR, Jovicic N, Djonov V, Arsenijevic N, Volarevic V. Mesenchymal Stem Cell-Derived Exosomes and Other Extracellular Vesicles as New Remedies in the Therapy of Inflammatory Diseases. Cells. 2019 Dec 11;8(12):1605. Doi: 10.3390/cells8121605.

41. Zhao AG, Shah K, Cromer B, Sumer H. Mesenchymal Stem Cell-Derived Extracellular Vesicles and Their Therapeutic Potential. Stem Cells Int. 2020 Aug 24;2020:8825771. Doi: 10.1155/2020/8825771.

42. Hill L, Alousi A, Kebriaei P, Mehta R, Rezvani K, Shpall E. New and emerging therapies for acute and chronic graft versus host disease. Ther Adv Hematol. 2018 Jan;9(1):21-46. Doi: 10.1177/2040620717741860.

43. Liu C, Gao H, Lv P, Liu J, Liu G. Extracellular vesicles as an efficient nanoplatform for the delivery of therapeutics. Hum Vaccin Immunother. 2017 Nov 2;13(11):2678-2687. Doi: 10.1080/21645515.2017.1363935.

44. Meng W, He C, Hao Y, Wang L, Li L, Zhu G. Prospects and challenges of extracellular vesicle-based drug delivery system: considering cell source. Drug Deliv. 2020 Dec;27(1):585-598. Doi: 10.1080/10717544.2020.1748758.

45. Abhange K, Makler A, Wen Y, Ramnauth N, Mao W, Asghar W, Wan Y. Small extracellular vesicles in cancer. Bioact Mater. 2021 Apr 7;6(11):3705-3743. Doi: 10.1016/j.bioactmat.2021.03.015.

46. Liu S, Wu X, Chandra S, Lyon C, Ning B, Jiang L, Fan J, Hu TY. Extracellular vesicles: Emerging tools as therapeutic agent carriers. Acta Pharm Sin B. 2022 Oct;12(10):3822-3842. Doi: 10.1016/j.apsb.2022.05.002.

47. Van der Koog L, Gandek TB, Nagelkerke A. Liposomes and Extracellular Vesicles as Drug Delivery Systems: A Comparison of Composition, Pharmacokinetics, and Functionalization. Adv Healthc Mater. 2022 Mar;11(5):e2100639. Doi: 10.1002/adhm.202100639.

48. Murphy DE, de Jong OG, Brouwer M, Wood MJ, Lavieu G, Schiffelers RM, Vader P. Extracellular vesicle-based therapeutics: natural versus engineered targeting and trafficking. Exp Mol Med. 2019 Mar 15;51(3):1-12. Doi: 10.1038/s12276-019-0223-5.

49. György B, Hung ME, Breakefield XO, Leonard JN. Therapeutic applications of extracellular vesicles: clinical promise and open questions. Annu Rev Pharmacol Toxicol. 2015;55:439-464. Doi: 10.1146/annurev-pharmtox-010814-124630.

50. Gupta D, Zickler AM, El Andaloussi S. Dosing extracellular vesicles. Adv Drug Deliv Rev. 2021 Nov;178:113961. Doi: 10.1016/j.addr.2021.113961.

51. Zhang G, Huang X, Xiu H, Sun Y, Chen J, Cheng G, Song Z, Peng Y, Shen Y, Wang J, Cai Z. Extracellular vesicles: Natural liver-accumulating drug delivery

vehicles for the treatment of liver diseases. J Extracell Vesicles. 2020 Dec;10(2):e12030. Doi: 10.1002/jev2.12030.

52. Ginini L, Billan S, Fridman E, Gil Z. Insight into Extracellular Vesicle-Cell Communication: From Cell Recognition to Intracellular Fate. Cells. 2022 Apr 19;11(9):1375. Doi: 10.3390/cells11091375.

53. Szwedowicz U, Łapińska Z, Gajewska-Naryniecka A, Choromańska A. Exosomes and Other Extracellular Vesicles with High Therapeutic Potential: Their Applications in Oncology, Neurology, and Dermatology. Molecules. 2022 Feb 15;27(4):1303. Doi: 10.3390/molecules27041303.

54. Bobis-Wozowicz S, Marbán E. Editorial: Extracellular Vesicles as Next Generation Therapeutics. Front Cell Dev Biol. 2022 May 12;10:919426. Doi: 10.3389/fcell.2022.919426.

55. Claridge B, Lozano J, Poh QH, Greening DW. Development of Extracellular Vesicle Therapeutics: Challenges, Considerations, and Opportunities. Front Cell Dev Biol. 2021 Sep 20;9:734720. Doi: 10.3389/fcell.2021.734720.

56. Paunovska K, Loughrey D, Dahlman JE. Drug delivery systems for RNA therapeutics. Nat Rev Genet. 2022 May;23(5):265-280. Doi: 10.1038/s41576-021-00439-4.

57. Li S, Stöckl S, Lukas C, Herrmann M, Brochhausen C, König MA, Johnstone B, Grässel S. Curcumin-primed human BMSC-derived extracellular vesicles reverse IL-1β-induced catabolic responses of OA chondrocytes by upregulating miR-126-3p. Stem Cell Res Ther. 2021 Apr 29;12(1):252. Doi: 10.1186/s13287-021-02317-6.

58. Ye R, Lin Q, Xiao W, Mao L, Zhang P, Zhou L, Wu X, Jiang N, Zhang X, Zhang Y, Ma D, Huang J, Wang X, Deng L. miR-150-5p in neutrophil-derived extracellular vesicles associated with sepsis-induced cardiomyopathy in septic patients. Cell Death Discov. 2023 Jan 21;9(1):19. Doi: 10.1038/s41420-023-01328-x.

59. Wang Z, Mo H, He Z, Chen A, Cheng P. Extracellular vesicles as an emerging drug delivery system for cancer treatment: Current strategies and recent advances. Biomed Pharmacother. 2022 Sep;153:113480. Doi: 10.1016/j.biopha.2022.113480.

60. Herrmann IK, Wood MJA, Fuhrmann G. Extracellular vesicles as a next-generation drug delivery platform. Nat Nanotechnol. 2021 Jul;16(7):748-759. doi: 10.1038/s41565-021-00931-2.

61. Huda MN, Nafiujjaman M, Deaguero IG, Okonkwo J, Hill ML, Kim T, Nurunnabi M. Potential Use of Exosomes as Diagnostic Biomarkers and in Targeted Drug Delivery: Progress in Clinical and Preclinical Applications. ACS Biomater Sci Eng. 2021 Jun 14;7(6):2106-2149. Doi: 10.1021/acsbiomaterials.1c00217.

62. Wiklander OPB, Brennan MÁ, Lötvall J, Breakefield XO, El Andaloussi S. Advances in therapeutic applications of extracellular vesicles. Sci Transl Med. 2019 May 15;11(492):eaav8521. doi: 10.1126/scitranslmed.aav8521.

63. Gao X, Ran N, Dong X, Zuo B, Yang R, Zhou Q, Moulton HM, Seow Y, Yin H. Anchor peptide captures, targets, and loads exosomes of diverse origins for diagnostics and therapy. Sci Transl Med. 2018 Jun 6;10(444):eaat0195. doi: 10.1126/scitranslmed.aat0195

64. Haraszti RA, Miller R, Didiot MC, Biscans A, Alterman JF, Hassler MR, Roux L, Echeverria D, Sapp E, DiFiglia M, Aronin N, Khvorova A. Optimized Cholesterol-siRNA Chemistry Improves Productive Loading onto Extracellular Vesicles. Mol Ther. 2018 Aug 1;26(8):1973-1982. doi: 10.1016/j.ymthe.2018.05.024.

65. Tian Y, Li S, Song J, Ji T, Zhu M, Anderson GJ, Wei J, Nie G. A doxorubicin delivery platform using engineered natural membrane vesicle exosomes for targeted tumor therapy. Biomaterials. 2014 Feb;35(7):2383-90. doi: 10.1016/j.biomaterials.2013.11.083.

66. Alvarez-Erviti L, Seow Y, Yin H, Betts C, Lakhal S, Wood MJ. Delivery of siRNA to the mouse brain by systemic injection of targeted exosomes. Nat Biotechnol. 2011 Apr;29(4):341-5. doi: 10.1038/nbt.1807.

67. Kamerkar S, LeBleu VS, Sugimoto H, Yang S, Ruivo CF, Melo SA, Lee JJ, Kalluri R. Exosomes facilitate therapeutic targeting of oncogenic KRAS in pancreatic cancer. Nature. 2017 Jun 22;546(7659):498-503. doi: 10.1038/nature22341.

68. Kooijmans SAA, Stremersch S, Braeckmans K, de Smedt SC, Hendrix A, Wood MJA, Schiffelers RM, Raemdonck K, Vader P. Electroporation-induced siRNA precipitation obscures the efficiency of siRNA loading into extracellular vesicles. J Control Release. 2013 Nov 28;172(1):229-238. doi: 10.1016/j.jconrel.2013.08.014.

69. Mendt M, Kamerkar S, Sugimoto H, McAndrews KM, Wu CC, Gagea M, Yang S, Blanko EVR, Peng Q, Ma X, Marszalek JR, Maitra A, Yee C, Rezvani K, Shpall E, LeBleu VS, Kalluri R. Generation and testing of clinical-grade exosomes for pancreatic cancer. JCI Insight. 2018 Apr 19;3(8):e99263. doi: 10.1172/jci.insight.99263.

70. Pascucci L, Coccè V, Bonomi A, Ami D, Ceccarelli P, Ciusani E, Viganò L, Locatelli A, Sisto F, Doglia SM, Parati E, Bernardo ME, Muraca M, Alessandri G, Bondiolotti G, Pessina A. Paclitaxel is incorporated by mesenchymal stromal cells and released in exosomes that inhibit in vitro tumor growth: a new approach for drug delivery. J Control Release. 2014 Oct 28;192:262-70. doi: 10.1016/j.jconrel.2014.07.042.

71. Zhang Y, Liu D, Chen X, Li J, Li L, Bian Z, Sun F, Lu J, Yin Y, Cai X, Sun Q, Wang K, Ba Y, Wang Q, Wang D, Yang J, Liu P, Xu T, Yan Q, Zhang J, Zen K,

Zhang CY. Secreted monocytic miR-150 enhances targeted endothelial cell migration. Mol Cell. 2010 Jul 9;39(1):133-44. doi: 10.1016/j.molcel.2010.06.010.

72. Mizrak A, Bolukbasi MF, Ozdener GB, Brenner GJ, Madlener S, Erkan EP, Ströbel T, Breakefield XO, Saydam O. Genetically engineered microvesicles carrying suicide mRNA/protein inhibit schwannoma tumor growth. Mol Ther. 2013 Jan;21(1):101-8. doi: 10.1038/mt.2012.161.

73. Ohno S, Takanashi M, Sudo K, Ueda S, Ishikawa A, Matsuyama N, Fujita K, Mizutani T, Ohgi T, Ochiya T, Gotoh N, Kuroda M. Systemically injected exosomes targeted to EGFR deliver antitumor microRNA to breast cancer cells. Mol Ther. 2013 Jan;21(1):185-91. doi: 10.1038/mt.2012.180. Ohno S, Takanashi M, Sudo K, Ueda S, Ishikawa A, Matsuyama N, Fujita K, Mizutani T, Ohgi T, Ochiya T, Gotoh N, Kuroda M. Systemically injected exosomes targeted to EGFR deliver antitumor microRNA to breast cancer cells. Mol Ther. 2013 Jan;21(1):185-91. doi: 10.1038/mt.2012.180.

74. Kojima R, Bojar D, Rizzi G, Hamri GC, El-Baba MD, Saxena P, Ausländer S, Tan KR, Fussenegger M. Designer exosomes produced by implanted cells intracerebrally deliver therapeutic cargo for Parkinson's disease treatment. Nat Commun. 2018 Apr 3;9(1):1305. doi: 10.1038/s41467-018-03733-8.

75. Wani S, Kaul D. Cancer cells govern miR-2909 exosomal recruitment through its 3'-end post-transcriptional modification. Cell Biochem Funct. 2018 Mar;36(2):106-111. doi: 10.1002/cbf.3323.

76. Lee ST, Im W, Ban JJ, Lee M, Jung KH, Lee SK, Chu K, Kim M. Exosome-Based Delivery of miR-124 in a Huntington's Disease Model. J Mov Disord. 2017 Jan;10(1):45-52. doi: 10.14802/jmd.16054.

77. Johnson R, Zuccato C, Belyaev ND, Guest DJ, Cattaneo E, Buckley NJ. A microRNA-based gene dysregulation pathway in Huntington's disease. Neurobiol Dis. 2008 Mar;29(3):438-45. doi: 10.1016/j.nbd.2007.11.001.

78. Wang Q, Lu Q. Plasma membrane-derived extracellular microvesicles mediate non-canonical intercellular NOTCH signaling. Nat Commun. 2017 Sep 27;8(1):709. doi: 10.1038/s41467-017-00767-2.

79. Nabhan JF, Hu R, Oh RS, Cohen SN, Lu Q. Formation and release of arrestin domain-containing protein 1-mediated microvesicles (ARMMs) at plasma membrane by recruitment of TSG101 protein. Proc Natl Acad Sci U S A. 2012 Mar 13;109(11):4146-51. doi: 10.1073/pnas.1200448109.

80. Wang Q, Yu J, Kadungure T, Beyene J, Zhang H, Lu Q. ARMMs as a versatile platform for intracellular delivery of macromolecules. Nat Commun. 2018 Mar 6;9(1):960. doi: 10.1038/s41467-018-03390-x.

81. Sato YT, Umezaki K, Sawada S, Mukai SA, Sasaki Y, Harada N, Shiku H, Akiyoshi K. Engineering hybrid exosomes by membrane fusion with liposomes. Sci Rep. 2016 Feb 25;6:21933. doi: 10.1038/srep21933.

82. Votteler J, Ogohara C, Yi S, Hsia Y, Nattermann U, Belnap DM, King NP, Sundquist WI. Designed proteins induce the formation of nanocage-containing extracellular vesicles. Nature. 2016 Dec 8;540(7632):292-295. doi: 10.1038/nature20607.

83. Zhang X, Zhang H, Gu J, Zhang J, Shi H, Qian H, Wang D, Xu W, Pan J, Santos HA. Engineered Extracellular Vesicles for Cancer Therapy. Adv Mater. 2021 Apr;33(14):e2005709. Doi: 10.1002/adma.202005709.

84. Vader P, Mol EA, Pasterkamp G, Schiffelers RM. Extracellular vesicles for drug delivery. Adv Drug Deliv Rev. 2016 Nov 15;106(Pt A):148-156. doi: 10.1016/j.addr.2016.02.006.

85. Wiklander OPB, Brennan MÁ, Lötvall J, Breakefield XO, El Andaloussi S. Advances in therapeutic applications of extracellular vesicles. Sci Transl Med. 2019 May 15;11(492):eaav8521. Doi: 10.1126/scitranslmed.aav8521.

86. Sun Y, Liu G, Zhang K, Cao Q, Liu T, Li J. Mesenchymal stem cells-derived exosomes for drug delivery. Stem Cell Res Ther. 2021 Oct 30;12(1):561. doi: 10.1186/s13287-021-02629-7.

87. Witwer KW, Wolfram J. Extracellular vesicles versus synthetic nanoparticles for drug delivery. Nat Rev Mater. 2021 Feb;6(2):103-106. doi: 10.1038/s41578-020-00277-6.

88. Paganini C, Capasso Palmiero U, Pocsfalvi G, Touzet N, Bongiovanni A, Arosio P. Scalable Production and Isolation of Extracellular Vesicles: Available Sources and Lessons from Current Industrial Bioprocesses. Biotechnol J. 2019 Oct;14(10):e1800528. doi: 10.1002/biot.201800528.

89. Pérez-Bermúdez P, Blesa J, Soriano JM, Marcilla A. Extracellular vesicles in food: Experimental evidence of their secretion in grape fruits. Eur J Pharm Sci. 2017 Feb 15;98:40-50. Doi: 10.1016/j.ejps.2016.09.022.

90. Barone ME, Murphy E, Parkes R, Fleming GTA, Campanile F, Thomas OP, Touzet N. Antibacterial Activity and Amphidinol Profiling of the Marine Dinoflagellate Amphidinium carterae (Subclade III). Int J Mol Sci. 2021 Nov 11;22(22):12196. Doi: 10.3390/ijms222212196.

91. Ampofo J, Abbey L. Microalgae: Bioactive Composition, Health Benefits, Safety and Prospects as Potential High-Value Ingredients for the Functional Food Industry. Foods. 2022 Jun 14;11(12):1744. Doi: 10.3390/foods11121744.

92. Barkia I, Saari N, Manning SR. Microalgae for High-Value Products Towards Human Health and Nutrition. Mar Drugs. 2019 May 24;17(5):304. Doi: 10.3390/md17050304.

93. Sathasivam R, Radhakrishnan R, Hashem A, Abd Allah EF. Microalgae metabolites: A rich source for food and medicine. Saudi J Biol Sci. 2019 May;26(4):709-722. Doi: 10.1016/j.sjbs.2017.11.003.

94. Barone ME, Parkes R, Herbert H, McDonnell A, Conlon T, Aranyos A, Fierli D, Fleming GTA, Touzet N. Comparative Response of Marine Microalgae to H2O2-Induced Oxidative Stress. Appl Biochem Biotechnol. 2021 Dec;193(12):4052-4067. Doi: 10.1007/s12010-021-03690-x.

95. Olasehinde TA, Olaniran AO, Okoh AI. Therapeutic Potentials of Microalgae in the Treatment of Alzheimer's Disease. Molecules. 2017 Mar 18;22(3):480. Doi: 10.3390/molecules22030480.

96. Ryckebosch E, Bruneel C, Termote-Verhalle R, Goiris K, Muylaert K, Foubert I. Nutritional evaluation of microalgae oils rich in omega-3 long chain polyunsaturated fatty acids as an alternative for fish oil. Food Chem. 2014 Oct 1;160:393-400. doi: 10.1016/j.foodchem.2014.03.087.

97. Chang CL, Deckelbaum RJ. Omega-3 fatty acids: mechanisms underlying 'protective effects' in atherosclerosis. Curr Opin Lipidol. 2013 Aug;24(4):345-50. doi: 10.1097/MOL.0b013e3283616364.

98. Falaise C, François C, Travers MA, Morga B, Haure J, Tremblay R, Turcotte F, Pasetto P, Gastineau R, Hardivillier Y, Leignel V, Mouget JL. Antimicrobial Compounds from Eukaryotic Microalgae against Human Pathogens and Diseases in Aquaculture. Mar Drugs. 2016 Sep 2;14(9):159. doi: 10.3390/md14090159.

99. Khan MI, Shin JH, Kim JD. The promising future of microalgae: current status, challenges, and optimization of a sustainable and renewable industry for biofuels, feed, and other products. Microb Cell Fact. 2018 Mar 5;17(1):36. doi: 10.1186/s12934-018-0879-x.

100. Burja AM, Abou-Mansour E, Banaigs B, Payri C, Burgess JG, Wright PC. Culture of the marine cyanobacterium, Lyngbya majuscula (Oscillatoriaceae), for bioprocess intensified production of cyclic and linear lipopeptides. J Microbiol Methods. 2002 Feb;48(2-3):207-19. doi: 10.1016/s0167-7012(01)00324-4.

101. Costa M, Costa-Rodrigues J, Fernandes MH, Barros P, Vasconcelos V, Martins R. Marine cyanobacteria compounds with anticancer properties: a review on the implication of apoptosis. Mar Drugs. 2012 Oct;10(10):2181-2207. doi: 10.3390/md10102181.

102. Gupta, V.; Ratha, S.K.; Sood, A.; Chaudhary, V.; Prasanna, R. New insights into the biodiversity and applications of cyanobacteria (blue-green algae)—Prospects

and challenges. Algal Res. 2013, 2, 79–97. https://doi.org/10.1016/j.algal.2013.01.006

103. Vijayakumar, S.; Menakha, M. Pharmaceutical applications of cyanobacteria— A review. J. Acute Med. 2015, 5, 15–23. https://doi.org/10.1016/j.jacme.2015.02.004

104. Li F, Li Y, Novoselov KS, Liang F, Meng J, Ho SH, Zhao T, Zhou H, Ahmad A, Zhu Y, Hu L, Ji D, Jia L, Liu R, Ramakrishna S, Zhang X. Bioresource Upgrade for Sustainable Energy, Environment, and Biomedicine. Nanomicro Lett. 2023 Jan 11;15(1):35. doi: 10.1007/s40820-022-00993-4.

Chapter 2

Scope of this thesis and introduction to the experimental work

2.1 Introduction to the experimental work

The development of a theranostic approach using EVs is challenged by their heterogeneity in size, composition, and function. Further, upscaling of the upstream cultivation of EV-producer human cells (*i.e.*, MSCs) to satisfy the demand from the pharmaceutical and cosmetic industries is economically and technologically challenging. This hinders the practical use of EVs in clinical practice, despite significant attention from the scientific community and industry. The collection procedures of EVs have a significant impact on their yield, measurement, and composition, suggesting that the chosen isolation method can shape the identity of the EVs. Based on these challenges, this PhD project aims to advance the development of new and improved bioprocesses for producing EVs from a renewable biological source and functionalizing them. The goal is to facilitate their clinical translation and minimize the side effects that have hindered their use until now. After identifying microalgae as a sustainable and natural bio-source for the mass production of EVs, as discussed in **Chapter 3**[1] the subsequent critical step was to identify the optimal species in collaboration with Dr. Nicolas Touzet of Atlantic Technology University (ATU) in Sligo, Ireland. Through the examination of nanoscale extracellular structures generated by eighteen species of microalgae, we discovered seven potential strains capable of producing EVs that belonged to distinct lineages. These findings indicate that the ability to produce EVs is a conserved evolutionary trait in microalgae. Specifically, two EV purification techniques were carried out: differential ultracentrifugation (dUC) and Tangential Flow Filtration (TFF). While both methods aim to separate vesicles based on their size, the focus has been on Tangential Flow Filtration due to its ability to preserve the integrity of liposomes and its capacity to handle larger starting volumes. Indeed, in **Chapter 4**[2] and in **Chapter 5**[3] it is discussed the optimal conditions for Tangential Flow Filtration, compared to differential ultracentrifugation. Subsequently, the isolation and preservation process of EVs was validated and standardized by evaluating their yield, heterogeneity, and presence of protein biomarkers characteristic of exosomes and/or microvesicles (such as Alix, Enolase, and ß-Actin proteins), using a multidisciplinary approach in collaboration with Dr. Mauro Manno's group at Institute of Biophysics (IBF) at CNR, Palermo and Prof. Paolo Arosio at ETHZ, Switzerland. In more detail, the size has been evaluated by Dynamic Light Scattering, the number of nanoparticles and their size distribution has been evaluated via the use of nanoparticle tracking analysis (NTA) and the analysis of morphology was performed using Scanning electron microscope (SEM), and atomic force microscopy. These results allowed us to define the microalgal-derived EVs, that we called

"nanoalgosomes", as a new type of EV that can be produced at large scale through a scalable, GMP-compliant and sustainable bioprocess.

Following on from the establishment of the optimal experimental parameters for vesicle isolation, the **Chapter 6**[4] reports the biological activity and toxicity of nanoalgosomes and how human and *Caenorhabditis elegans* cells take up labelled nanoalgosomes; we found that that is an energy-dependent mechanism and are localized in specific cells' cytoplasm for a prolonged period. Our results demonstrate that nanoalgosomes can be actively taken up by human cells in vitro and C. elegans cells in vivo (in collaboration with Dr. Elia di Schiavi, CNR, Napoli), supporting their potential use as nanocarriers for bioactive compounds in theranostic applications.

Chapter 7[5] reports the results obtained during the experience conducted at ETHZ in the laboratories of Prof. Paolo Arosio. Specifically, the development of programmable coacervates made from zwitterionic polymers with ion exchange properties has created a new method for bioseparation. These coacervates are highly effective for purifying soft nanoparticles like extracellular vesicles (EVs) and liposomes. By designing the polymers, the coacervates can respond to different stimuli and recruit specific molecules. These polymeric coacervates have been shown to efficiently recruit and release intact liposomes, human EVs. In this scenario, this new approach has been applied on EVs derived microalgae for separating them from impurities such as proteins and nucleic acids. This innovative approach combines the simplicity and speed of precipitation methods, the programmability of chromatography, and the gentleness of aqueous two-phase separation to ensure product stability. This material has the potential to provide an alternative, low-shear, gentle, and selective purification process for EVs.

References:

1. Picciotto S, Barone ME, Fierli D, Aranyos A, Adamo G, BoŽič D, Romancino DP, Stanly C, Parkes R, Morsbach S, Raccosta S, Paganini C, Cusimano A, Martorana V, Noto R, Carrotta R, Librizzi F, Capasso Palmiero U, Santonicola P, Iglič A, Gai M, Corcuera L, Kisslinger A, Di Schiavi E, Landfester K, Liguori GL, Kralj-Iglič V, Arosio P, Pocsfalvi G, Manno M, Touzet N, Bongiovanni A. Biomater Sci. 2021 Apr 21;9(8):2917-2930. doi: 10.1039/d0bm01696a. Epub 2021 Feb 23. PMID: 33620041.

2. Adamo G, Fierli D, Romancino DP, Picciotto S, Barone ME, Aranyos A, Božič D, Morsbach S, Raccosta S, Stanly C, Paganini C, Gai M, Cusimano A, Martorana V, Noto R, Carrotta R, Librizzi F, Randazzo L, Parkes R, Capasso Palmiero U, Rao E, Paterna A, Santonicola P, Iglič A, Corcuera L, Kisslinger A, Di Schiavi E, Liguori GL, Landfester K, Kralj-Iglič V, Arosio P, Pocsfalvi G, Touzet N, Manno M, Bongiovanni A. Nanoalgosomes: Introducing extracellular vesicles produced by microalgae. J Extracell Vesicles. 2021 Apr;10(6):e12081. doi: 10.1002/jev2.12081. Epub 2021 Apr 27. PMID: 33936568; PMCID: PMC8077145. Co-first Author.

3. Paterna A, Rao E, Adamo G, Raccosta S, Picciotto S, Romancino D, Noto R, Touzet N, Bongiovanni A, Manno M. Isolation of Extracellular Vesicles From Microalgae: A Renewable and Scalable Bioprocess. Front Bioeng Biotechnol. 2022 Mar 14;10:836747. doi: 10.3389/fbioe.2022.836747. PMID: 35360396; PMCID: PMC8963918.

4. Picciotto S, Santonicola P, Paterna A, Rao E, Raccosta S, Romancino DP, Noto R, Touzet N, Manno M, Di Schiavi E, Bongiovanni A, Adamo G. Extracellular Vesicles From Microalgae: Uptake Studies in Human Cells and Caenorhabditis elegans. Front Bioeng Biotechnol. 2022 Mar 24;10:830189. doi: 10.3389/fbioe.2022.830189. PMID: 35402397; PMCID: PMC8987914. First-Author.

5. C. Paganini, U. Capasso Palmiero, S. Picciotto, A. Molinelli, I. Porello, G. Adamo, M. Manno, A. Bongiovanni, P. Arosio. High-Yield Separation of Extracellular Vesicles Using Programmable Zwitterionic Coacervates. Small 2022, 2204736. https://doi.org/10.1002/smll.202204736. Co-Author. Impact Factor: 15.153

Chapter 3

Isolation of extracellular vesicles from microalgae: towards the production of sustainable and natural nanocarriers of bioactive compounds

Picciotto S, Barone ME, Fierli D, Aranyos A, Adamo G, BoŽič D, Romancino DP, Stanly C, Parkes R, Morsbach S, Raccosta S, Paganini C, Cusimano A, Martorana V, Noto R, Carrotta R, Librizzi F, Capasso Palmiero U, Santonicola P, Iglič A, Gai M, Corcuera L, Kisslinger A, Di Schiavi E, Landfester K, Liguori GL, Kralj-Iglič V, Arosio P, Pocsfalvi G, Manno M, Touzet N, Bongiovanni A. Biomater Sci. 2021 Apr 21;9(8):2917-2930. doi: 10.1039/d0bm01696a. Epub 2021 Feb 23. PMID: 33620041.

Abstract

Safe, efficient and specific nano-delivery systems are essential for current and emerging therapeutics, precision medicine and other biotechnology sectors. Novel bio-based nanotechnologies have recently arisen, which are based on the exploitation of extracellular vesicles (EVs). In this context, it has become essential to identify suitable organisms or cellular types to act as reliable sources of EVs and to develop their pilot- to large-scale production. The discovery of new biosources and the optimisation of related bioprocesses for the isolation and functionalisation of nano-delivery vehicles are fundamental to further develop therapeutic and biotechnological applications. Microalgae constitute sustainable sources of bio-active compounds with a range of sectorial applications including for example the formulation of health supplements, cosmetic products or food ingredients. In this study, we demonstrate that microalgae are promising producers of EVs. By analysing the nanosized extracellular nano-objects produced by eighteen microalgal species, we identified seven promising EV-producing strains belonging to distinct lineages, suggesting that the production of EVs in microalgae is an evolutionary conserved trait. Here we report the selection process and focus on one of this seven species, the glaucophyte *Cyanophora paradoxa*, which returned a protein yield in the small EV fraction of 1 μg of EV proteins per mg of dry weight of microalgal biomass (corresponding to 10^9 particles per mg of dried biomass) and EVs with a diameter of 130 nm (mode), as determined by the micro bicinchoninic acid assay, nanoparticle tracking and dynamic light scattering analyses. Moreover, the extracellular nanostructures isolated from the conditioned media of microalgae species returned positive immunoblot signals for some commonly used EV-biomarkers such as Alix, Enolase, HSP70, and β-actin. Overall, this work establishes a platform for the efficient production of EVs from a sustainable bioresource and highlights the potential of microalgal EVs as novel biogenic nanovehicles.

1. Introduction

A major therapeutic objective of modern medicine has been the development of novel treatment strategies that can target specific organs, tissues and cells.[1] As such, a variety of nano- particle-based drug delivery systems has been tested over the last decades, including synthetic polymer- and lipid-based nanoparticles as well as other organic and inorganic material- based nanovectors.[2] Therapeutic agents such as RNA molecules, which are effective *in vitro*, often fail *in vivo* due to rapid clearance or biological barriers that prevent site-specific accumulation.[3,4] Further, despite the appreciable success of synthetic nanomaterials to date, technical challenges involving their large-scale, cost-effective production and intrinsic toxicity still hinder their clinical and market translation.[2] Biogenic nanovesicles have shown potential to naturally perform cell-specific drug release.[5,6] Cell-secreted extracellular vesicles (EVs) are an example of biogenic lipid bilayer delimited nanocarriers.[7] They have been observed in many human and animal body fluids including blood, urine, saliva, semen, bronchoalveolar lavage, bile, ascitic fluid, breast milk or cerebrospinal fluid.[8,9] EVs are physiological nanocarriers recognised as mediators of inter-cellular signaling by which even distant cells can exchange membrane and cytosolic contents, including proteins and RNA.[7,10,11] EVs are also important mediators of cell–cell communication in conditions such as metabolic, cardiovascular, neural and neoplastic pathologies. Interestingly, EVs can act by either promoting or counteracting the disease.[12,13] Moreover, they are naturally stable in various biological fluids, immunologically inert and able to pass through some biological barriers due to their small size, which could potentially overcome some of the limitations currently associated with synthetic liposomes.[5,14] It has also been shown that EVs can exhibit organ-specific targeting abilities that are attributed to the interplay of several EV components.[15] The finding that EVs may be used as natural carriers of small bioactive molecules has hence raised great interest from a number of scientific disciplines given that they could find promising applications for the delivery of miRNA, siRNA, mRNA, lncRNA, proteins, peptides, lipids, synthetic drugs or other cargo.[16] EVs constitute vehicles for inter-species communication, as evidenced from the microbiota and human gut cell

interactions, and from the interactions between plants and their pathogens; EVs have been indeed found in all the three domains of life: archaea, bacteria and eukarya.[17–21] There are various cell sources available to produce EVs and indeed several have been in the process of being exploited for therapeutic applications.[22] However, one attractive source that has remained largely unexplored to date is microalgae. Microalgae are a heterogeneous group of protistean organisms of polyphyletic origins that constitute a rich reservoir of bioactive metabolites, including polysaccharides, lipids, proteins, pigments, vitamins, antioxidants and other bioactive compounds.[23–25] Microalgae are perceived as renewable bioreources which have been considered for applications in a variety of fields including wastewater treatment, atmospheric CO_2 sequestration, bioenergy, drug development, biofertilisation, feed manufacture or nutraceutical formulations.[26–32] As such, a range of microalgae species interspersed in a variety of lineages have the capacity to synthesise high-value metabolites such as xantophyll pigments or the omega-3 long chain poly- unsaturated fatty acids EPA and DHA, which have been claimed to have a wide range of beneficial health effects (e.g.antioxidant, anti-inflammation and antibacterial activities) and have high potential for niche markets.[33–35] Microalgae are believed to hold a number of advantages over other photosynthetic crops as they have higher growth rates and can be cultivated on non-arable land. They also do not depend on seasonal fluctuation limitations as their growth requirements can be tailored all year round under controlled conditions in specifically designed photobioreactors.

In the context of the H2020-FETOpen project VES4US (http://www.ves4us.eu) and in the present work we propose microalgae as novel sources of EVs to be used as tailor-made products for different industrial sectors such as nutraceutics, cosmetics or nanomedicine. To this end, we developed a plat- form for the production, isolation and characterisation of EVs from microalgae. Our results demonstrate that EVs can be isolated from different microalgae strains, exhibiting all the key features of EVs. As an important first step towards scaling-up production, we analysed a number of species interspersed across several microalgal lineages and identified those best suited for the future biorefining of EVs.

2. Materials and methods

2.1 Microalgae strain selection and cultivation

18 microalgae strains were grown for 30 days in triplicate borosilicate glass tubes containing 60 ml of f/2 medium.[36] The selection of the strains was based on including members from the main microalgal lineages as well as considering a variety of features such as seawater and freshwater inhabitants, small and large sized cells, colonial and single cells and species with sequenced genomes (ESI File 1‡). The cultures were initiated with a 10% (v/v) starting inoculum from actively dividing stocks at 1.67 mg ml−1 (wet biomass). The incubation conditions consisted of a temperature of 20 °C ± 1 °C and an illumination regime of 100 μmol m−2 s−1 with a light : darkness photoperiod of 14 : 10. The biomass of the strains was collected at day 30 of culture by centrifugation (2000g, 10 min) and freeze-dried overnight prior to subsequent analyses. The biomass of marine species was treated with 1 ml of 0.5 M ammonium formate for desalting prior to freeze-drying.

2.2 Pigment extraction and analysis

Pigment extraction was carried out according to Mc Gee et al.[37] Samples of freeze-dried biomass (2–3 mg) were mixed with 500 μl of ice cold 100% acetone and glass beads and placed in a FastPrep FP120 ribolyser for 40 s at full speed. Deionised water was added to bring the solution to 80% acetone (v/v) and vortexed. The extracts were then filtered through 0.22 μm PTFE membrane syringe filters to remove any residual particulate material. The extracts were transferred into amber vials and analysed within 24 hours. Pigment extracts were analysed at constant room temperature on a Varian ProStar HPLC binary solvent delivery system equipped with a 20 μl sample loop, ProStar 310 UV and 335 PDA detectors. Pigments were separated using a Phenomenex Onyx C18 100 × 4.6 mm ID monolithic column fitted with a Phenomenex Onyx C18 guard cartridge 10 × 4.6 mm ID employing a stepped gradient solvent programme with a flow rate of 3 ml min−1. Pigments were resolved using a gradient profile consisting of 10% B starting condition for 0.10 min, followed by a linear gradient to 65% B from 0:10–2:00 min, isocratic hold at 65% B from 2:00 to 4:00 min, linear gradient from 4:00 to 5:00 min followed by hold at 90% B for 1:00 min and a final re-equilibration at initial conditions from 6:01–7:50 min. The mobile phase A consisted of methanol : ammonium acetate (0.5 M) (80 : 20 v/v) and mobile phase B was acetone : acetonitrile (70 : 30 v/v). Prior to injection, extracts were diluted (1 : 5) with 0.5 M ammonium acetate when necessary. Carotenoids and chlorophylls were detected with a diode-array detector, scanning absorbance spectra from 360 to 700 nm and monitoring at 450 nm

Biomaterials Science

ROYAL SOCIETY
OF CHEMISTRY

PAPER

View Article Online
View Journal

for optimal carotenoid detection. Probable pigment identification was achieved by comparing retention times and UV-vis spectral fine structures to pigment standards, DHI phytoplankton pigment Mix-115 and reference data sheets.[38]

2.3 Lipid extraction and fame analysis

The freeze-dried microalgal biomass of the 18 strains was extracted according to Ryckebosch et al.[39] with slight modifications. First, 400 µl of methanol was added to dried biomass (2–15 mg), followed with 200 µl of chloroform and 40 µl of deionised water. The sample was then vortexed and centrifuged (2000 rpm, 10 min). The supernatant was discarded and the bottom chloroform layer collected. The residual biomass in the tube was re-extracted using 200 µl of methanol and chloroform, vortexed and centrifuged again. The upper layer was collected and the extraction was carried out twice more on the residual biomass. The four lipid extract layers were then pooled together into a 15 ml tube and Na2SO4 salts added for dewatering. Upon further centrifugation, the solution was placed in a new tube and the sample was then evaporated to dryness under a nitrogen stream. The residue was then resuspended in 500 µl of chloroform : methanol (50 : 50) as final extract. Prior to analysis, 200 µl of sample was placed in a GC-MS vial fitted with a glass insert and supplemented with 50 µl of trimethylsulfonium hydroxide (TMSH) for transesterification. The samples were maintained for at least 1 hour at room temperature prior to analysis by GC-MS. The separation of fatty acid methyl esters (FAMEs) in the microalgal extracts was carried out using a BPX70 120 m column with an internal diameter of 0.25 mm on an Agilent7890A/5975C GC-MS system equipped with the MassHunter software. Samples were injected at a split ratio of 100 : 1 at an inlet temperature of 250 °C with the helium flow rate set at 2 ml min^{-1} (48.51 psi) and the transfer line at 280 °C. The oven gradient temperature was as follows: an initial hold at 50 °C for 2 min followed by 20 °C min^{-1} ramp to 160 °C for 0 min, a 4 °C min^{-1} ramp to 220 °C for 5 min and finally a 4 °C min^{-1} ramp to 240 °C for 12.5 min. The mass spectrometry conditions had a solvent delay of 10.5 minutes. Identifications were carried out by comparing retention times against standards of the Supelco® 37 Component FAME Mix and using the MS NIST 08 library.

2.4 Isolation and characterisation of microalgal EVs

2.4.1 Microalgal EV isolation. The microalgae cultures were centrifuged on day 30 at low speed (2000g) for 10 minutes to separate cells from the culture medium. Then, the isolation of EVs from the supernatant was performed by differential ultracentrifugation (dUC). Large EV nanoparticles (lEVs) were isolated in 50 ml Eppendorf polypropylene conical tubes at 10 000g for 30 minutes at 4 °C using an Eppendorf rotor F34-6-38. The resulting supernatant was then used to isolate small EVs (sEVs) that were collected into Beckman Coulter polypropylene open top tubes via centrifugation at 118 000g for 70 minutes at 4 °C using a Beckman SW28 rotor. After a PBS washing step, the pellet was re-suspended in PBS for subsequent analyses.

2.4.2 BCA assay and immunoblotting. The protein concentration of EV nanoparticles was measured using the BCA protein assay kit (Thermo Fisher Scientific, Rockford, IL, USA). This colorimetric method provides a relative concentration to a protein standard (bovine serum albumin, BSA), which is used for the preparation of a calibration curve. The relative absorbance of the BCA soluble compound was measured at 562 nm using a GloMax® Discover Microplate Reader. The signal rises linearly with protein concentration over a protein range of 20–2000 μg ml−1.

Proteins were resolved by sodium dodecyl-sulfate polyacrylamide gel electrophoresis (SDS-PAGE). 30 μg of cell lysate and EV samples (in PBS) were mixed with 5× loading buffer (0.25 M Tris-Cl pH 6.8, 10% SDS, 50% glycerol, 0.25 M dithiothreitol (DTT) and 0.25% bromophenol blue) at 100 °C for 5 min and loaded on 10% SDS-PAGE for electrophoretic analyses. Proteins were blotted onto polyvinylidene fluoride (PVDF) membranes. The membranes were blocked with BSA-TBS-T solution (3% powdered with bovine serum albumin in TBST (50 mM Tris HCl pH 8.0, 150 mM NaCl,0.05% Tween 20)) for 1 hour at room temperature, followed by primary antibody incubation overnight at 4 °C. We tested different antibodies and found that antibodies anti-Alix (clone 3A9, dil. 1 : 150 in 3% BSA/TBS-T1X), anti-Enolase (clone A5, dil. 1 : 400 in 3% BSA/TBS-T1X), anti-βActin (clone AC15, dil. 1 : 400 in 3% BSA/TBS-T1X) and anti-HSP70 (clone W27, dil. 1 : 500 in 5% milk/TBS-T1X) (Santa Cruz Biotechnology, USA), raised against different mammalian EV markers,[7] also showed cross-reactivity to microalgae and were used in the present study. After washing, membranes were incubated for 1 hour with secondary antibodies according to the manufacturer's instructions (horseradish peroxidase-conjugated secondary anti-mouse or anti-rabbit antibodies, cell signalling). Membranes were washed four times in TBST for 20 min. Immunoblots were revealed using SuperSignal™, Pierce™ ECL (Thermo Fisher Scientific). Densitometric analyses of protein bands in the immunoblot assays

Biomaterials Science

ROYAL SOCIETY
OF CHEMISTRY

PAPER

View Article Online
View Journal

were performed using the ImageJ software; biomarker optical densities (OD) were normalised against their equivalent band ODs measured in the positive control (C2C12 lysate).

2.4.3 Nanoparticle tracking analysis (NTA). Nanoparticle size distribution and concentration were measured using a NanoSight NS300 (Malvern Panalytical, UK). The instrument was equipped with a 488 nm laser, a high sensitivity sCMOS camera and a syringe pump. The EV particles were diluted in particle-free water to generate a dilution in which 20–120 particles per frame were tracked to obtain a concentration within the recommended measurement range (1–10×10^8 particles per ml). For each sample, 5 experiment videos of 60 seconds duration were analysed using NTA 3.4 Build 3.4.003 (camera level 15–16) with syringe pump speed 30. A total of 1500 frames were examined per sample, which were captured and analysed by applying instrument-optimised settings using a suitable detection threshold so that the observed particles are marked with a red cross and that no more than 5 blue crosses are seen. Further settings, such as blur size and Max Jump Distance were set to "automatic" and viscosity was set to water (0.841–0.844 cP).

2.4.4 Dynamic light scattering (DLS). Scattered light intensity and its time autocorrelation function g2(t) were measured simultaneously on different samples at 20 °C using a Brookhaven BI-9000 correlator (Brookhaven Instruments, Holtsville, NY, USA) equipped with a solid state laser tuned at 532 nm. The samples were diluted to a final total protein concentration ≤ 50 μg ml^{-1} for both sEVs and lEVs to avoid vesicle interaction and multiple scattering artefacts. Absolute values for scattered intensity (Rayleigh ratio) were obtained by normalisation to toluene, whose Rayeigh ratio at 532 nm was taken as 28×10^{-6} cm^{-1}. Absolute intensity values were used to estimate the total content in small and large EVs. The intensity-averaged size distribution, namely the distribution of hydrodynamic radii Dh, was derived by fitting the autocorrelation function with a multi-peaked Schultz distribution for the particle diffusion coefficients D and then using the classical Stokes–Einstein relation D = (kBT)/(3πηDh), where kB is the Boltzmann constant, T is the temperature and η is the solvent viscosity.[41]

2.4.5 Scanning electron microscopy (SEM). Samples were fixed in 0.4% paraformaldehyde and 2.5% glutaraldehyde in 300 mM PBS, at 4 °C. The pre-fixed samples were applied onto polycarbonate filters with pore-diameter of 0.05 μm (STERLITECH). The EV-containing filters were post-fixed in bath following the protocol of Lešer et al.[42] Briefly, the primary fixatives were removed by three steps of

washing with distilled water (10 min incubation in each step). Samples were then incubated for 1 hour in 2% OsO4. They were washed with distilled water (three washing steps with 10 min incubation time), treated with saturated water solution of thiocarbohydrazide (15 min incubation time), washed again (three washing steps in distilled water, 10 min incubation time each) and subjected to 2% OsO4 again for 1 hour. After the second incubation in OsO4, the unbound osmium was removed in another three steps of washing (in distilled water, 10 min incubation time each). The samples were dehydrated in graded series of ethanol (30–100%, 10 min incubation in each solution; absolute ethanol was replaced three times), followed by graded series of hexamethyldisilizane (mixed with absolute ethanol; 30%, 50% and 100%, 10 min in each solution) and finally air dried. The dried samples were Au/Pd coated (PECS Gatan 682) and examined using a JSM-6500F field emission scanning electron microscope (JEOL Ltd, Tokyo, Japan).

2.5 Decision grid for ranking strains according to their EV production potential

A decision matrix was compiled to identify the species best suited for EV production.[43,44] Each strain was given a score against a set number of selected criteria. A score of 0 or 1 was assigned for settling velocity based on the absence/presence of residual cells as determined by microscopy after low-speed centrifugation. The susceptibility to contamination was deemed more elevated for freshwater species (score = 1) than marine species (score = 2). Species with a sequenced genome (yes = 1, no = 0) were given extra weighting in the context of facilitating subsequent proteomic analyses. For biochemical analyses, EV protein concentration (assessed with the BCA assay) and number of particles (assessed by NTA) were given a score of 3 for protein concentration greater than 0.6 μg ml^{-1} and number of particles per ml greater than 10^8, a score of 2 for values less than 0.6 μg ml^{-1} and number of particles per ml between 10^7 and 10^8, a score of 1 for values equal to 0 μg ml^{-1} and equal or lower than 10^7 particles per ml. The matrix also included information derived from biophysical analyses: DLS signal quality (scores of 0 and 1 for low and good signals, respectively) and size distribution by DLS and NTA analyses (scores of 1, 2 and 3 for wide, medium and narrow distributions, respectively). For protein markers, densitometric analyses of protein bands in the immunoblot assays were performed using the ImageJ software; biomarker optical densities (OD) were normalised against their equivalent band ODs measured in the positive control (C2C12 cell lysate). Scores of 2, 1 and 0 were assigned

to each marker for OD ratios >1, <1 and = 0, respectively. Finally, strains were given scores of 3, 2 and 1 for good, medium and bad shapes and features as determined by SEM analysis (or score of 0 when not determined for samples with low EV yield and concentration). These criteria were also given differential weights (1 = low; 2 = medium; 3 = high impact) based on their relative importance in the decision process (ESI File 2‡). The tallies for all the criteria were then added to give each strain a final score.

2.6 Toxicity analyses on mammalian cell lines

2.6.1 Cell cultures. C2C12 cell line is a myoblast line established from normal adult mouse muscle. MDA-MB 231 cell line is an epithelial, human breast cancer cell line. Both cell lines were obtained from ATCC (ATCC-LGC, Wesel, Germany) and were maintained at 37 °C in a humidified atmosphere (5% CO2) in Dulbecco's modified Eagle's medium (DMEM) (Sigma-Aldrich, St Louis, MO, USA) containing 15% (v/v) fetal bovine serum (FBS) (Gibco, Life Technologies) plus 2 mM L-glutamine, 100 U ml^{-1} penicillin and 100 mg ml^{-1} streptomycin (Sigma-Aldrich) for the C2C12 cell line, and 10% (v/v) FBS plus 2 mM L-glutamine, 100 U ml^{-1} penicillin and 100 mg ml^{-1} streptomycin for the MDA-MB-231 cell line.

2.6.2 Cell viability assay. Tumoral (MDA-MB 231) and normal (C2C12) cell lines were seeded in 96-well plates at a density of 2×10^3 cells per well and maintained using suitable culture conditions. The assay was carried out with EVs isolated from *Cyanophora paradoxa*, which scored as one of the most promising strains in the screening analysis. Similar to other studies carried, the EVs were used at concentrations ranging 0.1 to 2.0 μg ml^{-1}.[45–47] Under our experimental conditions, this is equivalent to $\sim 10^4$–10^5 EVs per cell, the estimated number of vesicles considered necessary to cover the surface of a cell.[48] Thus, 24 hours after seeding, the cells were incubated for 24, 48 and 72 hours with *Cyanophora paradoxa*-derived EVs. The cells treated with PBS alone were used as control. Cell viability was evaluated using the CellTiter 96® AQueous one solution reagent (Promega) according to the manufacturer's instructions. The mean optical density (OD, absorbance) of four wells in the indicated groups was used to calculate the percentage of cell viability as follows: percentage of cell viability = (Atreatment − Ablank)/(Acontrol (untreated) − Ablank) × 100 (where, A = absorbance at 490 nm). Values were expressed as means ± SD of three biological samples, each performed in triplicate.

2.6.3 Genotoxicity assay. MDA MB 2311 cells were plated onto glass coverslips and grown in DMEM complete medium for 24 hours. Cells were then incubated with 2 μg ml^{-1} of Cyanophora paradoxa-derived EVs for 48 and 72 hours. Thereafter, the medium was removed and cells were washed twice with PBS and subsequently stained with Acridine orange/PBS solution (Sigma) at 100 μg ml^{-1} for 10 seconds at room temperature and quickly examined by epi-fluorescence microscopy (Leica, DFC450C). Acridine orange is a cell permeating nucleic acid binding dye that emits green fluorescence when bound to double-strand DNA and red fluorescence when bound to single-strand DNA or RNA. This staining technique allows discriminating between intact (green nuclei) and damaged DNA in cells (red nuclei).

2.7 Quality management system

We developed a quality management system (QMS) compatible with UNI EN ISO 9001:2015 standard to efficiently deal with the targeted innovation level of this work, its interdisciplinarity and the multi-site structure of the study. Our QMS supported all scientific activities inside the study, including the identification and sharing of best practice and standard operating procedures (SOPs) so as to increase the reliability and reproducibility of the results as well as the overall performance of the project. Customised lab notebooks and SOP models were developed, distributed and utilised among the participating laboratories. Quality assurance and quality control activties, including checklists, audit and review meetings were regularly performed to monitor the specific activities of partners and associated deliverables and outcomes.[49]

2.8 EV-track

We have submitted all relevant data of our experiments to the EV-TRACK knowledgebase (EV-TRACK ID: EV200076). [50]

3. Results

3.1 Pigment profiling and fame signature of microalgae

Prior to characterise the attributes of EVs isolated from the cultures, the chemical signatures of the microalgal biomass of each strain were first determined in terms of pigment and FAME contents. The pigment composition of the 18 strains selected were
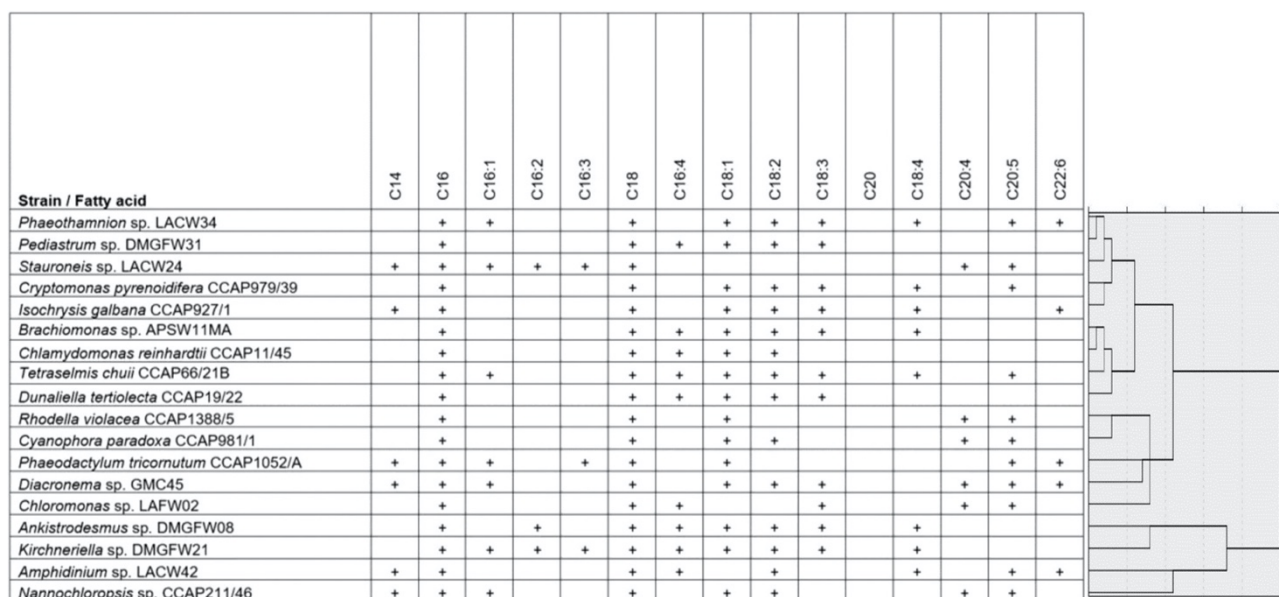
typical of their corresponding phytoplankton groups (Fig. 1). For example, similarities in pigment profiles were visible amongst the chlorophyte species or fucoxanthin-containing chromophytes. Promising contents in the high value xantophylls fucoxanthin, lutein and zeaxanthin were identified in strains *Phaeothamnion sp*. LACW34, *Ankistrodesmus sp*. DMGFW08 and *Cyanophora paradoxa* CCAP981/1, respectively. The carotenoid ß, ß carotene was also prominent in the strain *Tetraselmis chuii* CCAP66/21B. Cluster analysis of the strains based on pigment profile composition largely grouped them according to their evolutionary history with two main groups, one containing the stramenopiles and a second one with two sister clades of mostly chlorophytes. An example of chromatogram obtained for the Glaucophyte species *Cyanophora paradoxa* is provided in Fig. 2. The fatty acid methyl ester (FAME) signatures of the 18 microalgae strains were analysed by GC-MS (Fig. 3). The profiles were complex and showed amongst the strains sub- stantial variation in saturated and unsaturated fatty acids content. Interestingly, the high-value long chain PUFAs EPA (C20:5) and/or DHA (C22:6) were found in 12 strains. Of those, *Nannochloropsis sp*. CCAP211/46, *Amphidinium sp*. LACW42 and *Diacronema sp*. GMC45 showed higher contents in EPA and DHA. The clustering of the strains based on FAME compo- sition did not group them according to their overall phylogeny but rather on their relative content in fatty acids with *Ankistrodesmus sp*., *Kirchneriella sp*., *Nannochloropsis sp*. and *Amphidinium sp*. clustering together as the species with the highest yields. An example of FAME profile obtained for the Glaucophyte species *Cyanophora paradoxa* is provided in Fig. 4.
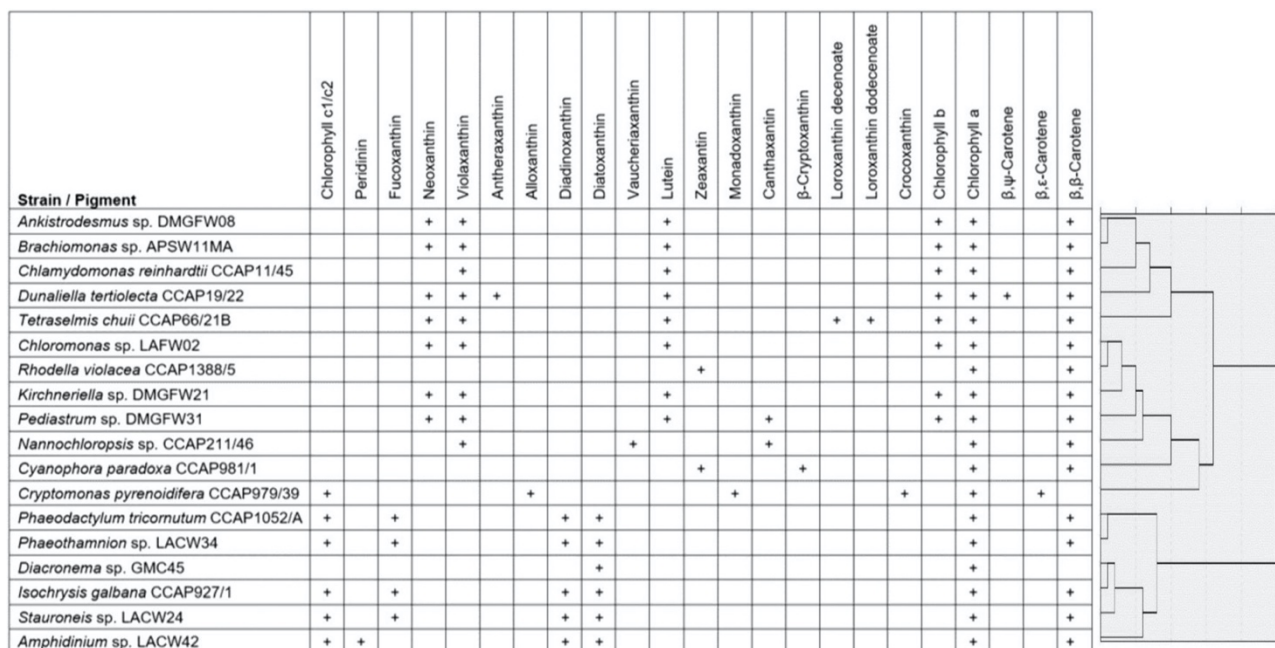
Fig. 1 HPLC-UV-DAD based pigment profiling in extracts of 18 microalgae strains. The right panel delineates groups of strains based on hierarchical clustering analysis (Ward's method and square Euclidean distance measure). Pigment presence is indicated by the '+' sign. The cluster analysis was carried out after column standardisation to return values comprised between 0 and 1.
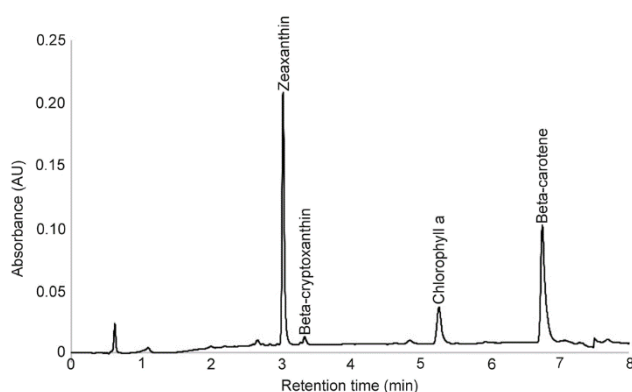
Fig. 2 HPLC-UV-DAD chromatogram obtained for an extract of the glaucophyte *Cyanophora paradoxa* CCAP981/1 indicating the main pigments detected.

| Strain / Fatty acid	C14	C16	C16:1	C16:2	C16:3	C18	C16:4	C18:1	C18:2	C18:3	C20	C18:4	C20:4	C20:5	C22:6
Phaeothamnion sp. LACW34		+	+			+		+	+	+		+		+	+
Pediastrum sp. DMGFW31		+					+	+	+	+					
Stauroneis sp. LACW24	+	+	+	+	+	+							+	+	
Cryptomonas pyrenoidifera CCAP979/39		+				+		+	+	+		+		+	
Isochrysis galbana CCAP927/1	+	+				+		+	+	+		+			+
Brachiomonas sp. APSW11MA		+					+	+	+	+		+			
Chlamydomonas reinhardtii CCAP11/45		+				+	+	+	+						
Tetraselmis chuii CCAP66/21B		+	+			+	+	+	+	+		+		+	
Dunaliella tertiolecta CCAP19/22		+				+	+	+	+	+					
Rhodella violacea CCAP1388/5		+				+		+					+	+	
Cyanophora paradoxa CCAP981/1		+				+		+					+	+	
Phaeodactylum tricornutum CCAP1052/A	+	+	+		+	+								+	+
Diacronema sp. GMC45	+	+	+			+		+	+	+			+	+	+
Chloromonas sp. LAFW02		+				+	+			+			+	+	
Ankistrodesmus sp. DMGFW08		+		+		+	+	+	+	+		+			
Kirchneriella sp. DMGFW21		+	+	+	+	+	+	+	+	+		+			
Amphidinium sp. LACW42	+	+				+	+		+			+		+	+
Nannochloropsis sp. CCAP211/46	+	+	+			+		+	+				+	+	

Fig. 3 GC/MS based FAME profiling in extracts of 18 microalgae strains. The right panel delineates groups of strains based on hierarchical clustering analysis (Ward's method and square Euclidean distance measure). Fatty acid presence is indicated by the '+' sign. The cluster analysis was carried out after column standardisation to return values comprised between 0 and 1.
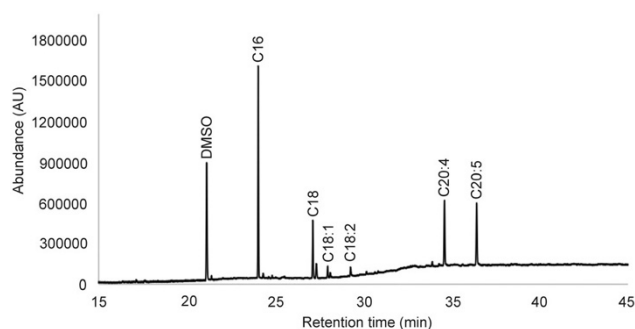

Fig. 4 GC/MS chromatogram obtained for an extract of the glaucophyte Cyanophora paradoxa CCAP981/1 indicating the fatty acids detected.

3.2 Microalgal EVs: purification and characterisation

After the removal of cells and cellular debris from the microalgae-conditioned media, the samples were processed using a well-established and standardised differential ultracentrifugation (dUC) protocol.[40,51] EV fractions were characterised following the recommendations of the International Society for Extracellular Vesicles known as MISEV guidelines.[7] The analyses focused on sEV enriched fractions. Specifically, dUC-isolated particles from each strain were biochemically and biophysically analysed

in two independent experiments. As such, total protein content and the expression of selected cellular and EV markers (Alix, Enolase, HSP70, and à-actin) cross-reacting with microalgal proteins were determined together with the number and size distribution of EV particles. The morphology of the sEVs was analysed by SEM. Negative control samples with no EVs were also prepared with the same SEM protocol and did not return major artefacts (ESI File 3‡). Far more nanoobjects were visible by SEM in the microalgae-derived sEV preparations with sizes and shapes aligned with what is expected of EV morphology. Results were used to prepare a microalgae-derived sEV identity card for each strain (ESI 4–9‡). Fig. 5 provides an example of identity card for the EV particles isolated from the glaucophyte *Cyanophora paradoxa*. BCA assay-based analysis of samples from this strain returned for the sEV fraction a yield of 1.45 ± 0.3 µg of total EV-protein per ml of microalgal conditioned media, corresponding to ~ 2 µg of proteins per mg of dry weight of microalgal biomass. The subsequent immunoblot analyses showed strong positive signals for Alix, enolase, HSP70 and à-actin proteins in the sEV fractions. Weaker signals were observed for the lEV preparations for all EV markers. The sEV preparations showed the highest Alix expression compared to both microalgal lysates and lEVs. Particle quantification in the samples by NTA showed a high concentration of extracellular nano-objects in the conditioned medium ($1.1 \times 10^9 \pm 3.8 \times 10^7$ sEV particles per ml in microalgal conditioned medium, corresponding to ~ 2×10^9 particles per mg of dry weight microalgal biomass). SEM analysis of the ultracentrifuge-processed sEV samples of the conditioned medium of *Cyanophora paradoxa* also revealed the presence of nano-objects with expected EV morphologies. The size distribution as determined by NTA of this particular fraction showed a main population of particles with a mode of 122.0 nm and average size of 170 ± 10 nm (polydispersity index: 0.25), which corroborated the DLS results (mode: 125 nm; average size: 180 ± 10 nm; polydispersity index: 0.30).
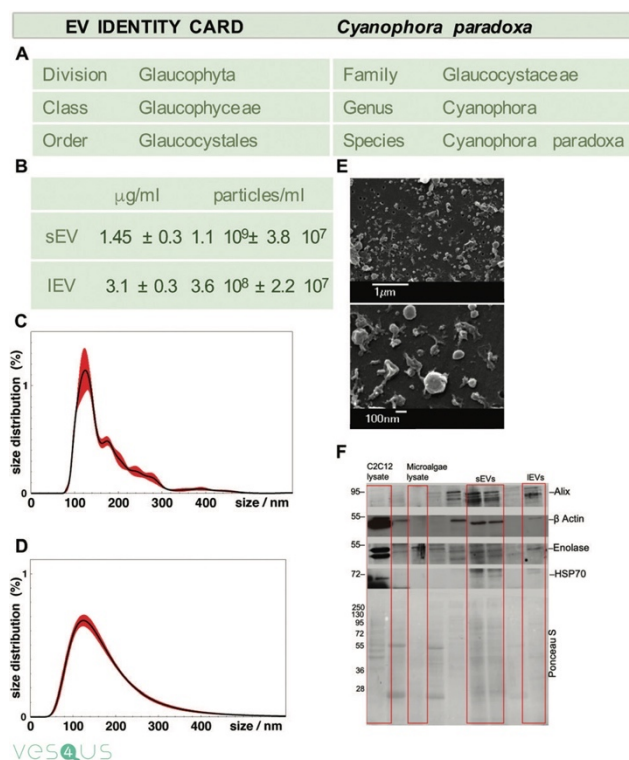
Fig. 5. Microalgal EV identity card: characterisation of extracellular nanoparticles isolated from *Cyanophora paradoxa* conditioned media. (A) Summary scheme on the taxonomy of *Cyanophora paradoxa*; (B) total protein quantification and number of particles of sEV and lEV fractions (data were calculated in triplicate cultures; results are presented by the average value ± standard deviation); (C) nanoparticle tracking analysis (NTA) of sEVs (the distribution error, in red, is calculated using 5 measurements of the same sample); (D) dynamic light scattering (DLS) analysis of sEVs (the distribution error, in red, is calculated using 3 measurements of 3 different samples); (E) representative images of SEM of the sEV fractions; (F) a representative immunoblot of a positive control (lysate of a mammalian cell line, C2C12), *Cyanophora paradoxa* lysate, sEV, and lEV fractions.

3.3 Identification of promising EV-producing microalgae strains

In order to select the most promising EV-producing microalgae strains, several properties related to the quality and quantity of the sEV population were considered to build a "performance" matrix for all the strains, including (i) the EV protein content, (ii) the expression of protein markers (e.g., Alix, Hsp70, enolase, ß-actin), (iii) the total scattering signal or the total particle number, as measured by DLS and NTA, respectively, and (iv) the sEV average size and size range. An initial statistical analysis was carried out by computing the correlation matrix of these variables for all the strains

(ESI File 10‡). The overall correlation between each pair of variables was always lower than 50%. In addition, a principal component analysis (PCA) highlighted a lack of correlation between each pair of variables measured over the observed samples with no distinct clustering of samples on the basis of the considered properties (data not shown). This confirmed the suitability of these variables as independent criteria for sample screening. As described in the methods, these EV attributes were hence considered along with other criteria to construct a matrix for the selection of the best EV-producing microalgae strains (ESI File 2‡). The sum of the weighted scores returned a final tally for each strain based on which the most promising ones could be identified (Table 1). *Cyanophora paradoxa* obtained the highest score of 31, followed by *Tetraselmis chuii*, *Amphidinium sp.* and *Rhodella violacea*. *Diacronema sp.*, *Dunaliella tertiolecta*, and *Phaeodactylum tricornutum* also returned high scores, but below 26. *Pediastrum sp.* and *Phaeothamnion sp.* returned the lowest score of 11.

Table 1 Ranking of the first seven EV-producing microalgal strains. Data refer to the sEVs isolated by dUC, starting from 50 ml of total culture volume

Rank	Species	Lineage	Score	µg sEV proteins per mg dry weight mass[a]	sEV particle numbers per mg dry weight mass[a]	Diameters (NTA mode)[a]
1	*Cyanophora paradoxa*	Glaucophyte	31	2.0 ± 0.2	$2.0 \times 10^9 \pm 3 \times 10^8$	130 ± 5
2	*Tetraselmis chuii*	Chlorophyte	28	0.4 ± 0.0	$2.6 \times 10^8 \pm 3 \times 10^7$	140 ± 5
3	*Amphidinium* sp.	Dinoflagellate	28	1.0 ± 0.1	$6.0 \times 10^8 \pm 2 \times 10^7$	120 ± 5
4	*Rhodella violacea*	Rhodophyte	28	0.4 ± 0.0	$8.0 \times 10^8 \pm 4 \times 10^7$	140 ± 5
5	*Diacronema* sp.	Haptophyte	25	0.3 ± 0.0	$1.0 \times 10^8 \pm 1 \times 10^7$	150 ± 10
6	*Dunaliella tertiolecta*	Chlorophyte	25	0.6 ± 0.0	$5.0 \times 10^9 \pm 9 \times 10^7$	160 ± 5
7	*Phaeodactylum tricornutum*	Diatom	25	0.2 ± 0.0	$2.4 \times 10^8 \pm 3 \times 10^7$	90 ± 5

[a] Technical replicates ($n = 6$).

3.4 Cellular response to *Cyanophora paradoxa*-derived EVs

After identifying *Cyanophora paradoxa* as the most promising strain, we tested the cytotoxicity and genotoxicity of sEVs obtained by this species using well-established assays on a mammalian normal cell line (myoblast C2C12 cell line) and a tumoral cell line (breast cancer MDA-MB 231 cell line). Cell viability was first assessed using the MTS assay (Fig. 6). sEVs derived from *Cyanophora paradoxa* did not show toxicity both on the tumorigenic MDA-MB 231 breast cancer and C2C12 myoblast cell lines, over time and at different concentrations (Fig. 6A and B, respectively). A slightly beneficial effect of sEVs at the higher dose tested was observed, mainly after 72 hours, for the C2C12 normal cell line (Fig. 6B). This may result from an experimental fluctuation or may correspond to cell viability enhancement by possibly bioactive metabolites in the microalgal sEVs used, making the future 49rganized49zation of the

cargo content of microalgal EVs an important task. Orange acridine staining was also carried out to evaluate the genotoxic effect of *Cyanophora paradoxa*-isolated sEVs (2 µg ml⁻1) on MDA-MB 231 cells incubated for 48 or 72 hours (Fig. 7b and b'). EV-treated MDA MB 231 cells showed mainly uniform bright green nuclei with 50rganized structures similar to the untreated controls (Fig. 7 a and a'), thereby excluding the presence of morphological nuclear changes associated with apoptotic events (Fig. 7b').
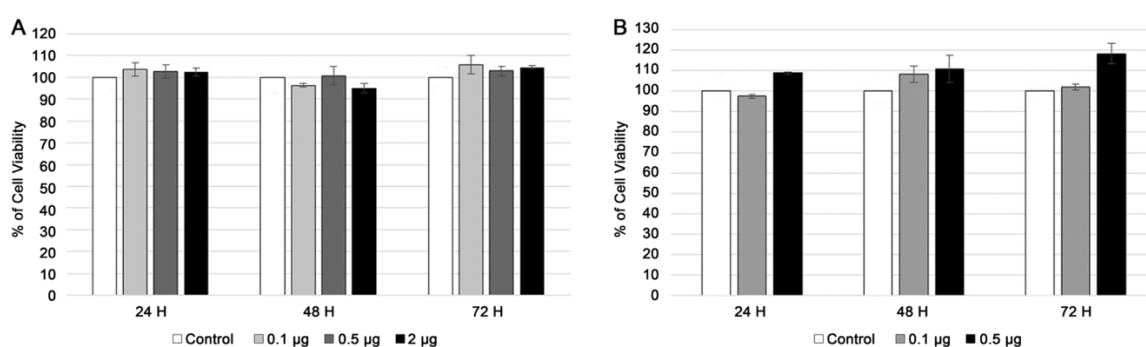

Fig. 6 Cytotoxicity of *Cyanophora paradoxa*-derived sEVs in (A) tumoral (MDA-MD 231 cell) and (B) normal mammalian cell lines (C2C12 cells), at different concentrations and for different timing of incubation (24, 48, and 72 hours). Values were expressed as means ± SD of three independent experiments.
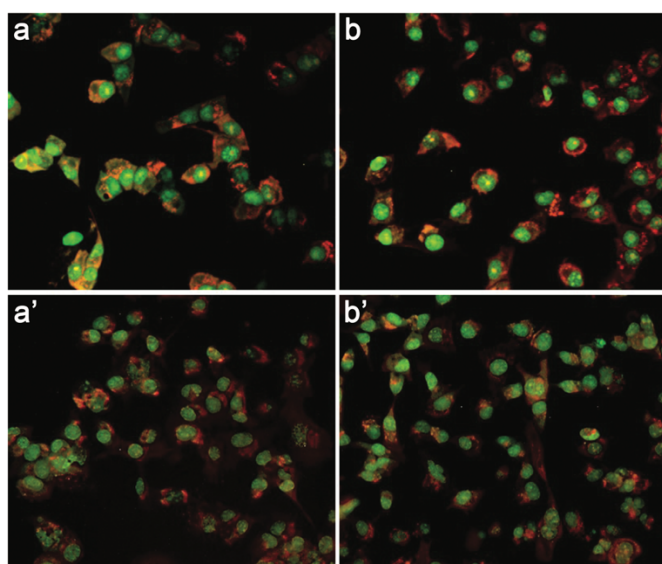
Fig. 7 Epi-fluorescence microscopy images of MDA-MB 231 cells treated with 2 µg ml⁻1 of *Cyanophora paradoxa*-derived sEVs (b and b') and untreated cells (control, a and a') for 48 (a and b) and 72 hours (a' and b'). Magnification 20×.

4. Discussion

Native and drug-loaded EVs obtained from mammalian cells (e.g., mesenchymal stem cells, MSCs) have been the focus of a rapidly growing research field known as "cell-free therapy".[52] As such, recent clinical trials evaluating MSC-derived EVs in different diseases (including diabetes, ischemic stroke, melanoma and lung cancer) have been ongoing, suggesting the feasibility and short-term safety of EV administration. [12, 53] Alternative cell sources, including bovine milk or bacteria derived EVs, have shown limited pharmaceutical acceptability because of their provenance.[54,55] In spite of the appreciable success of synthetic nanomaterials or EVs as drug delivery vehicles, technical challenges involving their large-scale, cost- effective production and intrinsic toxicity have limited to date their clinical and market translation[22]. In the present study, microalgae are proposed as novel and sustainable sources of EVs. Microalgae are polyphyletic unicellular organisms for which mechanisms of secretion of EVs are apparently known only in relation to primary and motile cilia/ flagella; for example, in the chlorophyte *Chlamydomonas reinhardtii*, extracellular particles, named ectosomes, are derived from the flagellar membrane and are involved in flagellar resorption [56, 57]. However, the isolation and description of EVs obtained from photosynthetic microalgal sources do not seem to have previously been reported with much detail. The capacity for microalgae to produce EVs is somehow curious; similar to plants, microalgae possess outside their plasma membrane a cell wall of varying thickness and chemical composition, which would have been expected to act as a physical barrier to the release of EVs. Yet, both plants and microalgae such as *Chlamydomonas sp*. appear able to do so. In addition, other major lineages of microalgae such as diatoms and dinoflagellates possess a silica frustule or a cell wall equipped with ornamental thecal plates, which might have made them less suitable as possible candidates for EV production. Yet, the present study still showed the presence of EVs in the culture medium of all the strains tested. The nanoparticles isolated from batch cultures of microalgae were characterised using biophysical and biochemical methods, showing attributes expected of sEVs as detailed in the literature in terms of morphology, size distribution protein content and immunoreactivity. [58] sEVs from the six best-scoring strains had size distributions with modes ranging 90–160 nm (Table 1). The information and data retrieved from the screening of the selected microalgae was summarised into EV identity cards for each strain considering some of the criteria listed in the MISEV 2018 guidelines for describing EVs.[7] Under the cultivation regime and conditions used in this study, the freshwater glaucophyte *Cyanophora paradoxa*, marine chlorophyte *Tetraselmis chuii*, marine dinoflagellate *Amphidinium s*p. and

rhodophyte *Rhodella violacea* returned the highest scores. These results represent a milestone in microalgal EV studies and exploitation, constituting the foundations for their future production and their potential use as tailor-made bio-products. Focusing on *Cyanophora paradoxa*, we reported here bio-chemical and biophysical results and carried out an evaluation of the biological activity of sEVs produced by this microalgae. Analysis of the sEV fraction isolated as a 100 000g pellet via a dUC based protocol returned a yield of ~ 2 µg of total sEV- protein (corresponding to $\sim 2 \times 10^9$ particles as per DLS and NTA measurements) per ml of microalgal conditioned media, or ~ 2 µg of proteins per mg of dry weight of microalgal biomass. These results are consistent with the estimate of 10^9 EV particles per µg-protein.[48] The subsequent immunoblot analyses showed strong positive signals for EV markers (e.g., Alix, enolase, HSP70 and ß-actin). Higher lEV protein yield (3 µg proteins per ml), smaller particle number (10^8 µg^{-1} of lEV proteins) and substantially weaker EV marker signals were observed for the lEV preparations (10 000g pellet of dUC protocol), suggesting the presence of contaminants in the lEV preparations. Focusing on ultracentrifuge-processed sEV samples, SEM analysis revealed the presence of nano-objects with expected EV morphologies together with other types of particles. Other methods of EV isolation such as gradient ultracentrifugation, size exclusion chromatography or tangential flow filtration may improve the purity and the homogeneity of preparations in future work. Nevertheless, the size distribution showed a main sEV population of particles with a mode of 130 ± 5 nm. These results obtained for *Cyanophora paradoxa* sEVs are in line with those obtained from plant-derived vesicles, which include both intra- and extra-cellular vesicles, as reported for citrus juice, in which EVs showed a smaller size but similar yield (2.5 µg ml^{-1} of lemon juice) [45]. This is also aligned with the yields of 4–24 µg ml^{-1} (or $4-16 \times 10^9$ ml^{-1}) of GMP-grade MSC-derived exosomes obtained from a 250 ml bioreactor.[59] Greater yield (451 µgr ml^{-1}, or 2×10^{13} ml^{-1}) were however retrieved from prolific exosome producing B16F10 tumor cells (from murine melanoma) cultured in a flask (CELLine AD1000 type, 72 ml).[60] Nevertheless, the apparent lack of toxicity of Cyanophora paradoxa sEVs on mammalian cells supports the long-term possibility of using microalgae as novel bio-resources for medium- to large-scale production of EVs for human-centered applications. The development of new therapies using functionalised microalgal EVs may be conceivable once their uptake by mammalian cells is confirmed. As a further step in this direction, we developed a QMS compatible with the UNI ISO9001:2015 standard and all the experiments were performed according to the agreed standard operating procedures

identified.[49] Microalgae constitute a rich reservoir of bioactive metabolites such as pigments and PUFAS that have already application in a variety of sectors.[61,62] The results of this study and the mechanisms underlying their ability to release EVs now allow exploiting the potential of these microalgal EVs as novel membranous bionanomaterials. Significantly, several species of microalgae have now obtained GRAS status (generally regarded as safe) and are increasingly being considered as health foods and ingredients in nutraceutical formulations.[63] The potential exploitation of microalgae as novel biofactories of EVs hinges on their natural and sustainable origins, making them probably more societally acceptable (and less risky in terms of bioethics) as EV sources for formulation preparations, especially when considering the medicinal and cosmetic sectors. The use of these protistean photosynthetic microorganisms as novel producers of EVs to be further functionalised as nanovehicles of bioactive chemicals has not been explored yet and appears promising. As such, biorefining pipelines could be designed on the one hand to isolate EVs from the microalgal cultivation medium and on the other hand to exploit the variety of high-value metabolites present in the residual biomass. Adapting the cultivation process from glass tubes to large reactors is not a trivial scale-up since additional growth parameters need consideration, in particular for semi- and continuous production systems.[25] However, given that microalgae can be grown in industrial contexts in thousands of litres volumes in closed photobioreactors,[23] the refining of large amounts of microalgal EVs and their post-harvest purification will make future pre-clinical trials largely feasible. The study of EVs is a rapidly expanding emerging field that still needs harmonisation with respect to the best practice approaches needed to isolate, purify, store and characterise such promising nano-biomaterials. Further investigations are now needed to acquire more in-depth biophysical and bio- chemical knowledge on microalgal EVs. Their potential bioactivity also needs to be further explored using a variety of in vivo and in vitro models together with the possibility of functionalising their membranes or loading them with bioactive molecules such as siRNA.

5. Conclusion

Extracellular nanoparticles were purified from batch cultures of several microalgae species and were characterised using bio-physical and biochemical methods, indicating attributes of small EVs (e.g., exosomes) as detailed in the literature from other biological sources. This is the first biophysical and bio- chemical description of such

membranous nanovesicles from photosynthetic microalgae. These results indicate that some strains are better suited for the isolation of EVs. Follow-on experiments will further assess their potential as new generation biogenic nanocarriers of bioactive molecules.

6. Conflicts of interest

There are no conflicts to declare.

7. Acknowledgements

8. References

1. G. Tiwari, R. Tiwari, B. Sriwastawa, L. Bhati, S. Pandey, P. Pandey and S. K. Bannerjee, Drug delivery systems: An updated review, Int. J. Pharm. Invest., 2012, 2, 2–11.

2. S. Busatto, A. Pham, A. Suh, S. Shapiro and J. Wolfram, Organotropic drug delivery: Synthetic nanoparticles and extracellular vesicles, Biomed. Microdevices, 2019, 21, 46.

3. E. Blanco, H. Shen and M. Ferrari, Principles of nano- particle design for overcoming biological barriers to drug delivery, Nat. Biotechnol., 2015, 33(9), 941–951.

4. S. F. Dowdy, Overcoming cellular barriers for RNA thera- peutics, Nat. Biotechnol., 2017, 35, 222–229.

5. S. A. Kooijmans, P. Vader, S. M. Van dommelen, W. W. Van solinge and R. M. Schi!elers, Exosome mimetics: a novel class of drug delivery systems, Int. J. Nanomed., 2012, 7, 1525–1541.

6. J. P. Armstrong, M. N. Holme and M. M. Stevens, Re- Engineering Extracellular Vesicles as Smart Nanoscale Therapeutics, ACS Nano, 2017, 11(1), 69–83.

7. C. Théry, K. W. Witwer, et al., Minimal information for studies of extracellular vesicles 2018 (MISEV2018): a position statement of the International Society for

Extracellular Vesicles and update of the MISEV2014 guidelines, J.Extracell. Vesicles, 2018, 7(1), 1535750.

8. M. Yáñez-Mó, P. R. Siljander, Z. Andreu, A. B. Zavec, F. E. Borràs, E. I. Buzas, K. Buzas, E. Casal, F. Cappello, J. Carvalho, E. Colás, A. Cordeiro-da Silva, S. Fais, J. M. Falcon-Perez, I. M. Ghobrial, B. Giebel, M. Gimona, M. Graner, I. Gursel, M. Gursel, N. H. Heegaard, A. Hendrix, P. Kierulf, K. Kokubun, M. Kosanovic, V. Kralj- Iglic, E. M. Krämer-Albers, S. Laitinen, C. Lässer, T. Lener, E. Ligeti, A. Lin , G. Lipps, A. Llorente, J. Lötvall, M. ManÊek-Keber, A. Marcilla, M. Mittelbrunn, I. Nazarenko, E. N. Nolte-'t Hoen, T. A. Nyman, L. O'Driscoll, M. Olivan, C. Oliveira, É. Pállinger, H. A. Del Portillo, J. Reventós, M. Rigau, E. Rohde, M. Sammar, F. Sánchez-Madrid, N. Santarém, K. Schallmoser, M. S. Ostenfeld, W. Stoorvogel, R. Stukelj, S. G. Van der Grein, M. H. Vasconcelos, M. H. Wauben and O. De Wever, Biologicalproperties of extracellular vesicles and their physiological functions, J.Extracell. Vesicles, 2015, 4, 27066.

9. A. Mrvar-Brecko, V. Sustar, V. Jansa, R. Stukelj, R. Jansa, E. Mujagi¬, P. Kruljc, A. Iglic, H. Hägerstrand and V. Kralj-Iglic, Isolated microvesicles from peripheral blood and body fluids as observed by scanning electron microscope,Blood Cells, Mol., Dis., 2010, 44(4), 307– 312.

10. S. Busatto, G. Vilanilam, T. Ticer, W. L. Lin, D. W. Dickson, S. Shapiro, P. Bergese and J. Wolfram, Tangential Flow Filtration for Highly E"cient Concentration of Extracellular Vesicles from Large Volumes of Fluid, Cells, 2018, 7(12),DOI: 10.3402/jev.v4.27066.

11. P. Vader, E. A. Mol, G. Pasterkamp and R. M. Schi!elers, Extracellular vesicles for drug delivery, Adv. Drug Delivery. Rev., 2016, 106(Pt A), 148–156.

12. R. Kalluri and V. S. LeBleu, The biology, function, and bio- medical applications of exosomes, Science, 2020,367(6478), DOI: 10.1126/science.aau6977.

13. F. Mantile, P. Franco, M. P. Stoppelli and G. L. Liguori, Biological role and clinical relevance of extracellular vesi- cles as key mediators of cell communication in cancer, in Advances in Biomembranes and Lipid Self-Assembly, AcademicPress, 2020, vol. 32, in press.

14. K. I. Mentkowski, J. D. Snitzer, S. Rusnak and J. K. Lang, Therapeutic Potential of Engineered Extracellular Vesicles,AAPS J., 2018, 20(3), 50.

15. A. Hoshino, B. Costa-Silva, T. L. Shen, G. Rodrigues, A. Hashimoto, M. T. Mark, H. Molina, S. Kohsaka, A. Di Giannatale, S. Ceder, S. Singh, C. Williams, N. Soplop, K. Uryu, L. Pharmer, T. King, L. Bojmar, A. E. Davies, Y. Ararso, T.

Zhang, H. Zhang, J. Hernandez, J. M. Weiss, V. D. Dumont-Cole, K. Kramer, L. H. Wexler, A. Narendran, G. K. Schwartz, J. H. Healey, P. Sandstrom, K. J. Labori, E. H. Kure, P. M. Grandgenett, M. A. Hollingsworth, M. de Sousa, S. Kaur, M. Jain, K. Mallya, S. K. Batra, W. R. Jarnagin, M. S. Brady, O. Fodstad, V. Muller, K. Pantel, A. J. Minn, M. J. Bissell, B. A. Garcia, Y. Kang, V. K. Rajasekhar, C. M. Ghajar, I. Matei, H. Peinado, J. Bromberg and D. Lyden, Tumour exosome integrinsdetermine organotropic metastasis, Nature, 2015, 527(7578), 329–335.

16. D. E. Murphy, O. G. de Jong, M. Brouwer, M. J. Wood, G. Lavieu, R. M. Schi!elers and P. Vader, Extracellular vesiclebased therapeutics: natural versus engineered targeting and tra"cking, Exp. Mol. Med., 2019, 51, 1–12.

17. M. Muraca, L. Putignani, A. Fierabracci, A. Teti and G. Perilongo, Gut microbiotaderived outer membrane vesi- cles:under-recognized major players in health and disease?, Discovery Med., 2015, 19(106), 343–348.

18. G. Sukhvinder, R. Catchpole and P. Forterre, Extracellular membrane vesicles in the three domains of life andbeyond, FEMS Microbiol. Rev., 2019, 43(3), 273–303.

19. R. P. Soares, P. Xander, A. O. Costa, A. Marcilla, A. Menezes-Neto, H. Del Portillo, K. Witwer, M. Wauben, E. Nolte-'t Hoen, M. Olivier, M. F. Criado, L. L. P. da Silva, M. M. Abdel Baqui, S. Schenkman, W. Colli, M. J. M. Alves, K. S. Ferreira, R. Puccia, P. Nejsum, K. Riesbeck, A. Stensballe, E. P. Hansen, L. M. Jaular, R. Øvstebø, L. de la Canal, P. Bergese, V. Pereira-Chioccola, M. W. Pfa#, J. Fritz, Y. S. Gho and A. C. Torrecilhas, Highlights of the São Paulo ISEV workshop onextracellular vesicles in cross- kingdom communication, J. Extracell. Vesicles, 2017, 6(1), 1407213.

20. M. R. Bleackley, M. Samuel, D. Garcia-Ceron, J. A. McKenna, R. G. T. Lowe, M. Pathan, K. Zhao, C. S. Ang, S. Mathivanan and M. A. Anderson, Extracellular Vesicles From the Cotton Pathogen Fusarium oxysporum f. sp. vasinfectum Inducea Phytotoxic Response in Plants, Front. Plant Sci., 2020, 10, 1610.

21. Q. Cai, L. Qiao, M. Wang, B. He, F. Lin, J. Palmquist, S. Huang and H. Jin, Plants send small RNAs in extracellu- larvesicles to fungal pathogen to silence virulence genes, Science, 2018, 360(6393), 1126–1129.

22. C. Paganini, U. C. Palmiero, G. Pocsfalvi, N. Touzet, A. Bongiovanni and P. Arosio, Scalable Production and Isolation of Extracellular Vesicles: Available Sources and Lessons from Current Industrial Bioprocesses, Biotechnol. J., 2019,14(10), DOI: 10.1002/biot.201800528.

23. S. Leu and S. Boussiba, Advances in the production of high-value products by microalgae, Ind. Biotechnol., 2014, 10,169–183.

24. S. P. Cuellar-Bermudez, I. Aguilar-Hernandez, D. L. Cardenas-Chavez, N. Ornelas-Soto, M. A. Romero- Ogawa and R. Parra-Saldivar, Extraction and purification of high-value metabolites from microalgae: essential lipids, astaxanthinand phycobiliproteins, Microb. Biotechnol., 2015, 8, 190–209.

25. L. Zhu, Biorefinery as a promising approach to promote microalgae industry: an innovative framework, Renewable Sustainable Energy Rev., 2015, 41, 1376– 1384.

26. H. Pereira, K. N. Gangadhar, P. S. C. Schulze, T. Santos, C. B. de Sousa, L. M. Schueler, L. Custódio, F. X. Malcata, L. Gouveia, J. C. S. Varela and L. Barreira, Isolation of a eur- yhaline microalgal strain, Tetraselmis sp. CTP4, as a robustfeedstock for biodiesel production, Sci. Rep., 2016, 6(1), 35663.

27. P. K. Sarker, A. R. Kapuscinski, A. J. Lanois, E. D. Livesey, K. P. Bernhard and M. L. Coley, Towards sustainable aqua- feeds: Complete substitution of fish oil with marine micro- alga Schizochytrium sp. improves growth and fatty aciddeposition in juvenile Nile tilapia (Oreochromis niloticus), PLoS One, 2016, 11(6), 156684.

28. S. M. Arad and A. Yaron, Natural pigments from red micro- algae for use in foods and cosmetics, Trends Food Sci.Technol., 1992, 3, 92–97.

29. C. Juin, V. Thiéry, J. P. Cadoret and L. Picot, Towards the clinical use of phytoplankton carotenoid pigments to cure cancer, Oceanography, 2013, 1, DOI: 10.4172/2332- 2632.1000e105.

30. B.G.Ryu,K.Kim,J.Kim,J.I.HanandJ.W.Yang,Useof organic waste from the brewery industry for high-density cultivation of the docosahexaenoic acid-rich microalga, Aurantiochytrium sp. KRS101, Bioresour. Technol., 2013, 129, 351– 359.

31. C. Falaise, C. Francois, M. A. Travers, B. Morga, J. Haure, R. Tremblay, F. Turcotte, P. Pasetto, R. Gastineau, Y. Hardivillier, V. Leignel and J. L. Mouget, Antimicrobial Compounds from Eukaryotic Microalgae against Human Pathogens and Diseases in Aquaculture, Mar. Drugs, 2016, 159, DOI: 10.3390/md14090159.

32. B. da Silva Vaz, J. B. Moreira, M. G. de Morais and J. A. V. Costa, Microalgae as a new source of bioactive com- pounds in food supplements, Curr. Opin. Food Sci., 2016, 7, 73–77.

33. P. Guesnet and J. M. Alessandri, Docosahexaenoic acid (DHA) and the developing central nervous system (CNS) e Implications for dietary recommendations, Biochimie, 2011, 93, 7–12.

34. C. Lauritano, J. H. Andersen, E. Hansen, M. Albrigtsen, L. Escalera, F. Esposito, K. Helland, K.Ø. Hanssen, G. Romano and A. Ianora, Bioactivity screening of micro- algae for antioxidant, anti-inflammatory, anticancer, anti- diabetes and antibacterial activities, Front. Mar. Sci., 2016, 3, 1–12.

35. Z. Sun, X. Wang and J. Liu, Screening of Isochrysis strains for simultaneous production of docosahexaenoic acid and fucox- anthin, Algal Research, Elsevier B.V., 2019, p. 41.

36. R. R. L. Guillard, Culture of Phytoplankton for Feeding Marine Invertebrates, Culture of Marine Invertebrate Animals, Springer US, Boston, MA, 1975, pp. 29–60.

37. D. Mc Gee, L. Archer, A. Paskuliakova, G. McCoy, G. Fleming, E. Gillespie and N. Touzet, Rapid chemotaxo- nomic profiling for the identification of high-value caroten- oids in microalgae, J. Appl. Phycol., 2018, 30, 385–399

38. E. S. Egeland, J. L. Garrido, L. Clementson, K. Andersen, C. S. Thomas, M. Zapata, R. Airs, C. A. Llewellyn, G. L. Newman, F. Rodriguez and S. Roy, Part VII Data sheets aiding identification of phytoplankton carotenoids and chlorophylls, in Phytoplankton pigments: characteriz- ation, chemotaxonomy and applications in oceanography, ed. S. Roy, C. A. Llewellyn, E. S. Egeland and G. Johnson, Cambridge University Press, Cambridge, 2011, pp. 665–822.

39. E. Ryckebosch, K. Muylaert and I. Foubert, Optimization of an Analytical Procedure for Extraction of Lipids from Microalgae, J. Am. Oil Chem. Soc., 2012, 89, 189–198.

40. D. P. Romancino, G. Paterniti, Y. Campos, A. De Luca, V. Di Felice, A. d'Azzo and A. Bongiovanni, Identification and characterization of the nano-sized vesicles released by muscle cells, FEBS Lett., 2013, 587, 1379–1384.

41. D. Romancino, V. Bu!a, S. Caruso, I. Ferrara, S. Raccosta, A. Notaro, Y. Campos, R. Noto, V. Martorana, A. Cupane, A. Giallongo, A. d'Azzo, M. Manno and A. Bongiovanni, Palmitoylation is a post-translational modification of Alix regulating the membrane organization of exosome-like small extracellular vesicles, Biochim. Biophys. Acta, Gen. Subj., 2018, 1862, 2879–2887.

42. V. LeÊer, D. Drobne, Ê. Pipan, M. Milani and F. Tatti, Comparison of di!erent preparation methods of biological samples for FIB milling and SEM investigation, J. Microsc., 2009, 233, 309–319.

43. A. Bongiovanni, G. Colotti, G. L. Liguori, M. Di Carlo, F. A. Digilio, G. Lacerra, A. Mascia, A. M. Cirafici, A. Barra, A. Lanati and A. Kisslinger, Applying quality and project management methodologies in biomedical research lab- oratories: a public network's case study, Accredit. Qual. Assur., 2015, 20, 203–213.

44. F. A. Digilio, A. Lanati, A. Bongiovanni, A. Mascia, M. Di Carlo, A. Barra, A. M. Cirafici, G. Colotti, A. Kisslinger, G. Lacerra and G. L. Liguori, Quality-based model for life sciences research guidelines, Accredit. Qual. Assur., 2016, 21, 221–230.

45. S. Raimondo, F. Naselli, S. Fontana, F. Monteleone, A. Lo Dico, L. Saieva, G. Zito, A. Flugy, M. Manno, M. A. Di Bella, G. De Leo and R. Alessandro, Citrus limon-derived nano- vesicles inhibit cancer cell proliferation and suppress CML xenograft growth by inducing TRAIL-mediated cell death, Oncotarget, 2015, 6, 19514–19527.

46. H. Kim, D. Choi, S. J. Yun, S. Choi, J. W. Kang, J. W. Jung, D. Hwang, K. P. Kim and D. W. Kim, Proteomic analysis of microvesicles derived from human mesenchymal stem cells, J. Proteome Res., 2012, 11(2), 839–849.

47. S. Busatto, A. Giacomini, C. Montis, R. Ronca and P. Bergese, Uptake Profiles of Human Serum Exosomes by Murine and Human Tumor Cells through Combined Use of Colloidal Nanoplasmonics and Flow Cytofluorimetric Analysis, Anal. Chem., 2018, 90(13), 7855–7861, DOI: 10.1021/acs.analchem.7b04374.

48. E. D. Sverdlov, Amedeo Avogadro's cry: What is 1 µg of exosomes?, Bioessays, 2012, 34, 873–875.

49. G. Liguori and A. Kisslinger, Standardization and reproducibility in EV research: the support of a Quality manage- ment system. Biological membrane vesicles: scientific, bio- technological and clinical considerations, Adv.Biomembr. Lipid Self-Assem., 2020, DOI: 10.1016/bs.abl.2020.05.005, ISSN: 2451-9634.

50. J. Van Deun, P. Mestdagh, P. Agostinis, Ö. Akay, S. Anand, J. Anckaert, Z. A. Martinez, T. Baetens, E. Beghein, L. Bertier, G. Berx, J. Boere, S. Boukouris, M. Bremer, D. Buschmann, J. B. Byrd, C. Casert, L. Cheng, A. Cmoch, D. Daveloose, E. De Smedt, S. Demirsoy, V. Depoorter, B. Dhondt, T. A. Driedonks, A. Dudek, A. Elsharawy, I. Floris, A. D. Foers, K. Gärtner, A. D. Garg, E. Geeurickx, J. Gettemans, F. Ghazavi, B. Giebel, T. G. Kormelink, G. Hancock, H. Helsmoortel,

A. F. Hill, V. Hyenne, H. Kalra, D. Kim, J. Kowal, S. Kraemer, P. Leidinger, C. Leonelli, Y. Liang, L. Lippens, S. Liu, A. Lo Cicero, S. Martin, S. Mathivanan, P. Mathiyalagan, T. Matusek, G. Milani, M. Monguió-Tortajada, L. M. Mus, D. C. Muth, A. Németh, E. N. Nolte-'t Hoen, L. O'Driscoll, R. Palmulli, M. W. Pfa#, B. Primdal-Bengtson, E. Romano, Q. Rousseau, S. Sahoo, N. Sampaio, M. Samuel, B. Scicluna, B. Soen, A. Steels, J. V. Swinnen, M. Takatalo, S. Thaminy, C. Théry, J. Tulkens, I. Van Audenhove, S. van der Grein, A. Van Goethem, M. J. van Herwijnen, G. Van Niel, N. Van Roy, A. R. Van Vliet, N. Vandamme, S. Vanhauwaert, G. Vergauwen, F. Verweij, A. Wallaert, M. Wauben, K. W. Witwer, M. I. Zonneveld, O. De Wever, J. Vandesompele and A. Hendrix, EV-TRACK: transparent reporting and centralizing knowledge in extracellular vesicle research, Nat. Methods, 2017, 14, 228–232.

51. C. Théry, S. Amigorena, G. Raposo and A. Clayton, Isolation and Characterization of Exosomes from Cell Culture Supernatants and Biological Fluids, Curr. Protoc. Cell Biol., 2006, 30, 3.22.1–3.22.29.

52. S. Samanta, S. Rajasingh, N. Drosos, Z. Zhou, B. Dawn and J. Rajasingh, Exosomes: new molecular targets of diseases, Acta Pharmacol. Sin., 2018, 39, 501–513.

53. T. Lener, M. Gimona, L. Aigner, V. et al., Applying extracellular vesicles based therapeutics in clinical trials - an ISEV posi- tion paper, J. Extracell. Vesicles, 2015, 4, 30087.

54. O. P. Wiklander, J. Z. Nordin, A. O'Loughlin, Y. Gustafsson, G. Corso, I. Mäger, P. Vader, Y. Lee, H. Sork, Y. Seow, N. Heldring, L. Alvarez-Erviti, C. I. Smith, K. Le Blanc, P. Macchiarini, P. Jungebluth, M. J. Wood and S. E. Andaloussi, Extracellular vesicle in vivo biodistribu- tion is determined by cell source, route of administration and targeting, J. Extracell. Vesicles, 2015, 4, 26316.

55. G. Carobolante, J. Mantaj, E. Ferrari and D. Vllasaliu, Cow Milk and Intestinal Epithelial Cell-derived Extracellular Vesicles as Systems for Enhancing Oral Drug Delivery, Pharmaceutics, 2020, 12(3), 226.

56. C. R. Wood and J. L. Rosenbaum, Ciliary ectosomes: trans- missions from the cell's antenna, Trends Cell Biol., 2015, 25(5), 276–285.

57. J. Wang and M. M. Barr, Ciliary extracellular vesicles: Txt Msg organelles, Cell. Mol. Neurobiol., 2016, 36, 449–457.

58. A. E. Russell, A. Sneider, K. W. Witwer, P. Bergese, S. N. Bhattacharyya, A. Cocks, E. Cocucci, U. Erdbrügger, J. M. Falcon-Perez, D. W. Freeman, T. M.

Gallagher, S. Hu, Y. Huang, S. M. Jay, S. I. Kano, G. Lavieu, A. Leszczynska, A. M. Llorente, Q. Lu, V. Mahairaki, D. C. Muth, N. Noren Hooten, M. Ostrowski, I. Prada, S. Sahoo, T. H. Schøyen, L. Sheng, D. Tesch, G. Van Niel, R. E. Vandenbroucke, F. J. Verweij, A. V. Villar, M. Wauben, A. M. Wehman, H. Yin, D. R. F. Carter and P. Vader, Biological membranes in EV biogenesis, stability, uptake, and cargo transfer: an ISEV position paperarising from the ISEV membranes and EVs workshop, J. Extracell. Vesicles, 2019, 8(1), 1684862.

59. M. Mendt, S. Kamerkar, H. Sugimoto, K. M. McAndrews, C. C. Wu, M. Gagea, S. Yang, E. V. Rodriges Blanko, Q. Peng, X. Ma, J. R. Marszalek, A. Maitra, C. Yee, K. Rezvani, E. Shpall, V. S. LeBleu and R. Kalluri, Generation and testing of clinical-grade exosomes for pan- creatic cancer, JCI Insight, 2018, 3, e99263.

60. F. N. Faruqu, J. T. Wang, L. Xu, L. McNickle, E. M. Y. Chong, A. Walters, M. Gurney, A. Clayton, L. A. Smyth, R. Hider, J. Sosabowski and K. T. Al-Jamal, Membrane Radiolabelling of Exosomes for Comparative Biodistribution Analysis in Immunocompetent and Immunodeficient Mice - A Novel and Universal Approach, Theranostics, 2019, 9, 1666-1682.

61. M. G. De morais, S. Vaz Bda, E. G. De morais and J. A. Costa, Biologically Active Metabolites Synthesized by Microalgae, BioMed Res. Int., 2015, 835761.

62. R. Sathasivam, R. Radhakrishnan, A. Hashem and E. F. Abd allah, Microalgae metabolites: A rich source for food and medicine, Saudi J. Biol. Sci., 2019, 26(4), 709– 722

63. J. Matos, C. Cardoso, N. M. Bandarra and C. Afonso, Microalgae as healthy ingredients for functional food: a review, Food Funct., 2017, 8(8), 2672–2685.

ISEV

Chapter 4

Nanoalgosomes: Introducing extracellular vesicles produced by microalgae

Correspondence

Mauro Manno, Institute of Biophysics (IBF) - National Research Council of Italy (CNR), Palermo, Italy.
Email: mauro.manno@cnr.it

Antonella Bongiovanni, Institute for Research and Biomedical Innovation (IRIB) - National Research Council of Italy (CNR), Palermo, Italy.
Email: antonella.bongiovanni@cnr.it

Giorgia Adamo, David Fierli, Daniele P. Romancino, Sabrina Picciotto, Maria E. Barone, Anita Aranyos, Darja Božič, Svenja Morsbach, Samuele Raccosta, Christopher Stanly and Carolina Paganini are first authors and they contributed equally to this study.

Mauro Manno and Antonella Bongiovanni are last authors and they contributed equally to this study.

All the listed Authors are members of the VES4US consortium (H2020 grant agreement #801338).

Adamo G, Fierli D, Romancino DP, **Picciotto S,** Barone ME, Aranyos A, Božič D, Morsbach S, Raccosta S, Stanly C, Paganini C, Gai M, Cusimano A, Martorana V, Noto R, Carrotta R, Librizzi F, Randazzo L, Parkes R, Capasso Palmiero U, Rao E, Paterna A, Santonicola P, Iglič A, Corcuera L, Kisslinger A, Di Schiavi E, Liguori GL, Landfester K, Kralj-Iglič V, Arosio P, Pocsfalvi G, Touzet N, Manno M, Bongiovanni A. J Extracell Vesicles. 2021 Apr;10(6):e12081. doi: 10.1002/jev2.12081. Epub 2021 Apr 27. PMID: 33936568; PMCID: PMC8077145.

RESEARCH ARTICLE

ISEV

Abstract

Cellular, inter-organismal and cross kingdom communication via extracellular vesicles (EVs) is intensively studied in basic science with high expectation for a large variety of bio-technological applications. EVs intrinsically possess many attributes of a drug delivery vehicle. Beyond the implications for basic cell biology, academic and industrial interests in EVs have increased in the last few years. Microalgae constitute sustainable and renewable sources of bioactive compounds with a range of sectoral applications, including the formulation of health supplements, cosmetic products and food ingredients. Here we describe a newly discovered subtype of EVs derived from microalgae, which we named nanoalgosomes. We isolated these extracellular nano-objects from cultures of microalgal strains, including the marine photosynthetic chlorophyte *Tetraselmis chuii*, using differential ultracentrifugation or tangential flow fractionation and focusing on the nanosized small EVs (sEVs). We explore different biochemical and physical properties and we show that nanoalgosomes are efficiently taken up by mammalian cell lines, confirming the cross kingdom communication potential of EVs. This is the first detailed description of such membranous nanovesicles from microalgae. With respect to EVs isolated from other organisms, nanoalgosomes present several advantages in that microalgae are a renewable and sustainable natural source, which could easily be scalable in terms of nanoalgosome production.

ISEV

1 Introduction

Cells communicate with each other and respond to a variety of stimuli by releasing membrane-enclosed vesicles, which are found in extracellular fluids (Yáñez-Mó et al., 2015). Several types of cell-derived vesicles are commonly distinguished according to their formation mechanism and size. Extracellular vesicles (EVs) have recently emerged as important entities used by cells to mediate several physiological processes or affect various pathological conditions associated with the activation of an immune response or the spread of cancer and virus infections (Dhondt et al., 2020; Maacha et al., 2019; Urbanelli et al., 2019). EVs constitute also cross-species communication means and have been found in all kingdoms of life (Bleackley et al., 2020; Cai et al., 2018; Gill et al., 2019; Muraca et al., 2015; Soares et al., 2017). Beside mammalian cells, there are various sources available to produce EVs, including bacteria, bovine milk and plants, and indeed several have been studied for therapeutic applications (Bitto & Kaparakis-Liaskos, 2017; Gerritzen et al., 2017; Kim et al., 2015; Munagala et al., 2016; Paganini et al., 2019; Pocsfalvi et al., 2018; Raimondo et al., 2015; Wang et al., 2013). The exploitation of the biotechnological potential of EVs as carriers of bioactive compounds for different theranostic applications is of increasing interest. The growth of this field is evident from the surge in recent years in the number of publications, patents, companies, and clinical trials related to EVs (Kosaka et al., 2019; Shaimardanova et al., 2020; Zipkin, 2019). As such, in the context of better harmonizing research efforts also aimed at valorising the potential of EVs, Théry and Witwer et al. (2018) recently revised the required parameters for the robust description of EVs (Théry et al., 2018). Microalgae are microorganisms constituting a rich reservoir of bioactive metabolites such as pigments, polyunsaturated fatty acids, antioxidants or antimicrobial compounds, which are being increasingly exploited in commercial ventures (Cuellar-Bermudez et al., 2015; Friedl et al., 2021; Khan et al., 2018; Leu & Boussiba, 2014; Zhu, 2015). Microalgae are also heralded as promising feedstock in the context of the bio-based economy and the better valorisation of natural and renewable bioresources for the production of biofuels, animal feeds and other valuable commodities. This polyphyletic group of microorganisms shows high genetic diversity and has colonised many habitats due to the unique metabolic attributes that some species possess (Friedl et al., 2021). Many microalgae species are suitable for growth in industrial scale photobioreactors under controlled cultivation conditions and are seen as highly productive crops when compared with terrestrial plants (Khan et al., 2018). In the context of the H2020-FETOpen project VES4US (www.ves4us.eu) here

RESEARCH ARTICLE

we propose microalgae as potential bioresources for the production of EVs with applications for the nanomedicine, cosmetics or nutraceutics sectors. In this study, we considered the guidelines of MISEV 2018 and the well-established knowledge in the EV research field (EV-TRACK) (Théry et al., 2018; Van Deun et al., 2017) to define a new generation of microalgal EV-based nanoproducts, using different methodologies and specific approaches for EV bio-refinement, separation and characterisation. Our check-list (developed from MISEV guidelines and applied in the framework of the VES4US project) includes the identification of methods for the microalgal-derived EV separation, enrichment and characterization (including EV quantification, EV identity in terms of protein composition, size, morphology, topology, EV stability, EV quality in terms of purity and density and EV bioactivity), as well as protocols for microalgae cultivation and quantification (Table 1). This list is also reported as supporting information with more details (Supporting Table 1), with the purpose to highlight and list the different items we addressed within MISEV 2018. Since the microalgal EVs have to our best knowledge never been described in detail, in accordance with the MISEV 2018 recommendation, we decided to use its suggested nomenclature. Indeed, we refer to the small extracellular particles separated either by differential ultracentrifugation or tangential flow fractionated. The term "nanoalgosome" is here then introduced to describe such microalgal small EVs (sEVs) isolated from the marine photosynthetic microalgal chlorophyte *Tetraselmis chuii*, which is surrounded by a membrane, contains EV biomarkers and has a typical EV size distribution and density (Théry et al., 2006, 2018). *Tetraselmis chuii* is a chlorophyceaen photosynthetic marine microalgae possessing an array of bioactive pigments and essential fatty acids (Pereira et al., 2019), which contribute to making it a promising source of EVs. The production of nanoalgosomes is an evolutionarily conserved trait within the microalgae strain as demonstrated by similar results obtained using the sEVs isolated from batch cultures of other microalgae species, including another chlorophyte strain, the *Dunaliella tertiolecta*, and the dinoflagellate strain *Amphidinium sp.* A drawback limiting progress in current EV research has been the typically low EV yields obtained for subsequent clinical trials, making the roll out of EV-based treatments for humans still some distance away (György et al., 2015; Paganini et al., 2019). In this context, we envision that microalgae such as *Tetraselmis chuii* can offer a remarkable opportunity to overcome this limitation thanks to their scalable EV production and increased EV yield.

RESEARCH ARTICLE

ISEV

TABLE 1   MISEV inspired checklist of minimal information for studies of nanoalgosomes

1. Source features	(a) Microalgal strain, cultivation protocol, and biomass weight
	(b) Pigment and lipid profiling
2. EV Purification/Enrichment	(a) Differential Ultra Centrifugation (dUC)
	(b) Tangential Flow Filtration (TFF)
	(c) gradient Ultra Centrifugation (gUC)
3. EV quantification	(a) Nanoparticle number (by Nanoparticle Tracking Analysis, NTA)
	(b) Amount of protein (by BCA colorimetric assay)
4. EV identity (size)	(a) Multi angle dynamic light scattering (Multi angle DLS)
	(b) Nanoparticle tracking analysis (NTA)
	(c) Fluorescence nanoparticle tracking analysis (F-NTA)
	(d) Fluorescence correlation spectroscopy (FCS)
5. EV identity (morphology, shape and membrane presence and structure)	(a) Scanning electron microscopy (SEM)
	(b) Atomic force microscopy (AFM)
	(c) Cryogenic transmission electron microscopy (cryo-TEM)
	(d) Static light scattering (SLS)
	(e) Fluorescence nanoparticle tracking analysis (F-NTA)
6. EV identity (proteins and density)	(a) Immunoblot analysis of EV protein markers
	(b) Density determination by gUC
7. EV identity (topology)	(a) Fluorescamine assay
8. EV Stability	(a) Zeta potential measurement
	(b) Stability test/quality control in biological fluids
	(c) Resistance to detergents
9. EV Bioactivity	(a) In vitro cytotoxicity
	(b) Cellular uptake
10. Quality control (purity)	(a) Negative control on EV identity and preparation on culture media – throughout the manuscript
	(b) EV quantification by labelling with fluorescent lipid specific dye, to assess the presence of non-EV particles – see also 5.e
	(c) Density measurement and separation by density gradient, to assess the ratio between EVs and aggregates – see also 6b
	(d) Application of a tailor-made Quality Management System (QMS)

2 Materials and methods

2.1 Microalgae cultivation

A stock culture of the marine chlorophyte *Tetraselmis chuii* CCAP 66/21b was grown in borosilicate glass vessels in f/2 medium (Guillard, 1975) into its exponential phase growth and used via a 10% v/v inoculum to start 50 ml batch-cultures, in glass tubes, or 7.5 litre cultures, in a photobioreactor PB 200 (GroTech GmbH, Germany), at an initial concentration of 0.5 mg/ml (wet weight). Tubes and reactor were maintained at a temperature of $20 \pm 2°C$, a white light intensity of 100 µE m−2 s−1 and 14:10 light/dark photoperiod for 30 days prior to processing by EVs separation. Aeration was provided using a 0.22 µm airline and homogenisation was carried out manually every 3–4 days. The same batch cultivation procedures were used for other two microalgal strains: *Dunaliella tertiolecta* and the *Amphidinium sp*. An aliquot of the biomass of microalgal cells was collected at day 30 by centrifugation ($2000 \times g$ 10 min) and

freeze-dried overnight prior to weight or storage at -20°C. The biomass was treated with 1 ml of 0.5 M ammonium formate for desalting prior to freeze-drying.

2.1.1 Pigment extraction and analysis: Pigment extraction was carried out according to Mc Gee et al. (2018). Samples of freeze-dried biomass (2-3 mg) were mixed with 500 μl of ice cold 100% acetone and glass beads and placed in a FastPrep FP120 ribolyser for 40 s at full speed. Deionised water was added to bring the solution to 80% acetone (v/v) and vortexed. The extracts were then filtered through 0.22 μm PTFE membrane syringe filters to remove any residual particulate material. The extracts were transferred into amber vials and stored at -80°C and analyzed within 24 h. Pigment extracts were analysed at constant room temperature on a Varian ProStar HPLC binary solvent delivery system equipped with a 20 μl sample loop, ProStar 310 UV and 335 PDA detectors. Pigments were separated using a Phenomenex Onyx C18 100 × 4.6 mm ID monolithic column fitted with a Phenomenex Onyx C18 guard cartridge 10 × 4.6 mm ID employing a stepped gradient solvent programme with a flow rate of 3 ml/min. Pigments were resolved using a gradient profile consisting of 10% B starting condition for 0:10 min, followed by a linear gradient to 65% B from 0:10–2:00 min, isocratic hold at 65% B from 2:00 to 4:00 min, linear gradient from 4:00 to 5:00 min followed by hold at 90 B for 1:00 min and a final re-equilibration at initial conditions from 6:01–7:50 min. The mobile phase A consisted of methanol: 0.5 M ammonium acetate (80:20 v/v) and mobile phase B was acetone: acetonitrile (70:30 v/v). Prior to injection, extracts were diluted (1:5) with 0.5 M ammonium acetate when necessary. Carotenoids and chlorophylls were detected with a diode-array detector, scanning absorbance spectra from 360 to 700 nm and monitoring at 450 nm for optimal carotenoid detection. Probable pigment identification was achieved by comparing retention times and UV-vis spectral fine structures to pigment standards, DHI phytoplankton pigment Mix-115 and reference data-sheets.

2.1.2 Lipid extraction and fame analysis: The freeze-dried microalgal biomass was extracted according to Ryckebosch et al. (2012) with slight modifications. First, 400 μl of methanol was added to dried biomass (2-15 mg), followed with 200 μl of chloroform and 40 μl of deionised water. The sample was then vortexed and centrifuged (2,000 rpm, 10 min). The supernatant was discarded and the bottom chloroform layer collected. The residual biomass in the tube was re-extracted using 200 μl of methanol and chloroform, vortexed and centrifuged again. The upper layer was collected, and the extraction was carried out twice more on the residual biomass. The four lipid extract layers were then pooled together into a 15 ml tube and Na2SO4 salts added for dewatering. Upon further centrifugation, the solution was placed in a new tube and the

ôISEV

sample was then evaporated to dryness under a nitrogen stream. The residue was then resuspended in 500 µl of chloroform:methanol (50:50) as the final extract. Prior to analysis, 200 µl of the sample was placed in a GC-MS vial fitted with a glass insert and supplemented with 50 µl of trimethylsulfonium hydroxide (TMSH) for transesterification. The samples were left for at least 1 h at room temperature prior to analysis by GC-MS. The separation of Fatty Acid Methyl Esters (FAMEs) in the microalgal extracts was carried out using a BPX70 120 m column with an internal diameter of 0.25 mm on an Agilent7890A/5975C GC-MS system equipped with the MassHunter software. Samples were injected at a split ratio of 100:1 at an inlet temperature of 250°C with the helium flow rate set at 2 ml/min (48.51 psi) and the transfer line at 280°C. The oven gradient temperature was as follows: an initial hold at 50°C for 2 min followed by 20°C/min ramp to 160°C for 0 min, a 4°C/min ramp to 220°C for 5 min and finally a 4°C/min ramp to 240°C for 12.5 min. The mass spectrometry conditions had a solvent delay of 10.5 min. Identifications were carried out by comparing retention times against standards of the Supelco 37 Component FAME Mix and using the MS NIST 08 library.

2.2 Separation of nanoalgosomes from microalgae-conditioned media

2.2.1 Centrifugation-based EV purification methods: differential centrifugation

The 50 ml batch-cultures were centrifuged on day 30 at low speed to separate cells from the culture medium. Then, the separation of microalgae-derived EVs was performed by differential centrifugation (dUC) (Romancino et al., 2013). Large EVs (lEVs) were isolated in 50 ml Eppendorf polypropylene conical tubes at 10,000 × g for 30 min at 4°C using an Eppendorf rotor F34-6-38. Small EV (sEVs) were then collected from the supernatant into Beckman Coulter polypropylene open top tubes via centrifugation at 118,000 × g for 70 min at 4°C using a Beckman SW28 rotor. After a Phosphate-buffered saline (PBS 1X, without Calcium and magnesium, Thermo Fisher Scientific) washing step, the pellet was re-suspended in PBS for subsequent analyses, these sEV preparations are the dUC-isolated nanoalgosomes.

2.2.2 Filtration-based EV purification methods: Tangential flow filtration Cell
clarification and EV concentration were performed using a TFF ÄKTA Crossflow system (GE Healthcare, USA) and three GE Healthcare polysulfone hollow fibre membranes. After 30 days of cultivation, the reactor (containing typically 7.5 L of cell culture) was connected to the TFF system and the cell suspension was clarified by microfiltration with a 450 nm hollow fibre cartridge housed in the ÄKTA Crossflow.

Feed flow and transmembrane pressure (TMP) were kept constant at 110 ml/min and 0.05 bar, respectively. The first retentate (> 450 nm sized particles) was concentrated into a final volume of 100–200 ml and used to observe by light microscopy the integrity of cells. The 450 nm permeate (< 450 nm sized particles) was processed for a second microfiltration step using a 200 nm hollow fibre membrane with a 140 ml/min feed flow and 0.05 bar TMP. The ensuing permeate (< 200 nm sized particles) was concentrated using a 50 kDa MWCO hollow fibre membrane with feed flow and TMP of 42 ml/min and 0.45 bar, respectively; these TFF preparations corresponds to the sEVs and are considered as the TFF-isolated nanoalgosomes.

2.2.3 Density-based EV purification methods: gradient ultracentrifugation Gradient ultracentrifugation was used to further purify selected samples enriched in sEVs either by TFF or dUC. Samples containing about 200 µg of sEVs (expressed in protein content and measured by BCA) were concentrated by ultracentrifugation at 110,000 × g for 2 h at 4°C using a Ti70 rotor. The resulting pellets were homogenized in 10 mM Tris-HCL pH 8.6 buffer in a final volume of 50 µl. Samples were vigorously mixed for 20 min to disaggregate vesicles. A 50% (w/v) iodixanol working solution was prepared by diluting OptiPrep (Merck) according to the manufacturer's instruction. A discontinuous gradient containing 1.5 ml of 50%, 30% and 10% gradient cushions was prepared and the samples containing the EVs of interest were layered on top of the gradient. Ultracentrifugation was carried out at 110,000 x g for 24 h at 4°C using an SW55Ti rotor. Ten fractions of 500 µl each were collected from the top of the tubes. The percentage of iodixanol in each fraction was measured using a UV spectrophotometer (Nanodrop 200, Thermo Scientific) at 340 nm, from which the density was calculated according to the manufacturer's method. Protein concentration in each fraction was measured by micro-BCA (Thermo Scientific) using a UV spectrophotometer (Nanodrop 200, Thermo Scientific) at 562 nm.

2.3 Characterisation of nanoalgosomes

2.3.1 BCA assay and immunoblotting: The protein content of microalgal EVs was measured using the micro-bicinchoninic BCA Protein Assay Kit (Thermo Fishers Scientific). This colorimetric method provides a relative concentration to a protein standard (bovine serum albumin, BSA), which is used for the preparation of a calibration curve. The relative absorbance of the BCA soluble compound was measured at 562 nm using a GloMax Discover Microplate Reader. Proteins were separated by sodium dodecyl-sulfate polyacrylamide gel electrophoresis (SDS-PAGE)

∂ISEV

(10%). A total of 30 μg of cell lysate and EV samples (in PBS) were mixed with proper volumes of 5X loading buffer (0.25 M Tris-Cl pH 6.8, 10% SDS, 50% glycerol, 0.25 M dithiothreitol (DTT), 0.25% bromophenol blue). Then, the samples were heated at 100°C for 5 min and loaded in a 10% sodium dodecyl sulfate-polyacrylamide gel for electrophoretic analyses. Proteins were blotted onto polivinilidenfluoro-membranes (PVDF), which were blocked with BSA-TBS-T solution (3% powdered with bovine serum albumin in TBST (50 mM Tris HCl pH 8.0, 150 mM NaCl with 0.05% Tween 20) for 1 h at room temperature, followed by primary antibody incubation overnight at 4°C. The antibodies anti-Alix (clone 3A9, dil. 1:150 in 3%BSA/TBS-T1X), anti-Enolase (clone A5, dil. 1:400 in 3%BSA/TBS-T1X), anti-β-actin (clone AC15 dil. 1:400 in 3%BSA/TBS-T1X) and anti-HSP70 (clone W27 dil. 1:500 in 5% Milk/TBS-T1X) (Santa Cruz Biotechnology, USA), raised against different mammalian EV markers (MISEV 2018), also showed cross-reactivity to microalgae and were used in the present study. Anti H+/ATPase (dil. 1:1000 in 3% BSA/TBS-T1x, Agrisera), with a predicted reactivity for microalgae, are incubated for 1 h at room temperature. After washing, the membranes were incubated for 1 h with secondary antibodies according to the manufacturer's instructions (horseradish peroxidase-conjugated secondary anti-mouse or anti-rabbit antibodies, Cell Signaling). The membranes were washed four times in TBST for 20 min. The immunoblots were revealed using SuperSignal Pierce ECL (Thermo Fisher Scientific).

2.3.2 **Nanoparticle tracking analysis**: Nanoparticle size distribution and concentration were measured using a NanoSight NS300 (Malvern Panalytical, UK) at CNR and a ZetaView instrument (Particle Metrix) at ETH Zurich. The first instrument was equipped with a 488 nm laser, a high sensitivity sCMOS camera and a syringe pump and the second a 405 laser and a CMOS camera. At CNR, EV samples were diluted in particle-free water (Water, HPLC grade, Sigma-Aldrich, filtered by 20 nm using Whatman Anotop filters) to generate a dilution in which 20–120 particles per frame were tracked, to obtain a concentration within the recommended measurement range (1–10×108 particles/ml). Five experiment videos of 60-s duration were analyzed using NTA 3.4 Build 3.4.003 (camera level 15–16). A total of 1500 frames were examined per sample, which were captured and analysed by applying instrument-optimized settings with a suitable detection threshold so that the observed particles are marked with red crosses and that no more than 5 blue crosses are seen. Further settings, such as blur size and Max Jump Distance were set to 'automatic' and viscosity to that of water (0.841 - 0.844 cP). At ETH Zurich, the EV samples were diluted in particle-free PBS to obtain particle concentrations between 107 and 109 particles/ml. Each

RESEARCH ARTICLE

sample was injected with a 1 ml syringe in the sample chamber which was calibrated daily with polystyrene nanoparticles. Videos were acquired at 11 positions in the chamber at a frame rate of 30/s, with a trace length of 15 frames and using 80% scattering intensity and 150 shutter in light scattering mode. The experiments were repeated in triplicates and analysed with the ZetaView analysis software (ZetaView 8.04.02 SP2).

2.3.3 Fluorescence nanoparticle tracking analysis (F-NTA): We explored several staining strategies including commercial apolar dyes for lipid membrane staining (e.g., DiI and DIOC16) and photoactivatable probes to stain apolar environments (e.g. Di-8-ANEPPS). Therefore, we labelled nanoalgosomes with the dye Di-8-ANEPPS, whose fluorescence is activated in apolar environments, and specifically enhanced when bound to the lipid membrane of EVs, with a higher quantum yield with respect to any binding to hydrophobic protein regions. This makes it the Di-8-ANEPPS fluorescent signal highly EV-specific. For F-NTA, the fluorescent Tetraselmis chuii-derived EVs (f-EVs) were produced as follows: 5×10^{10} EV particles/ml were stained with 500 nM of 4-(2-[6-(dioctylamino)-2-naphthalenyl]ethenyl)-1-(3-sulfopropyl)pyridinium, DI-8-ANEPPS (Ex/Em: 467/631 nm, ThermoFisher Scientific), previously filtered by 20 nm filters (Whatmann Anotop filters). After 1 h at room temperature, NTA analyses were carried out by using NanoSight NS300 (Malvern Panalytical, UK) with a 500LP filter (laser wavelength 488 nm), with optimized manual settings for camera level and with high flow rate for the syringe pump (setting 150 μl/s) so that fluorescent EVs (f-EVs) cross the field of view of the main NTA screen in 5 to 10 s. Further settings were set as described in the previous NTA section. As negative control, we tested that the probe alone does not emit fluorescence signal with F-NTA.

2.3.4 Fluorescence correlation spectroscopy (FCS): FCS experiments were performed on nanoalgosomes labelled with Di-8-ANEPPS by using a Hamamatsu C9413-01 instrument equipped with a 473 nm excitation source. Along with the samples, a 10 nM Alexa-488 solution was used in the multi-well glass container as a calibrant for concentration and characteristic diffusion times to optimize the optical setup (Montis et al., 2017; Pánek et al., 2018; Ries & Schwille, 2012). In the Supporting Information, further details are reported on the experimental set up and the analysis to obtain the size distribution function.

2.3.5 Multi angle dynamic light scattering (DLS): Multi angle DLS experiments were repeated at two different laboratories of our consortium, CNR (Italy) and MPIP (Germany), by using a slightly different procedure. Briefly, samples were diluted to a final total protein content below 50 μg/ml to avoid vesicle interaction and multiple

ISEV

RESEARCH ARTICLE

scattering, and then either centrifuged at $1000 \times g$ for 10 min and poured into a quartz cylindrical cell or directly filtered into the cell by Millex-LCR 0.45 μm syringe filters (Merck, Germany) at CNR or MPIP, respectively. At CNR, cells were placed at 20°C in a thermostated cell compartment of a Brookhaven Instrument BI200-SM goniometer equipped with a solid state laser tuned at a wavelength $\lambda = 532$ nm, and a Brookhaven BI-9000 correlator (Brookhaven Instruments, Holtsville, NY, USA). At MPIP, multi-angle DLS was performed with an ALV spectrometer (ALV-GmbH, Germany), including a goniometer and an ALV/ LSE-5004 multiple-tau full-digital correlator with 320 channels and equipped with a He-Ne laser with $\lambda = 632.8$ nm. Scattered intensity and intensity autocorrelation function $g_2(t)$ were measured simultaneously at different scattering angle ϑ to measure the z-averaged hydrodynamic diameters Dh0, the average diameter Dg, which is twice the radius of gyration, and eventually the fullsize distribution (Mailer et al., 2015; Noto et al., 2012; Prima et al., 2020; Schmitz, 1990). Full details about the analysis are reported in the Supporting Materials and Method's Section and Supporting Figure S1.

Analogous DLS experiments were performed at different pHs. The TFF-separated sEVs were pelleted by ultracentrifugation and then resuspended in a 10 mM buffer solution with 150 mM NaCl. The buffers used were phosphate buffer (pH 6.1, 7.4 and 7.8), acetate buffer (pH 4.3 and 5.3), or carbonate buffer (pH 8.8).DLS experiments with detergents were performed at the same vesicle concentration using different detergents concentrations. Samples were incubated overnight, centrifuged at $1000 \times g$ for 10 min and supernatants poured in quartz cells for DLS measurements. Both SDS and Triton X-100 were purchased from Sigma Aldrich, diluted in buffer solution and filtered using 200 nm syringe filters. For comparison the same experiments were performed on large unilamellar vesicles (LUV) made with 2-Oleoyl-1-palmitoyl-sn-glycero-3-phosphocholine (POPC), 2-Oleoyl-1-palmitoyl-sn-glycero-3-phospho-L-serine sodium salt (POPS), both purchased from Avanti Polar Lipids Inc. (Alabaster, AL, USA), and Cholesterol (Merck Life Science). LUV were made with the relative content of POPC:POPS:Cholesterol (81:9:10) by extrusion through a 100 nm polycarbonate filter by using a miniextruder (AVESTIN, Germany).

2.3.6 Atomic force microscopy (AFM): Atomic Force Microscopy images were captured by using a Nanowizard III scanning probe microscope (JPK instruments, AG Germany) equipped with a 12 μm scanner. Nanoalgosomes were initially concentrated by ultracentrifugation and resuspended in MilliQ water to a final concentration of 5×10^{11} particles/ml, as previously estimated by NTA.

For measurements on dry samples, a 30 μl drop of the samples was directly deposited on freshly cleaved mica, incubated for 10 min, and then gently dried under nitrogen flow. Measurements were performed in tapping mode by using a NSC-15 (Mikromasch) cantilever (spring constant 40 N/m, typical tip radius 8 nm). Measurements with softer cantilevers (data not shown) were carried out with MSNL-10 cantilevers (Bruker; lever D, spring constant 0.03 N/m, nominal tip radius 2 nm).

2.3.7 Scanning electronic microscopy: Samples were fixed in 0.4% paraformaldehyde and 2.5% glutaraldehyde in 300 mM PBS at 4°C. The pre-fixed samples were applied onto polycarbonate filters with pore-diameter of 0.05 μm (STERLITECH) until the filter got blocked. Then, the EV-covered filters were taken from holders and post-fixed in a bath following the protocol adopted from (Lešer et al. (2009). In brief, the primary fixatives were removed by three washing steps with distilled water (10 min incubation for each). Samples were then incubated for 1 h in 2% OsO4. They were washed with distilled water (three washing steps with 10 min incubation time), treated with saturated water solution of thiocarbohydrazide (15 min incubation time), washed again (three washing steps in distilled water, 10 min incubation time each), and subjected to 2% OsO4 again for 1 h. After the second incubation in OsO4, the unbound osmium was removed in three additional washing steps (in distilled water, 10 min incubation time in each step). The samples were dehydrated in graded series of ethanol (30%-100%, 10 min incubation in each solution; absolute ethanol was replaced three times), followed by graded series of HMDS (mixed with absolute ethanol; 30%, 50% and 100%, 10 min in each solution) and finally air dried. The dried samples were Au/Pd coated (PECS Gatan 682) and examined by JSM-6500F Field Emission Scanning Electron Microscope (JEOL Ltd., Tokyo, Japan).

2.3.8 Cryo-transmission electron microscopy (cryo-TEM): The sEV samples, with an original particle concentration of 5 × 1010 per ml, were concentrated 10x (using Amicon Ultra-2 μl Centrifugal Filters, Molecular weight cut-off (MWCO): 30 kDa, Merck, Germany) and afterwards 10 μl were placed onto a 400 mesh copper grid covered with lacey film, which was treated with oxygen plasma to make it hydrophilic, and immobilized using high pressure freezing (Engineering Office M. Wohlwend GmbH, Switzerland). The specimen (sapphire discs with cells) was enclosed and protected in a small volume between two specimen carriers and locked inside the specimen pressure chamber by blotting two times for 3 s each. Liquid nitrogen was used as cooling medium. After the preparation, the samples were carefully transferred into liquid nitrogen for further imaging. Imaging was performed on a TEM (FEI Tecnai

F20) microscope. For the Cryo-TEM analysis, the acceleration voltage was 200 kV and the device was coupled with an axis Gatan US1000 2k CCD camera.

2.3.9 Stability and surface properties: zeta-potential and amino-groups of nanoalgosome surface A Zetasizer Nano Z (Malvern Panalytical GmbH, Germany) with disposable folded capillary cells was used to determine the zeta-potential (ζ-potential) of the nanoalgosomes. Basically, 50 μl of each sample were diluted with 1 μl of a 1 mM potassium chloride (KCl) solution. The measurement was performed at 25°C after 2 min of equilibration. Each measurement was repeated in triplicate and mean values, as well as standard deviations, were calculated. The amount of NH2 groups present on the nanoalgosome surface was determined based on a fluorescamine assay (FA assay). Hexylamine, which contains primary amine groups, was selected as a reference for establishing the standard calibration curve. For the assay, 250 μl fluorescamine stock solution (concentration of 0.3 mg/μl) and 25 μl sample solution (H_2O as the control), as well as 725 μl borate buffer (0.1 M, pH = 9.5), were added into a 2 μl Eppendorf tube. The mixture was vortexed (Heidolph REAX2000 at maximum speed) for 30 s and then immediately analyzed in a plate reader (Tecan AG, Switzerland) at 25°C by exciting at 410 nm and detecting the fluorescence emission at 470 nm. Samples were concentrated 10x before the quantification using Amicon Ultra-2 μl Centrifugal Filters, Molecular weight cut-off (MWCO): 30 kDa, Merck, Germany. All fluorescence measurements were repeated three times (3 × 100 μl in a well of a 96-well-plate).

2.3.10 Stability in biological fluids: The stability of nanoalgosomes was analysed in undiluted human blood plasma using multiangle dynamic light scattering. Human citrate blood plasma was collected from 10 healthy donors at the Transfusion Centre of the University Clinic of Mainz, Germany, according to standard guidelines. It was pooled and stored at -20°C. To remove cell fragments and additional protein precipitates, it was centrifuged at 20,000 × g and 4°C for 1 h (Sigma 3–30K, Germany) before use. The nanoalgosome samples were centrifuged at 10,000 × g for 10 min prior to analysis to remove dust. The citrate plasma (200 μl) was filtered through 0.2 μm Millex-GS syringe filters (Merck, Germany) directly into cylindrical quartz cuvettes (18 mm diameter, Hellma, Germany). The cuvettes were cleaned in an acetone fountain prior to usage for removing dust. Then, 10 μl of *Tetraselmis chuii*-derived nanoalgosomes were added. For reference, 10 μl of pure nanoalgosomes were diluted in 200 μl PBS buffer. Similarly, 200 μl of plasma were measured without the addition of nanoalgosomes. Samples were incubated at 37°C for 1 h before the measurement.

RESEARCH ARTICLE

Multi-angle DLS was performed with an ALV spectrometer (ALV-GmbH, Germany) at 37°C. The set-up consisted of a goniometer and an ALV/LSE-5004 multiple-tau full-digital correlator with 320 channels. As a light source, a He-Ne laser was used at a wavelength of 632.8 nm. Data analysis was performed using a multicomponent fitting method according to Rausch et al. (2010).

2.4 Bioactivity and cellular uptake of nanoalgosomes

2.4.1 Cell cultures: The following cell lines were used for the bioactivity and cellular uptake analyses: (i) 1–7 HB2, a normal mammary epithelial; (ii) MDA-MB 231, an epithelial human breast cancer and (iii) HepG2 a human hepatocarcinoma (ECACC cell lines). All cell lines were maintained at 37°C in a humidified atmosphere (5% CO_2) in Dulbecco's Modified Eagle's Medium (DMEM) (Sigma-Aldrich) containing 10% (v/v) Fetal Bovine Serum (FBS) (Gibco, Life Technologies) plus 2 mM L-glutamine, 100 U/ml Penicillin and 100 mg/ml Streptomycin (Sigma-Aldrich) for the MDA-MB-231; DMEM low glucose plus 5 µg/ml Hydrocortisone and 10 µg/ml, Bovine Insulin (Sigma-Aldrich) for 1–7 HB2 cell line; RPMI 1640 Medium containing 10% (v/v) Fetal Bovine plus mM L-glutamine, 100 U/ml Penicillin and 100 mg/ml Streptomycin was used for HepG2 cell line.

2.4.2 Cell viability assay: Tumoral (MDA-MB 231 and HepG2) and normal (1-7 HB2) cell lines were seeded in 96-well plates at a density of 2×10^3 cells per well and maintained using suitable culture conditions. The assay was carried out with EVs isolated from Tetraselmis chuii conditioned media. Similar to other studies carried out with plant-derived EVs, the nanoalgosomes were used at concentrations ranging from 0.1 to 2.0 µg/ml (Kim et al., 2015; Montis et al., 2017; Raimondo et al., 2015). This is equivalent to ~104-105 EVs/cell, corresponding to the estimated number of vesicles considered necessary to cover the surface of a cell (Sverdlov, 2012). 24 h after seeding, the cells were incubated for 24, 48 and 72 h with Tetraselmis chuii-derived EVs. The cells treated with PBS alone were used as control. Cell viability was evaluated using the CellTiter 96 AQueous One Solution Reagent (Promega) according to the manufacturer's instructions. The mean optical density (OD, absorbance) of four wells in the indicated groups was used to calculate the percentage of cell viability as follows: percentage of cell viability = (Atreatment − Ablank)/(Acontrol (untreated) − Ablank) × 100% (where, A = absorbance490nm). Values were expressed as means ± SD of three biological samples, each performed in triplicate.

ISEV

RESEARCH ARTICLE

2.4.3 Genotoxicity assay: MDA-MB 231, HepG2 and 1–7 HB2 cells were plated in 24-well plates containing sterile coverslips in complete medium, for 24 h. Cells were then incubated with 2 μg/ml of Tetraselmis chuii-derived EVs for 48 and 72 h. Thereafter, the medium was removed and the cells were washed twice with PBS and subsequently stained with Acridine Orange/PBS solution (Sigma) at 100 μg/ml for 10 s at room temperature and quickly examined by epi-fluorescence microscopy (Leica, DFC450C). Acridine Orange is a cell permeating nucleic acid binding dye that emits green fluorescence when bound to double-strand DNA and red fluorescence when bound to single-strand DNA, RNA or lysosomes. This staining technique allows for discrimination between intact (green nuclei) and damaged DNA in cells (red nuclei).

2.4.4 Cellular uptake: MDA-MB 231 and 1–7 HB2 cell lines were grown at a density of 5×10^3 cells/well in 12-well plates containing sterile coverslips in complete medium for 24 h. F-EV samples (see F-NTA section), were dialysed to remove free probe (D-Tube Dialyzer Midi, MWCO 3.5 KDa, Sigma-Aldrich) against PBS, for 24 h at 4°C. As negative control, we used dUC isolates (at 118,000 × g) using not-conditioned f/2 media incubated with Di-8-ANEPPS, similarly to f-EV samples. Before and after dialysis, both f-EVs and negative control were checked for fluorescence and size distribution by NTA. Next, cell lines were incubated with different amount of f-EVs (0.5 and 2 μg/ml) at 37°C or 4°C, as well as with an equivalent amount of negative control. After different incubation times (3, 6 and 24 h), cells were washed twice with PBS, fixed with 3.7% paraformaldehyde for 15 min, and washed again twice with PBS. F-actin cytoskeleton was detected by staining with Alexa Fluor 594 phalloidin (ThermoFisher Scientific) in 1% BSA-PBS solution at 400 μgr/ml for 60 min at room temperature. Afterwards, the nuclei were stained with VECTASHIELD Mounting Medium with DAPI. The f-EV cellular localization was monitored by fluorescence microscopy analysis (Nikon Eclipse 80i), confocal laser scanning microscopy (Olympus FV10i, 1 μm thickness optical section was taken on total of about 15 sections for each sample) and analysed using ImageJ 1.52t. The reported relative green fluorescence intensities correspond to the fluorescence intensities of 5 different images of each sample, normalized to the number of nuclei, and relative to the control sample (i.e., cells treated with the dUC-isolates from not-conditioned f/2 media). Experiments were repeated using three independent nanoalgosome preparations; data were expressed as the mean ± standard deviation (SDs).

2.4.5 Statistical analyses: Experiments were independently repeated at least in triplicate. Error bars in the graphical data represent standard deviations. A Student's t-

ISEV

RESEARCH ARTICLE

test was used for statistical analysis, and statistical significance was claimed when the P-values were ≤ 0.0001 (****) and ≤ 0.001 (***).

2.5 Quality management system

We validate and applied a Quality Management System (QMS) compatible with UNI EN ISO 9001:2015 standard to assure standardization of the procedures as well as reliability and reproducibility of the results among the different laboratories. Our QMS supported the scientific activities of the study, including the sharing of standard operating procedures (SOPs) to increase the reliability and reproducibility of the results. Customized lab notebooks and SOP models were developed, distributed and utilized among the participating laboratories. Quality Assurance and Quality Control activities, including checklists and review meetings, were performed to monitor the specific activities of partners (Liguori & Kisslinger, 2020).

2.6 EV-track

We have submitted all relevant data of our experiments to the (EV-TRACK ID: EV200075) (Van Deun et al., 2017).

3 Results

The following paragraphs describe an in depth biochemical, biophysical and biological characterization of the microalgal-derived small extracellular vesicles, sEVs, which we named nanoalgosomes.

3.1 Characterization of the nanoalgosome bioresource: *Tetraselmis chuii*

The marine photosynthetic chlorophyte species *Tetraselmis chuii* CCAP66/21b was identified in the present study as a new source of nanoalgosomes. First, we determined the chemical signatures of the microalgal biomass in terms of pigment and fatty acid methyl ester (FAME) contents. Interestingly, we found high-value carotenoid (e.g., Neoxanthin, Violaxanthin, Lutein, and β carotene) and long-chain polyunsaturated fatty acids (LC-PUFA), such as the eicosapentaenoic (EPA, 20:5n-3) (Supporting Figure S2).

3.2 Separation and quantification of microalgal extracellular vesicles

ISEV

Next, from the microalgae-conditioned culture media we isolated extracellular by-products, which consist of two EVs sub-populations: nanovesicles (small EVs, sEVs) and microvesicles (large EVs, lEVs). While differential ultracentrifugation (dUC) is the classical method for EV enrichment (Romancino et al., 2013; Théry et al., 2006), tangential flow filtration (TFF) has been increasingly applied in the field, as gentler (low shear stress) purification method to optimise the recovery of intact EVs with consistent purity both in small and large-scale processes (Busatto et al., 2018; Paganini et al., 2019). Both dUC and TFF procedures allowed a reproducible separation of sEVs; the yield of sEV production was slightly affected by the scaling-up of the microalgal culture from small- (50 ml) to medium-scale (7.5 L) and the use of two different separation protocols (Table 2). The EV yields, in terms of sEV protein content and sEV number, were consistent with the estimate of 10^9 EV particles/µg EV proteins, as reported by Sverdlov (2012) (Sverdlov, 2012). Based on the above analyses, we have validated and optimized the TFF separation method and were able to produce sufficient amount of sEVs for the in-depth characterization, in line with those obtained from plant-derived vesicles, as reported for citrus juice-derived nanovesicles (Raimondo et al., 2015).

TABLE 2   Yield of nano-algosomes (microalgal-derived sEVs) from six biological replicates of *Tetraselmis chuii*-conditioned media from small- (50 ml) to medium-scale (7.5 L) volume

Isolation method	Culture Volume	sEV pt µg/mg biomass	n. sEVs/mg biomass
dUC (118,000 × g pellet)	50 ml	0.40 ± 0.03	$(2.00 \pm 0.08) \times 10^9$
TFF (< 200 nm)	7500 ml	0.30 ± 0.05	$(1.00 \pm 0.20) \times 10^9$

The sEV yields is based on EV protein concentration (sEV pt), measured by micro-bicinchoninic (BCA) colorimetric assay, and particle numbers (n. sEVs), measured by Nanoparticle Tracking Analysis (NTA), both expressed per mg of dry weight microalgal biomass.

3.3 Nanoalgosome identity: biophysical analyses of particle size

Microalgal sEVs, i.e. nanoalgosomes, were analyzed by different techniques for determination of their average size and size distributions.

Multi-angle dynamic light scattering (DLS). Simultaneous static and dynamic light scattering measurements were performed at multiple scattering angles on TFF-isolated nanoalgosomes to derive the average diameter D_g and the z-averaged hydrodynamic diameters D_{h0}, as shown in Figure 1a. In order to validate the experimental outcomes, the experiments were repeated at two different laboratories of our consortium, by using a slightly different procedure. The average values obtained after sample filtration at MPIP ($D_g = 120$ nm, $D_{h0} = 100$ nm) are slightly lower than those obtained after sample

δISEV

RESEARCH ARTICLE

centrifugation at CNR (D_g = 135 nm, D_{h0} = 113 nm), since in the first case a more effective depletion of the EV population with larger size may be expected. In both cases, the ratio D_g/D_{h0} is about 1.2. While for monodisperse colloidal particles a value larger than 1 indicates a non-spherical shape, for the heterogeneous nanoalgosome mixture this value is likely due to the sample polydispersity and to the asymmetric shape of its size distribution. To account also for smaller size objects such as proteins, which were sporadically observable in the sample, from the DLS measurements we derived the complete distribution of hydrodynamic diameters $P(D_h)$ (Figure 1b). The distribution of the nanoalgosome samples are typically peaked at D_{mode} = 70 nm and have a tail at larger sizes; nanoalgosomes have the corresponding average size of D_{avg} = 135 nm. We note that the latter moment of the distribution is not equivalent to the z-averaged size, obtained e.g. by cumulant method, which is a harmonic average of hydrodynamic diameters and therefore attains a lower value (D_{ho} = 95 nm, Figure 1b).

Nanoparticle tracking analysis (NTA). The size distribution of diluted sEV samples was measured by nanoparticle tracking which was also used to measure the particle concentration (Figure 1b). Two NTA experiments are reported on the same samples, made by using two different equipment (namely NanoSight NS300 at CNR and ZetaView at ETH). As NTA is typically more accurate on larger size particles, we observed a distribution peaked at Dmode = 125 nm, with a slightly higher average size. Comparison of size distribution of nanoalgosomes isolated by dUC and TFF . We next applied the techniques described above to compare the size distribution of dUC- and TFF-isolated Tetraselmis chuii-sEVs. The NTA and DLS analyses showed that both separation methods produce sEVs with comparable size distributions (Figure 1c). As a minor difference, one notes that TFF-isolated sEVs have a slightly sharper size range with respect to dUC-isolated sEVs. Also, a residual population of larger vesicles is more often observed in dUC-isolated sEVs.

Fluorescence nanoparticle tracking analysis (F-NTA). To confirm the presence of lipid membranes in the isolated nanoalgosomes, we applied F-NTA to determine the size distribution of particles stained with Di-8-ANEPPS, an EV specific fluorescent dye (inset of Figure 1b). Both F-NTA and standard (scattering mode) NTA give a largely overlapping distribution and also a comparable particle number (Supporting Figure S3). In addition to validate the presence of nanoalgosomes with lipid membranes, this analysis shows the absence of large number of non-vesicle contaminants, such as lipoproteins and protein aggregates.

Fluorescence Correlation Spectroscopy (FCS). To further confirm this result, we applied the same fluorescence staining used for F-NTA experiments to perform FCS

RESEARCH ARTICLE

measurements and determine the distribution of the hydrodynamic radii of fluorescent labelled species (inset of Figure 1b). It is worth noting that FCS is more accurate in detecting smaller particles with respect to F-NTA. The analysis further confirmed the presence of lipid membranes in the isolated nanoalgosomes.

Size distribution of nanoalgosomes by different techniques: conclusion. Overall, the different techniques and analyses described above provided consistent size distributions, with slight differences depending on the weight given to large and small particles and to the sampling method (Supporting Figure S4). With respect to NTA, DLS has no limit in the detection of diffusing vesicles also smaller than 70 nm. On the other hand, it measures a size distribution that is weighted on the square of particle mass. Thus, while the z-averaged hydrodynamic diameter is a robust experimental parameter (multi angle DLS cumulant analysis, Figure 1a), one can obtain a more reliable esteem of the size of greatest number of particles by referring to the mode of the distribution (DLS analytic fit, Figure 1b). NTA is able to track single particles in the sample and, therefore, by definition it measures a number size distribution (NTA, Figure 1b). However, its capability for sampling small particles is affected by the detection sensibility and the tracking speed, as well as by lower light scattering of small particles, which is covered by the signal of larger particles. This determines a closer analogy between NTA distribution and the weight average distribution observed in DLS experiments. A further drawback of NTA is due to its intrinsic limitation in the lower particle range; a limitation that can be overcome by using fluorescent dyes (F-NTA, inset of Figure 1b). When we deal with a broad size distribution, as in the present case and in the case of EVs in general, NTA represents a routinely tool to identify the average size of a broad population. Indeed, the peak observed by NTA typically mirrors the average values measured by DLS. As a second step, one can perform a more detailed DLS analysis, as we highlight in the present work, to pin point the sEV size that appears most frequently in the distribution (DLS_{mode}).

⟐ ISEV
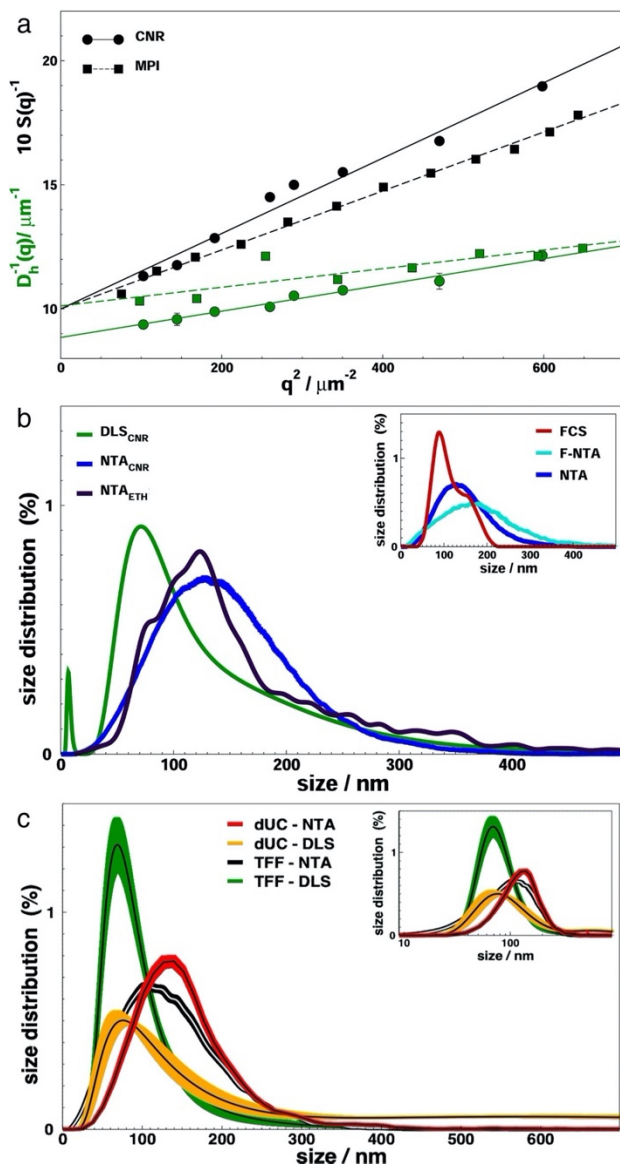
FIGURE 1 Size and size distribution of nanoalgosomes isolated by TFF. (**a**) Multi Angle Light Scattering (MALS) experiments. Form factor S(q), black, and apparent hydrodynamic diameter $D_h(q)$, green, as a function of the square of the scattering vector q^2. Two experiments are reported on the same samples, performed at CNR (CNR, circles, solid curves) and MPIP (MPI, squares, dashed curves). The continuous curve represents a linear regression to data, as described in the text. The parameters D_{h0}, derived from the intercept in the fit of $D_h(q)^{-1}$, are the z-averaged hydrodynamic diameters; the parameters D_g, derived from the slope in the fit of $S(q)^{-1}$, are the double of the average radius of gyration. (**b**) Nanoalgosome size distribution by Dynamic Light Scattering (DLS), green curve, and Nanoparticle Tracking Analysis (NTA), performed at CNR, blue curve, and ETH, black curve. **Inset**: Size distribution of nanoalgosomes stained with Di-8-ANEPPS measured by fluorescence NTA (F-NTA), cyan curve, and Fluorescence Correlation Spectroscopy (FCS), red curve. NTA

♪ ISEV

analysis is also shown (blue). (**c**) Size distribution of nanoalgosomes isolated by TFF and dUC and analyses by DLS and NTA. The bold solid lines represent the distributions errors, that are calculated either on 5 replica of the same sample or on 3 different preparations of the same sample for NTA or DLS, respectively. Inset: Size distributions of the main panel displayed in log scale.

3.4 Nanoalgosome identity: morphology

Since morphology is another important property of EVs, after characterizing the size distribution of our nanoalgosomes we applied different microscopy techniques to define their morphology and shape.

Atomic force microscopy (AFM). Figures 2a-d show AFM images of nanoalgosomes at different magnifications allowing to observe the details of single particles and the heterogeneity of a complete sEV sample. The close-up image in Figure 2b and its 3D reconstruction in Figure 2d highlight a small dip in the middle of sEVs. This dip is caused by the strength of the AFM cantilever, which actually pushes the sEV surface causing the curvature of the membrane and of the whole particle since the edges cannot be adequately squeezed. To verify this hypothesis, we repeated the measurements with a softer cantilever and no depression was indeed observed. This observation supports the potential of AFM to study the structural and mechanical properties of EVs (Paolini et al., 2020; Ridolfi et al., 2020).

Scanning electron microscopy (SEM). SEM images of nanoalgosomes isolated from Tetraselmis chuii show globular particles, heterogeneous in size and shape, sometimes organized in clusters. Images of sEVs of isolates obtained by TFF are shown in Figure 2e-f, while additional images of dUC- and TFF-isolated sEVs are given in Supporting Figures S5-S6.

Cryo-Transmission Electron Microscopy (cryo-TEM). In cryo-TEM imaging, the nanoalgosome samples are directly applied onto an EM grid, vitrified and visualized, therefore allowing us for characterization near their native state, avoiding dehydration, chemical fixation, and/or staining which can alter the sample (as in SEM). The cryo-TEM imaging revealed that the nanoalgosomes are spherical core-shell nanoparticles, possessing a lipid bilayer structure, which is expected for these vesicles (Figure 2e-f). Smaller amorphous structures, which are currently under investigation, are barely observable in the background.

: ISEV

RESEARCH ARTICLE
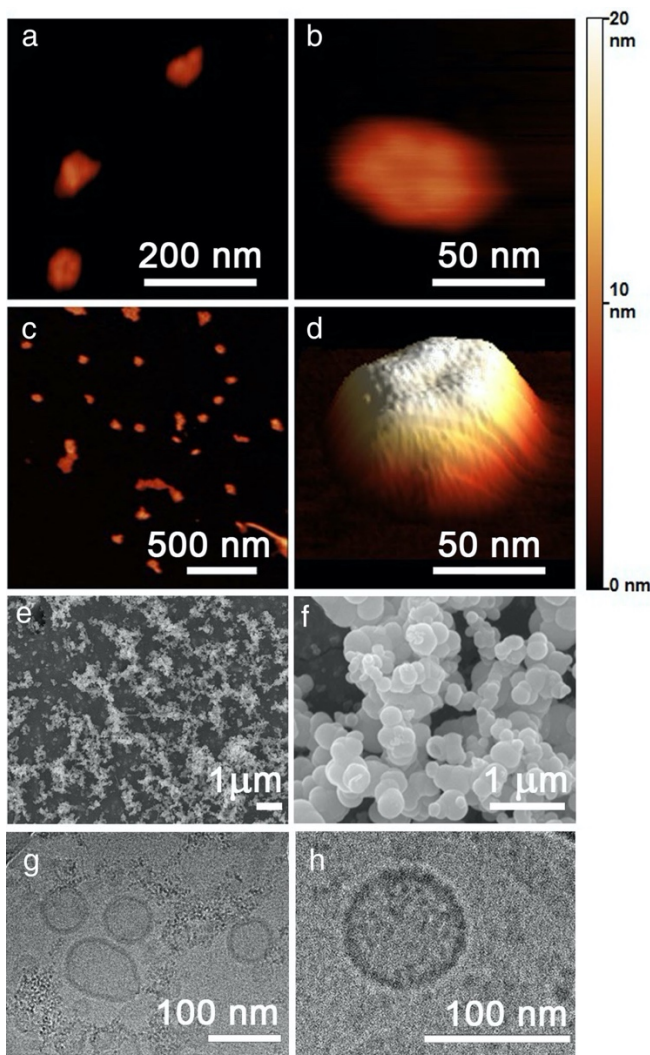
FIGURE 2. Morphology of T*etraselmis chuii* nanoalgosomes isolated by TFF. (a) and (b) Zoom-up tapping mode AFM images in air of selected nanoalgosomes. (c) Wide-field tapping mode AFM images in air showing several sEVs. The coloured scale on the right indicates the height for all AFM images. (d) 3D reconstruction of a single nanoalgosomes from panel (b). (e) and (f) SEM and (g) and (h) cryo-TEM images. Representative images are presented of three independent experiments (n = 3).

3.5 Nanoalgosomes identity: protein markers and density

After determining size distribution, morphology and shape, following the VES4US-MISEV guidelines, we evaluated the biochemical features of nanoalgosomes purified from *Tetraselmis chuii* culture.

Vesicle protein biomarkers. Selected biomarkers enriched in the EV fraction and putatively conserved during evolution were evaluated by immunoblot analyses. First, we checked for their cross-reactivity against the relative microalgal orthologs, then, we compared their expression in the lysates as well as in the sEVs and lEVs fractions

RESEARCH ARTICLE

obtained by Tetraselmis chuii. Target protein biomarkers, chosen according with MISEV guidelines, were Alix, Enolase, HSP70, and β-actin. This analysis was crucial to discriminate EVs from other contaminants. Immunoblot results showed the enrichment of three target proteins (i.e., Alix, Enolase, and β-actin) in the sEV samples compared to the lysates and lEVs (Figure 3).

Plasma membrane H+/ATPase as a biomarker of nanoalgosomes. The plasma membrane H+/ATPase is a transmembrane protein of about 100 kDa, which extrudes protons to generate electrochemical proton gradients, using ATP energy. The generation of this gradient is critical in providing energy for secondary active transport through the plasma membrane (Stevens & Forgac, 1997). The plasma membrane H+/ATPase plays a key role in plant physiology, in normal growth conditions and under abiotic stresses (Zhang et al., 2019). It is present also in several intracellular compartments of mammalian cells, including clathrin-coated vesicles, endosomes, lysosomes, Golgi-derived vesicles, chromaffin granules, synaptic vesicles, and multivesicular bodies (Han et al., 2017; Moriyama et al., 1992). It is of note that the high concentrations of solutes in secretory organelles such as chromaffin granules, synaptic vesicles, and microvesicles is allowed by specific transporters that are coupled to the proton gradient or to the membrane potential generated by the H+/ATPase. In this context, the presence of H+/ATPase was reported in human prostasomes and its expression alteration in urinary exosomes (Pathare et al., 2018). Most studies regarding H+/ATPase have been performed in plants and fungi and, due to the lack of genetic information, much less is known about plasma membrane H+/ATPase in microalgae (Pertl-Obermeyer et al., 2018).

To find a possible biomarker of nanoalgosomes, we evaluated the presence of this highly conserved plasma membrane H+/ATPase in nanoalgosome samples. For this purpose, here, we use H+/ATPase polyclonal antibody with high reactivity and specificity for microalgae. Figure 3 shows the presence of H+/ATPase in nanoalgosome samples, isolated by TFF from two independent sEV preparations from Tetraselmis chuii (Figure 3). To support the specificity of H+/ATPase for sEVs, we demonstrated the presence of this protein marker in Tetraselmis chuii sEV fraction isolated by dUC and TFF and separated by iodixanol gradient (Figure 4d).

Determination of nanoalgosome density. Density gradient ultracentrifugation in iodixanol was used to determine the nanoalgosome density and to purify and further separate sEVs isolated either by dUC or TFF. After 24 h of centrifugation, a light coloured band was observed in the tube with dUC sample but none was observed in

ISEV

the tube with the TFF sample. Ten fractions were collected from the top of each tube to determine the density and the protein concentration (Figure 4a).

Mammalian cell-derived sEVs (i.e., exosomes) are characterized by density between 1.15 – 1.19 g/ml (Théry et al., 2006). The density of the fraction containing the visible band (Fraction 5) was measured to be slightly lower (i.e., 1.13 g/ml) than the density of mammalian exosomes.

Fractions 1–4 corresponding to the soluble protein fractions showed very less to no protein content in both the samples (Figure 4b). Fraction 6 (partially could be overlapping with 5 and 7) has a density of 1.12 ± 0.01 g/ml (n = 3) that corresponds to the density of mammalian exosomes showed high protein content in the TFF sample. Fraction 5 (the visible layer) has a density of 1.16 ± 0.1 g/ml showed high protein content in dUC sample. Fractions 8–10 had higher densities than sEVs, and they could be nuclei, DNA, proteins, cell fragments that co-purify with dUC and TFF separation methods.

DUC and TFF isolated sEVs separated by gUC were analysed by immunoblotting (Figure 4d). In fractions 5 and 6 where sEVs were expected based on density, the presence of nanoalgosomes could be confirmed by Alix and H+/ATPase positivity. Based on these analyses we can conclude that the nanoalgosomes have a slightly lower density than mammalian sEVs and it is 1.13 g/ml.
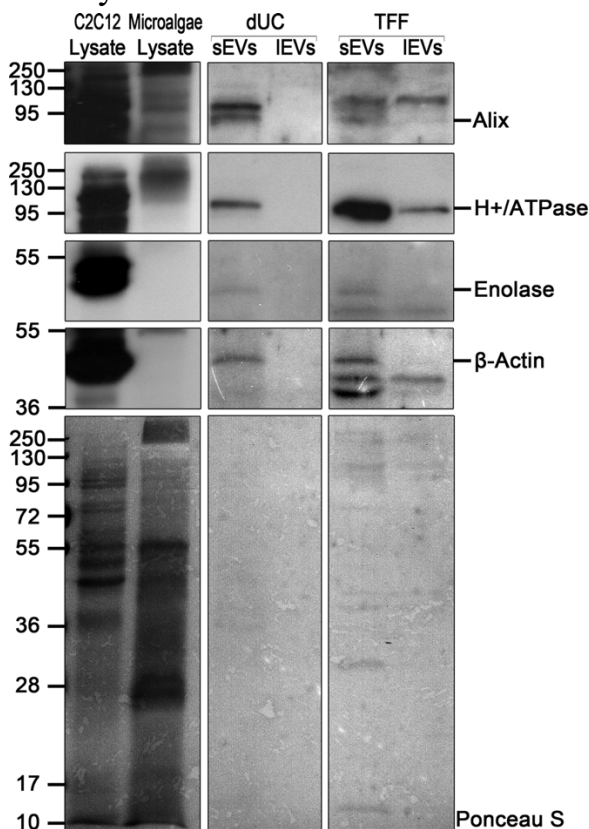
RESEARCH ARTICLE

FIGURE 3. Representative immunoblot analyses of Alix, H+/ATPase, Enolase and β-actin in *Tetraselmis chuii* cell lysates (Microalgae lysate), sEVs and lEVs isolated by dUC and TFF from Tetraselmis chuii cultures; a mammalian cell line is used as positive control (C2C12 lysate). [C2C12 (10 μg) and microalgae (20 μg) lysates, dUC-isolated and TFF-isolated sEV (13 μg) and lEV (equal volumes) samples were loaded on gels. Alix, H+/ATPase, Enolase, and β-actin are enriched in the sEV samples. Three independent experiments (n = 3) were performed. Ponceau red staining is shown as loading control (bottom panel); lower exposures of lysate immunoblots are shown to indicate the specific bands
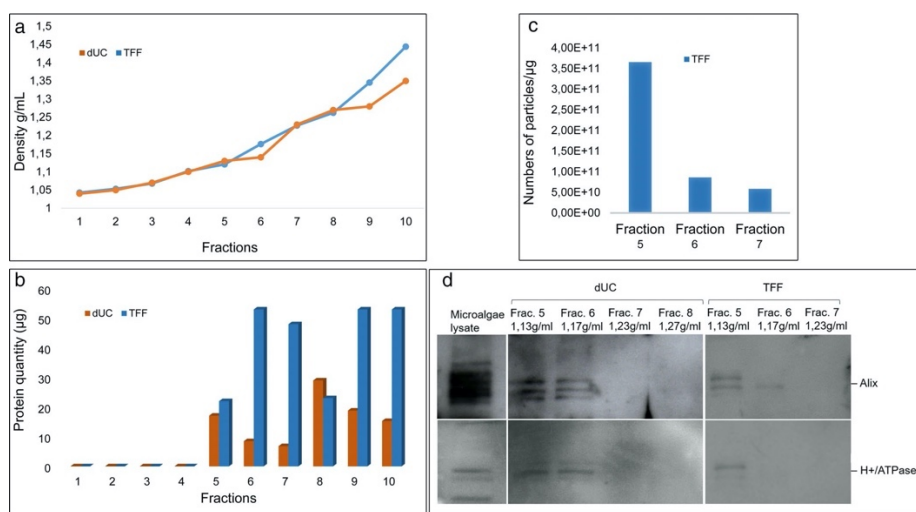
FIGURE 4 Iodixanol gradient to determine the nanoalgosome density. (a)The density of the ten fractions measured in the gradient ultracentrifugation (gUC) of TFF and dUC samples. (b) The quantity of protein measured in each gUC fraction. (c) The ratio of numbers of particles (determined by NTA) relative to μg of proteins measured in 5-6-7 gUC fractions of TFF samples. (d) Representative immunoblot analyses of nanoalgosomes isolated by dUC and TFF, and loaded on iodixanol density gradient. 20 μg of microalgae lysate and whole fractions were loaded on gel. Fraction 5 (density 1.13 g/ml) of dUC and TFF separated nanoalgosomes and at a less extent the fraction 6 (density 1.2 g/ml) are positive for EV specific biomarkers (Alix and H+/ATPase). Two independent biological replicas (n = 2) were performed.

3.6 Nanoalgosome identity: topology

The topology of different components of EVs, as recently pin-pointed by the MISEV 2018, is an important characteristic in defining EVs functionality. Here we report a first assay performed on nanoalgosomes in regard of surface functionality.

Amino-groups on nanoalgosome surface: Amino groups on the nanoalgosome surface are originating from amino acid side chains of membrane proteins. These groups can later be utilized as an anchoring point for further functionalization. The presence of functional amino groups (-NH2) on the EVs surface was quantified by a fluorescamine assay (FA) in TFF-isolated sEVs. For the FA assay, we assumed that the diameter of sEVs is 100 nm, therefore, around 15000 ± 2500 NH2 groups per EV, which were isolated from Tetraselmis chuii, were detected. This is the first step to consider a functionalization strategy by click chemistry (Tian et al., 2018). Indeed, the presence and quantification of NH2 groups allow the conjugation of sEVs with linkers via the NHS ester reaction, e.g. NHS-PEG4-DBCO. Different biomacromolecules, e.g. CD11c antibody for dendritic cell targeting (Gai et al., 2020) or apolipoprotein A1 for brain endothelial cells targeting (Zensi et al., 2010), can be clicked on the EVs surface after their azidation (-N3 groups) via bio-orthogonal strain-promoted alkyne–azide cycloaddition (SPAAC) click chemistry reaction, where Cu (I) as a catalyst can be avoided.

3.7 Vesicle stability

Zeta-potential: Biological membranes of cells (including EV membranes) possess a negative surface charge, mainly due to the negatively charged network of glycosylated proteins intercalated within the lipid bilayer. The surface charge of EV is reflected by its zeta potential, in turn, specific populations of EVs are expected to have certain surface charges (Midekessa et al., 2020). Large differences in zeta potential values have been reported for sEVs from different body fluids, tissues or cell cultures (Beit-Yannai et al., 2018). For these highly heterogeneous lipid-bilayer nanovesicles, the surface potential of the EVs, which is measured by zeta potential, is a crucial parameter for the colloidal stability study. Furthermore, it is also a key indicator for characterizing the EVs' surface before/after functionalization with various conjugated linkers (e.g., antibody, protein, peptide) as these change the zeta potential depending on their own net charge. It also worth to point out that the surface charge of the EVs could be changed significantly while changing its dispersion phase conditions: e.g. saltwater, phosphate-buffered saline (PBS) of various phosphate ionic concentrations (0.01, 0.1, and 1 mM), with or without detergent (Tween-20), or in the presence of different salts (10 mM NaCl, KCl, CaCl2 or AlCl3) and at different pH values (Midekessa et al., 2020). The zeta potential of nanoalgosome samples TFF-isolated from Tetraselmis

RESEARCH ARTICLE

chuii cultures in neutral pH (7) buffer (KCl 0.1 M) was equal to -13 ± 12 mV, which confirms the expectation of a negative surface charge due to the presence of proteins.

Stability at different pH and temperature. DLS measurements were performed upon the same TFF isolated nanoalgosome samples buffered at different pH in the range 4–9. The size distribution of nanoalgosome sample completely unchanged over the all pH range (Supporting Figure S7), eliciting a striking stability at acidic and basic environments, which may be important for different biomedical applications. The same stability is preserved up to 50°C.

Stability in biological fluids. The stability of EVs obtained from the microalgae Tetraselmis chuii was assessed in human blood plasma after 1 h incubation at 37°C. DLS measurements were subjected to a multicomponent fitting procedure as described by Rausch et al. (2010) (Rausch et al., 2010), and showed that no aggregates were present and the analyzed nanoalgosomes were stable in blood plasma (Supporting Figure S8). This is a key prerequisite for further application in a biomedical context.

 Stability against detergents. Detergents are a powerful mean to solubilize and disassemble lipid structure. To determine the detergent resistance of the nanoalgosome membranes, we incubated the nanoalgosomes with different concentrations of SDS, Triton X-100, and Nonidet P. We then checked EV integrity by measuring the size distribution by DLS, as well as the total scattering signal, in terms of Rayleigh ratio. Our experiments show that a fraction of nanoalgosomes is destroyed upon incubation, thus giving an additional assessment to the lipid nature of the nanoalgosome envelope. Interestingly, the larger fraction of EVs resisted the incubation with detergent (Supporting Figure S9), while liposomes, prepared as a positive control, were immediately dissolved under the same conditions. This opens novel perspective to the study of EV resistance in relation to their membrane composition.

3.8 Bioactivity and cellular uptake of nanoalgosomes

Finally, after characterizing several biophysical and biochemical properties, we studied the biological activity, toxicology and cellular uptake of nanoalgosomes using a series of well-established in vitro assays.

Toxicity assays. The cytotoxicity of microalgal sEVs was evaluated by the cell viability MTS (3-(4,5-dimethylthiazol-2-yl)-5-(3-carboxymethoxyphenyl)-2-(4-sulfophenyl)-2H-tetrazolium) assay. Nanoalgosomes derived from *Tetraselmis chuii* did not show significant toxicity both on the tumorigenic MDA-MB 231 breast cancer

♦ ISEV

RESEARCH ARTICLE

cell line and on the non-tumorigenic 1–7 HB2 mammary luminal epithelial cell line, over time and at different concentration (Figure 5a). For the genotoxicity assay, we used the Acridine Orange (AO) staining. As it can be observed in Figure 5b (a-a''), 1–7 HB2 cells, treated or untreated, show a normal epithelial disposition and cell shape, with well-organized nuclear structures and no signs of DNA damage (i.e., the number of damaged red nuclei were unchanged compared to control cells). Also, MDA-MB 231 cells show uniform bright green nuclei with organized structures, similarly to the untreated cells, excluding the classical morphological changes associated with apoptotic events, also after 72 h of treatment (Figure 5b, b-b''), in agreement with the cell viability assay. Subsequently, we tested the effect of *Tetraselmis chuii* nanoalgosomes on human hepatocarcinoma cell (Hep G2 cell line), as a useful model to obtain data on any EV-effects on the metabolism of cells of hepatic origin and to assess the risk of hepatotoxicity. To this aim we analysed the in vitro hepatotoxicity by using the MTS assay (Figure 5a) and observed no significant toxic or metabolic effects induced by the microalgal sEVs on the hepatic cells, at different concentrations and over time (Figure 5a). The AO staining was used for hepato-genotoxicity evaluations, following treatment with microalgal EVs. Figure 5b (c-c'') shows the AO images of Hep G2 cells incubated with Tetraselmis chuii nanoalgosomes, for 48 or 72 h. Also in this case, we observed no genotoxic changes after nanoalgosome treatment with respect to the control ones.
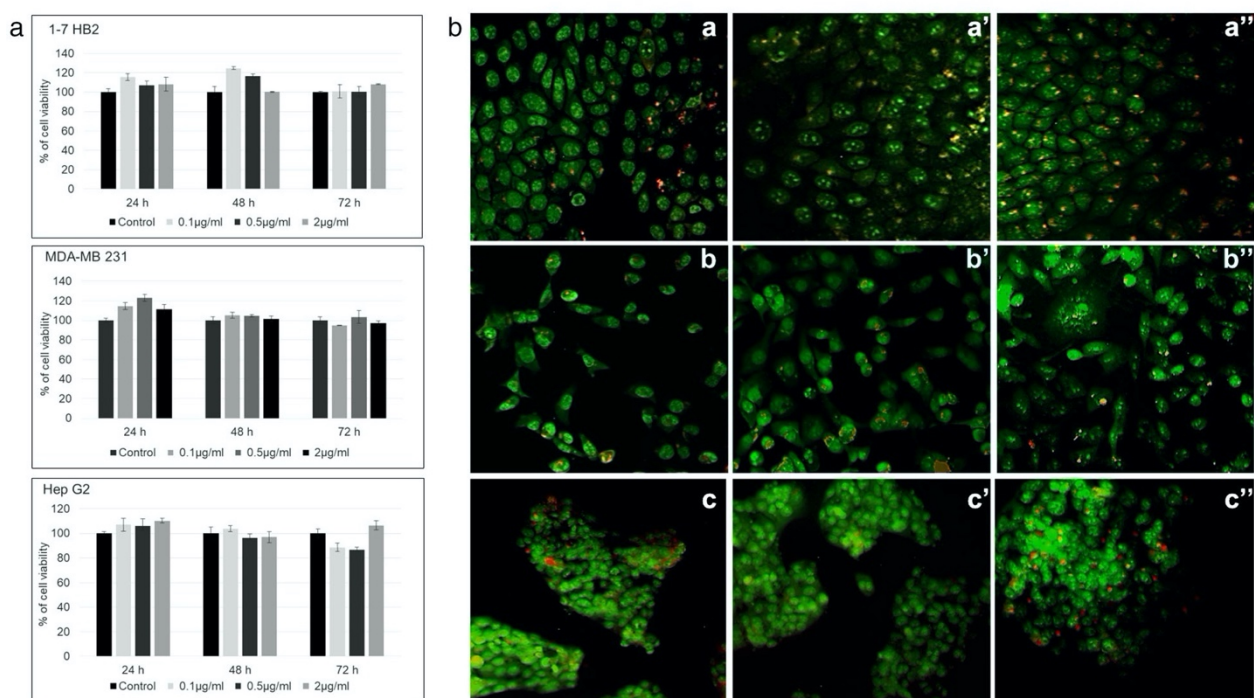
FIGURE 5 (a) Test of cytotoxicity activities of Tetraselmis chuii nanoalgosomes in: normal (1-7 HB2), tumoral (MDA-MB 231), and Hep G2 at different EVs

RESEARCH ARTICLE

concentrations (0.1-0.5-2 µg/ml) and for different time of incubation (24, 48 and 72 h). Cell viability is assessed by using MTS (3-(4,5-dimethylthiazol-2-yl)-5-(3-carboxymethoxyphenyl)-2-(4-sulfophenyl)-2H-tetrazolium) assays. Values were expressed as means ± SD of three independent experiments. By Student's t-test, differences of treated cells were determined not statistically significant when compared with the control ($p > 0.6$). (b) Genotoxicity assay by Acridine Orange staining on three different cell lines: (a) untreated 1–7 HB2, (a') 1–7 HB2 treated with 2 µg/ml Tetraselmis chuii sEVs for 48 h and (a'') 1–7 HB2 treated with 2µg/ml Tetraselmis chuii sEVs for 72 h; (b) untreated MDA-MB 231, (b') MDA-MB 231 treated with 2µg/ml Tetraselmis chuii sEVs for 48 h and (b'') MDA-MB 231 treated with 2µg/ml *Tetraselmis chuii* EVs for 72 h; (c) untreated Hep G2, (c') Hep G2 treated with 2µg/ml *Tetraselmis chuii* EVs for 48 h and (c'') Hep G2 treated with 2µg/ml Tetraselmis chuii EVs for 72 h. Representative images of three independent experiments are showed. Magnification 20X.

Cellular uptake. Once established that *Tetraselmis chuii* EVs are not cytotoxic, hepatotoxic or genotoxic at different concentrations and timing, we have determined the cross-kingdom communication among the microalgal sEVs and the human cells, by testing the cellular uptake. Cells were incubated with different concentrations of Di-8-ANEPPS-stained *Tetraselmis chuii*-derived sEVs (f-EVs) (i.e., 0.5 and 2 µg/ml) for different incubation times, namely 3, 6 and 24 h. To confirm that nanoalgosomes actively bypass cell membrane and that they were uptaken through an energy dependent mechanism, we incubated cells at 4°C, as negative control. As shown in Figure 6a, the f-EVs rapidly bypass the cellular membrane in MDA-MB 231 cells, to accumulate intracellularly after 3 h, only at the temperature of 37°C. Their distribution in the cytoplasm compartment was mostly evident after 24 h (Figure 6a, c), respect to samples incubated at 4°C in which there were no detectable fluorescence (Figure 6a, left rows). Similarly, the normal 1–7 HB2 cells have uptaken the f-EVs, although slowly (> 6 h) and in a significant lower amount (Figure 6b-c). In addition, we excluded aspecific green fluorescence by repeating the same studies using as a further negative control the dUC-isolates using not-conditioned f/2 media and stained with DI-8-ANEPPS. No fluorescence signal was detected from negative control images, for all the conditions analysed (Figure 6a-b). These results are confirmed by confocal analyses that show the intracellular localization of fluorescent nanoalgosomes in MDA-MB 231 cells (Figure 7a-d). Thus, we could conclude that both human cell lines were able to uptake nanoalgosomes in a specific dose- and time-dependent manner (Figure 6a-c, 7a-d).

RESEARCH ARTICLE
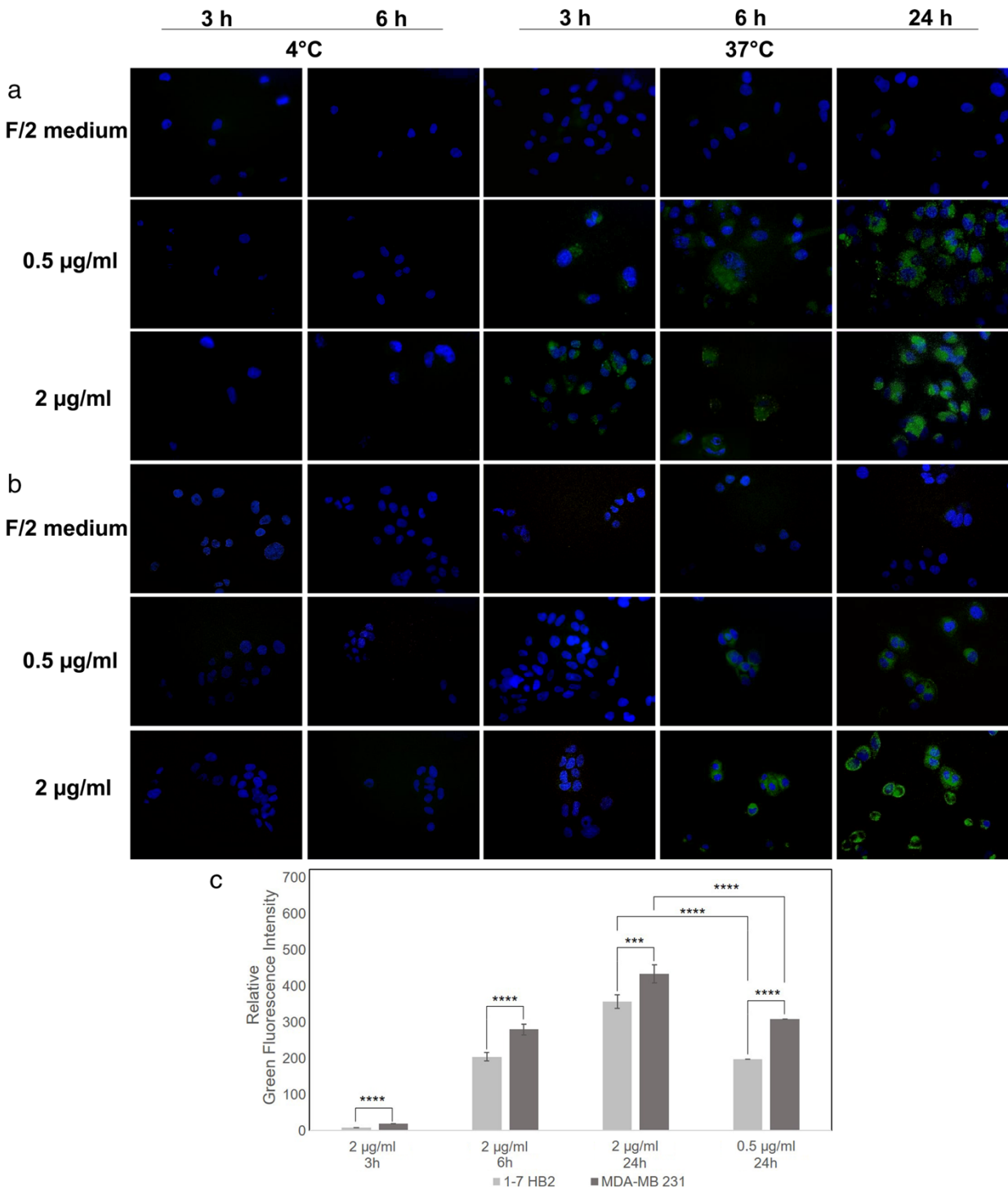
FIGURE 6 Representative fluorescence microscopy images showing the cellular uptake of Di-8-ANEPPS fluorescent nanoalgosomes (green) in MDA-MB 231 (a) and 1–7 HB2 (b) cell lines (nuclei in blue), incubated with different concentrations of f-EVs at 37°C for 3, 6 and 24 h. DUC-isolates using not-conditioned f/2 media and stained with DI-8-ANEPPS and 4°C incubation are shown as negative controls. Magnification 40X. (c) The relative green fluorescence intensities of MDA-MB 231 and 1–7 HB2 cell lines incubated with 2 μg/ml f-EVs, at 37°C for 3, 6 and 24 h, or with 0.5 μg/ml f-EVs at 37°C for 24 h are reported as relative values against the green

RESEARCH ARTICLE

fluorescent intensities of cells treated with the dUC-isolates from not-conditioned f/2 media at 37°C for 24 h. The data are presented as means ± SD (*** P < 0.001, **** P < 0.0001)
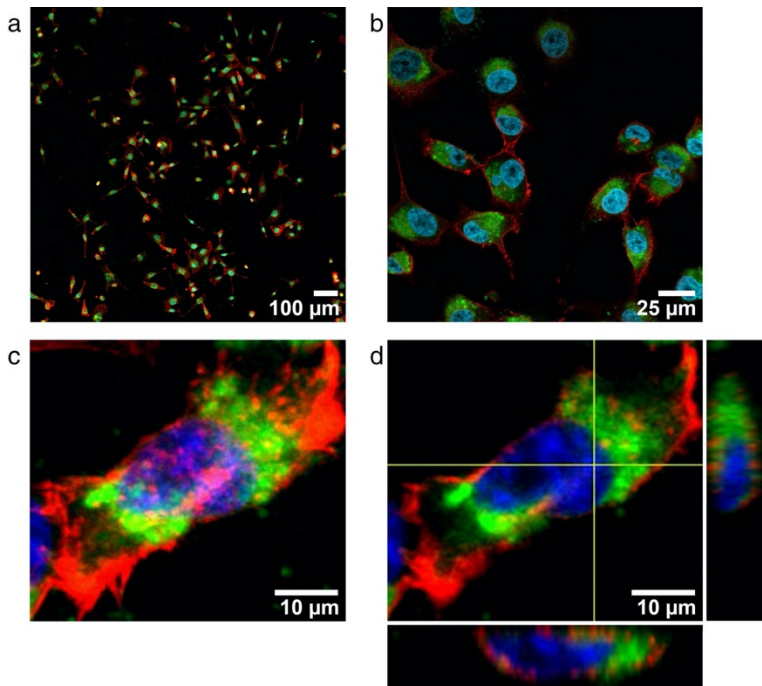
FIGURE 7 Confocal microscopy analysis of nanoalgosome internalization in MDA-MB 231 cells (nuclei stained with DAPI in blue; F-actin stained with Alexa Fluor 594 phalloidin in red), incubated with 2 μg/ml of Di-8-ANEPPS fluorescent nanoalgosomes (green) at 37°C for 24 h. (a-b) Representative confocal microscopy images showing optical mid-sections (at focal depth of 7 μm over a total scanning thickness of ∼15 μm), at 10x and 60x of magnification, respectively. (c) Representative confocal Z-stack acquisition and (d) its orthogonal projections. Scale bars are showed. Three independent biological replicas were performed.

4 Discussion

Nanoalgosomes are novel membranous biogenic nanomaterial refined for the first time from a sustainable and renewable bioresource (i.e., microalgae), which can be used as a new natural delivery system for high-value microalgal substances (such as antioxidants, pigments, lipids and complex carbohydrates), bioactive biological molecules (e.g., proteins, miRNA, siRNA, mRNA, lncRNA, peptides) and/or synthetic drugs. Different separation procedures (e.g., dUC, TFF and gUC) allowed to isolate nanoalgosomes from the Tetraselmis chuii-conditioned media. As experimentally demonstrated by their sensitivity to the detergent SDS and their positivity to the membrane staining with Di-8-ANEPPS, we could conclude that nanoalgosomes are biogenic lipidic membranous nanovesicles. They contain one or more established EV protein markers, such as Alix

RESEARCH ARTICLE

and the additional protein marker, plasma membrane H+/ATPase, and can be efficiently and safely taken up by mammalian cells, confirming the cross kingdom communication potential of EVs (Gill et al., 2019). The study presented here is promising in using nanoalgosomes in therapy. Also, future in vivo, pre-clinical and clinical testing would allow to evaluate whether nanoalgosomes are not toxic, low immunogenic, and well-tolerated by the organism. Further, their engineering is already ongoing to confer targetability feature to specific cell or tissue. Also, we have been able to isolate EV-like nanoparticles from several microalgae strains. In particular, nanoalgosomes were purified and characterized from two other strains: the *Tetraselmis chuii*-related chlorophyte *Dunaliella tertiolecta*, and the distant phytoplankton group dinoflagellate *Amphidinium sp.* (Supporting Figure S10). Despite the polyphyletic origin, we can conclude that the nanoalgosome production is an evolutionary conserved trait within this heterogeneous group of protistean organisms. It is well known that EVs constitute vehicles for inter-organisms communication. For instance, bacterial EVs perform several functions, including molecular transport, mediation of stress response, biofilm formation and the influence on hosts (Bleackley et al., 2020; Cai et al., 2018; Gill et al., 2019; Muraca et al., 2015; Soares et al., 2017; Yáñez-Mó et al., 2015). Vesicle release has been also observed in a variety of cultured marine cyanobacteria (Biller et al., 2014). Further, field studies demonstrated that in natural environments, such as the aquatic ecosystem, bacterial-derived extracellular vesicles are abundant, and they likely play a role in the ecology of marine microbial ecosystems (Biller et al., 2014). It has been postulated that the cyanobacteria vesicles can serve as food parcels for marine organisms and/or as a defence agent against phage attack (cellular decoys), and with implications for marine carbon cycling, mechanisms of horizontal gene transfer (Biller et al., 2014). The concentration of vesicles would vary from place to place in ocean ecosystems, reflecting the balance between species-specific production rates, degradation rates, and consumption rates by the marine food web. In this context, future studies may help to establish the biological function of the extracellular vesicles produced by microalgae, the most abundant primary unicellular organism found in all the aquatic systems. The use of microalgae as a natural source for EVs would provide a number of advantages. Indeed, the metabolic attributes of microalgae are actively researched worldwide to address strategic priorities, with a particular focus on biofuel generation, bioremediation developments and biosynthesis of high-added value biochemicals (Blanch, 2012; Khozin-Goldberg et al., 2016; Pulz & Gross, 2004; Sun et al., 2013; Yáñez-Mó et al., 2015). Recent advances in microalgal biotechnology have generated much optimism for a viable industrial production of microalgae-derived compounds such as antioxidants or

ISEV

RESEARCH ARTICLE

omega-3 polyunsaturated fatty acids. Nanoalgosomes presented here would offer a number of advantages compared to mammalian cell-, plant-, bacteria-, and milk-derived EVs in that microalgae cells have high growth rates, can be cultured on non-arable land under controlled environmental conditions in large scale photobioreactors and produce nanoalgosomes with a yield comparable to other sources (Bitto & Kaparakis-Liaskos, 2017; Gerritzen et al., 2017; Kim et al., 2015; Munagala et al., 2016; Paganini et al., 2019) (Figure 8; Pocsfalvi et al., 2018; Raimondo et al., 2015; Wang et al., 2013). In addition, the natural and sustainable origin of nanoalgosomes grants them a likely greater societal acceptance (with reduced sensitive ethical questions) as a source for formulation preparations.
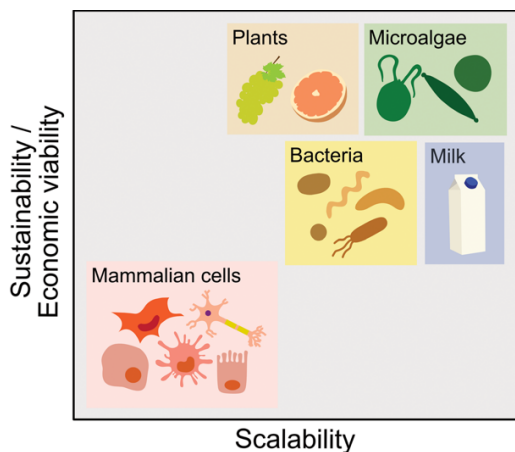
FIGURE 8.The scalability, sustainability and economical viability of nanoalgosome production compared to the most common sources of therapeutic vesicles. [The ranking represents an arbitrary evaluation based on the analysis of the nanoalgosome production in the context of current bioprocesses (Paganini et al., 2019)]

DISCLOSURE STATEMENT

ISEV

The authors report no conflict of interest.

References

1. Beit-Yannai, E. , Tabak, S. , & Stamer, W. D. (2018). Physical exosome: eXosome interactions. *Journal of Cellular and Molecular Medicine*, 22, 2001–2006. 10.1111/jcmm.13479 [PMC free article] [PubMed] [CrossRef] [Google Scholar]

2. Biller, S. J. , Schubotz, F. , Roggensack, S. E. , Thompson, A. W. , Summons, R. E. , & Chisholm, S. W. (2014). Bacterial vesicles in marine ecosystems. *Science*, 343(6167), 183–186. 10.1126/science.1243457 [PubMed] [CrossRef] [Google Scholar]

3. Bitto, N. , & Kaparakis-Liaskos, M. (2017). The Therapeutic Benefit of Bacterial Membrane Vesicles. *International Journal of Molecular Sciences*, 18(6), 1287. 10.3390/ijms18061287 [PMC free article] [PubMed] [CrossRef] [Google Scholar]

4. Blanch, H. W. (2012). Bioprocessing for biofuels. *Current Opinion in Biotechnology*, 23(3), 390–395. 10.1016/j.copbio.2011.10.002 [PubMed] [CrossRef] [Google Scholar]

5. Bleackley, M. R. , Samuel, M. , Garcia-Ceron, D. , Mckenna, J. A. , Lowe, R. G. T. , Pathan, M. , Zhao, K. , Ang, C.-S. , Mathivanan, S. , & Anderson, M. A. (2020). Extracellular Vesicles From the Cotton Pathogen Fusarium oxysporum f. sp. vasinfectum Induce a Phytotoxic Response in Plants. *Frontiers in plant science*, 10, 1610. 10.3389/fpls.2019.01610 [PMC free article] [PubMed] [CrossRef] [Google Scholar]

6. Busatto, S. , Vilanilam, G. , Ticer, T. , Lin, W.-L. , Dickson, D. , Shapiro, S. , Bergese, P. , & Wolfram, J. (2018). Tangential flow filtration for highly efficient concentration of extracellular vesicles from large volumes of fluid. *Cells*, 7(12), 273. 10.3390/cells7120273. [PMC free article] [PubMed] [CrossRef] [Google Scholar]

7. Cai, Q. , Qiao, L. , Wang, M. , He, B. , Lin, F.-M. , Palmquist, J. , Huang, S.-D. , & Jin, H. (2018). Plants send small RNAs in extracellular vesicles to fungal pathogen to silence virulence genes. *Science*, 360(6393), 1126–1129. 10.1126/science.aar4142 [PMC free article] [PubMed] [CrossRef] [Google Scholar]

8. Cuellar-Bermudez, S. P. , Aguilar-Hernandez, I. , Cardenas-Chavez, D. L. , Ornelas-Soto, N. , Romero-Ogawa, M. A. , & Parra-Saldivar, R. (2015). Extraction and purification of high-value metabolites from microalgae: Essential lipids, astaxanthin and phycobiliproteins. *Microbial Biotechnology*, 8, 190–209.

ISEV

RESEARCH ARTICLE

10.1111/1751-7915.12167 [PMC free article] [PubMed] [CrossRef] [Google Scholar]

9. Dhondt, B. , Geeurickx, E. , Tulkens, J. , Van Deun, J. , Vergauwen, G. , Lippens, L. , Miinalainen, I. , Rappu, P. , Heino, J. , Ost, P. , Lumen, N. , De Wever, O. , & Hendrix, A. (2020). Unravelling the proteomic landscape of extracellular vesicles in prostate cancer by density-based fractionation of urine. *Journal of Extracellular Vesicles*, 9, 1736935. 10.1080/20013078.2020.1736935. [PMC free article] [PubMed] [CrossRef] [Google Scholar]

10. Friedl, T. , Rybalka, N. , & Kryvenda, A. (2021). Phylogeny and systematics of microalgae: An overview. *Microalgal Biotechnology: Potential and Production*, 11–38. 10.1515/9783110225020.11 [CrossRef] [Google Scholar]

11. Gai, M. , Simon, J. , Lieberwirth, I. , Mailänder, V. , Morsbach, S. , & Landfester, K. (2020). A bio-orthogonal functionalization strategy for site-specific coupling of antibodies on vesicle surfaces after self-assembly. *Polymer Chemistry*, 11(2), 527–540. 10.1039/C9PY01136F [CrossRef] [Google Scholar]

12. Gerritzen, M. J.H. , Martens, D. E. , Wijffels, R. H. , Van Der Pol, L. , & Stork, M. (2017). Bioengineering Bacterial Outer Membrane Vesicles as Vaccine Platform. *Biotechnology Advances*, 35(5), 565–574. 10.1016/j.biotechadv.2017.05.003 [PubMed] [CrossRef] [Google Scholar]

13. Gill, S. , Catchpole, R. , & Forterre, P. (2019). Extracellular membrane vesicles in the three domains of life and beyond, *FEMS Microbiology Reviews*, 43(3), 273–303. 10.1093/femsre/fuy042 [PMC free article] [PubMed] [CrossRef] [Google Scholar]

14. Guillard, R. R. L. (1975). *Culture of Phytoplankton for Feeding Marine Invertebrates, Culture of Marine Invertebrate Animals*. Boston, MA: Springer US; 29–60. 10.1007/978-1-4615-8714-9_3 [CrossRef] [Google Scholar]

15. György, B. , Hung, M. E. , Breakefield, X. O. , & Leonard, J. N. (2015). Therapeutic applications of extracellular vesicles: Clinical promise and open questions. *Annual Review of Pharmacology and Toxicology*, 55, 439–464. 10.1146/annurev-pharmtox-010814-124630 [PMC free article] [PubMed] [CrossRef] [Google Scholar]

16. Han, X. , Yang, Y. , Wu, Y. , Liu, X. , Lei, X. , & Guo, Y. (2017). A bioassay-guided fractionation system to identify endogenous small molecules that activate plasma membrane H+-ATPase activity in Arabidopsis. *Journal of Experimental Botany*, 68(11), 2951–2962. 10.1093/jxb/erx156. [PMC free article] [PubMed] [CrossRef] [Google Scholar]

ISEV

RESEARCH ARTICLE

17. Khan, M. I. , Shin, J. H. , & Kim, J. D. (2018). The promising future of microalgae: Current status, challenges, and optimization of a sustainable and renewable industry for biofuels, feed, and other products. *Microbial cell factories*, 17(1), 36. 10.1186/s12934-018-0879-x [PMC free article] [PubMed] [CrossRef] [Google Scholar]

18. Khozin-Goldberg, I. , Leu, S. , & Boussiba, S. (2016). Microalgae as a source for VLC-PUFA production. *Subcellular biochemistry*, 86, 471–510. 10.1007/978-3-319-25979-6_19 [PubMed] [CrossRef] [Google Scholar]

19. Kim, J. H. , Lee, J. , Park, J. , & Gho, Y. S. (2015). Gram-negative and Gram-positive bacterial extracellular vesicles. *Seminars in Cell & Developmental Biology*, 40, 97–104. 10.1016/j.semcdb.2015.02.006 [PubMed] [CrossRef] [Google Scholar]

20. Kosaka, N. , Kogure, A. , Yamamoto, T. , Urabe, F. , Usuba, W. , Prieto-Vila, M. , & Ochiya, T. (2019). Exploiting the message from cancer: The diagnostic value of extracellular vesicles for clinical applications. *Experimental & Molecular Medicine*, 51, 1–9. 10.1038/s12276-019-0219-1 [PMC free article] [PubMed] [CrossRef] [Google Scholar]

21. Lešer, V. , Drobne, D. , Pipan, Ž. , Milani, M. , & Tatti, F. (2009). Comparison of different preparation methods of biological samples for FIB milling and SEM investigation. *Journal of Microscopy*, 233, 309–319. 10.1111/j.1365-2818.2009.03121.x [PubMed] [CrossRef] [Google Scholar]

22. Leu, S. , & Boussiba, S. (2014). Advances in the production of high-value products by microalgae. *Industrial Biotechnology*, 10, 169–183. 10.1089/ind.2013.0039 [CrossRef] [Google Scholar]

23. Liguori, G. , & Kisslinger, A. (2020). Standardization and reproducibility in EV research: The support of a Quality management system. Biological membrane vesicles: Scientific, biotechnological and clinical considerations, *Advances in Biomembranes and Lipid Self-Assembly*, 202032. 10.1016/bs.abl.2020.05.005 [CrossRef] [Google Scholar]

24. Maacha, S. , Bhat, A. A. , Jimenez, L. , Raza, A. , Haris, M. , Uddin, S. , & Grivel, J.-C. (2019). Extracellular vesicles-mediated intercellular communication: Roles in the tumor microenvironment and anti-cancer drug resistance. *Molecular Cancer [Electronic Resource]*, 18(1), 55. 10.1186/s12943-019-0965-7 [PMC free article] [PubMed] [CrossRef] [Google Scholar]

25. Mailer, A. G. , Clegg, P. S. , & Pusey, P. N. (2015). Particle sizing by dynamic light scattering: Non-linear cumulant analysis. *Journal of Physics: Condensed*

∂ ISEV

RESEARCH ARTICLE

Matter, 27,   145102.   10.1088/0953-8984/27/14/145102   [PubMed] [CrossRef] [Google Scholar]

26. Mc Gee, D. , Archer, L. , Paskuliakova, A. , Mc Coy, G. R. , Fleming, G. T. A. , Gillespie, E. , & Touzet, N. (2018). Rapid chemotaxonomic profiling for the identification of high-value carotenoids in microalgae. *Journal of Applied Phycology*, 30,   385–399.   10.1007/s10811-017-1247-7   [CrossRef] [Google Scholar]

27. Midekessa, G. , Godakumara, K. , Ord, J. , Viil, J. , Lättekivi, F. , Dissanayake, K. , Kopanchuk, S. , Rinken, A. , Andronowska, A. , Bhattacharjee, S. , Rinken, T. , & Fazeli, A. (2020). Zeta Potential of Extracellular Vesicles: Toward Understanding the Attributes that Determine Colloidal Stability. *ACS Omega*, 5(27), 16701–16710.   10.1021/acsomega.0c01582 [PMC free article] [PubMed] [CrossRef] [Google Scholar]

28. Montis, C. , Zendrini, A. , Valle, F. , Busatto, S. , Paolini, L. , Radeghieri, A. , Salvatore, A. , Berti, D. , & Bergese, P. (2017). Size distribution of extracellular vesicles by optical correlation techiniques. *Journal of Colloid and Interface Science*, 158,   331–338.   10.1016/j.colsurfb.2017.06.047   [PubMed] [CrossRef] [Google Scholar]

29. Moriyama, Y. , Maeda, M. , & Futai, M. (1992). The role of V-ATPase in neuronal and endocrine systems. *Journal of Experimental Biology*, 172, 171–178. [PubMed] [Google Scholar]

30. Munagala, R. , Aqil, F. , Jeyabalan, J. , & Gupta, R. C. (2016). Bovine Milk-Derived Exosomes   for   Drug   Delivery. *Cancer   Letters*, 371(1),   48–61. 10.1016/j.canlet.2015.10.020 [PMC free article] [PubMed] [CrossRef] [Google Scholar]

31. Muraca, M. , Putignani, L. , Fierabracci, A. , Teti, A. , & Perilongo, G. (2015). Gut microbiotaderived outer membrane vesicles: Under-recognized major players in health and disease? *Discovery Medicine*, 19(106), 343–348. [PubMed] [Google Scholar]

32. Noto, R. , Santangelo, M. G. , Ricagno, S. , Mangione, M. R. , Levantino, M. , Pezzullo, M. , Martorana, V. , Cupane, A. , Bolognesi, M. , & Manno, M. (2012). The tempered polymerisation of human neuroserpin. *PLoS One*, 7, e32444. 10.1371/journal.pone.0032444 [PMC free article] [PubMed] [CrossRef] [Google Scholar]

33. Paganini, C. , Capasso Palmiero, U. , Pocsfalvi, G. , Touzet, N. , Bongiovanni, A. , & Arosio, P. (2019). Scalable Production and Isolation of Extracellular Vesicles:AVailable   Sources   and   Lessons   from   Current   Industrial

ò ISEV

RESEARCH ARTICLE

Bioprocesses. *Biotechnology Journal*, 14(10), 1800528. 10.1002/biot.201800528 [PubMed] [CrossRef] [Google Scholar]

34. Pánek, J. , Loukotová, L. , Hrubý, M. , & Štěpánek, P. (2018). Distribution of Diffusion Times Determined by Fluorescence (Lifetime) Correlation Spectroscopy. *Macromolecules*, 51(8), 2796–2804. 10.1021/acs.macromol.7b02158 [CrossRef] [Google Scholar]

35. Paolini, L. , Federici, S. , Consoli, G. , Arceri, D. , Radeghieri, A. , Alessandri, I. , & Bergese, P. (2020). Fourier-transform Infrared (FT-IR) spectroscopy fingerprints subpopulations of extracellular vesicles of different sizes and cellular origin, *Journal of Extracellular Vesicles*, 9(1), 1741174. 10.1080/20013078.2020.1741174 [PMC free article] [PubMed] [CrossRef] [Google Scholar]

36. Pathare, G. , Dhayat, N. A. , Mohebbi, N. , Wagner, C. A. , Bobulescu, I. A. , Moe, O. W. , & Fuster, D. G. (2018). Changes in V-ATPase subunits of human urinary exosomes reflect the renal response to acute acid/alkali loading and the defects in distal renal tubular acidosis. *Kidney International*, 93(4), 871–880. 10.1016/j.kint.2017.10.018 [PMC free article] [PubMed] [CrossRef] [Google Scholar]

37. Pereira, H. , Silva, J. , Santos, T. , Gangadhar, K. N. , Raposo, A. , Nunes, C. , Coimbra, M. A. , Gouveia, L. , Barreira, L. , & Varela, J. (2019). Nutritional Potential and Toxicological Evaluation of sp. CTP4 Microalgal Biomass Produced in Industrial Photobioreactors. *Molecules (Basel, Switzerland)*, 24(17), 3192. 10.3390/molecules24173192 [PMC free article] [PubMed] [CrossRef] [Google Scholar]

38. Pertl-Obermeyer, H. , Lackner, P. , Schulze, W. X. , Hoepflinger, M. C. , Hoeftberger, M. , Foissner, I. , & Obermeyer, G. (2018). Dissecting the subcellular membrane proteome reveals enrichment of H+ (co-)transporters and vesicle trafficking proteins in acidic zones of Chara internodal cells. *PLoS One*, 13(8), e0201480. 10.1371/journal.pone.0201480 [PMC free article] [PubMed] [CrossRef] [Google Scholar]

39. Pocsfalvi, G. , Turiák, L. , Ambrosone, A. , Del Gaudio, P. , Puska, G. , Fiume, I. , Silvestre, T. , & Vékey, K. (2018). Protein Biocargo of Citrus Fruit-Derived Vesicles Reveals Heterogeneous Transport and Extracellular Vesicle Populations. *Journal of Plant Physiology*, 229, 111–121. 10.1016/j.jplph.2018.07.006 [PubMed] [CrossRef] [Google Scholar]

40. Prima, G. D , Librizzi, F. , & Carrotta, R. (2020). Light Scattering as an Easy Tool to Measure Vesicles Weight Concentration. *Membranes*, 10, 222.

ᴊISEV

RESEARCH ARTICLE

10.3390/membranes10090222 [PMC free article] [PubMed] [CrossRef] [Google Scholar]

41. Pulz, O. , & Gross, W. (2004). Valuable products from biotechnology of microalgae. *Applied Microbiology and Biotechnology*, 65(6), 635–648. [PubMed] [Google Scholar]

42. Raimondo, S. , Naselli, F. , Fontana, S. , Monteleone, F. , Lo Dico, A. , Saieva, L. , Zito, G. , Flugy, A. , Manno, M. , Di Bella, M. A. , De Leo, G. , & Alessandro, R. (2015). Citrus Limon-Derived Nanovesicles Inhibit Cancer Cell Proliferation and Suppress CML Xenograft Growth by Inducing TRAIL-Mediated Cell Death. *Oncotarget*, 6(23), 19514–19527. 10.18632/oncotarget.4004 [PMC free article] [PubMed] [CrossRef] [Google Scholar]

43. Rausch, K. , Reuter, A. , Fischer, K. , & Schmidt, M. (2010). Evaluation of nanoparticle aggregation in human blood serum. *Biomacromolecules*, 11(11), 2836–2839. 10.1021/bm100971q [PubMed] [CrossRef] [Google Scholar]

44. Ridolfi, A. , Brucale, M. , Montis, C. , Caselli, L. , Paolini, L. , Borup, A. , Boysen, A. T. , Loria, F. , Van Herwijnen, M. J. C. , Kleinjan, M. , Nejsum, P. , Zarovni, N. , Wauben, M. H. M. , Berti, D. , Bergese, P. , & Valle, F. (2020). AFM-Based High-Throuput Nanomechanical Screening of Single Extracellular Vesicles. *Analytical Chemistry*, 92, 10274–10282. 10.1021/acs.analchem.9b05716 [PubMed] [CrossRef] [Google Scholar]

45. Ries, J. , & Schwille, P. (2012). Fluorescence Correlation Spectroscopy. *Bioessays*, 34, 361–368. 10.1002/bies.201100111. [PubMed] [CrossRef] [Google Scholar]

46. Romancino, D. P. , Paterniti, G. , Campos, Y. , De Luca, A. , Di Felice, V. , D'azzo, A. , & Bongiovanni, A. (2013). Identification and characterization of the nano-sized vesicles released by muscle cells. *FEBS Letters*, 587, 1379–1384. 10.1016/j.febslet.2013.03.012 [PMC free article] [PubMed] [CrossRef] [Google Scholar]

47. Ryckebosch, E. , Muylaert, K. , & Foubert, I. (2012). Optimization of an Analytical Procedure for Extraction of Lipids from Microalgae. *Journal of the American Oil Chemists Society*, 89, 189–198. 10.1007/s11746-011-1903-z [CrossRef] [Google Scholar]

48. Schmitz, K. S. (1990). *An Introduction to Dynamic Light Scattering by Macromolecules*. Academic Press, Inc. ISBN: 9780323140355 [Google Scholar]

49. Shaimardanova, A. , Solovyeva, V. , Chulpanova, D. , James, V. , Kitaeva, K. , & Rizvanov, A. (2020). Extracellular vesicles in the diagnosis and treatment of central

RESEARCH ARTICLE

ISEV

nervous system diseases. *Neural Regeneration Research*, 15(4), 586–596. 10.4103/1673-5374.266908 [PMC free article] [PubMed] [CrossRef] [Google Scholar]

50. Soares, R. P. , Xander, P. , Costa, A. O. , Marcilla, A. , Menezes-Neto, A. , Del Portillo, H. , Witwer, K. , Wauben, M. , Nolte-`T Hoen, E. , Olivier, M. , Criado, M. F. , Da Silva, L. L. P. , Abdel Baqui, M. M. , Schenkman, S. , Colli, W. , Alves, M. J. M. , Ferreira, K. S. , Puccia, R. , Nejsum, P. … Torrecilhas, A. C. (2017). Highlights of the São Paulo ISEV workshop on extracellular vesicles in cross-kingdom communication. *Journal of Extracellular Vesicles*, 6(1), 1407213. 10.1080/20013078.2017.1407213 [PMC free article] [PubMed] [CrossRef] [Google Scholar]

51. Stevens, T. H. , & Forgac, M. (1997). Structure, function and regulation of the vacuolar (H+)-ATPase. *Annual Review of Cell and Developmental Biology*, 13, 779–808. 10.1146/annurev.cellbio.13.1.779 [PubMed] [CrossRef] [Google Scholar]

52. Sun, H. , Zhao, W. , Mao, X. , Li, Y. , Wu, T. , & Chen, F. (2013). Use of organic waste from the brewery industry for high-density cultivation of the docosahexaenoic acid-rich microalga, Aurantiochytrium sp. KRS101. *Bioresource Technology*, 11, 351–359. 10.1186/s13068-018-1253-2 [PubMed] [CrossRef] [Google Scholar]

53. Sverdlov, E. D. (2012). Amedeo Avogadro's cry: What is 1 μg of exosomes? *Bioessay*, 34, 873–875. 10.1002/bies.201200045 [PubMed] [CrossRef] [Google Scholar]

54. Théry, C. , Amigorena, S. , Raposo, G. , & Clayton, A. (2006). Isolation and Characterization of Exosomes from Cell Culture Supernatants and Biological Fluids. *Current Protocols in Cell Biology*, 30, 3.22.1–3.22.29. 10.1002/0471143030.cb0322s30 [PubMed] [CrossRef] [Google Scholar]

55. Théry, C. , Witwer, K. W. , Aikawa, E. , Alcaraz, M. J. , Anderson, J. D. , Andriantsitohaina, R. , Antoniou, A. , Arab, T. , Archer, F. , Atkin-Smith, G. K. , Ayre, D. C. , Bach, J.-M. , Bachurski, D. , Baharvand, H. , Balaj, L. , Baldacchino, S. , Bauer, N. N. , Baxter, A. A. , Bebawy, M. … Zuba-Surma, E. K. (2018). Minimal information for studies of extracellular vesicles 2018 (MISEV2018): A position statement of the International Society for Extracellular Vesicles and update of the MISEV2014 guidelines, *Journal of Extracellular Vesicles*, 7, 1535750. 10.1080/20013078.2018.1535750 [PMC free article] [PubMed] [CrossRef] [Google Scholar]

56. Tian, T. , Zhang, H.-X. , He, C.-P. , Fan, S. , Zhu, Y.-L. , Qi, C. , Huang, N.-P. , Xiao, Z.-D. , Lu, Z.-H. , Tannous, B. A. , & Gao, J. (2018). Surface functionalized

ISEV

RESEARCH ARTICLE

exosomes as targeted drug delivery vehicles for cerebral ischemia therapy. *Biomaterials*, 150, 137–149. 10.1016/j.biomaterials.2017.10.012 [PubMed] [CrossRef] [Google Scholar]

57. Urbanelli, L. , Buratta, S. , & Tancini, B. et al. (2019). The Role of Extracellular Vesicles in Viral Infection and Transmission. *Vaccines (Basel)*, 7(3), 102. 10.3390/vaccines7030102 [PMC free article] [PubMed] [CrossRef] [Google Scholar]

58. Van Deun, J. , Mestdagh, P. , Agostinis, P. , Akay, Ö. , Anand, S. , Anckaert, J. , Martinez, Z. A. , Baetens, T. , Beghein, E. , Bertier, L. , Berx, G. , Boere, J. , Boukouris, S. , Bremer, M. , Buschmann, D. , Byrd, J. B. , Casert, C. , Cheng, L. , Cmoch, A. … Hendrix, A. (2017). EV-TRACK: Transparent reporting and centralizing knowledge in extracellular vesicle research. *Nature Methods*, 14, 228–232. 10.1038/nmeth.4185 [PubMed] [CrossRef] [Google Scholar]

59. Wang, Q. , Zhuang, X. , Mu, J. , Deng, Z.-B. , Jiang, H. , Zhang, L. , Xiang, X. , Wang, B. , Yan, J. , Miller, D. , & Zhang, H.-G. (2013). Delivery of Therapeutic Agents by Nanoparticles Made of Grapefruit-Derived Lipids. *Nature Communications*, 4(1), 1867. 10.1038/ncomms2886 [PMC free article] [PubMed] [CrossRef] [Google Scholar]

60. Yáñez-Mó, M. , Siljander, P. R.-M. , Andreu, Z. , Bedina Zavec, A. , Borràs, F. E. , Buzas, E. I. , Buzas, K. , Casal, E. , Cappello, F. , Carvalho, J. , Colás, E. , Cordeiro-Da Silva, A. , Fais, S. , Falcon-Perez, J. M. , Ghobrial, I. M. , Giebel, B. , Gimona, M. , Graner, M. , Gursel, I. … De Wever, O. (2015). Biological properties of extracellular vesicles and their physiological functions. *Journal of Extracellular Vesicles*, 4, 27066. 10.3402/jev.v4.27066 [PMC free article] [PubMed] [CrossRef] [Google Scholar]

61. Zensi, A. , Begley, D. , Pontikis, C. , Legros, C. , Mihoreanu, L. , Büchel, C. , & Kreuter, J. (2010). Human serum albumin nanoparticles modified with apolipoprotein A-I cross the blood-brain barrier and enter the rodent brain. *Journal of Drug Targeting*, 18(10), 842–848. 10.3109/1061186X.2010.513712. [PubMed] [CrossRef] [Google Scholar]

62. Zhang, S. , Habets, M. , Breuninger, H. , Dolan, L. , Offringa, R. , & Van Duijn, B. (2019). Evolutionary and functional analysis of a plasma membrane H-ATPase. *Frontiers in Plant Science*, 10, 1707. 10.3389/fpls.2019.01707 [PMC free article] [PubMed] [CrossRef] [Google Scholar]

63. Zhu, L. (2015). Biorefinery as a promising approach to promote microalgae industry: An innovative framework. *Renewable and Sustainable Energy Reviews*, 41, 1376–1384. 10.1016/j.rser.2014.09.040 [CrossRef] [Google Scholar]

RESEARCH ARTICLE

64. Zipkin, M. (2019). Exosome redux *Nature Biotechnology*, 37, 1395–1400. 10.1038/s41587-019-0326-5 [PubMed] [CrossRef] [Google Scholar]

frontiers
in Bioengineering and Biotechnology

Check for
updates

Chapter 5

Isolation of Extracellular Vesicles From Microalgae: A Renewable and Scalable Bioprocess

Paterna A, Rao E, Adamo G, Raccosta S**, Picciotto S**, Romancino D, Noto R, Touzet N, Bongiovanni A, Manno M. Front Bioeng Biotechnol. 2022 Mar 14;10:836747. doi: 10.3389/fbioe.2022.836747. PMID: 35360396; PMCID: PMC8963918.

104

Abstract

Extracellular vesicles (EVs) play a crucial role as potent signal transducers among cells, with the potential to operate cross-species and cross-kingdom communication. Nanoalgosomes are a subtype of EVs recently identified and isolated from microalgae. Microalgae represent a natural bioresource with the capacity to produce several secondary metabolites with a broad range of biological activities and commercial applications. The present study highlights the upstream and downstream processes required for the scalable production of nanoalgosomes from cultures of the marine microalgae *Tetraselmis chuii*. Different technical parameters, protocols, and conditions were assessed to improve EVs isolation by tangential flow filtration (TFF), aiming to enhance sample purity and yield. The optimization of the overall bioprocess was enhanced by quality control checks operated through robust biophysical and biochemical characterizations. Further, we showed the possibility of recycling by TFF microalgae cells post-EVs isolation for multiple EV production cycles. The present results highlight the potential of nanoalgosome production as a scalable, cost-effective bioprocess suitable for diverse scientific and industrial exploitations.

1 Introduction

Extracellular vesicles (EVs) are a diverse group of membranous nanoparticles originated from cells and involved in several biological processes (Yáñez-Mó et al., 2015; Margolis and Sadovsky, 2019). EVs perform specific and selective cargo release to cells or target tissues via different mechanisms, including endocytosis, fusion, or receptor interaction, and in general they take part in intercellular signal transduction (Van Niel et al., 2018; Raposo and Stahl, 2019; Limongi et al., 2021a). Beyond their physiological functions, EVs have a role in several diseases, including cancer (Vagner et al., 2018; Raimondi et al., 2020), and in numerous pathological conditions, for instance, in stimulating an immune response (Zhou et al., 2020) or intervening in multidrug resistance in cancer treatments (Samuel et al., 2017; Pasini and Ulivi, 2020) and in virus infections and transmission (Urbanelli et al., 2019; Pocsfalvi et al., 2020). Due to their intrinsic capability to vehicle biological materials and information, EVs have high potential as drug delivery systems (Armstrong and Stevens, 2018; Kooijmans et al., 2021). Indeed, there is an increasing interest to exploit EVs as therapeutics (Witwer et al., 2019; Silva et al., 2021; Limongi et al., 2021b) and in a large variety of biotechnological applications (Paganini et al., 2019). A growing interest is also arising from the study and exploitation of EVs or, more in general, of micro- and nano-sized vesicles, derived from non-human sources, such as bacteria (Bitto and Kaparakis-Liaskos, 2017), bovine milk (Kleinjan et al., 2021; Samuel et al., 2021), and edible plants (Wang et al., 2014; Raimondo et al., 2015; Bokka et al., 2020; Stanly et al., 2020; Raimondo et al., 2021). In particular, plant-derived vesicles are currently considered as biocompatible, sustainable, green, next-generation nanocarriers (Kameli et al., 2021; Urzì et al., 2021). In such a context, we recently identified microalgae as a novel natural source of EVs, called nanoalgosomes or simply algosomes (Adamo et al., 2021; Picciotto et al., 2021). Microalgae are microorganisms (mostly photosynthetic and autotrophic) considered a promising source of natural bioactive macromolecules such as pigments, polyunsaturated fatty acids, vitamins, and polysaccharides (Cuellar-Bermudez et al., 2015; Khan et al., 2018). These compounds are well known to possess a wide range of biological functions including antioxidant, antibacterial, antiviral, and anticancer activities. Microalgae operate the biosynthesis of numerous health beneficial compounds; thus, they are exploitable as natural ingredients in functional foods or cosmetics, with a corresponding attention from industries (Caporgno and Mathys, 2018; Khan et al., 2018; Jacob-Lopes et al., 2019; Morocho-Jácome et al., 2020). In our previous studies, we evaluated different

microalgal species for their capability to produce EVs (Picciotto et al., 2021) and we identified the marine chlorophyte microalga *Tetraselmis chuii (T. chuii)* as one of the most promising biosource for a large-scale production of EVs (Adamo et al., 2021). Beyond its capability to produce EVs with a high yield, *T. chuii* has also an interesting content of valuable natural pigments, including lutein and *β*-carotene (Picciotto et al., 2021), and it has been approved as a novel food for human consumption (European Commission, 2017). Nanoalgosomes exhibit remarkable benefits in comparison with EVs derived from other sources, such as mammalian cells, plant, bacteria, or milk, since microalgae are a non-animal, sustainable biosource and also a fast-growing organism that can be easily cultured in large scale under controlled conditions (Adamo et al., 2021). In the present work, we focus on the isolation of nanoalgosomes and we optimize an efficient bioprocess for a sustainable, scalable, and renewable EVs production, along with a robust quality control procedure, as defined in our previous work (Adamo et al., 2021) in accord to the guidelines and the consensus from the scientific community (Théry et al., 2018). A cost-effective and reliable EVs production, which is also suitable for an industrial or large scale exploitation, requires a fine tuning of both upstream and downstream processes (Paganini et al., 2019; Buschmann et al., 2021; Grangier et al., 2021; Staubach et al., 2021). Here, we discuss and define a clear manufacturing practice for the implementation of nanoalgosome production, with optimized protocols for microalgal cultivation (*upstream processing*) and isolation of EVs by Tangential Flow Filtration (TFF), an isolation technique allowing to process large volumes of microalgae cultures, reaching concentrated EV samples (*downstream processing*). Our production pipeline is optimized thanks to quality controls, ensured by an extensive biophysical and biochemical characterization by different techniques, including dynamic light scattering (DLS), nanoparticle tracking analysis (NTA), immunoblot analysis (IB analysis) of protein markers, atomic force microscopy (AFM), and BicinChoninic Acid assay (BCA assay) (Romancino et al., 2018; Adamo et al., 2021; Paganini et al., 2021). Moreover, we demonstrate the possibility to recycle microalgal biomass after EVs harvesting to renew the cell culture and continue EVs production in a cyclic bioprocess (*renewable processing*). This capability to go through several production/isolation cycles further increases the interest of microalgae as a sustainable and renewable biosources of EVs.

2 Materials and methods

2.1 Microalgae cultivation

A stock culture of the microalgae *Tetraselmis chuii (T. chuii)* (CCAP 66/21b) was grown in borosilicate glass bottles in modified f/2 medium (Guillard, 1975) and used to start new cultures in bottles via a 25% v/v inoculum. Cultures were kept for 4 weeks at a temperature of 22°C ± 2°C under continuous air flow and exposed to white light with a photoperiod of 14 h light and 10 h dark. Bottles were gently shaken every 2 days in order to homogenize cultures. Microalgae were cultured in sterile conditions by using 0.22 μm filters at the bottle inlets. The cell growth was monitored every week by optical density at 600 nm, and cell counting (see Supplementary Figure S1).

2.2 Tangential flow filtration

The KrosFlo® KR2i TFF System from Repligen (Spectrum Labs, Los Angeles, CA, USA) was used to isolate microalgae-derived EVs. Microalgae cultures (1.6 L) were clarified by sequential micro- and ultra-filtration using TFF hollow fiber filters (MiniKros Sampler) with cut-off of 650 nm (S04-E65U-07-N, Spectrum Labs), 200 nm (S04-P20-10-N, Spectrum Labs), and 500-kDa (S04-E500-10-N, Spectrum Labs). Three different settings were evaluated: feed flow 750 ml/min and permeate flow 60 ml/min, feed flow 450 ml/min and permeate flow 6 ml/min, and feed flow 450 ml/min and permeate flow 6 ml/min followed by a wash of the TFF cartridges with 100 ml of culture medium. During all filtration processes transmembrane pressure (TMP) was kept constant at 0.02 bar. The small and large EVs recovered from the retentate of the 500-kDa and 200 nm cut-off TFF filter modules, respectively, were concentrated until a final volume of almost 150 ml. Subsequently, using a smaller 500-kDa cut-off TFF filter module (C02-E500-10-N, Spectrum Labs, MicroKros) with a feed flow 75 ml/min and a permeate flow 2 ml/min, samples were further concentrated and diafiltrated seven times with PBS, reaching a final volume of approximately 5 ml.

2.3 Microalgae cultivation recycling protocol

After culture clarification, the retentate obtained from the 650 nm cut-off TFF cartridge (100 ml) was diluted in modified f/2 medium to reach the initial batch volume (1.6 L) and used to start renewed cultures in bottles via a 25% v/v inoculum. After 4 weeks of cultivation, microalgae were again processed by TFF to isolate EVs. In order to maintain sterile conditions, necessary for the recycle of the microalgae cell culture, the 650 nm TFF membrane filter was washed with 1 L of sterile water before starting the

clarification process. Moreover, for the first TFF step the instrument and the bioreactors are connected in a closed system to maintain sterility.

2.4 Nanoparticle tracking analysis

Measurement of nanoparticle size distribution and concentration was performed using NanoSight NS300 (Malvern Panalytical, United Kingdom). The NTA instrument is composed of a 488 nm laser, a high sensitivity sCMOS camera, and a syringe pump. In order to achieve the suggested concentration measurement range ($107 \div 108$ particles per ml) in which $20 \div 120$ particles per frame were tracked, the EVs-enriched samples have been diluted in particle-free water. The analysis of the samples was executed using the NanoSight Software NTA 3.4 Build 3.4.003 (camera level 15–16, syringe pump speed 30) acquiring five videos of 60s duration and examining 1,500 frames for each sample. The frame analysis was carried out setting a detection threshold so that the observed particles are marked (red crosses in the software) and no more than five particles are rejected (blue crosses). Medium viscosity was set to water viscosity. As in our previous work (Adamo et al., 2021), nanoalgosomes may be equivalently diluted both in water and in PBS since ionic strength has no effect on their integrity (see supporting information, Supplementary Figure S2).

2.5 Protein content (BCA assay)

The EVs protein content was quantified using the colorimetric BCA protein assay (Thermo Fisher Scientific, Rockford, IL, USA). The protein concentration was measured at 562 nm, according to the manufacturer's instructions, using a GloMax® Discover Microplate Reader.

2.6 Immunoblotting

The Western blot analysis was executed using sodium dodecyl-sulfate (SDS) polyacrylamide gel electrophoresis (PAGE); 10 μg of cell lysate and 5 μg EV samples (in PBS) were incubated at 100°C for 5 min with 5× loading buffer (0.25 M Tris-Cl pH 6.8, 10% SDS, 50% glycerol, 0.25 M dithiothreitol, 0.25% bromophenol blue) and loaded on 10% SDS polyacrylamide gel for electrophoresis. Polyvinylidene fluoride (PVDF) membranes are used to blot proteins. The membranes were blocked with BSA-TBS-T solution [3% powdered with bovine serum albumin in TBST (50 mM Tris HCl pH 8.0, 150 mM NaCl, 0.05% Tween 20)] for 1 h at room temperature, followed by

primary antibody incubation. The antibody anti-Alix (clone 3A9, dil. 1:150 in 3% BSA/TBS-T1X), incubated overnight at 4°C, is raised against a mammalian EV marker and is cross-reactive for microalgae. The antibody anti-H+/ATPase (dil. 1:1,000 in 3% BSA/TBS-T1x, Agrisera), incubated for 1 h at room temperature, is raised against H+/ATPase a membrane protein specific for plants and protists. After washing, membranes were incubated for 1 h with secondary antibodies according to the manufacturer's instructions (horseradish peroxidase-conjugated secondary anti-mouse or anti-rabbit antibodies, cell signaling), and then washed four times in TBST for a total of 20 min. Immunoblots were revealed using SuperSignal™, Pierce™ ECL (Thermo Fisher Scientific).

2.7 Dynamic light scattering

An aliquot of vesicle solution was pipetted and centrifuged at 1,000×*g* for 10 min at 4°C in order to remove any dust particles. The supernatant was withdrawn by pipet tips (previously washed by MilliQ water), put directly into a quartz cuvette and incubated at 20°C in a thermostated cell compartment of a BI200-SM goniometer (Brookhaven Instruments) equipped with a He-Ne laser (JDS Uniphase 1136P) with wavelength $\lambda = 633$ nm and a single pixel photon counting module (Hamamatsu C11202-050). Scattered light intensity and its autocorrelation function $g_2(t)$ were measured simultaneously at a scattering angle $\vartheta = 90°$ by using a BI-9000 correlator (Brookhaven Instruments). Absolute scattered intensity, namely excess Rayleigh ratio, R_{ex}, was obtained by normalization with respect to toluene: $R_{ex} = [I - I_B] \cdot I_T^{-1} \cdot \tilde{n}^2 \cdot \tilde{n}_T^{-2} \cdot R_T$, where I, I_B, and I_T are the scattered intensities of sample, buffer, and toluene, respectively; $\tilde{n} = 1.3367$ and $\tilde{n}_T = 1.4996$ are the refractive indexes of buffer and toluene at 633 nm, respectively; and R_T is the toluene Rayleigh ratio at 633 nm ($R_T = 14 \times 10^{-6}$ cm^{-1}) (Noto et al., 2012). The intensity autocorrelation function $g_2(t)$ is related to the size σ of diffusing particles and to their size distribution $P_q(\sigma)$, by the relation $g_2(t) = 1 + |\beta \int P_q(\sigma) \exp[-D(\sigma)q^2t]|^2$, where β is an instrumental parameter, $q = 4\pi\tilde{n}\lambda^{-1} sin[\vartheta/2]$ is the scattering vector, and $D(\sigma)$ is the diffusion coefficient of a particle of hydrodynamic diameter $D_h = \sigma$, determined by the Stokes-Einstein relation $D(\sigma) = k_B T [3\pi\eta\sigma]^{-1}$, with T being the temperature, η the medium viscosity, and k_B the Boltzmann constant (Berne and Pecora, 1990). The size distribution $P_q(\sigma)$ is calculated by assuming that the diffusion coefficient distribution is shaped as a Schultz distribution, which is a two-parameter asymmetric distribution, determined by the average diffusion coefficient $\bar{D}$ and its variance $\bar{\nu}$ (Berne and Pecora, 1990; Romancino et al., 2018). This approach is justified by the typical noise level in the autocorrelation functions (Mailer et al., 2015). Two robust parameters may be derived from this analysis: D_z, the z-averaged hydrodynamic diameter (the diameter

corresponding to the average diffusion coefficient $\bar{D}$), and *PDI*, the polydispersity index $\left(PDI = \bar{v}\bar{D}^{-2}\right)$, which is an estimate of the distribution width. The integrity of nanoalgosomes has been shown by measuring DLS autocorrelation function in different hypo and hyper tonic solutions from 0 to 300 mM NaCl. The same EVs sample has been dialyzed against the different solutions for 2 h at room temperature and, after dialysis buffers change, overnight at 4°C. No effect is observable in both size distribution and particle number (see supporting information, Supplementary Figure S2).

2.8 Atomic force microscopy

A 40μl vesicle solution, diluted in MilliQ water to a final concentration of a few μg/ml, was deposited onto freshly cleaved mica, incubated for 20 min, and gently dried under nitrogen flow. Tapping mode AFM measurements were carried out by using a Nanowizard III scanning probe microscope (JPK Instruments AG, Germany) equipped with a 15 μm z-range scanner and NSC-15 (Mikromasch) cantilevers (spring constant 40 N/m, typical tip radius 8 nm); 2 × 2 $\mu m2$ images were acquired at 256 × 256pixel resolution. Setpoint was fixed at 70% of free oscillation amplitude (20 nm). Other measurements were performed in liquid by quantitative imaging upon deposition on a functionalized substrate (see supporting information, Supplementary Figure S3).

3 Results and discussion
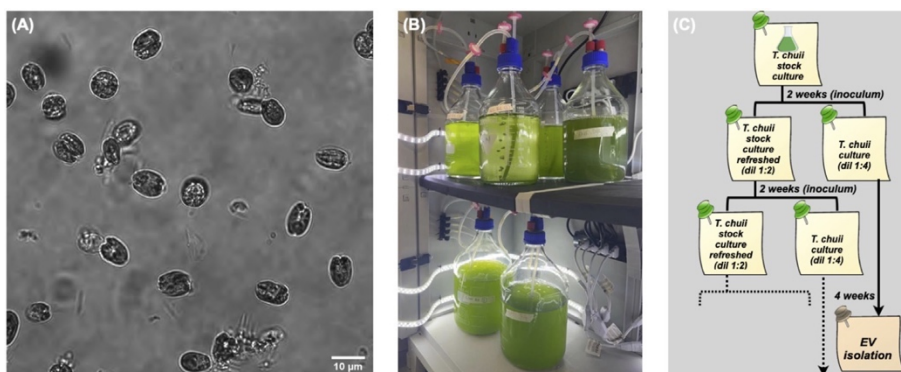
3.1 Upstream processing

In the present work, we isolated EVs from the marine chlorophyte microalgae *T. chuii* (Figure 1A). This species was selected from a set of several microalgal strains as one of the best candidates for EVs production (Adamo et al., 2021; Picciotto et al., 2021). We established a permanent platform for microalgae cultivation at pilot scale. Different cultivation methods are available for microalgae, in brief (Henley, 2019):

• batch —a given volume of culture medium is inoculated with cell culture at low density and then processed during exponential growth to obtain a maximum yield;

• fed batch —a supplement of culture medium and nutrients periodically feeds the cell culture without removing the biomass before harvesting;

• semicontinuous —a fixed volume of cell culture is harvested at given time intervals and replaced with fresh culture medium;

• continuous —the harvested culture is drained out of and the fresh medium is fluxed in the bioreactor continuously to maintain a constant biomass concentration.

Although a continuous method may in principle allow a higher yield, we preferred to implement on a lab/pilot scale a batch cultivation in small bioreactors (a few liters each), since it is reliable and it facilitates the setting of sterile conditions. Both the method and the apparatus are well suitable for scaling-out. Thus, we typically cultivate several liters of cultures, which are synchronously inoculated, grown, and distributed in different bioreactors, as shown in Figure 1B. The harvested cultures are then pooled and processed at the same time. The harvesting time depends upon the life cycle of *T. chuii* as well as the culture conditions, such as the amount of the inoculated culture. Specifically, after 4 weeks the cell density increases to reach a maximum, as measured by periodic optical density measurements and cell counting. Along with the cultures fated to EV production, we maintained a refreshed stock culture, as described in the general flow chart of Figure 1C.

FIGURE 1 | Microalgal cultivation. (A) Microscopy image (60×) of T. Chuii cells. (B) Lab cabinet with parallel bioreactors. (C) Flow chart of the cultivation timing.

3.2 Downstream processing

3.2.1 Isolation by differential tangential flow filtration. Differential ultra-centrifugation (dUC) is the classical methods for EV isolation and purification (Théry et al., 2006). It consists of a series of subsequent centrifugation and eventually ultracentrifugation steps to progressively remove and fractionate cells, debris, large particles, and small particles. While its protocols are well established (Théry et al., 2018), dUC is not easily suitable for large-scale EV production, since it is time-consuming and low throughput, due to the various centrifugation steps (Coumans et al., 2017). Also, it presents further drawbacks, including EV aggregation (Linares et

al., 2015; Yuana et al., 2015); coisolation of contaminants, e.g. protein aggregates (György et al., 2011; Paolini et al., 2016); and damage of EV structure due to high shear forces (Ismail et al., 2013; Coumans et al., 2017). Other isolation methods have been used for viruses or virus-like particles and then exploited for EV isolation, due to their close structural analogy (Merten et al., 2016). These methods include density gradient ultracentrifugation (gUC), filtration, and various chromatographies (Staubach et al., 2021), such as size exclusion chromatography (SEC), ion exchange chromatography (IEX), and affinity chromatography (AC) (Paganini et al., 2019). A reliable method extensively used for liposomes (Worsham et al., 2019) as well as for virus isolation (Loewe et al., 2019) and now adopted in the EV field is tangential flow filtration (TFF) (Heinemann et al., 2014; Busatto et al., 2018; Haraszti et al., 2018). In TFF, the particle solution, or the cell culture, flows tangentially over a membrane with a given size cut-off. The feed solution is circulated with low pressure by a peristaltic pump in a closed loop through the reservoir and the filter unit (which it typically a hollow fiber). A part of the solution permeates the filter and is then recovered with a content of particle with a size smaller than the pore size (permeate). At the same time, the feed volume is reduced and depleted of small particles (retentate). The same process may be used for diafiltration or effective volume reduction of the retentate, which is extremely important for subsequent use of EV products, e.g. for therapeutic application (Witwer et al., 2019). With respect to dead-end filtration, TFF considerably reduces membrane fouling and the formation of the undesirable filter cake due to the crowding of small-size particles. With respect to dUC, TFF induces a low shear stress, thus providing more gentle processing and resulting in high yield (Busatto et al., 2018; Haraszti et al., 2018). In general, TFF allows the processing of large volumes in a short time with high reliability and reproducibility. The process is then easily scalable and suitable for the production of GMP-compliant products (Bari et al., 2018). In our previous work, we have used both differential ultracentrifugation (dUC) and tangential flow filtration (TFF) to isolate EVs from microalgae, confirming the above described expectations for TFF performance (Adamo et al., 2021). Thus, we implemented the following procedure based on sequential TFF filtration steps (Figure 2).

1) Clarification

The harvested cell culture is fluxed through a fiber with a cut-off of 650 nm to remove the biomass.

2) Isolation

The clarified permeate from the previous step is fluxed through a fiber with a cut-off of 200 nm; this step allows to isolate EVs smaller than 200 nm in the permeate by

removing larger objects, including large EVs or cellular debris which escaped the first clarification.

3) Ultrafiltration and volume reduction

The isolated permeate from the previous step is fluxed through a fiber with a cut-off of 500 kDa, which corresponds to approximately 20 nm; this step allows to remove small particles, such as proteins, maintaining small EVs in the retentate; at the same time, the retentate volume is reduced down to the fiber volume (150 ml in the current setting).

4) Concentration and diafiltration

The ultrafiltered retentate from the previous step is fluxed through a fiber with the same cut-off (500 kDa) and a lower volume and filter surface; this step allows to further concentrate the sample by reducing the volume down to the volume of the filter module and the tubing (5 ml in the current setting).

The isolation of nanoalgosomes actually occurs in step 2 after filtration via a 200 nm filter. At this stage, the retentate mainly consists of a subpopulation of large particles at very low concentration as well as a fraction of small EVs that were not brought in the permeate. The subsequent TFF ultrafiltration steps (3 and 4) are quite important to achieve a rapid volume reduction. Moreover, they are very efficient in removing any small particle, such as freely diffusing proteins. In the case of T. chuii culture, this purification step is made easier by the simplicity of the microalgal culture medium. At the opposite, EV purification from a complex culture medium, such as for instance in the case of mammalian cells, may require a further purification step to remove small particles (typically size exclusion chromatography), as reported in other studies and according to our own experience (Staubach et al., 2021). Indeed, a culture with high protein content may result in quick membrane fouling affecting all TFF steps and preventing an efficient recovery.
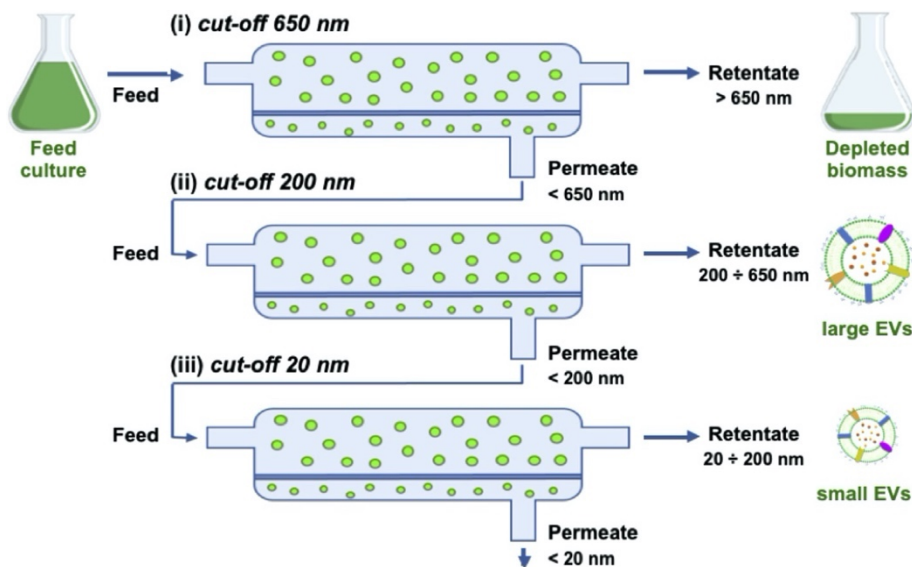
FIGURE 2 | Scheme of TFF steps showing the retentate, permeate, and feed for the three filters used in sequence: (i) 650 nm, (ii) 200 nm, (iii) 20 nm (namely 500 kDa).

3.2.2 TFF parameters optimization. In order to optimize the TFF protocol, the specific parameters controlling the process must be adjusted individually for each type of culture medium (Moleirinho et al., 2019). Two important parameters to maximize EV yield are the inlet and outlet flow rates: more specifically, the feed flow rate, F in, and the permeate flow rate, F out. We evaluated three different conditions for each filtration step:

(A) F_{in} = 750 ml min^{-1}, F_{out} = 60 ml min^{-1};

(B) F_{in} = 450 ml min^{-1}, F_{out} = 6 ml min^{-1};

(C) F_{in} = 450 ml min^{-1}, F_{out} = 6 ml min^{-1} and filter module wash.

The condition (C) adds to condition (B) the eventual wash of each cartridge with a 100 ml culture medium to avoid EVs losses on the filter membrane. In order to compare the different TFF conditions, a 1.6 L microalgae culture was portioned in three equal volume samples (≈530 ml), which were then processed by TFF. The EV-enriched samples (5 ml) resulting from the retentate of the last small column (step 4), underwent several biophysical and biochemical analyses aiming to quantify small EV isolation yields. EVs yields, for each small EVs sample obtained by TFF, were evaluated in term of protein content using the BCA assay and in terms of particles number calculated by NTA (both normalized per mg of dry microalgal biomass). Additionally, their average size and size distributions were determined by DLS and NTA (Figure 3 and Table 1). The biophysical characterization allows a straightforward evaluation of the EV yield in the chosen conditions. Figure 3 and Table 1 show that the size distribution, along

with the average size, are identical in the three preparations. Other parameters are related to the amount of isolated particles, namely, the particle number measured by NTA, the total protein mass measured by BCA assay, and the excess Rayleigh ratio, corresponding to the absolute value of scattered intensity and proportional to particle concentration. Therefore, Table 1 shows that a slow flow rate determines a higher EV recovery (conditions B and C), likely due to the prevention of any membrane fouling. An additional washing step (condition C) may also improve particle recovery.
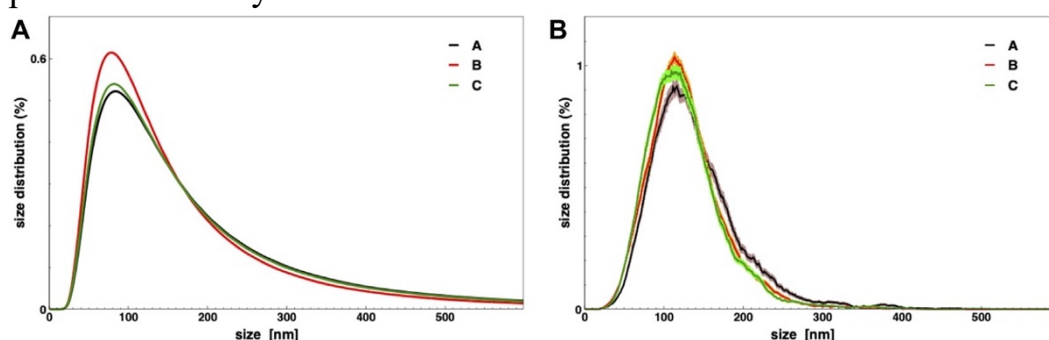
FIGURE 3 | Nanoalgosomes size distribution in three TFF conditions as described in the text, measured by DLS (A) and NTA (B).

TABLE 1 | Characterization of nanoalgosomes obtained from the three different TFF conditions (A, B, and C). D_z: z-averaged hydrodynamic diameter; PDI: polydispersity index; R_{ex}/biomass: excess Rayleigh ratio, measured by DLS, over dry biomass; N_P (*NTA*): particle number, measured by NTA, over dry biomass; c_p (*BCA*): Protein mass, measured by BCA assay, over dry biomass.

TFF	D_z	PDI	R_{ex}/biomass	N_P (*NTA*)	c_p (*BCA*)
Conditions	(nm)		(10^{-6} cm^{-1} g^{-1}L)	(10^9 g^{-1})	(μg g^{-1})
A	85 ± 5	0.5	1.05 ± 0.01	320 ± 25	50 ± 7
B	85 ± 5	0.5	1.90 ± 0.01	760 ± 10	29 ± 7
C	85 ± 5	0.5	2.90 ± 0.01	810 ± 45	42 ± 4

3.3 Renewable processing

After the optimization of upstream and downstream processing, we were able to produce EVs at a lab scale, with a maximum yield of 2 mg EVs for every 5 L of cell culture and approximately every 5 g of dry biomass. Also, our production platform showed high reproducibility and quality over different production cycles, as discussed in the present work and in our previous studies (Adamo et al., 2021; Picciotto et al., 2021). Now, we explore the possibility to link upstream and downstream processes by implementing a cyclic bioprocess for nanoalgosomes isolation. Since microalgae cells are concentrated during the first TFF filtration step, the corresponding retentate could

be used to seed a new culture via appropriate dilution with fresh medium (modified f/2 medium) and subjected to further sequential filtration after 4 weeks. This requires that microalgal cells are not damaged during the first TFF step, when the cell culture is depleted from the released vesicles. In order to demonstrate the capability of such a production for high throughput EVs production, we characterized the nanoalgosomes obtained from a fresh culture and its subsequent TFF-based subculture cycles (up to 3). BCA assay and NTA were performed to compare and quantify the EV sample yields (Table 2). Furthermore, the average size and size distributions of the small vesicles were measured by DLS and NTA (Figure 4). Finally, the biochemical characterization was completed by assessing the presence of EVs in each sample by immunoblot analysis, emphasizing the expression of particular biomarkers (e.g., H+/ATPase and Alix) in accord with the MISEV 2018 guidelines (Théry et al., 2018) and our previous work (Adamo et al., 2021). Immunoblot results showed the enrichment of specific biomarkers (H+/ATPase and Alix) in Nanoalgosomes samples Figure 5. Specifically, semiquantitative densitometric analysis of immunoblotting showed an increase in the expression of target proteins in nanoalgosomes isolated from renewals of the T. chuii cultures. As a negative control, we perform immunoblot analysis to verify the absence of the biomarker TET8, which is an orthologue of mammalian tetraspanins in plants and bacteria, that is not present in T. chuii and here used as a negative control for the presence of bacterial contaminants. In addition to the enrichment of biomarkers, we can also observe a slight increase of EV amount over subsequent recycling, in terms of protein mass, measured by BCA assay and of total particle number determined by NTA (Table 2). The overall population of nanolgosomes was not altered by TFF-based recycling, as shown by the unchanged size distributions, measured by DLS and NTA (Figure 4). Also the morphology of nanoalgosome was not altered, as clearly shown in the AFM images of Figure 6. Other AFM images were taken by using a functionalized substrate for amine groups, and no significant changes were observed after TFF-based subcultivation cycles (see supporting information, Supplementary Figure S3). In some cases, we observed that the recycled samples displayed a wider concentration of particles, namely, sample impurities. This may warrant further purification steps, for instance by size exclusion chromatography. The functional behavior of nanoalgosomes, which is currently under study, is not addressed in the present work. Nevertheless, given the growth of cells in culture after each TFF-based recycling regime (see supporting information, Supplementary Figure S1), it is possible that their functional properties would not be altered.

TABLE 2 | Characterization of nanoalgosomes obtained from a fresh culture (R0) and after 1, 2 and 3 recycling (R1, R2, and R3, respectively). D_z: z-averaged hydrodynamic diameter; PDI: polydispersity index; R_{ex}/biomass: excess Rayleigh ratio, measured by DLS, over dry biomass; N_P (*NTA*): Particle number, measured by NTA, over dry biomass; c_p (*BCA*): Protein mass, measured by BCA assay, over dry biomass.

Samples	D_z	PDI	R_{ex}/biomass	N_P (*NTA*)	c_p (*BCA*)
Recycling	(nm)		$(10^{-6}\ cm^{-1}\ g^{-1}L)$	$(10^9\ g^{-1})$	$(\mu g\ g^{-1})$
R0	85 ± 5	0.50	21.00 ± 0.01	5,500 ± 300	375 ± 4
R1	85 ± 5	0.55	17.70 ± 0.01	5,500 ± 700	383 ± 8
R2	100 ± 5	0.60	19.10 ± 0.01	5,400 ± 300	425 ± 7
R3	90 ± 5	0.45	15.55 ± 0.02	11,400 ± 500	435 ± 4
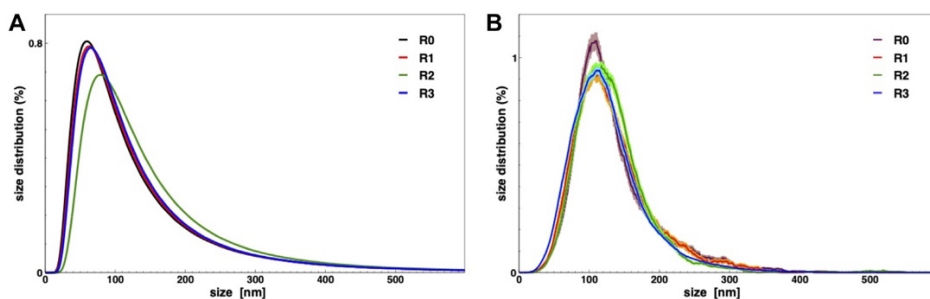
FIGURE 4 | Nanoalgosomes size distribution from a fresh culture (R0) and after 1, 2, and 3 recycling (R1, R2 and R3, respectively), measured by DLS (A) and NTA (B).
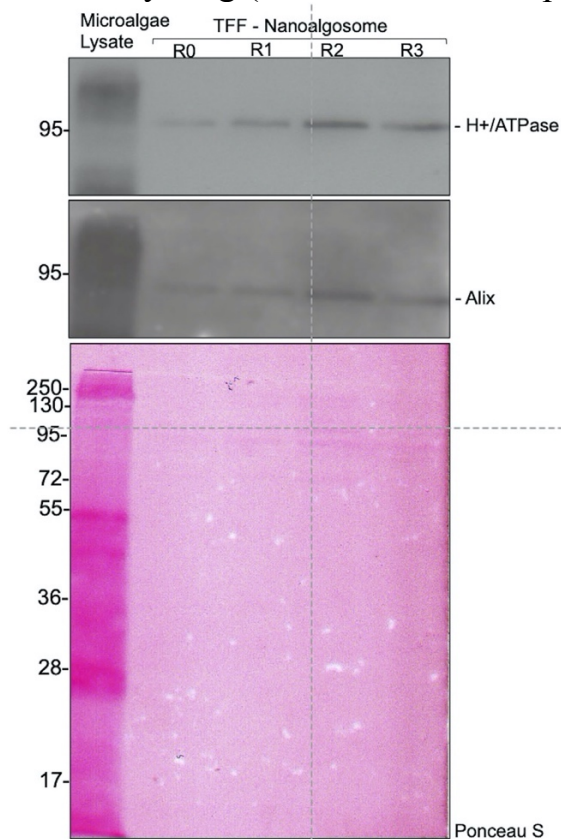
FIGURE 5 | Immunoblot analysis of specific biomarkers (H+/ATPase and Alix) in Tetraselmis chuii cells lysate (Microalgae lysate; 10 μg) and nanoalgosomes isolated by TFF from Tetraselmis chuii fresh culture (R0), and after 1, 2, and 3 subculturing steps (R1, R2, and R3, respectively) (upper panel). Ponceau red staining is shown as loading control (bottom panel). Three independent experiments (n = 3) were performed
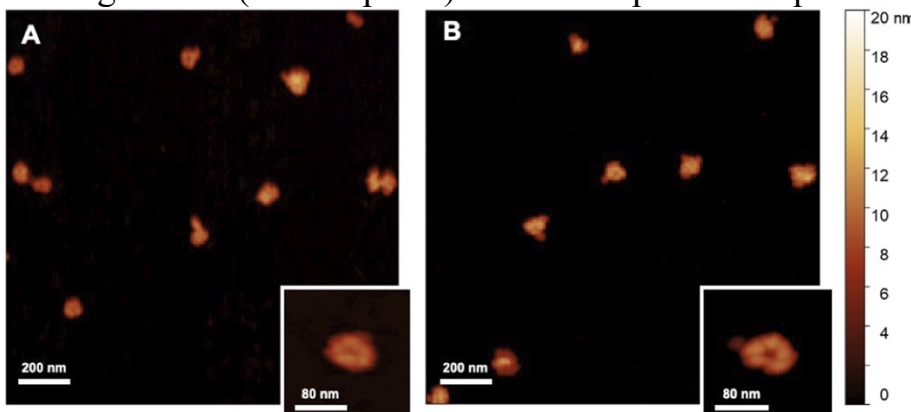
FIGURE 6 | AFM images (2 × 2 μm2) of nanoalgosomes (A) from a fresh culture and (B) from a culture after multiple recycles.

3.4 Hard numbers for a fast quality check

We reported different quantities related to the amount of vesicles in solution:

1) c_p , protein mass concentration determined by BCA assay

This quantity is a standard parameter in the EV field; its measure can be done by using a specific kit and a spectrophotometer or a colorimeter; thus it is quite cheap and easily accessible in every laboratory. Also, it is a widely used procedure and thus it is very useful to compare measurements from different studies and different samples. Other colorimetric methods measuring protein mass concentration, such as the popular Bradford assay, may be equivalently performed. On the other hand, an accurate measurement of protein concentration typically requires a concentrated sample, so it is often taken after a concentration step, which introduces the possibility of sample loss and a biased measurement.

2) N_p, particle number concentration measured by NTA

The number of particles is the ideal quantification for each sample and it is becoming another standard parameter with the increasing availability of NTA instruments, or also Resistive Pulse Sensing techniques, which allow to track and count each particle in a sample. There are two main drawbacks: the first is the intrinsic limit of detection of NTA instruments which are less sensitive to objects with a size below 100 nm (or with a very large size), giving a constitutive bias to the measure of number concentration;

119

the second is the intrinsic incomplete sampling of the particle population; indeed, both a short experimental duration and a different setting of the acquisition parameters may lead to large differences in the particle count, and hence in the particle concentration, which only a highly trained operator can reliably and partly suppress.

3) R_{ex}, excess Rayleigh ratio measured by DLS

This quantity is an absolute measure of the intensity scattered at a given angle. While the measure requires an appropriate instrumentation (not every light scattering commercial device is adequate), it is very easy and requires a very low sample amount, if taken at 90°. Most importantly, since DLS intrinsically performs an exhaustive ergodic sampling of all the particles in solution, the measure is quite robust, carries an almost irrelevant error, and is not biased by any instrumental parameter or analytic method. For such a reason, it is a reliable quantity suited for the comparison of different samples or different batches. On the other hand, its physical meaning is not straightforward. It is proportional to the total mass concentration c of the particles in solution. However, it also proportional to the weight average mass of the particles Mw and to their z-averaged form factor $P_z(q)$, which is related to the average shape of the particles and depends upon the scattering angle ϑ, or the scattering vector q: $R_{ex}(q) \sim cM_w P_z(q)$ (Berne and Pecora, 1990).

After several iterations of different purifications of nanoalgosomes with different yield but comparable quality, we are able to put some order in the information derived from these quantities. First, we observed an expected correlation between the protein concentration c_p and the particle number N_p, as shown in Figure 7A: $N_p = Sc_p$, where $S = 10.5 \times 10^9 \ \mu g^{-1}$, which is slightly higher than the constant calculated by Sverdlov (Sverdlov, 2012). If the correlation is evident, one may note that the variability in the data does not allow to infer one quantity by simply measuring the other one. For this reason, we recommend to measure both quantities to complete any batch characterization.

Furthermore, Figure 7B shows that both quantities are correlated with R_{ex}. This result is not trivial in the case of particles with a heterogeneous size distribution. One may argue that the two quantities, the weight average mass Mw (proportional to D^2), and the z-averaged form factor $P_z(q)$ (roughly proportional to D^{-2} at high q) average out, thus making R_{ex} directly proportional to the mass concentration c (Montis et al., 2017). However this could be assumed for large particles and at large angle (i.e. in back scattering). Otherwise, in order to unravel the relation between scattered intensity and particle concentration, a more complex multi-angle analysis would be required. In our

case, the strict correlation between particle number and Rayleigh ratio is likely due to the reproducible size distribution of our preparations (as observable in the quite constant average size of Figure 7B).

In any case, the correlation shown in Figure 7B works as an a posteriori calibration of the particle number with respect to the "hard number" of Rayleigh ratio, which can be quickly measured to assess EV concentration and make a reliable and accurate batch to batch comparison. For instance, a 90° excess Rayleigh ratio of 42×10^{-6} cm $^{-1}$ corresponds to a number concentration of 10^{10} particles mL^{-1}.
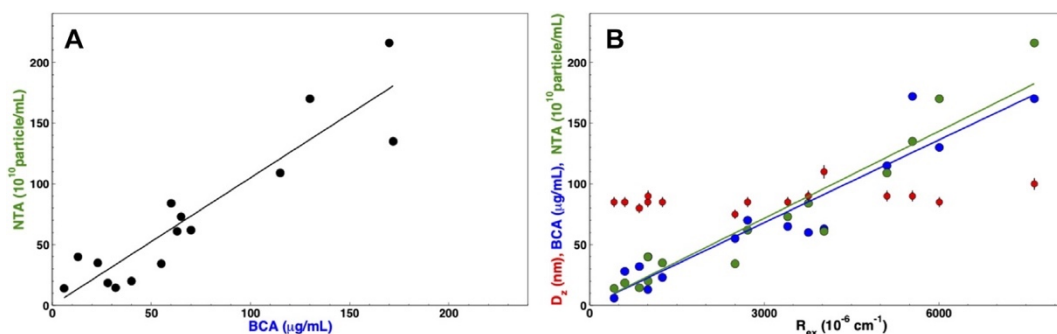
FIGURE 7 | Correlation among concentration parameters: (A) particle concentration measured by NTA (black circles) vs. protein concentration measured by BCA assay. (B) Protein concentration measured by BCA assay (blue circles), particle concentration measured by NTA (green circles), and z-averaged hydrodynamic diameter (red circles) vs. excess Rayleigh ratio, Rex; The solid lines show a linear regression to data for BCA vs. Rex (blue line) and NTA vs. Rex (green line).

4 Conclusion

The role of EVs in cell communication is attracting increasing interest from several clinical and biological fields. This emerging relevance is also supported by the application of EVs for clinical diagnosis and liquid biopsy (Ayers et al., 2019; Trino et al., 2021). Also, their potential exploitation as efficient drug delivery systems boosted the interest in their biotechnological exploitation. In order to fulfill the increasing demand for EVs, it is required to adopt new strategies for their massive production at high purity level or, at least, with a controlled batch reproducibility. Here, we addressed the production of nanoalgosomes, EVs derived from microalgae recently identified and characterized in our recent work (Adamo et al., 2021; Picciotto et al., 2021). Both upstream and downstream processing steps have been optimized to maximize EV yields. Moreover, we showed that it is possible to operate microalgal production cycles

using TFF-derived culture inocula to facilitate a cyclical production of nanoalgosomes. The optimization of EV production was achieved by implementing quality control checks, which included the use of several biophysical and biochemical methods for EV characterization. As highlighted in the present work and accounted in previous studies (Paganini et al., 2019; Adamo et al., 2021), nanoalgosomes have different competitive advantages with respect to EVs derived from other sources (Figure 8): 1) Sustainability. They are obtained by a sustainable "green" biosource: they can be seen as more appealing for an exploitation as drug carriers than EVs from human or animal sources, which have inherent safety and ethical issues. 2) Scalability. The optimized TFF based bioprocess is suitable for a large scale production: for any large-scale exploitation, a cell suspension has a definitive advantage with respect to other green sources, such as higher plants, which require more time-consuming and expensive treatments. 3) Renewability—the potential recycling of TFF-concentrated microalgal cells to facilitate the scaled production.
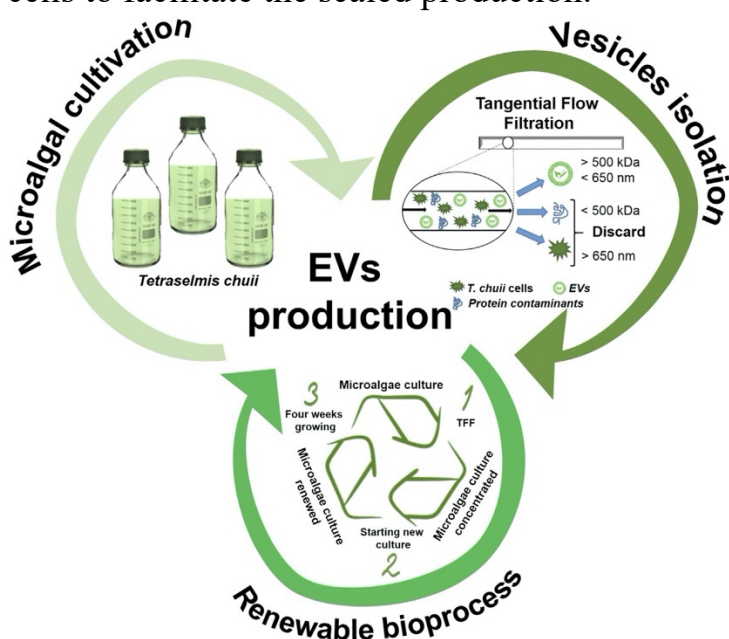
FIGURE 8 | Schematic representation of EV production as a sustainable (cultivation of microalgae), scalable (isolation by TFF), and renewable bioprocess.

Data Availability Statement

The raw data supporting the conclusion of this article will be made available by the authors, without undue reservation.

Author Contributions

Conceptualization, NT, AB, and MM; funding acquisition, NT, AB, and MM; investigation, AP, ER, GA, SP, DR, RN, and SR; methodology, NT, AB, and MM; project administration, AB and MM; visualization, AP, ER, GA, SP, and SR; writing + original draft preparation, AP, ER, and MM; writing + review and editing, AP, ER SR, RN, NT, AB, and MM; All authors have read and agreed to the published version of the manuscript.

Funding

Conflict of Interest

The authors declare that the research was conducted in the absence of any commercial or financial relationships that could be construed as a potential conflict of interest.

Publisher's Note

All claims expressed in this article are solely those of the authors and do not necessarily represent those of their affiliated organizations, or those of the publisher, the editors, and the reviewers. Any product that may be evaluated in this article, or claim that may be made by its manufacturer, is not guaranteed or endorsed by the publisher.

Supplementary Material

The Supplementary Material for this article can be found online at: https://www.frontiersin.org/articles/10.3389/fbioe.2022.836747/full#supplementary-material

References

1. Adamo G., Barone M. E., Fierli D., Aranyos A., Romancino D. P., Picciotto S., et al. (2021). Nanoalgosomes: Introducing Extracellular Vesicles Produced by Microalgae. *J. Extracellular Vesicles* 10, e12081. 10.1002/jev2.12081 [PMC free article] [PubMed] [CrossRef] [Google Scholar]

2. Armstrong J. P., Stevens M. M. (2018). Strategic Design of Extracellular Vesicle Drug Delivery Systems. *Adv. Drug Deliv. Rev.* 130, 12–16. 10.1016/j.addr.2018.06.017 [PMC free article] [PubMed] [CrossRef] [Google Scholar]

3. Ayers L., Pink R., Carter D. R. F., Nieuwland R. (2019). Clinical Requirements for Extracellular Vesicle Assays. *J. Extracellular Vesicles* 8, 1593755. 10.1080/20013078.2019.1593755 [PMC free article] [PubMed] [CrossRef] [Google Scholar]

4. Bari E., Perteghella S., Di Silvestre D., Sorlini M., Catenacci L., Sorrenti M., et al. (2018). Pilot Production of Mesenchymal Stem/Stromal Freeze-Dried Secretome for Cell-free Regenerative Nanomedicine: A Validated GMP-Compliant Process. *Cells* 7, 190. 10.3390/cells7110190 [PMC free article] [PubMed] [CrossRef] [Google Scholar]

5. Berne B. J., Pecora R. (1990). *Dynamic Light Scattering with Applications to Chemistry, Biology, and Physics*. Hoboken: John Wiley & Sons. [Google Scholar]

6. Bitto N. J., Kaparakis-Liaskos M. (2017). The Therapeutic Benefit of Bacterial Membrane Vesicles. *Int. J. Mol. Sci.* 18, 1–15. 10.3390/ijms18061287 [PMC free article] [PubMed] [CrossRef] [Google Scholar]

7. Bokka R., Ramos A. P., Fiume I., Manno M., Raccosta S., Turiák L., et al. (2020). Biomanufacturing of Tomato-Derived Nanovesicles. *Foods* 9, 1852. 10.3390/foods9121852 [PMC free article] [PubMed] [CrossRef] [Google Scholar]

8. Busatto S., Vilanilam G., Ticer T., Lin W.-l., Dickson D. W., Shapiro S., et al. (2018). Tangential Flow Filtration for Highly Efficient Concentration of Extracellular Vesicles from Large Volumes of Fluid. *Cells* 7, 1–11. 10.3390/cells7120273 [PMC free article] [PubMed] [CrossRef] [Google Scholar]

9. Buschmann D., Mussack V., Byrd J. B. (2021). Separation, Characterization, and Standardization of Extracellular Vesicles for Drug Delivery Applications. *Adv. Drug Deliv. Rev.* 174, 348–368. 10.1016/j.addr.2021.04.027 [PMC free article] [PubMed] [CrossRef] [Google Scholar]

10. Caporgno M. P., Mathys A. (2018). Trends in Microalgae Incorporation into Innovative Food Products with Potential Health Benefits. *Front. Nutr.* 5, 1–10. 10.3389/fnut.2018.00058 [PMC free article] [PubMed] [CrossRef] [Google Scholar]

11. Coumans F. A., Brisson A. R., Buzas E. I., Dignat-George F., Drees E. E., El-Andaloussi S., et al. (2017). Methodological Guidelines to Study Extracellular Vesicles. *Circ. Res.* 120, 1632–1648. 10.1161/CIRCRESAHA.117.309417 [PubMed] [CrossRef] [Google Scholar]

12. Cuellar-Bermudez S. P., Aguilar-Hernandez I., Cardenas-Chavez D. L., Ornelas-Soto N., Romero-Ogawa M. A., Parra-Saldivar R. (2015). Extraction and Purification of High-Value Metabolites from Microalgae: Essential Lipids,

Check for updates

Astaxanthin and Phycobiliproteins. *Microb. Biotechnol.* 8, 190–209. 10.1111/1751-7915.12167 [PMC free article] [PubMed] [CrossRef] [Google Scholar]

13. European Commission (2017). Commission Implementing Regulation (EU) 2017/2470of 20 December 2017 Establishing the Union List of Novel Foods in Accordance with Regulation (EU)2015/2283of the European Parliament and of the Council on Novel Foods. *Official J. Eur. Union* 351, 1–188. [Google Scholar]

14. Grangier A., Branchu J., Volatron J., Piffoux M., Gazeau F., Wilhelm C., et al. (2021). Technological Advances towards Extracellular Vesicles Mass Production. *Adv. Drug Deliv. Rev.* 176, 113843. 10.1016/j.addr.2021.113843 [PubMed] [CrossRef] [Google Scholar]

15. Guillard R. R. L. (1975). "Culture of Phytoplankton for Feeding Marine Invertebrates," in *Culture of Marine Invertebrate Animals*. Editors Smith W. L., Chanley M. H. (Boston, MA: Springer;), 29+60. 10.1007/978-1-4615-8714-9_3 [CrossRef] [Google Scholar]

16. György B., Módos K., Pállinger v., Pálóczi K., Pásztói M., Misják P., et al. (2011). Detection and Isolation of Cell-Derived Microparticles Are Compromised by Protein Complexes Resulting from Shared Biophysical Parameters. *Blood* 117, 39–48. 10.1182/blood-2010-09-307595 [PubMed] [CrossRef] [Google Scholar]

17. Haraszti R. A., Miller R., Stoppato M., Sere Y. Y., Coles A., Didiot M. C., et al. (2018). Exosomes Produced from 3D Cultures of MSCs by Tangential Flow Filtration Show Higher Yield and Improved Activity. *Mol. Ther.* 26, 2838–2847. 10.1016/j.ymthe.2018.09.015 [PMC free article] [PubMed] [CrossRef] [Google Scholar]

18. Heinemann M. L., Ilmer M., Silva L. P., Hawke D. H., Recio A., Vorontsova M. A., et al. (2014). Benchtop Isolation and Characterization of Functional Exosomes by Sequential Filtration. *J. Chromatogr. A* 1371, 125+135. 10.1016/j.chroma.2014.10.026 [PubMed] [CrossRef] [Google Scholar]

19. Henley W. J. (2019). The Past, Present and Future of Algal Continuous Cultures in Basic Research and Commercial Applications. *Algal Res.* 43, 101–636. 10.1016/j.algal.2019.101636 [CrossRef] [Google Scholar]

20. Ismail N., Wang Y., Dakhlallah D., Moldovan L., Agarwal K., Batte K., et al. (2013). Macrophage Microvesicles Induce Macrophage Differentiation and miR-223 Transfer. *Blood* 121, 984–995. 10.1182/blood-2011-08-374793 [PMC free article] [PubMed] [CrossRef] [Google Scholar]

21. Jacob-Lopes E., Maroneze M. M., Deprá M. C., Sartori R. B., Dias R. R., Zepka L. Q. (2019). Bioactive Food Compounds from Microalgae: an Innovative Framework on Industrial Biorefineries. *Curr. Opin. Food Sci.* 25, 1–7. 10.1016/j.cofs.2018.12.003 [CrossRef] [Google Scholar]

22. Kameli N., Dragojlovic-kerkache A., Savelkoul P., Stassen F. R. (2021). Plant-derived Extracellular Vesicles: Current Findings, Challenges, and Future Applications. *Membranes* 11, 1–9. 10.3390/membranes11060411 [PMC free article] [PubMed] [CrossRef] [Google Scholar]

23. Khan M. I., Shin J. H., Kim J. D. (2018). The Promising Future of Microalgae: Current Status, Challenges, and Optimization of a Sustainable and Renewable Industry for Biofuels, Feed, and Other Products. *Microb. Cell Factories* 17, 1–21. 10.1186/s12934-018-0879-x [PMC free article] [PubMed] [CrossRef] [Google Scholar]

24. Kleinjan M., Van Herwijnen M. J., Libregts S. F., Van Neerven R. J., Feitsma A. L., Wauben M. H. (2021). Regular Industrial Processing of Bovine Milk Impacts the Integrity and Molecular Composition of Extracellular Vesicles. *J. Nutr.* 151, 1416–1425. 10.1093/jn/nxab031 [PubMed] [CrossRef] [Google Scholar]

25. Kooijmans S. A., de Jong O. G., Schiffelers R. M. (2021). Exploring Interactions between Extracellular Vesicles and Cells for Innovative Drug Delivery System Design. *Adv. Drug Deliv. Rev.* 173, 252–278. 10.1016/j.addr.2021.03.017 [PubMed] [CrossRef] [Google Scholar]

26. Limongi T., Susa F., Dumontel B., Racca L., Perrone Donnorso M., Debellis D., et al. (2021a). Extracellular Vesicles Tropism: A Comparative Study between Passive Innate Tropism and the Active Engineered Targeting Capability of Lymphocyte-Derived Evs. *Membranes* 11, 886. 10.3390/membranes11110886 [PMC free article] [PubMed] [CrossRef] [Google Scholar]

27. Limongi T., Susa F., Marini M., Allione M., Torre B., Pisano R., et al. (2021b). Lipid-Based Nanovesicular Drug Delivery Systems. *Nanomaterials* 11, 3391. 10.3390/nano11123391 [PMC free article] [PubMed] [CrossRef] [Google Scholar]

28. Linares R., Tan S., Gounou C., Arraud N., Brisson A. R. (2015). High-speed Centrifugation Induces Aggregation of Extracellular Vesicles. *J. Extracellular Vesicles* 4, 29509. 10.3402/jev.v4.29509 [PMC free article] [PubMed] [CrossRef] [Google Scholar]

29. Loewe D., Grein T. A., Dieken H., Weidner T., Salzig D., Czermak P. (2019). Tangential Flow Filtration for the Concentration of Oncolytic Measles

Virus: The Influence of Filter Properties and the Cell Culture Medium. *Membranes* 9, 160. 10.3390/membranes9120160 [PMC free article] [PubMed] [CrossRef] [Google Scholar]

30. Mailer A. G., Clegg P. S., Pusey P. N. (2015). Particle Sizing by Dynamic Light Scattering: Non-linear Cumulant Analysis. *J. Phys. Condensed matter : Inst. Phys. J.* 27, 145102. 10.1088/0953-8984/27/14/145102 [PubMed] [CrossRef] [Google Scholar]

31. Margolis L., Sadovsky Y. (2019). The Biology of Extracellular Vesicles: The Known Unknowns. *PLoS Biol.* 17, 1–12. 10.1371/journal.pbio.3000363 [PMC free article] [PubMed] [CrossRef] [Google Scholar]

32. Merten O. W., Hebben M., Bovolenta C. (2016). Production of Lentiviral Vectors. *Mol. Ther. - Methods Clin. Dev.* 3, 16017. 10.1038/mtm.2016.17 [PMC free article] [PubMed] [CrossRef] [Google Scholar]

33. Moleirinho M. G., Silva R. J., Alves P. M., Carrondo M. J., Peixoto C. (2019). Current Challenges in Biotherapeutic Particles Manufacturing. *Expert Opin. Biol. Ther.* 20, 451–465. 10.1080/14712598.2020.1693541 [PubMed] [CrossRef] [Google Scholar]

34. Montis C., Zendrini A., Valle F., Busatto S., Paolini L., Radeghieri A., et al. (2017). Size Distribution of Extracellular Vesicles by Optical Correlation Techniques. *Colloids Surf. B: Biointerfaces* 158, 331–338. 10.1016/j.colsurfb.2017.06.047 [PubMed] [CrossRef] [Google Scholar]

35. Morocho-Jácome A. L., Ruscinc N., Martinez R. M., de Carvalho J. C. M., Santos de Almeida T., Rosado C., et al. (2020). Bio)Technological Aspects of Microalgae Pigments for Cosmetics. *Appl. Microbiol. Biotechnol.* 104, 9513–9522. 10.1007/s00253-020-10936-x [PubMed] [CrossRef] [Google Scholar]

36. Noto R., Santangelo M. G., Ricagno S., Mangione M. R., Levantino M., Pezzullo M., et al. (2012). The Tempered Polymerization of Human Neuroserpin. *PLoS ONE* 7, e32444. 10.1371/journal.pone.0032444 [PMC free article] [PubMed] [CrossRef] [Google Scholar]

37. Paganini C., Capasso Palmiero U., Pocsfalvi G., Touzet N., Bongiovanni A., Arosio P. (2019). Scalable Production and Isolation of Extracellular Vesicles: Available Sources and Lessons from Current Industrial Bioprocesses. *Biotechnol. J.* 14, 1800528. 10.1002/biot.201800528 [PubMed] [CrossRef] [Google Scholar]

38. Paganini C., Hettich B., Kopp M. R., Eördögh A., Capasso Palmiero U., Adamo G., et al. (2021). Rapid Characterization and Quantification of Extracellular Vesicles

by Fluorescence-Based Microfluidic Diffusion Sizing. *Adv. Healthc. Mater.* 11, 2100021. 10.1002/adhm.202100021 [PubMed] [CrossRef] [Google Scholar]

39. Paolini L., Zendrini A., Noto G. D., Busatto S., Lottini E., Radeghieri A., et al. (2016). Residual Matrix from Different Separation Techniques Impacts Exosome Biological Activity. *Scientific Rep.* 6, 1–11. 10.1038/srep23550 [PMC free article] [PubMed] [CrossRef] [Google Scholar]

40. Pasini L., Ulivi P. (2020). Extracellular Vesicles in Non-small-cell Lung Cancer: Functional Role and Involvement in Resistance to Targeted Treatment and Immunotherapy. *Cancers* 12, 40. 10.3390/cancers12010040 [PMC free article] [PubMed] [CrossRef] [Google Scholar]

41. Picciotto S., Barone M. E., Fierli D., Aranyos A., Adamo G., Božič D., et al. (2021). Isolation of Extracellular Vesicles from Microalgae: towards the Production of Sustainable and Natural Nanocarriers of Bioactive Compounds. *Biomater. Sci.* 9, 2917–2930. 10.1039/d0bm01696a [PubMed] [CrossRef] [Google Scholar]

42. Pocsfalvi G., Mammadova R., Ramos Juarez A. P., Bokka R., Trepiccione F., Capasso G. (2020). COVID-19 and Extracellular Vesicles: An Intriguing Interplay. *Kidney Blood Press. Res.* 45, 661–670. 10.1159/000511402 [PMC free article] [PubMed] [CrossRef] [Google Scholar]

43. Raimondi L., De Luca A., Giavaresi G., Raimondo S., Gallo A., Taiana E., et al. (2020). Non-Coding RNAs in Multiple Myeloma Bone Disease Pathophysiology. *Non-coding RNA* 6, 1–22. 10.3390/NCRNA6030037 [PMC free article] [PubMed] [CrossRef] [Google Scholar]

44. Raimondo S., Naselli F., Fontana S., Monteleone F., Lo Dico A., Saieva L., et al. (2015). Citrus limon-derived Nanovesicles Inhibit Cancer Cell Proliferation and Suppress CML Xenograft Growth by Inducing TRAIL-Mediated Cell Death. *Oncotarget* 6, 19514–19527. 10.18632/oncotarget.4004 [PMC free article] [PubMed] [CrossRef] [Google Scholar]

45. Raimondo S., Nikolic D., Conigliaro A., Giavaresi G., Sasso B. L., Giglio R. V., et al. (2021). Preliminary Results of citraves™ Effects on Low Density Lipoprotein Cholesterol and Waist Circumference in Healthy Subjects after 12 Weeks: A Pilot Open-Label Study. *Metabolites* 11, 276. 10.3390/metabo11050276 [PMC free article] [PubMed] [CrossRef] [Google Scholar]

46. Raposo G., Stahl P. D. (2019). Extracellular Vesicles: a New Communication Paradigm? *Nat. Rev. Mol. Cell Biol.* 20, 509–510. 10.1038/s41580-019-0158-7 [PubMed] [CrossRef] [Google Scholar]

47. Romancino D. P., Buffa V., Caruso S., Ferrara I., Raccosta S., Notaro A., et al. (2018). Palmitoylation Is a post-translational Modification of Alix Regulating the Membrane Organization of Exosome-like Small Extracellular Vesicles. *Biochim. Biophys. Acta - Gen. Subjects* 1862, 2879–2887. 10.1016/j.bbagen.2018.09.004 [PubMed] [CrossRef] [Google Scholar]

48. Samuel M., Fonseka P., Sanwlani R., Gangoda L., Chee S. H., Keerthikumar S., et al. (2021). Oral Administration of Bovine Milk-Derived Extracellular Vesicles Induces Senescence in the Primary Tumor but Accelerates Cancer Metastasis. *Nat. Commun.* 12, 3950. 10.1038/s41467-021-24273-8 [PMC free article] [PubMed] [CrossRef] [Google Scholar]

49. Samuel P., Fabbri M., Carter D. R. F. (2017). Mechanisms of Drug Resistance in Cancer: The Role of Extracellular Vesicles. *Proteomics* 17, 1600375. 10.1002/pmic.201600375 [PubMed] [CrossRef] [Google Scholar]

50. Silva A. K., Morille M., Piffoux M., Arumugam S., Mauduit P., Larghero J., et al. (2021). Development of Extracellular Vesicle-Based Medicinal Products: A Position Paper of the Group "Extracellular Vesicle translatiOn to clinicaL perspectiVEs + EVOLVE France". *Adv. Drug Deliv. Rev.* 179, 114001. 10.1016/j.addr.2021.114001 [PubMed] [CrossRef] [Google Scholar]

51. Stanly C., Alfieri M., Ambrosone A., Leone A., Fiume I., Pocsfalvi G. (2020). Grapefruit-Derived Micro and Nanovesicles Show Distinct Metabolome Profiles and Anticancer Activities in the A375 Human Melanoma Cell Line. *Cells* 9, 2722. 10.3390/cells9122722 [PMC free article] [PubMed] [CrossRef] [Google Scholar]

52. Staubach S., Bauer F. N., Tertel T., Börger V., Stambouli O., Salzig D., et al. (2021). Scaled Preparation of Extracellular Vesicles from Conditioned media. *Adv. Drug Deliv. Rev.* 177, 113940. 10.1016/j.addr.2021.113940 [PubMed] [CrossRef] [Google Scholar]

53. Sverdlov E. D. (2012). Amedeo Avogadro's Cry: What Is $1\mu g$ of Exosomes? *BioEssays* 34, 873–875. 10.1002/bies.201200045 [PubMed] [CrossRef] [Google Scholar]

54. Théry C., Amigorena S., Raposo G., Clayton A. (2006). Isolation and Characterization of Exosomes from Cell Culture Supernatants and Biological Fluids. *Curr. Protoc. Cell Biol.* 30, 1–29. 10.1002/0471143030.cb0322s30 [PubMed] [CrossRef] [Google Scholar]

55. Théry C., Witwer K. W., Aikawa E., Alcaraz M. J., Anderson J. D., Andriantsitohaina R., et al. (2018). Minimal Information for Studies of

Extracellular Vesicles 2018 (MISEV2018): a Position Statement of the International Society for Extracellular Vesicles and Update of the MISEV2014 Guidelines. *J. Extracellular Vesicles* 7, 1535750. 10.1080/20013078.2018.1535750 [PMC free article] [PubMed] [CrossRef] [Google Scholar]

56. Trino S., Lamorte D., Caivano A., De Luca L., Sgambato A., Laurenzana I. (2021). Clinical Relevance of Extracellular Vesicles in Hematological Neoplasms: from Liquid Biopsy to Cell Biopsy. *Leukemia* 35, 661–678. 10.1038/s41375-020-01104-1 [PMC free article] [PubMed] [CrossRef] [Google Scholar]

57. Urbanelli L., Buratta S., Tancini B., Sagini K., Delo F., Porcellati S., et al. (2019). The Role of Extracellular Vesicles in Viral Infection and Transmission. *Vaccines* 7, 1–20. 10.3390/vaccines7030102 [PMC free article] [PubMed] [CrossRef] [Google Scholar]

58. Urzì O., Raimondo S., Alessandro R. (2021). Extracellular Vesicles from Plants: Current Knowledge and Open Questions. *Int. J. Mol. Sci.* 22, 5366. 10.3390/ijms22105366 [PMC free article] [PubMed] [CrossRef] [Google Scholar]

59. Vagner T., Spinelli C., Minciacchi V. R., Balaj L., Zandian M., Conley A., et al. (2018). Large Extracellular Vesicles Carry Most of the Tumour DNA Circulating in Prostate Cancer Patient Plasma. *J. Extracellular Vesicles* 7, 1505403. 10.1080/20013078.2018.1505403 [PMC free article] [PubMed] [CrossRef] [Google Scholar]

60. Van Niel G., D'Angelo G., Raposo G. (2018). Shedding Light on the Cell Biology of Extracellular Vesicles. *Nat. Rev. Mol. Cell Biol.* 19, 213–228. 10.1038/nrm.2017.125 [PubMed] [CrossRef] [Google Scholar]

61. Wang B., Zhuang X., Deng Z.-B., Jiang H., Mu J., Wang Q., et al. (2014). Targeted Drug Delivery to Intestinal Macrophages by Bioactive Nanovescicles Released from Grapefruit. *Mol. Ther.* 22, 522–534. 10.1038/mt.2013.190 [PMC free article] [PubMed] [CrossRef] [Google Scholar]

62. Witwer K. W., Van Balkom B. W., Bruno S., Choo A., Dominici M., Gimona M., et al. (2019). Defining Mesenchymal Stromal Cell (MSC)-derived Small Extracellular Vesicles for Therapeutic Applications. *J. Extracellular Vesicles* 8, 1609206. 10.1080/20013078.2019.1609206 [PMC free article] [PubMed] [CrossRef] [Google Scholar]

63. Worsham R. D., Thomas V., Farid S. S. (2019). Potential of Continuous Manufacturing for Liposomal Drug Products. *Biotechnol. J.* 14, e1700740. 10.1002/biot.201700740 [PubMed] [CrossRef] [Google Scholar]

64. Yáñez-Mó M., Siljander P. R., Andreu Z., Zavec A. B., Borràs F. E., Buzas E. I., et al. (2015). Biological Properties of Extracellular Vesicles and Their Physiological Functions. *J. Extracellular Vesicles* 4, 1–60. 10.3402/jev.v4.27066 [PMC free article] [PubMed] [CrossRef] [Google Scholar]

65. Yuana Y., Böing A. N., Grootemaat A. E., van der Pol E., Hau C. M., Cizmar P., et al. (2015). Handling and Storage of Human Body Fluids for Analysis of Extracellular Vesicles. *J. Extracellular Vesicles* 4, 29260. 10.3402/jev.v4.29260 [PMC free article] [PubMed] [CrossRef] [Google Scholar]

66. Zhou X., Xie F., Wang L., Zhang L., Zhang S., Fang M., et al. (2020). The Function and Clinical Application of Extracellular Vesicles in Innate Immune Regulation. *Cell Mol. Immunol.* 17, 323–334. 10.1038/s41423-020-0391-1 [PMC free article] [PubMed] [CrossRef] [Google Scholar]

Check for updates

Chapter 6

Extracellular Vesicles From Microalgae: Uptake Studies in Human Cells and Caenorhabditis elegans

Picciotto S, Santonicola P, Paterna A, Rao E, Raccosta S, Romancino DP, Noto R, Touzet N, Manno M, Di Schiavi E, Bongiovanni A, Adamo G.. Front Bioeng Biotechnol. 2022 Mar 24;10:830189. doi: 10.3389/fbioe.2022.830189. PMID: 35402397; PMCID: PMC8987914.

132

Abstract

Extracellular vesicles (EVs) are lipid membrane nano-sized vesicles secreted by various cell types for intercellular communication, found in all kingdoms of life. Nanoalgosomes are a subtype of EVs derived from microalgae with a sustainable biotechnological potential. To explore the uptake, distribution and persistence of nanoalgosomes in cells and living organisms, we separated them from a culture of the chlorophyte Tetraselmis chuii cells by tangential flow filtration (TFF), labelled them with different lipophilic dyes and characterized their biophysical attributes. Then we studied the cellular uptake of labelled nanoalgosomes in human cells and in C. elegans, demonstrating that they enter the cells through an energy dependent mechanism and are localized in the cytoplasm of specific cells, where they persist for days. Our data confirm that nanoalgosomes are actively uptaken in vitro by human cells and in vivo by C. elegans cells, supporting their exploitation as potential nanocarriers of bioactive compounds for theranostic applications.

1 Introduction

Adhering to principles and practices of environmental sustainability in nanotechnology manufacturing is a multifaceted issue with myriads of applications, which range from the development of natural nanomedical devices to novel green nanomaterials suitable for several industrial sectors. The production of environmentally sustainable nanomaterials requires responsible nano-manufacturing practices so as to minimise the use of toxic chemicals, to reduce waste and to generate less greenhouse gases (Nel et al., 2013). Efforts are ongoing to develop new nanomaterials to be utilised as nanocarriers for specific targets or controlled drug delivery for diagnosis and disease treatment, but also as ingredients for new cosmetic and nutraceutical formulations (Arrad et al., 1992; Adamo et al., 2016; Adamo et al., 2017). There has been growing interest in microalgae, which are increasingly viewed as sustainable resources with applications in different fields (Sutherland et al., 2021). A range of microalgae species from varying lineages have been investigated for their potential to synthesise and accumulate value-added products with remarkable biological qualities (Orejuela-Escobar et al., 2021). For instance, it has been found that many microalgae can produce a variety of natural metabolites with high antioxidant potential (Tiwari et al., 2012; Zhu, 2015). Within the VES4US consortium, we developed a platform for the production of extracellular vesicles (EVs), called nanoalgosomes, which are isolated from the cultivation medium of microalgal reactors (Adamo et al., 2021; Picciotto et al., 2021). EVs, which are lipid membrane nano-sized vesicles secreted by various cell types, play critical roles in inter-cellular as well as inter-species communication (Muraca et al., 2015; Soareset al., 2017; Cai et al., 2018; Gill et al., 2019; Bleackley et al., 2020; Picciotto et al., 2020). Nanoalgosomes show several attributes expected from EVs in terms of morphology, size, distribution, protein content and immunoreactivity (Adamo et al., 2021; Picciotto et al., 2021). Moreover, nanoalgosomes offer a number of advantages compared to mammalian cell-, plant-, bacteria- or milk-derived EVs in that microalgal cells have high growth rates, can be cultured on non-arable land under controlled environmental conditions in photo-bioreactors, and can produce, in a renewable manner, nanoalgosomes with a yield comparable to those of other sources (Wang et al., 2013; Kim et al., 2015; Raimondo et al., 2015; Munagala et al., 2016; Bitto and Kaparakis-Liaskos, 2017; Gerritzen et al., 2017; Pocsfalvi et al., 2018; Paganini et al., 2019). In addition, the natural origin and sustainable trait of nanoalgosomes grant them greater societal acceptance and make them less subject to sensitive to ethical questions in the context of using them as new natural nano-materials. Previous results have shown nanoalgosomes to be uptaken by

different cellular systems and to be non-cytotoxic at the doses tested (Adamo et al., 2021; Picciotto et al., 2021). Here, a more detailed analysis is provided using different EV staining methods so as to better characterise their concentration, size distribution and cellular uptake in vitro (Verweij et al., 2021). Our knowledge is further extended by the use of an in vivo model organism Caenorhabditis elegans (Nematoda). This is carried out in the context of biosafety assessments in whole organisms of nanoparticles. As such, invertebrate in vivo assays have been recently considered highly suitable tests (Hunt, 2016; Wu et al., 2019). Unlike higher organisms, invertebrate models such as C. elegans are faster, less expensive and raise less ethical concerns for scientific research, hence fulfilling the 3R principles (Li et al., 2021). In addition, owing to its body transparency, C. elegans has been used to study nanoparticle uptake, toxicity and biodistribution (Scharf et al., 2013), to understand EVs secretion and function (Beer et al., 2016), or to explore the modulation of probiotic bacteria-derived EVs on host immune responses (Li et al., 2017). Our data show that nanoalgosomes can be efficiently taken up by mammalian cells in culture and by C. elegans intestinal cells, suggesting a potential role in cross-kingdom communication.

2 Materials and Methods

2.1 Microalgae Cultivation

A stock culture of the marine chlorophyte Tetraselmis chuii CCAP 66/21b was grown in borosilicate glass flask in f/2 medium (Guillard, 1975) up to its exponential growth phase and then used, via a 10% v/v inoculum, to inoculate a 7.5 L culture in a photobioreactor PB 200 (GroTech GmbH, Germany) at an initial concentration of 0.5 mg/ml (wet weight). The cultures were maintained at a temperature of $20 \pm 2°C$, with a white light intensity of 100 µE m^{-2} s^{-1} and a 14:10 light/dark photoperiod for 30 days.

2.2 Nanoalgosome Purification Methods: Tangential Flow Filtration

Nanoalgosome isolation was performed using the KrosFlo® KR2i TFF System from Repligen (Spectrum Labs., Los Angeles, CA, United States) and three modified polyethersulfone hollow fiber membranes (S04-E65U-07-N, S04-P20-10-N and S04-E500-10-N, Spectrum Labs.). Briefly, after 30 days, the microalgae cultures were clarified by microfiltration using a 650 nm hollow fiber cartridge housed in the KrosFlo® KR2i TFF System. Feed flow and transmembrane pressure (TMP) were kept constant at 450 ml/min and 0.05 bar, respectively. The first retentate (>650 nm sized

particles) was concentrated into a final volume of 150 ml, and the 650 nm permeate (<650 nm sized particles) was then processed for a second microfiltration step using a 200 nm hollow fiber membrane at a 450 ml/min feed flow and 0.05 bar TMP. The resulting permeate (<200 nm sized particles) was processed for the last ultrafiltration step using a 500 kDa MWCO hollow fiber membrane with a feed flow of 450 ml/min and 0.05 bar TMP, prior to concentration to a final volume of 150 ml. Subsequently, the samples were further concentrated and diafiltrated seven times with PBS using a smaller 500-kDa cutoff TFF filter module (C02-E500-10-N, Spectrum Labs., MicroKros) and a feed flow of 75 ml/min and 0.25 bar TMP, returning a final volume of approximately 5 ml.

## 2.3 Nanoalgosome Fluorescent Labelling

The protein content of nanoalgosomes was measured using the micro-bicinchoninic BCA Protein Assay Kit (Thermo Fishers Scientific) (Romancino et al., 2018) and the nanoparticle size distribution and concentration were measured using a NanoSight NS300 (Malvern Panalytical, United Kingdom) as described in Adamo et al., 2021. After performing nanoalgosome quality control checks (Figure 1), EV labelling was carried out using three specific lipophilic dyes (Di-8-Anepps, PKH26 and DiR). Nanoalgosome staining with the Di-8-Anepps was performed as in Adamo et al., 2021. Briefly, 500 nM of Di-8-Anepps (Invitrogen, filtered 20 nm with Anotop filter) was incubated with 5×10^{10} particles/mL for 30 min at room temperature. The samples were dialysed (Slide-A-Lyzer MINI Dialysis Device, 3.5 KDa MWCO, Thermo Fishers Scientific) against PBS to remove unbound fluorophore. The red fluorescent staining of nanoalgosomes was carried out using PKH26, a fluorescent cell linker used for cell membrane labelling (Ex/Em: 551/567 nm, Sigma-Aldrich). As for Di-8-Anepps, PKH26 fluorescence is activated in apolar environments and is specifically enhanced when bound to the lipid membrane of cells or EVs. The third lipophilic dye, DiR (1,1′-Dioctadecyl-3,3,3′,3′-Tetramethylindotricarbocyanine Iodide, Invitrogen, filtered 20nm, Anotop filter) is weakly fluorescent in H2O but fluorescent and photo-stable when incorporated into lipid membranes. Prior to staining, PKH26 in the Diluent C (supplied by Sigma-Aldrich with PKH26) vehicle was incubated at 37°C for 15 min to a final concentration of 3 μM (dye solution), while DiR was used at 0.5, 1, 3.5 μM (dye solutions). In parallel, particle-free PBS was used as a control for both dyes, using the specific amount of free probe for each. For the labelling of nanoalgosomes, 5×10^{10} particles/mL were incubated with dye solutions. After 1 h at room temperature, the stained nanoalgosomes were diluted to 3 ml with PBS and pelleted by

ultracentrifugation at $118{,}000 \times g$ for 70 min at 4°C using a Beckman SW55Ti rotor to remove the unbound dyes (Wiklander et al., 2015; Pužar et al., 2018). The pellet was gently resuspended in PBS overnight at 4°C. The quality check for Di-8-Anepps fluorescent nanoalgosomes was then monitored by Fluorescent Nanoparticle Tracking Analysis (NTA) using the Nanosight NS300 instrument (Malvern Panalytical, Malvern, United Kingdom). Dilution of the sample in PBS was performed in order to adjust the range of particles per frame to the working range of the system (108 particle/mL). A total of five videos were captured at a syringe speed of 60 in light scattering and 150 in fluorescence modes. Data were further processed using the NanoSight Software NTA 3.1 Build 3.1.46 with a detection threshold of 5. The absence of significant fluorescent signal after dialysis on labelled control samples, at an equivalent fluorophore concentration used to that of the labelled nanoalgosomes, was confirmed (data not shown). Quality check for PKH26-labelled nanoalgosomes was verified by spectrofluorimetric analysis (Spectrofluorometer Jasco fp-6500) and the size distribution and concentration were checked with NTA. The staining efficiency of DiR-labelled nanoalgosomes was verified by Odyssey infrared Imaging System (LiCor Biosciences, software V 3.0) and the size distribution and concentration were checked with NTA.
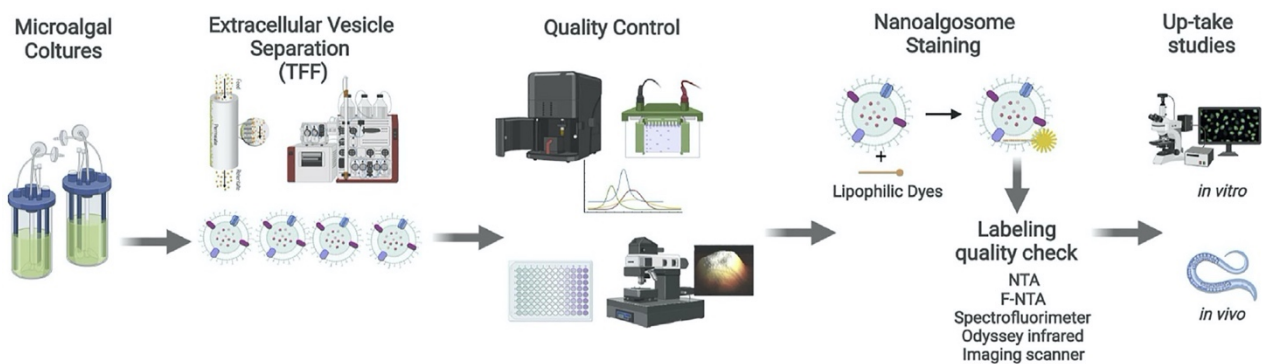
FIGURE 1. Nanoalgosome production workflow. Starting from the *T. chuii* culture medium, nanoalgosomes are separated by TFF and checked by quality control procedures. Downstream analyses include the staining of nanoalgosomes and in vitro and in vivo uptake studies. Created also with the support of BioRender.com.

2.4 In vitro Cellular Uptake of Nanoalgosomes

2.4.1 Cell Cultures

MDA-MB 231, an epithelial, human breast cancer cell line, was maintained at 37°C in a humidified atmosphere (5% CO_2) in Dulbecco's Modified Eagle Medium (DMEM)

(Sigma-Aldrich) containing 10% (v/v) Fetal Bovine Serum (FBS) (Gibco, Life Technologies) plus 2 mM L-glutamine, 100 U/mL penicillin and 100 mg/ml streptomycin (Sigma-Aldrich).

2.4.2 Cellular Uptake Study

For the PKH26-labelled nanoalgosome uptake experiment, the MDA-MB 231 cell line was grown at a density of 5×10^4 cells/well in 12-well plates containing sterile coverslips in complete medium for 24 h. Cells were then incubated with different amounts of nanoalgosomes (10 and 20 μg/ml) at 37°C or 4°C, as well as with an equivalent amount of the control samples. After different incubation times (3, 6 and 24 h), cells were washed twice with PBS, fixed with 3.7% paraformaldehyde for 15 min and washed again twice with PBS. The nuclei were then stained with VECTASHIELD Mounting Medium with DAPI. For the DiR-labelled nanoalgosome uptake experiment, MDA-MB 231 cells were plated at a density of 4×10^3 cells/well in 96-well plates in complete medium for 24 h. Cells were then incubated with different amount of nanoalgosomes (2 and 10 μg/ml, respectively stained with of 0.5, 1, 3.5 μM of DiR) at 37°C or 4°C, as well as with an equivalent amount of control samples. After different incubation times (3, 6 and 24 h), the fluorescence intensities inside the cells were monitored in real time, after removing the culture medium, with the Odyssey infrared Imaging System (LiCor Biosciences, software V 3.0). Cell viability assay was performed as previously described in Adamo et al., 2021, incubating MDA MB 231 cells with 10 and 20 μg/ml of nanoalgosomes for 24 and 48 h. All experiments were performed in three independent biological replicates. Statistical analysis was performed using a One-way ANOVA calculated by Statistics Kingdom online software.

2.4.3 Fluorescence and Confocal Microscopy Analysis

The PKH26-labelled nanoalgosomes cellular localization was monitored by fluorescence microscopy analysis (Nikon Eclipse 80i) and confocal laser scanning microscopy (Olympus FV10i; a 1 μm thick optical section was taken from a total of about 15 sections for each sample). The orthogonal projection of the Z-stack was obtained using the imageJ software.

2.5 In vivo Cellular Uptake of Nanoalgosomes

2.5.1 Animal Culture

Nanoalgosome uptake was assessed in wild type C. elegans strain N2, Bristol variety and in HA2031 strain, harboring rtIs31 transgene that expresses GFP in the intestinal

nuclei. These strains were provided by the Caenorhabditis Genetics Center (CGC), which is funded by the NIH Office of Research Infrastructure Programs (P40 OD010440). Animals were grown and handled following standard procedures under uncrowded conditions on nematode growth medium (NGM) agar plates seeded with Escherichia coli strain OP50, unless differently specified (Brenner, 1974).

2.5.2 In vivo Uptake of Nanoalgosomes by C. elegans

For the soaking experiments, thirty synchronized animals, at L4 larval stage, were manually transferred into a medium composed of OP50 bacteria, M9 buffer, antibiotic antimycotic solution (2x) (cat. n. A5955 Sigma-Aldrich®) and cholesterol (5 ng/ml), supplemented with Di-8-Anepps-nanoalgosomes (12 μg/ml or 20 μg/ml final concentrations) in a 96 multi-well plate (70 μl final volume/well). After 3, 6 and 24 h of treatment in the dark and mild agitation on a swinging oscillator (15 rpm), the animals were transferred to clean NGM plates with bacteria to allow the animals to crawl for 1 h, so as to remove the excess of dye. For the in solido experiments, twenty synchronized L4 larvae were transferred on freshly prepared NGM plates seeded with heat-killed OP50 bacteria and Di-8-Anepps-nanoalgosomes (20 μg/ml, final concentration), PKH26-nanoalgosomes (45 μg/ml), Di-8-Anepps (2.5 μM), PKH26 (7.5 μM), PBS buffer or unstained nanoalgosomes (20 μg/ml). The dilutions were performed considering the final volume of NGM (4 ml), meaning that to obtain a final concentration of 20 μg/ml of nanoalgosomes, 80 μg of EVs corresponding to ~4×10^{12} total particles were added to the solified agar in the plates. After 24 h of exposure in the dark, young adult animals were transferred to clean NGM plates with OP50 bacteria to let the animals crawl for 1 h and remove the excess of dye. For the injection experiments, ten animals were injected and were analyzed after 24 h. Young-adult animals were immobilised on agar pads with halocarbon oil 700 (cat. n.H8898 Sigma-Aldrich®) and injected in the pseudocoelom cavity near the pharynx (avoiding the intestine) with Di-8-Anepps-nanoalgosomes (20 μg/ml) (Mello et al., 1995; Mohan et al., 2010). Animals were then recovered on clean NGM plates with OP50 bacteria for 24 h. All experiments were performed in triplicates using at least two independent nanoalgosomes preparations.

2.5.3 Fluorescence and Confocal Microscopy Analysis

After allowing the animals to eliminate the excess of dye, they were transferred on glass slides with 4% agar pads and immobilized alive for microscopy analysis with 0.01% tetramisole hydrochloride (cat. N. T1512 Sigma-Aldrich®). Confocal and epi-fluorescence (FITC filter) images were collected with Leica TCS SP8 AOBS

microscope using a 40x objective. For persistence analysis, the animals were collected and observed after 24, 48 and 72 h from the treatment.

3 Results

3.1 Setting up of Efficient Staining of Nanoalgosomes Using Three Different Dyes

Nanoalgosomes were isolated from the conditioned medium of a *T. chuii* culture by TFF and were characterised using biophysical and biochemical approaches (see Figure 1). As previously described, the nanoalgosomes were stained with Di-8-Anepps, a lipophilic dye which is non-fluorescent until bound to membranes, to verify the presence of lipid bilayer-nanovesicles, and in turn to check the quality of nanoalgosome preparations (Adamo et al., 2021). Here, we assessed the uptake of Di-8-Anepps-labelled nanoalgosomes in *C. elegans*. Further, two additional nanoalgosome staining strategies were considered using red and infrared lipophilic fluorescent dyes for future applications in potency assays in vitro and in vivo (Gangadaran et al., 2018). A quality check of the staining procedure was performed by NTA and no variations in size and concentration were obtained for the nanoalgosomes labelled with the three lipophilic dyes compared to the unstained nanoalgosome controls (Figure 2). We monitored the size distribution of the fluorescent Di-8-Anepps-nanoalgosomes cleaned from the free dye using NTA in fluorescence and light scattering (Figure 2A). In this way, we excluded artifacts, like protein aggregates, nanobubbles and insoluble salts, which returned a green fluorescent nanoalgosome population (54% of the total nanoparticles as measured by light scattering) with the same size distribution and mode of the unstained control. NTA operated in standard scattering mode was also used for the PKH26- and DiR-based nanoalgosome staining to compare concentrations and size distributions between the original and stained samples. After PKH26-labelling, the nanoalgosome size distribution and concentration remained constant at 88 ± 2.5 nm and $1.8 \times 10^{12} \pm 9.8 \times 10^{10}$ particles/mL, respectively, confirming the absence of aggregates (Figure 2B). Figure 2B' shows the comparison of the fluorescence emission spectra of PKH26-labelled nanoalgosomes, unstained nanoalgosomes and free dye. Neither the raw nanoalgosomes nor the free dye emitted fluorescence when excited (λ551nm) whereas PKH26-labelled nanoalgosomes showed high red fluorescent emission (λ567nm), confirming successful staining. The DiR dye was selected based on its high stability in biological fluid for future in vivo applications. Based on literature data reported for the DiR staining of mammalian cell-derived extracellular vesicle (Gerwing et al., 2020; Samuel et al., 2021; Verweij et al.,

2021), we tested three different starting concentrations of the DiR dye (0.5, 1, 3.5 µM) to optimise the labelling of nanoalgosomes. The size distribution and concentration of the nanoalgosomes did not undergo changes following the removal of the free dye compared to unstained nanoalgosomes (Figure 2C). Figure 2C' shows the fluorescence emission images (λ800nm) obtained using an Odyssey infrared Imaging scanner, before and after removal of the free dye. A more effective staining of nanoalgosomes was obtained using 3.5 µM of DiR, which returned a higher fluorescence intensity compared to the other two other concentrations (i.e., 0.5 and 1 µM) and the negative controls (i.e., free DiR that showed no detectable fluorescence) after free dye removal.
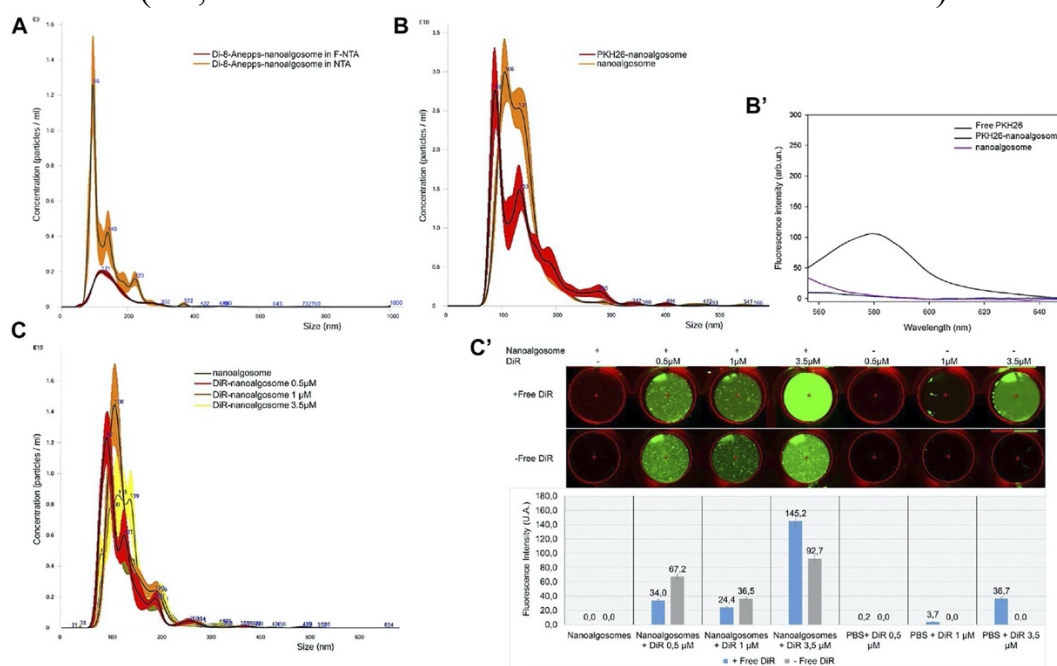
FIGURE 2. Fluorescent staining of nanoalgosomes with three different dyes (A) Fluorescent-NTA (F-NTA) and standard (scattering mode) NTA to determine the size distribution and concentration of nanoalgosomes stained with Di-8-ANEPPS. This comparative analysis gives the concentration of fluorescent nanoparticles, excluding non-vesicle contaminants. (B) Size distributions and concentrations by NTA of PKH26-labelled nanoalgosomes and unstained nanoalgosomes, showing a largely overlapping distribution. (B') Fluorescent emission spectra of PKH26-labelled nanoalgosomes compared to PKH26 free dye and unstained nanoalgosomes. (C) Size distribution and concentration analyses by NTA of nanoalgosomes stained with DiR at different concentrations show no variation compared to unstained nanoalgosomes after the free dye removal. (C') Infrared fluorescent emission imaging and intensities (λ800nm) obtained using an Odyssey IR scanner of DiR-labelled nanoalgosomes and free dye at different concentrations before and after free dye removal.

3.2 In vitro Uptake of PKH26 and DiR Labelled Nanoalgosomes

To study the intracellular uptake of isolated *T. chuii*-derived nanoalgosomes, we used PKH26 and DiR fluorescent dyes that were incorporated into the lipid membrane of nanoalgosomes. We previously demonstrated the biocompatibility of nanoalgosomes as well as the cellular uptake using nanoalgosomes stained with Di-8-Anepps, demonstrating that they are internalised by human cells over time through an energy dose-dependent mechanism (Adamo et al., 2021). First, we studied the uptake of red-fluorescent nanoalgosomes using MDA MB 231 cells treated with different doses (10–20 µg/ml), for 3, 6 and 24 h at 37 and 4°C (Figure 3). Moreover, we verified that incubation with nanoalgosomes (10 and 20 µg/ml up to 48 h) did not affect cell viability or induce cell proliferation in MDA MB 231 cells (Supplementary Figure S1). In Figure 3A, epifluorescence images resolve the positions of PKH26 labelled nanoalgosomes within tumor cells. Dose- and time-dependent uptakes were observed. The uptake increased with incubation time at 37°C, while it was inhibited by incubation at 4°C, indicating an energy-dependent endocytic process. The images in Figure 3A show a low PKH26-nanoalgosome internalization for short incubation times (i.e., 3 h). After 6 h of incubation, the amount of red fluorescent nanoalgosomes within the cells increased, reaching a maximum cytoplasmic/intracellular concentration after 24 h. No red fluorescent signal was observed for MDA-MB 231 cells incubated with the controls (staining-control samples after free dye removal) for all duration and temperature treatments used. Confocal microscopy analyses supported the specificity of PKH26-labelled nanoalgosome uptake as the orthogonal projections showed evident intracellular intracellular localization, in the mid-section focal plan of the cytoplasm closed to the nucleus (Figure 3B). Finally, to assess the DiR-labelled nanoalgosome uptake *in vitro*, the cellular internalisation was compared across the doses and durations tested. The Odyssey images showed that DiR-labelled nanoalgosomes were internalised over time, in a dose- and energy-dependent manner, as observed with the other two dyes (Figure 3C). The fluorescence intensities measured in real time inside the tumor cell line for all tested conditions at 37°C are shown in Figure 3C'. Interestingly, there was a higher level of internalization for the cells incubated with 10 µg/ml of nanoalgosomes stained with 3.5 µM of DiR, after 24 h of incubation compared to the other tested conditions. With these experiments we set-up a protocol for the best staining strategy of nanoalgosomes using three different fluorescence dyes, we confirmed the cellular uptake of nanoalgosomes and we established the best conditions for further in vivo experiments. Specifically, near-infrared dye is suitable for non-

invasive *in vivo* applications because of their high signal-to-noise ratio, low autofluorescence of biological tissue in the 700–900 nm spectral range, and deep tissue penetration of the near-infrared light.
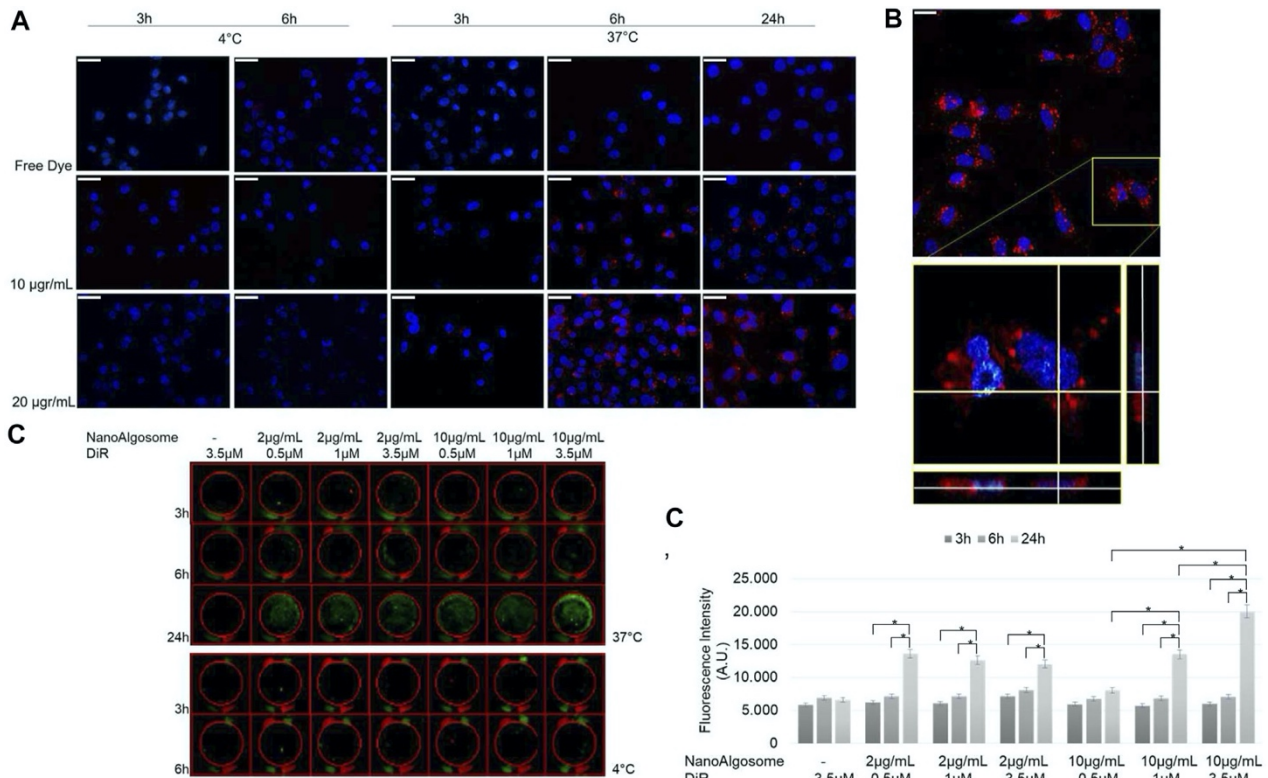
FIGURE 3. Nanoalgosome cellular uptake in vitro. (A) Representative fluorescence microscopy images showing the cellular uptake of PKH26-fluorescent nanoalgosomes (red) in MDA-MB 231 cells (nuclei in blue) incubated with different concentrations of PKH26-labelled nanoalgosomes (10 and 20 μg/ml) at 37°C for 3, 6 and 24 h. The free dye control and 4°C incubations are shown as negative controls (Magnification 40X). Scale bar 50 μm. (B) Confocal microscopy analysis of PKH26-labelled nanoalgosome internalization in MDA-MB 231 cells (nuclei in blue) incubated with 20 μg/ml of red fluorescent nanoalgosomes at 37°C for 24 h. The inset of confocal Z-stack acquisition shows its orthogonal projections at a focal depth of 9 μm over a total scanning thickness of ~18 μm (Magnification 60X). Scale bar 25 μm. (C) Representative infra-red scanner images showing the cellular uptake of DiR-labelled nanoalgosomes (green) in MDA-MB 231 cells incubated with different concentrations of DiR-labelled nanoalgosomes at 37°C for 3, 6 and 24 h. The corresponding IR fluorescence intensities are measured in triplicate (*$p < 0.0001$) and reported (C') through the in-cell function of Odyssey V3.0 software. Free dye and 4°C incubations are shown as negative controls.

**3.4 In vivo Cellular Uptake in C. elegans**

The animal model *C. elegans* was used for testing exogenous EVs uptake, distribution and persistence. First, we tested different times of treatment (3, 6 and 24 h) and two concentrations (12 µg/ml and 20 µg/ml) of Di-8-Anneps-labelled nanoalgosomes. Green fluorescent signal was observed only in the intestine of the animals (Figure 4). The best condition in terms of brightness was obtained using 20 µg/ml dose for 24 h treatment. In this case, the labelled particles were administered by immersing the animals in the nanoalgosome-containing solution (soaking), which allowed to rapidly test a high number of animals using several conditions at once together with limited manipulation and less nanoalgosomes being needed (Figures 4A,C). Then, to identify the best conditions to study EV uptake in a whole living animal, we compared three different administration methods: soaking (*in liquido*), *in solido*, and injection. These methods offer advantages and disadvantages in terms of costs, time, physiology of the animals, quantity and concentration of EVs, and number of animals treated (Figure 4A). After treating the animals with Di-8-Anneps-labelled nanoalgosomes a fluorescent signal was observed in their intestine in all conditions (Figures 4B–D). A faint fluorescent signal was also observed in the head of the animals when using the *in solido* administration (Figure 4D). To confirm the specificity of the fluorescence observed, Di-8-Anepps free dye and unlabeled nanoalgosomes were used as controls for all the administration methods and no signal was visible, except in the lumen *in solido* and faintly in the head after soaking (Figures 4B–D). The treatments did not affect animal survival with all concentrations and methods tested. *In solido* and injection administrations showed similar labelling in the animals analysed, while soaking was less efficient and not all the animals were labelled; moreover a fluorescent signal was also observed in the intestinal lumen. Since injection is a time-consuming technique, allowing the observation of only few animals, the *in solido* method was used for further analyses. The whole animal body was observed at higher magnification, but the fluorescent signal appeared mostly confined to intestinal cells (Figure 5A). Confocal images confirmed the observations, highlighting a punctuate fluorescent signal in the intestinal cells and in the head of all animals treated with Di-8-Anepps-nanoalgosomes, but no signal was observed in the animals treated with PBS or unlabelled nanoalgosomes (Figure 5A). An unexpected fluorescent signal was instead observed in the head of the animal, but not in the intestinal cells, after treatment with Di-8-Anepps free dye, albeit using higher concentrations compared to the dye incorporated in nanoalgosomes (arrowheads in Figure 5A). To further confirm our observations, animals were treated with nanoalgosomes stained with the lipophilic PKH26 dye for 24 h and similar results were observed (Figure 5A). C. elegans body

transparency allows the visualization of fluorescent proteins in specific tissues or cells when expressed through transgenics in living whole animals. Thus, we performed confocal analysis, on transgenic animals expressing the GFP only in intestinal nuclei after treatment with Di-8-Anepps-nanoalgosomes, confirming that the fluorescent signal is localized only in the cytoplasm of the intestinal cells (Figure 5B). The persistence of the fluorescent signal in a living whole organism was assessed by observing animals at 24, 48 and 72 h after injection or after interrupting the treatment *in solido*. Using both approaches, we observed that the specific intestinal fluorescent signal did persist, albeit becoming fainter after 72 h post-treatment; interestingly this time-window coincides with the entire fertile period of adult animals (Figures 5C,D). We demonstrated that C. elegans intestinal cells uptake labelled extracellular vesicles and this fluorescence persists for 3 days; thus nanoalgosomes can be recognized and internalized in living organisms.
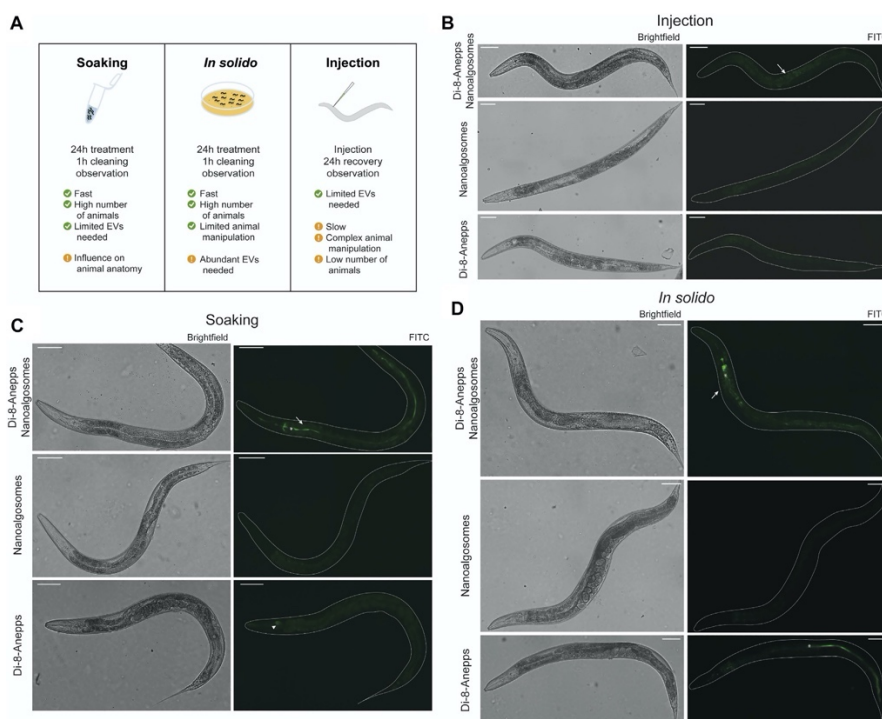
FIGURE 4. Set-up of labelled nanoalgosomes treatment in C. elegans. (A) Schematic representation of the administration methods used for testing the uptake in C. elegans of fluorescent nanoalgosomes. The best conditions used for treating animals as well as some advantages and disadvantages are listed. (B–D) Brightfield (left) and epifluorescence (with FITC filter, right) images of animals treated with Di-8-Anepps-nanoalgosomes, nanoalgosomes and free-dye (Di-8-Anepps) by injection (B), soaking (C) and *in solido* (D). A fluorescent signal was observed in the intestinal cells of the animals treated with labeled nanoalgosomes (arrows). Moreover, aspecific signals

were observed in the head after soaking (arrowhead) and *in solido* with free-dye (asterisks). Anterior is left and ventral is down. Scale bar 75 µm.
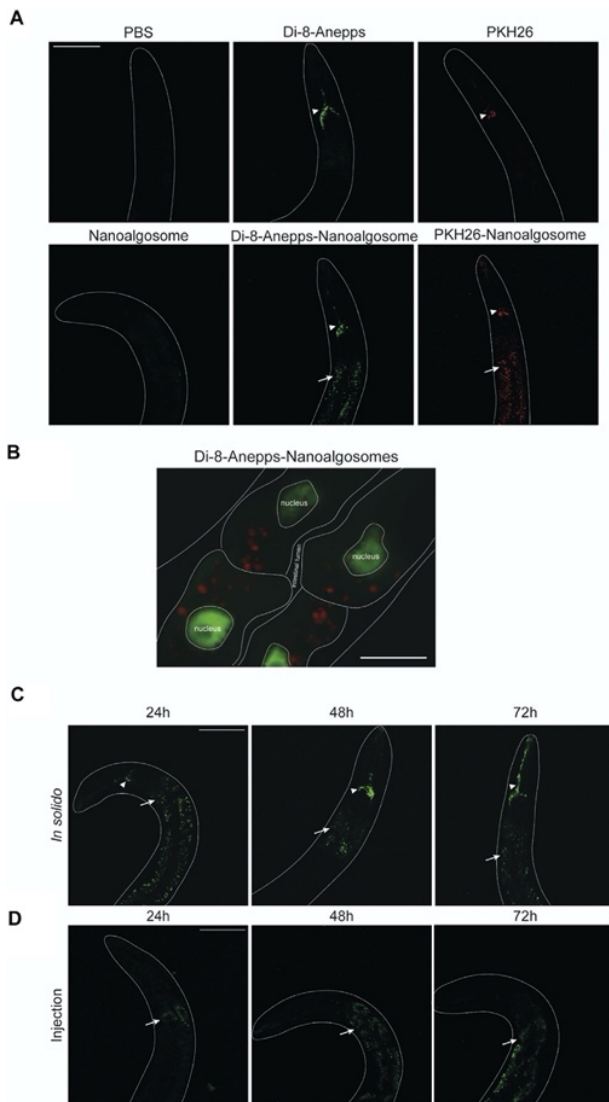
FIGURE 5. *C elegans* intestinal cells uptake and persistence of labelled nanoalgosomes.(A) Confocal images of animals treated with PBS, Di-8-Anepps free dye, PKH26 free dye for 24 h are shown in the upper panels; animals treated for 24 h with unstained nanoalgosomes, Di-8-Anepps-nanoalgosomes and PKH26-nanoalgosomes are shown in the lower panels. A fluorescent signal was observed in animals treated with labelled nanoalgosomes in the intestinal cells (arrows) and in the head (arrowheads). Anterior is up. Scale bar 75 µm. (B) Localisation of Di-8-Anepps-nanoalgosomes in the cytoplasm of intestinal cells expressing GFP in the nuclei thanks to *elt-2* promoter. The Di-8-Anepps-nanoalgosomes specific signal has been pseudo-colored in red. Scale bar 25 µm. (C,D) The persistence of the fluorescent signal (arrows) was assessed in animals treated with Di-8-Anepps-nanoalgosomes for 24, 48 and 72 h after treatments *in solido* (C) or injection (D). A fluorescent signal in the head (arrowheads) is also visible *in solido*. Anterior is up. Scale bar 75 µm.

4 Discussion

In this study, we explored the labelling of nanoalgosomes using three lipophilic dyes with different fluorescence emissions (green, red and infrared) and the monitoring of their uptake with in vitro and in vivo assays. The use of lipophilic dyes to study EV biogenesis and to carry out functional studies is quite common (Verweij et al., 2021). Microalgal derived extracellular vesicles have recently been characterised (Picciotto et al., 2021). Here, we report the isolation of nanoalgosomes from T. chuii culture medium by TFF, which were successfully labelled with three lipophilic dyes. The stained nanoparticles were then characterised in terms of size, concentration and fluorescence intensity using NTA, spectrofluorometric and infrared analyses. PKH26 and DiR labelled nanoalgosomes were successfully internalised by cultured tumoral cells in a way similar to that recently described for Di-8-Anepps labelled nanoalgosomes (Adamo et al., 2021). Epi-fluorescence microscopy confirmed that MDA MB231 cells can internalise PKH26-positive nanoalgosomes in a dose-, time- and energy-dependent manner. Subsequent confocal microscopy analysis of tumor cells revealed numerous red fluorescent puncta in the cell cytoplasm, while the orthogonal views showed the intracellular localisation of labeled nanoalgosomes closed to nucleus. The same uptake pattern was observed for nanoalgosomes labelled with the DiR dye. The biological model system C. elegans was used to ascertain, in a living multicellular-organism, whether unstained nanoalgosomes can be uptaken and in which body parts they accumulate. Since we evaluated for the first time, to the best of our knowledge, the uptake of exogenous labelled EVs in C. elegans, we initially compared three administration routes previously used for the delivery of nanoparticles (Mohan et al., 2010; Zhang et al., 2011; Perni et al., 2017). We successfully observed for the three approaches tested a specific fluorescent signal in the cytoplasm of intestinal cells, with minor differences among the three administration methods. By using these different administration methods we demonstrated that EVs could be uptaken by both apical and basolateral membrane of the intestinal cells, in line with the high endocytic and exocytic trafficking capability of the intestinal cells (Sato et al., 2014). Following the exposure of the animals to labelled nanoalgosomes via the *in solido* method, we also observed a fluorescent signal in the head, possibly in the neurons, which are mainly concentrated at the anterior end of the animals and able to sense the environment through cilia. A similar observation was made using a very high concentration of free dyes, which can be explained by the fact that lipophilic dyes have

been extensively used in *C. elegans* to label amphid neurons (Starich et al., 1995). Thus we cannot exclude that the labelling of neurons can be specifically obtained with labelled nanoalgosomes. Nevertheless, using all the three methods we did not observe any fluorescent signal in other animal tissues, suggesting a tissue-specific uptake of the nanoalgosomes. While the soaking and *in solido* exposure routes allow the simultaneous treatment and analysis of hundreds of animals, injection is performed one animal at a time, which it is time consuming and cannot be applied to many animals. On the other hand, considering the amount of starting material needed, both soaking and injection can be preferred as they require a lower amount of EVs compared to feeding. However, worms usually grow *in solido* and *in liquido* cultivation can alter animal anatomy and its physiology (Çelen et al., 2018). Considering the availability of nanoalgosomes and the importance of observing several animals under suitable physiological conditions, the *in solido* method was chosen as the preferred option. The specificity of the observed signal was assessed using controls and the two lipophilic free dyes Di-8-Anepps and PKH26, thus further confirming the robustness of our nanoalgosome labelling approach. Finally we demonstrated that C. elegans, with its body transparency and potent genetics, is a powerful model system to study exogenous EVs uptake, persistence and biodistribution. The data gathered in the present study showed that three different methods can be used to stain efficiently nanoalgosomes for in in vivo and in vitro uptake studies, and further applied in functional studies as nano-delivery system.

Data Availability Statement

The raw data supporting the conclusion of this article will be made available by the authors, without undue reservation.

Author Contributions

Study concepts and design: GA, ED, and AB; nanoalgosome staining and in vitro cellular uptake experiments and data evaluation: SP and GA; C. elegans experiments and data evaluation: PS and ED; manuscript preparation: SP, PS, GA, AB, and ED; support in microalgae cultures and nanoalgosome isolation: DR, AP, ER, SR, RN, MM, and NT. Approval of the final version of the manuscript submitted: all authors.

Funding

Conflict of Interest

The authors declare that the research was conducted in the absence of any commercial or financial relationships that could be construed as a potential conflict of interest.

Publisher's Note

All claims expressed in this article are solely those of the authors and do not necessarily represent those of their affiliated organizations, or those of the publisher, the editors and the reviewers. Any product that may be evaluated in this article, or claim that may be made by its manufacturer, is not guaranteed or endorsed by the publisher.

Acknowledgments

Supplementary Material

The Supplementary Material for this article can be found online at: https://www.frontiersin.org/articles/10.3389/fbioe.2022.830189/full#supplementary-material

References

1. Adamo, G., Fierli, D., Romancino, D. P., Picciotto, S., Barone, M. E., Aranyos, A., et al. (2021). Nanoalgosomes: Introducing Extracellular Vesicles Produced by Microalgae. J. Extracellular Vesicles 10, e12081. doi:10.1002/jev2.12081 CrossRef Full Text | Google Scholar.

2. Adamo, G., Grimaldi, N., Campora, S., Bulone, D., Bondì, M., Al-Sheikhly, M., et al. (2016). Multi-Functional Nanogels for Tumor Targeting and Redox-Sensitive Drug and siRNA Delivery. Molecules 21 (11), 1594.

doi:10.3390/molecules21111594 PubMed Abstract | CrossRef Full Text | Google Scholar

3. Adamo, G., Grimaldi, N., Sabatino, M. A., Walo, M., Dispenza, C., and Ghersi, G. (2017). E-beam Crosslinked Nanogels Conjugated with Monoclonal Antibodies in Targeting Strategies. Biol. Chem. 398 (2), 277–287. doi:10.1515/hsz-2016-0255 PubMed Abstract | CrossRef Full Text | Google Scholar

4. Arad, S., and Yaron, A. (1992). Natural Pigments from Red Microalgae for Use in Foods and Cosmetics. Trends Food Sci. Tech. 3, 92–97. doi:10.1016/0924-2244(92)90145-m. CrossRef Full Text | Google Scholar

5. Beer, K. B., and Wehman, A. M. (2016). Mechanisms and Functions of Extracellular Vesicle Release In Vivo-What We Can Learn from Flies and Worms. Cell Adhes. Migration 11 (2), 135–150. Epub 2016 Sep 30. doi:10.1080/19336918.2016.1236899.PubMed Abstract | CrossRef Full Text | Google Scholar

6. Bitto, N., and Kaparakis-Liaskos, M. (2017). The Therapeutic Benefit of Bacterial Membrane Vesicles. Ijms 18 (6), 1287. doi:10.3390/ijms18061287 PubMed Abstract | CrossRef Full Text | Google Scholar

7. Bleackley, M. R., Samuel, M., Garcia-Ceron, D., Mckenna, J. A., Lowe, R. G. T., Pathan, M., et al. (2020). Extracellular Vesicles from the Cotton Pathogen Fusarium Oxysporum F. Sp. Vasinfectum Induce a Phytotoxic Response in Plants, Frontiers in Plant Science, Frontiers in Plant Science, 1610. doi:10.3389/fpls.2019.01610. CrossRef Full Text | Google Scholar

8. Brenner, S. (1974). The Genetics of Caenorhabditis elegans. Genetics 77 (1), 71–94. doi:10.1093/genetics/77.1.71. PubMed Abstract | CrossRef Full Text | Google Scholar

9. Cai, Q., Qiao, L., Wang, M., He, B., Lin, F.-M., Palmquist, J., et al. (2018). Plants Send Small RNAs in Extracellular Vesicles to Fungal Pathogen to Silence Virulence Genes. Science 360 (6393), 1126–1129. doi:10.1126/science.aar4142. PubMed Abstract | CrossRef Full Text | Google Scholar

10. Çelen, İ., Doh, J. H., and Sabanayagam, C. R. (2018). Effects of Liquid Cultivation on Gene Expression and Phenotype of C. elegans. BMC Genomics 19 (1), 562. doi:10.1186/s12864-018-4948-7. PubMed Abstract | CrossRef Full Text | Google Scholar

11. Gangadaran, P., Hong, C. M., and Ahn, B.-C. (2018). An Update on In Vivo Imaging of Extracellular Vesicles as Drug Delivery Vehicles. Front. Pharmacol. 9, 169. doi:10.3389/fphar.2018.00169. PubMed Abstract | CrossRef Full Text | Google Scholar

12. Gerritzen, M. J. H., Martens, D. E., Wijffels, R. H., Van der Pol, L., and Stork, M. (2017). Bioengineering Bacterial Outer Membrane Vesicles as Vaccine Platform. Biotechnol. Adv. 35 (5), 565–574. Epub 2017 May 15. doi:10.1016/j.biotechadv.2017.05.003. PubMed Abstract | CrossRef Full Text | Google Scholar

13. Gerwing, M., Kocman, V., Stölting, M., Helfen, A., Masthoff, M., Roth, J., et al. (2020). Tracking of Tumor Cell-Derived Extracellular Vesicles In Vivo Reveals a Specific Distribution Pattern with Consecutive Biological Effects on Target Sites of Metastasis. Mol. Imaging Biol. 22 (6), 1501–1510. Epub 2020 Jul 31. doi:10.1007/s11307-020-01521-9. PubMed Abstract | CrossRef Full Text | Google Scholar

14. Gill, S., Catchpole, R., and Forterre, P. (2019). Extracellular Membrane Vesicles in the Three Domains of Life and beyond. FEMS Microbiol. Rev. 43 (3), 273–303. doi:10.1093/femsre/fuy042. PubMed Abstract | CrossRef Full Text | Google Scholar

15. Guillard, R. R. L. (1975). Culture of Phytoplankton for Feeding Marine Invertebrates, Culture of Marine Invertebrate Animals. Boston, MA: Springer US, 29–60. doi:10.1007/978-1-4615-8714-9_3Culture of Phytoplankton for Feeding Marine Invertebrates. CrossRef Full Text | Google Scholar

16. Hunt, P. R. (2016). The C. elegans Model in Toxicity Testing. J. Appl. Toxicol. 37 (1), 50–59. Epub 2016 Jul 22. doi:10.1002/jat.3357. CrossRef Full Text | Google Scholar

17. Kim, J. H., Lee, J., Park, J., and Gho, Y. S. (2015). Gram-negative and Gram-Positive Bacterial Extracellular Vesicles. Semin. Cel Dev. Biol. 40, 97–104. Epub 2015 Feb 1. doi:10.1016/j.semcdb.2015.02.006.9. CrossRef Full Text | Google Scholar

18. Li, M., Lee, K., Hsu, M., Nau, G., Mylonakis, E., and Ramratnam, B. (2017). Lactobacillus-derived Extracellular Vesicles Enhance Host Immune Responses against Vancomycin-Resistant Enterococci. BMC Microbiol. 17 (1), 66.

doi:10.1186/s12866-017-0977-7. PubMed Abstract | CrossRef Full Text | Google Scholar

19. Li, Y., Zhong, L., Zhang, L., Shen, X., Kong, L., and Wu, T. (2021). Research Advances on the Adverse Effects of Nanomaterials in a Model Organism, Caenorhabditis elegans. Environ. Toxicol. Chem. 40 (9), 2406–2424. Epub 2021 Jul 22. doi:10.1002/etc.5133. PubMed Abstract | CrossRef Full Text | Google Scholar

20. Mello, C., and Fire, A. (1995)., Vol. 48. Elsevier, 451–482. doi:10.1016/s0091-679x(08)61399-0Chapter 19 Dna TransformationMethods Cel Biol. CrossRef Full Text | Google Scholar

21. Mohan, N., Chen, C.-S., Hsieh, H.-H., Wu, Y.-C., and Chang, H.-C. (2010). In Vivo imaging and Toxicity Assessments of Fluorescent Nanodiamonds in Caenorhabditis elegans. Nano Lett. 10 (9), 3692–3699. doi:10.1021/nl1021909. PubMed Abstract | CrossRef Full Text | Google Scholar

22. Munagala, R., Aqil, F., Jeyabalan, J., and Gupta, R. C. (2016). Bovine Milk-Derived Exosomes for Drug Delivery. Cancer Lett. 371 (1), 48–61. Epub 2015 Nov 18. doi:10.1016/j.canlet.2015.10.020.PubMed Abstract | CrossRef Full Text | Google Scholar

23. Muraca, M., Putignani, L., Fierabracci, A., Teti, A., and Perilongo, G. (2015). Gut Microbiota-Derived Outer Membrane Vesicles: Under-recognized Major Players in Health and Disease? Discov. Med. 19 (106), 343–348. PubMed Abstract | Google Scholar

24. Nel, A., Zhao, Y., and Mädler, L. (2013). Environmental Health and Safety Considerations for Nanotechnology. Acc. Chem. Res. 46 (3), 605–606. doi:10.1021/ar400005v. PubMed Abstract | CrossRef Full Text | Google Scholar

25. Orejuela-Escobar, L., Gualle, A., Ochoa-Herrera, V., and Philippidis, G. P. (2021). Prospects of Microalgae for Biomaterial Production and Environmental Applications at Biorefineries. Sustainability 13, 3063. doi:10.3390/su13063063. CrossRef Full Text | Google Scholar

26. Paganini, C., Capasso Palmiero, U., Pocsfalvi, G., Touzet, N., Bongiovanni, A., and Arosio, P. (2019). Scalable Production and Isolation of Extracellular Vesicles: Available Sources and Lessons from Current Industrial Bioprocesses. Biotechnol.

J. 14 (10), 1800528. doi:10.1002/biot.201800528. PubMed Abstract | CrossRef Full Text | Google Scholar

27. Perni, M., Aprile, F. A., Casford, S., Mannini, B., Sormanni, P., Dobson, C. M., et al. (2017). Delivery of Native Proteins into C. elegans Using a Transduction Protocol Based on Lipid Vesicles. Sci. Rep. 7 (1), 15045. doi:10.1038/s41598-017-13755-9. PubMed Abstract | CrossRef Full Text | Google Scholar

28. Picciotto, S., Barone, M. E., Fierli, D., Aranyos, A., Adamo, G., Božič, D., et al. (2021). Isolation of Extracellular Vesicles from Microalgae: towards the Production of Sustainable and Natural Nanocarriers of Bioactive Compounds. Biomater. Sci. 9, 2917–2930. doi:10.1039/d0bm01696a. PubMed Abstract | CrossRef Full Text | Google Scholar

29. Picciotto, S., Romancino, D. P., Buffa, V., Cusimano, A., Bongiovanni, A., and Adamo, G. (2020). Post-translational Lipidation in Extracellular Vesicles: Chemical Mechanisms, Biological Functions and Applications, 83, 111. doi:10.1016/bs.abl.2020.05.001. CrossRef Full Text | Google Scholar

30. Pocsfalvi, G., Turiák, L., Ambrosone, A., Del Gaudio, P., Puska, G., Fiume, I., et al. (2018). Protein Biocargo of Citrus Fruit-Derived Vesicles Reveals Heterogeneous Transport and Extracellular Vesicle Populations. J. Plant Physiol. 229, 111–121. Epub 2018 Jul 21. doi:10.1016/j.jplph.2018.07.006. CrossRef Full Text | Google Scholar

31. Pužar Dominkuš, P., Stenovec, M., Sitar, S., Lasič, E., Zorec, R., Plemenitaš, A., et al. (2018). PKH26 Labeling of Extracellular Vesicles: Characterization and Cellular Internalization of Contaminating PKH26 Nanoparticles. Biochim. Biophys. Acta (Bba) - Biomembranes. 1860 (6), 1350–1361. Google Scholar

32. Raimondo, S., Naselli, F., Fontana, S., Monteleone, F., Lo Dico, A., Saieva, L., et al. (2015). Citrus Limon-Derived Nanovesicles Inhibit Cancer Cell Proliferation and Suppress CML Xenograft Growth by Inducing TRAIL-Mediated Cell Death. Oncotarget 6 (23), 19514–19527. doi:10.18632/oncotarget.4004. PubMed Abstract | CrossRef Full Text | Google Scholar

33. Romancino, D. P., Buffa, V., Caruso, S., Ferrara, I., Raccosta, S., Notaro, A., et al. (2018). Palmitoylation Is a post-translational Modification of Alix Regulating the Membrane Organization of Exosome-like Small Extracellular Vesicles. Biochim. Biophys. Acta (Bba) - Gen. Subjects 1862 (12), 2879–2887.

doi:10.1016/j.bbagen.2018.09.004. PubMed Abstract | CrossRef Full Text | Google Scholar

34. Samuel, M., Fonseka, P., Sanwlani, R., Gangoda, L., Chee, S. H., Keerthikumar, S., et al. (2021). Oral Administration of Bovine Milk-Derived Extracellular Vesicles Induces Senescence in the Primary Tumor but Accelerates Cancer Metastasis. Nat. Commun. 12 (1), 3950. doi:10.1038/s41467-021-24273-8. PubMed Abstract | CrossRef Full Text | Google Scholar

35. Sato, K., Norris, A., Sato, M., and Grant, B. D. The C. elegans Research Community.C. elegans as a Model for Membrane Traffic (April 25, 2014), WormBook. Google Scholar

36. Scharf, A., Piechulek, A., and von Mikecz, A. (2013). Effect of Nanoparticles on the Biochemical and Behavioral Aging Phenotype of the Nematode Caenorhabditis elegans. ACS Nano 7 (12), 10695–10703. Epub 2013 Nov 23. doi:10.1021/nn403443r. PubMed Abstract | CrossRef Full Text | Google Scholar

37. Soares, R. P., Xander, P., Costa, A. O., Marcilla, A., Menezes-Neto, A., Del Portillo, H., et al. (2017). Highlights of the São Paulo ISEV Workshop on Extracellular Vesicles in Cross-Kingdom Communication. J. Extracellular Vesicles 6 (1), 1407213. doi:10.1080/20013078.2017.1407213. PubMed Abstract | CrossRef Full Text | Google Scholar

38. Starich, T. A., Herman, R. K., Kari, C. K., Yeh, W. H., Schackwitz, W. S., Schuyler, M. W., et al. (1995). Mutations Affecting the Chemosensory Neurons of Caenorhabditis elegans. Genetics 139, 171–188. doi:10.1093/genetics/139.1.171. PubMed Abstract | CrossRef Full Text | Google Scholar

39. Sutherland, D. L., McCauley, J., Labeeuw, L., Ray, P., Kuzhiumparambil, U., Hall, C., et al. (2021). How Microalgal Biotechnology Can Assist with the UN Sustainable Development Goals for Natural Resource Management. Curr. Res. Environ. Sustainability 3, 100050. doi:10.1016/j.crsust.2021.100050. CrossRef Full Text | Google Scholar

40. Tiwari, G., Tiwari, R., Bannerjee, S., Bhati, L., Pandey, S., Pandey, P., et al. (2012). Drug Delivery Systems: An Updated Review. Int. J. Pharma Investig. 2 (1), 2–11. doi:10.4103/2230-973X.96920. CrossRef Full Text | Google Scholar

41. Verweij, F. J., Balaj, L., Boulanger, C. M., Carter, D. R. F., Compeer, E. B., D'Angelo, G., et al. (2021). The Power of Imaging to Understand Extracellular

Vesicle Biology In Vivo. Nat. Methods 18 (9), 1013–1026. Epub 2021 Aug 26. doi:10.1038/s41592-021-01206-3. PubMed Abstract | CrossRef Full Text | Google Scholar

42. Wang, Q., Zhuang, X., Mu, J., Deng, Z.-B., Jiang, H., Zhang, L., et al. (2013). Delivery of Therapeutic Agents by Nanoparticles Made of Grapefruit-Derived Lipids. Nat. Commun. 4 (1), 1867. doi:10.1038/ncomms2886. PubMed Abstract | CrossRef Full Text | Google Scholar

43. Wiklander, O. P. B., Nordin, J. Z., O'Loughlin, A., Gustafsson, Y., Corso, G., Mäger, I., et al. (2015). Extracellular Vesicle In Vivo Biodistribution Is Determined by Cell Source, Route of Administration and Targeting. J. Extracellular Vesicles 4 (1), 26316. doi:10.3402/jev.v4.26316. CrossRef Full Text | Google Scholar

44. Wu, T., Xu, H., Liang, X., and Tang, M. (2019). Caenorhabditis elegans as a Complete Model Organism for Biosafety Assessments of Nanoparticles. Chemosphere 221, 708–726. Epub 2019 Jan 14. doi:10.1016/j.chemosphere.2019.01.021. PubMed Abstract | CrossRef Full Text | Google Scholar

45. Zhang, W., Sun, B., Zhang, L., Zhao, B., Nie, G., and Zhao, Y. (2011). Biosafety Assessment of Gd@C82(OH)22 Nanoparticles on Caenorhabditis elegans. Nanoscale 3 (6), 2636–2641. Epub 2011 May 3. doi:10.1039/c1nr10239g. PubMed Abstract | CrossRef Full Text | Google Scholar

46. Zhu, L. (2015). Biorefinery as a Promising Approach to Promote Microalgae Industry: an Innovative Framework. Renew. Sust. Energ. Rev. 41, 1376–1384. doi:10.1016/j.rser.2014.09.040. CrossRef Full Text | Google Scholar

ADVANCED
SCIENCE NEWS
www.advancedsciencenews.com

NANO · MICRO
small
www.small-journal.com

Chapter 7

High-Yield Separation of Extracellular Vesicles Using Programmable Zwitterionic Coacervates

Paganini C, Capasso Palmiero U, **Picciotto S**, Molinelli A, Porello I, Adamo G, Manno M, Bongiovanni A, Arosio P.. Small. 2023 Jan;19(1):e2204736. doi: 10.1002/smll.202204736. Epub 2022 Nov 11. PMID: 36367966.

C. Paganini, U. Capasso Palmiero, A. Molinelli, I. Porello, P. Arosio
Department of Chemistry and Applied Biosciences
ETH Zürich
Vladimir-Prelog-Weg 1–5/10, Zürich 8093, Switzerland
E-mail: umberto.capasso@chem.ethz.ch; paolo.arosio@chem.ethz.ch

S. Picciotto, G. Adamo, A. Bongiovanni
Institute for Research and Biomedical Innovation
National Research Council of Italy
Via Ugo la Malfa 153, Palermo 90146, Italy

S. Picciotto
Department of Biological
Chemical and Pharmaceutical Sciences and Technologies
University of Palermo
Palermo 90146, Italy

M. Manno
Institute of Biophysics
National Research Council of Italy
Via Ugo la Malfa 153, Palermo 90146, Italy

The ORCID identification number(s) for the author(s) of this article can be found under https://doi.org/10.1002/smll.202204736.

156

Abstract

Programmable coacervates based on zwitterionic polymers are designed as dynamic materials for ion exchange bioseparation. These coacervates are proposed as promising materials for the purification of soft nanoparticles such as liposomes and extracellular vesicles (EVs). It is shown that the stimulus- responsiveness of the coacervates and the recruitment of desired molecules can be independently programmed by polymer design. Moreover, the polymeric coacervates can recruit and release intact liposomes, human EVs, and nanoalgosomes in high yields and separate vesicles from different types of impurities, including proteins and nucleic acids. This approach combines the speed and simplicity of precipitation methods and the programmability of chromatography with the gentleness of aqueous two-phase separation, thereby guaranteeing product stability. This material represents a promising alternative for providing a low-shear, gentle, and selective purification method for EVs.

ADVANCED
SCIENCE NEWS
www.advancedsciencenews.com

NANO · MICRO
small
www.small-journal.com

1. Introduction

In addition to vesicle-like compartments, cells can organize functions in space and time via membraneless organelles (MLOs) [1], which are associated with liquid–liquid phase separation of proteins and nucleic acids. A remarkable feature of MLOs is their ability to selectively recruit and dynamically exchange molecules with the surrounding environment.[2-4] Recapitulating this behavior using synthetic droplets would open attractive applications in bioseparation. A key prerequisite to achieve this goal is mimicking the ability of the scaffold molecules of MLOs to encode multiple types of interactions to simultaneously control different properties of the compartments, such as stimulus-responsiveness and recruitment of client molecules.[5] Inspired by this principle, we recently developed programmable liquid-like coacervates based on the phase separation of associative zwitterionic polymers that, in analogy with proteins commonly found in MLOs, encode multiple types of intermolecular interactions. [6]
The main characteristic of this strategy is the identification of zwitterionic coacervates with three key properties: i) they reversibly form and dissolve in response to external stimuli such as temperature, pH, and ionic strength; ii) they exhibit liquid-like properties; and iii) they exhibit anti-fouling properties and preferentially exclude most molecules as well as vesicles (Figure 1a). These baseline zwitterionic coacervates represent an ideal starting point for engineering liquid materials for biotechnological applications, particularly for the purification of biomolecules. In fact, our coacervates can be programmed to recruit target molecules by functionalizing the baseline zwitteri-onic polymers with specific ligands such as affinity tags or by introducing net charges, thereby attracting target compounds in the droplets based on affinity or electrostatic interactions, respectively. In the case of recruitment by electrostatic interactions, a remarkable feature of our material is the ability to independently program the stimulus-responsiveness and recruitment of the droplets by modifying the composition and architecture of the scaffold polymer. This property makes the polymeric coacervates designed in our study significantly different from complex coacervates, in which recruitment and phase separation are both modulated by a single type of interaction, that is, attractive electrostatic forces between polyelectrolytes of opposite charges. [7,8]
As a results, our material combines the advantages of a controlled partitioning with the use of a liquid and dynamic phase which responds to external stimuli. These features are particularly attractive for processing soft products such as extracellular vesicles (EVs), whose purification currently relies on techniques such as ultracentrifugation, precipitation, filtration, and chromatography.[9–16]. These methods have significant issues related to low purity, high shear, and aggregation of EVs, which can alter their integrity and functionality.[13,17] In this context, our zwitterionic coacervates offer a

gentler purification method. In this study, we introduced positively charged groups in the scaffold of our zwitterionic polymers to recruit anionic species following the principle of anion exchange chromatography. These polymeric coacervates could take up and release negatively charged vesicles upon changing the salt concentration of the solution. We applied these coacervates to liposomes and extracellular vesicles obtained from HEK-293F cells and microalgae[18,19]. Moreover, we showed that our material can purify vesicles from impurities such as small molecules, proteins and DNA, demonstrating the potential use of our programmable liquid coacervates for vesicle purification from conditioned media during bioprocessing. This approach shares several key advantages with precipitation techniques, such as large purification capacity, low cost, high speed, and simple instrumentation.[20] Moreover, the gentle conditions of this method and the aqueous environment in the coacervates enable the concentration of biomolecules without affecting their stability.
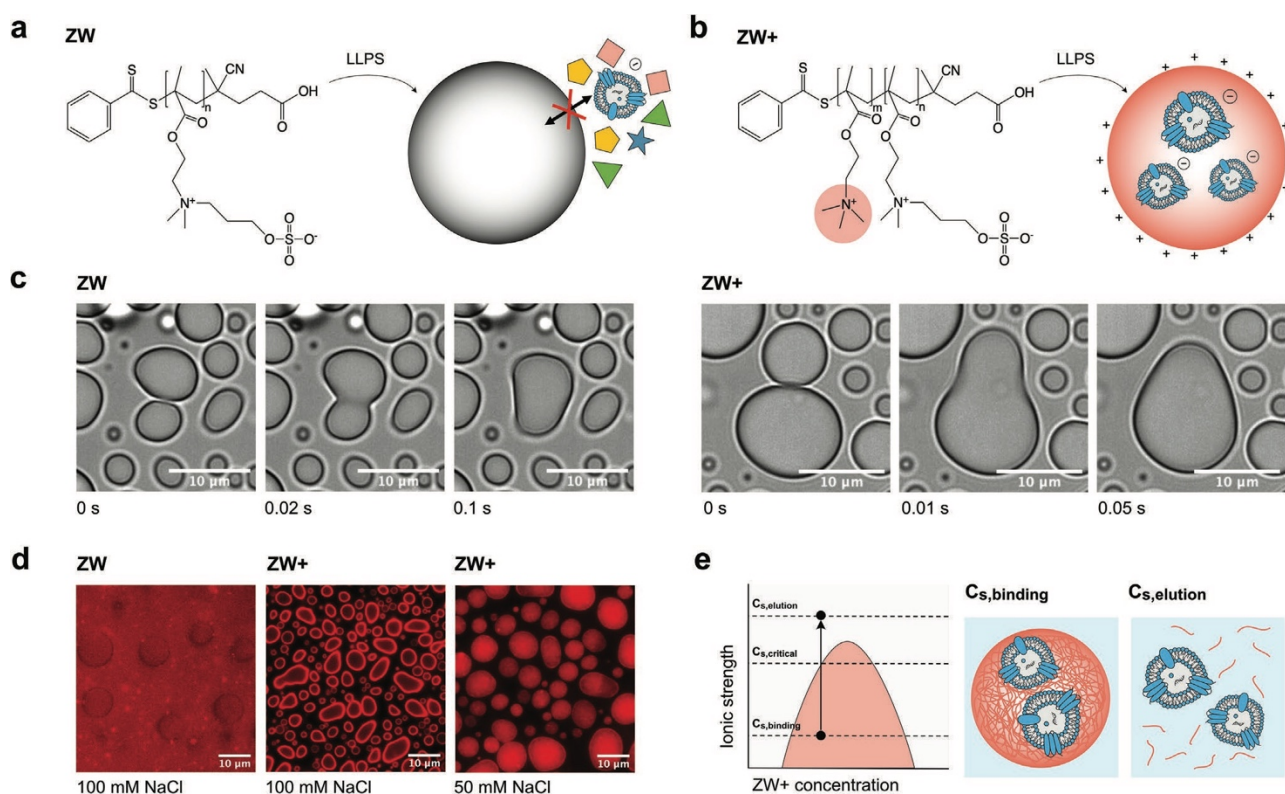
Figure 1. Purification of extracellular vesicles (EVs) with functionalized zwitterionic coacervates. a) The baseline zwitterionic polymer (ZW) forms coacervates that largely exclude biomolecules and vesicles.[6]. b) Using ZW as a starting material, we designed a polymer with both zwitterionic and unpaired positively charged monomers (ZW+), which forms coacervates capable of recruiting negatively charged vesicles via attractive electrostatic interactions. c) ZW and ZW+ coacervates behave like liquid-like material, as shown by coalescence events. d) Fluorescence microscopy images

ADVANCED
SCIENCE NEWS
www.advancedsciencenews.com

NANO · MICRO
small
www.small-journal.com

show that liposomes are excluded from ZW coacervates (left) and are recruited into ZW+ coacervates (middle and right). The location of the liposomes inside the coacervates changes with the salt concentration and therefore with the strength of the intermolecular interactions. e) Vesicles are recruited in the coacervates at low salt concentrations ($C_{s,binding}$), typically below the critical threshold required for phase separation ($C_{s,crit}$). When the salt concentration is increased above $C_{s,crit}$ ($C_{s,elution}$), coacervates dissolve and the vesicles are released in one single phase. Depending on material properties and solution conditions, $C_{s,elution}$ can be lower than $C_{s,crit}$ and vesicles can be eluted from intact coacervates.

2. Results

2.1. Design of Positively Charged Zwitterionic Coacervates

Starting from the baseline zwitterionic polymer (ZW) that we recently developed (Figure 1a), [6] we designed a polymer containing net positive charges (ZW+, Figure 1b). The polymer ZW+ consists of two monomers: sulfabetaine methacrylate (ZB), which is defined as the "sticker," and [2-(methacryloyloxy) ethyl]trimethylammonium (MQ), which is positively charged. ZB drives the phase separation by mediating ion-paired attractive interactions,[21] and MQ controls the uptake of negatively charged products.

First, we confirmed that the ZW+ coacervates retained the liquidity of the baseline ZW material, which is a key requirement for the purification of EVs. Initially, we used a ZW+ polymer with 20 MQ and 80 ZB monomers and observed the coalescence of the droplets formed by its liquid–liquid phase separation (LLPS) (Figure 1c).

Subsequently, we tested whether these positive coacervates could recruit negatively charged vesicles and, therefore, be used as dynamic materials for bioseparation based on ion exchange.

To this end, we initially considered using model liposomes composed of phosphatidylserine (DOPS) and rhodamine-B- labeled phosphatidylethanolamine (RhodB-PE) at a molar ratio of 200:1 and with an average diameter of 125 nm. Given the large excess of negatively charged DOPS, the charge of the final liposomes was only minimally influenced by the presence of the fluorophores. We analyzed the uptake of the coacervates using epifluorescence microscopy. The results in Figure 1d show that the labelled liposomes did not interact with the coacervates of the unfunctionalized polymer (ZW), but were recruited into the ZW+ coacervates at low salt concentrations. We observed that the location of the liposomes in the coacervates (in both the random and block copolymers) depended on the strength of the interactions between the ZW+ polymers and the liposome membrane. Indeed, the liposomes were recruited in the bulk

ADVANCED
SCIENCE NEWS
www.advancedsciencenews.com

NANO · MICRO
small
www.small-journal.com

of the droplets when the interactions between the polymers and vesicles were strengthened (for instance, by decreasing the salt concentration or increasing the number of positive charges) (Figure 1d; Figure S2, Supporting Information).

Owing to their liquidity and recruitment capability, ZW+ coacervates can be developed as materials for EV purification. Therefore, we designed the process shown in Figure 1e. Initially, at sufficiently low salt concentrations ($C_{s,binding}$), the polymer undergoes phase separation, and the resulting drop- lets recruit EVs. Under these conditions, droplets enriched with EVs can be separated from the supernatant containing impurities, for instance by precipitation. The increase in salt concentration ($C_{s,elution}$) screens electrostatic interactions and allows the separation of vesicles from the dissolved droplets. Finally, the purified vesicles can be separated from the polymer via filtration or a buffer exchange step.

Notably, the programmability of zwitterionic coacervates allows one to tune $C_{s,binding}$ and $C_{s,elution}$, depending on the specificity of the system and stability of the product. For instance, in the case of EVs, although NaCl concentrations up to 1 m can be used, [14,22,23] lower ionic strengths are preferable. These salt concentrations can be easily modulated by varying the amounts of ZB and unpaired charges (MQ). In addition to controlling the uptake of negatively charged products, MQ also behaves as a "spacer." Indeed, MQ affects phase separation by changing the local concentration of ZB stickers in the polymer,[6] and increasing the repulsion between the polymers at low ionic strength. Next, we studied the effect of unpaired positive charges on the phase separation of ZW+ to design polymers with stimulus- responsiveness in the desired salt concentration range. For this purpose, we synthesized polymers with different lengths and different numbers and distributions of unpaired positive charges (MQ). Here, the total degree of polymerization, "DPtot," indicates the total number of monomers in the polymer. We characterized the phase separation by microscopy and measured the critical salt concentration ($C_{s,crit}$), that is, the concentration required to suppress net electrostatic attractive forces and prevent phase separation. As expected, $C_{s,crit}$ decreased with an increase in the fraction of unpaired positive charges (MQ) and therefore of the amount of electrostatic repulsion, which decreased the net attractive interactions mediated by the paired ions of the ZB monomer (Figure 2a). No phase separation was observed for the polymers with an MQ fraction equal to or greater than 36% (Figure 2a). At a constant fraction of positive charges, $C_{s,crit}$ increased with increasing polymer length (Figure 2b). In agreement with Flory–Huggins theory, the critical salt concentration $C_{s,crit}$ scales with the polymer length N as per the following equation (inset Figure 2b)[24].

ADVANCED
SCIENCE NEWS
www.advancedsciencenews.com

NANO · MICRO
small
www.small-journal.com

$$\frac{1}{\sqrt{c_{s,\text{crit}}}} = \frac{1}{\alpha}\left(\frac{1}{2} + \frac{1}{\sqrt{N}} - A\right) - \frac{B/\alpha}{T} = A' + \frac{B'}{\sqrt{N}}$$

Here, α is a constant, A is the temperature-independent entropic term, and B/T is the temperature-dependent enthalpic term of the non-electrostatic (residual) component of the inter- action parameter χ.

$C_{s,\text{crit}}$ was only slightly affected by the distribution of the charges, as shown by the comparison between the random and block polymers (Figure 2c).

Next, we investigated the impact of the fraction and distribution of positive charges in ZW+ on the interactions between liposomes and coacervates. We incubated fluorescent liposomes with the different ZW+ polymers in a phosphate buffer containing 100 mm NaCl at pH 7.4. We characterized the partitioning by measuring the fluorescence intensity of the samples in the continuous aqueous phase. As expected, the number of liposomes recruited by the droplets increased with an increase in the fraction of positive charges (Figure 2d). Specifically, 96% of the liposomes were recruited when the fraction of positive charges was equal to or larger than 14%.

This result was independent of DP_{tot}, which was in the 100–600 range (Figure 2e). Combined with the data shown in Figure 2b, this result indicates that polymer length can be used as a design parameter to tune the $C_{s,\text{crit}}$ of the droplets independently of the recruitment. Therefore, the zwitterionic droplets could be adapted for specific process conditions required by the product.

Additionally, we observed that charge distribution had a significant effect on vesicle recruitment. In particular, the interactions between liposomes and droplets were strengthened when the monomers were organized into two blocks (Figure 2f). For instance, at an NaCl concentration of 150 mm, the coacervates of block and random polymers recruited 99% and 9% of the liposomes, respectively. The analysis of the distribution of condensed counterions on polymer chains with different charge patterns indicated that counterions are confined near the block charges.[25] Consequently, in the context of complex coacervation, block polymers mediate stronger attractive electrostatic interactions than random ones.[25] Our results, which can be explained by a similar mechanism, reveal that charge patterning is an important parameter for the recruitment of droplets at the desired process operating conditions.

ADVANCED
SCIENCE NEWS
www.advancedsciencenews.com

NANO · MICRO
small
www.small-journal.com
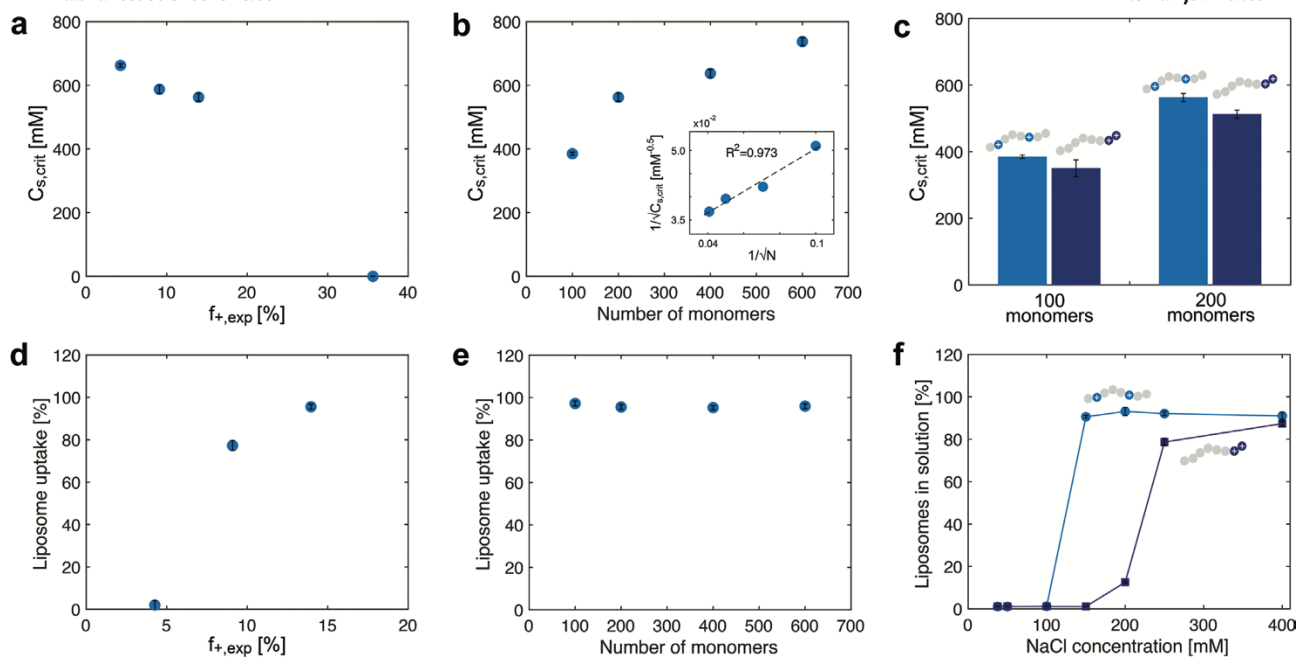
Figure 2. Independent modulation of a–c) the stimulus-responsiveness and d–f) recruitment of the ZW+ coacervates by polymer design. a) Effect of the fraction of positively charged monomers ($f_{+,exp}$) on the phase separation of ZW+ represented by the critical salt concentration ($C_{salt,crit}$). b) Effect of the length of the polymer (number of monomers, N) on the phase separation of ZW+ at a constant fraction of positively charged monomers. The inset shows predicted scaling according to the Flory-Huggins theory. c) Effect of charge distribution (random versus block) on $C_{salt,crit}$. d) Effect of the fraction of positively charged monomers on liposome recruitment. e) Effect of the length of ZW+ on liposome recruitment at a constant fraction of positively charged monomers. f) Effect of charge distribution (random vs block) on liposome recruitment. The interaction of the polymer with the liposomes increases when different monomers are organized in two blocks. All experiments were performed at constant polymer mass concentration.

2.2. Separation of Liposomes with Zwitterionic Coacervates

After designing the polymers to optimize liposome recruitment, we analyzed the release of liposomes from the coacervates upon increasing the ionic strength of the solution. Based on the results described in the previous section, we selected two polymers, ZW-R1 and ZW-B1, with $C_{s,crit}$ values below 500 mm. The polymers were chosen to avoid NaCl concentrations at which liposome aggregation occurs. The selected polymers had similar lengths and fractions of positively charged monomers but different charge distributions. Their properties are listed in **Table 1**.

After recruiting the liposomes into the ZW+ coacervates in 100 mm NaCl, the coacervates were removed from the solution by centrifugation, and the vesicles were

ADVANCED
SCIENCE NEWS
www.advancedsciencenews.com

NANO · MICRO
small
www.small-journal.com

recovered from the polymerrich pellet by increasing the salt concentration to 400 mm, that is, above the $C_{s,crit}$ required to dissolve the coacervates. This solution was centrifuged again to remove aggregated vesicles (Figure 3a).

Dynamic light scattering (DLS) measurements showed that the liposomes in the coacervates had similar size distribution before and after recruitment, demonstrating that the eluted liposomes were intact after uptake in the ZW+ coacervates (Figure 3b). We next evaluated the separation yield by measuring the amount of liposomes recruited and released from the coacervates. For this purpose, we counted the liposomes in the continuous phase by nanoparticle tracking analysis (NTA). The NTA measurements (Figure 3c) showed that ZW+ coacervates recruited most of the liposomes in 100 mm NaCl. Specifically, random and block polymers recruited $92 \pm 1\%$ and $96 \pm 1\%$ of liposomes, respectively. Interestingly, after increasing the salt concentration to $C_{s,elution}$ and removing the vesicle aggregates, we recovered $97 \pm 10\%$ and $78 \pm 8\%$ of the vesicles for random and block polymers, respectively. Control experiments indicated that the non-recovered fraction was formed by vesicle aggregation during centrifugation (Figure S3, Supporting Information).

Finally, we measured the binding capacity of the ZW-R1 coacervates; 0.25 mg mL^{-1} of ZW-R1 coacervates were incubated with increasing concentrations of liposomes differing over one order of magnitude. Liposome uptake was greater than 90% at all concentrations (Figure 3d). The binding of the vesicles to the coacervates decreased their surface tension and size (Figure 3e), thereby increasing the total area available for binding. Consequently, the binding area for a fixed amount of coacervate material is not a constant parameter and depends on the number of vesicles in the solution. This is a remarkable advantage of using a liquid material over the conventional solid stationary phases used in chromatography, which can exhibit saturation effects with increasing amounts of loaded material. In contrast, the same amount of liquid coacervates can recruit vesicles with similar efficiency over a wide range of product concentrations because liquid droplets can adjust their size distribution and binding area.

Table 1. Properties of the polymers used for vesicle isolation.

	Type	DP_{ZB} [—]	DP_{MQ} [—]	DP_{tot} [—]	$f_{MQ,exp}$ [%]
ZW-R1	Random	80	20	100	9.06
ZW-B1	Block	80	20	100	13.6

2.3. Separation of Purified Extracellular Vesicles with Zwitterionic Coacervates

ADVANCED
SCIENCE NEWS
www.advancedsciencenews.com

NANO · MICRO
small
www.small-journal.com

After demonstrating that the ZW+ coacervates can recruit and release intact liposomes in high yields and that the separation process is compatible with a wide range of product concentrations, we applied our polymeric coacervates on EVs produced from human HEK-293F cells (see characterization by microfluidic diffusion sizing, [26] NTA, AND TEM in Figure S4, Supporting Information) and microalgae (see comprehensive characterization in refs. [18,27]). We quantified the recruitment of human EVs using the ZW+ coacervates previously tested with liposomes, that is, random ZW-R1 and block ZW-B1 polymer droplets (Figure 4a). We quantified the recruitment of EVs by measuring their fraction remaining in the dilute phase via an ELISA assay based on tetraspanin CD81, a common EV marker[28,29] The CD81+ particles were recruited by the ZW-R1 and ZW-B1 polymer coacervates at NaCl concentrations below 25 and 37.5 mm, respectively. These NaCl concentrations were significantly lower than the values required to recruit liposomes because the negative charge on the EV membrane was weaker than that on the liposomes. In this case, the distribution of monomers in the two blocks did not significantly affect the salt concentration required for uptake.

The distribution of 293F-EVs inside the two different types of zwitterionic coacervates (Table 1) was investigated by imaging the coacervates using epifluorescence microscopy. EVs were labeled with a photoactivatable lipophilic dye[26,30] before incubation with ZW-R1 and ZW-B1 in 25 mm NaCl solutions and with ZW in 100 mm NaCl solutions (Figure 4b). We observed that under these conditions, EVs were concentrated mostly on the rim of the ZW-R1 and ZW-B1 coacervates. However, their locations in the droplets could be changed by tuning the strength of the interactions between the polymers and EV membrane, as demonstrated with the liposomes (Figure 1d). This mechanism is useful for controlling the local concentration of the product in the coacervates and for avoiding the potential aggregation of products at the coacervate interface due to local increase in concentration.

After identifying the conditions for EV binding, we applied the separation process previously developed for liposomes to 293F-EVs. We incubated EVs with ZW-R1 for one minute before separating the coacervates from the aqueous phase via centrifugation. The EVs were then eluted by increasing the ionic strength of the solution to 550 mm NaCl. DLS analysis of the eluates showed that the EVs recovered from the coacervates had a size distribution similar to that of the initial EV sample, indicating that most EVs remained intact throughout the process (Figure 4c). Moreover, TEM analysis of the eluates confirmed the presence and integrity of the isolated EVs, which exhibited the expected cup-shaped morphology (Figure 4d).

The yield of the process was measured by quantifying the amount of CD81+ particles in aqueous solutions using ELISA. We observed that most CD81+ vesicles were recruited in the ZW-R1 coacervates. Moreover, at the end of the process, we recovered

ADVANCED
SCIENCE NEWS
www.advancedsciencenews.com

small
NANO · MICRO
www.small-journal.com

86% of the initial EVs (Figure 4e). Notably, these experiments were performed using small EVs purified by size exclusion chromatography, and different recoveries can be expected for other types of EVs.

In the case of EVs, we noticed that aggregation was mainly caused by centrifugation (Figure S5, Supporting Information). Indeed, upon removal of the first centrifugation step, the EVs did not aggregate and nearly all EVs were recovered in the eluate (Figure S5, Supporting Information). Moreover, EV losses were significantly higher when the first centrifugation step was performed at 25 °C than at 4 °C (Figure S5, Supporting Information). Therefore, the yield can be further optimized by tuning the centrifugation settings. To further assess the versatility of our purification approach, we tested this process on nanoalgosomes, which are EVs derived from microalgae.[18] We followed the same protocol used for 293F-EVs and used ZW-R1 coacervates. DLS measurement of the eluate confirmed that the separation of nanoalgosomes with zwitterionic coacervates did not affect their size distribution (Figure 4f). Moreover, NTA measurements showed that most nanoalgosomes were recruited by the zwitterionic coacervates and released upon increasing the salt concentration (Figure 4g). Under all tested conditions, the time required to complete the separation process was in the order of minutes. After polymer addition, the first binding step occurred in one minute. Our experiments confirmed that the amount of EVs recruited was unaffected by the incubation time during the interval of 1–15 min (Figure S5, Supporting Information). The second step, involving pellet dissolution and EV resuspension, was quickly performed by gently mixing the solution for a few seconds. The liquidity of the coacervates prevented the formation of EV precipitates and facilitated pellet resuspension. This property of our coacervates is more advantageous than precipitation techniques, wherein the resuspension of the product complexes is typically a challenging step.[17,31]

ADVANCED
SCIENCE NEWS
www.advancedsciencenews.com

NANO · MICRO
small
www.small-journal.com
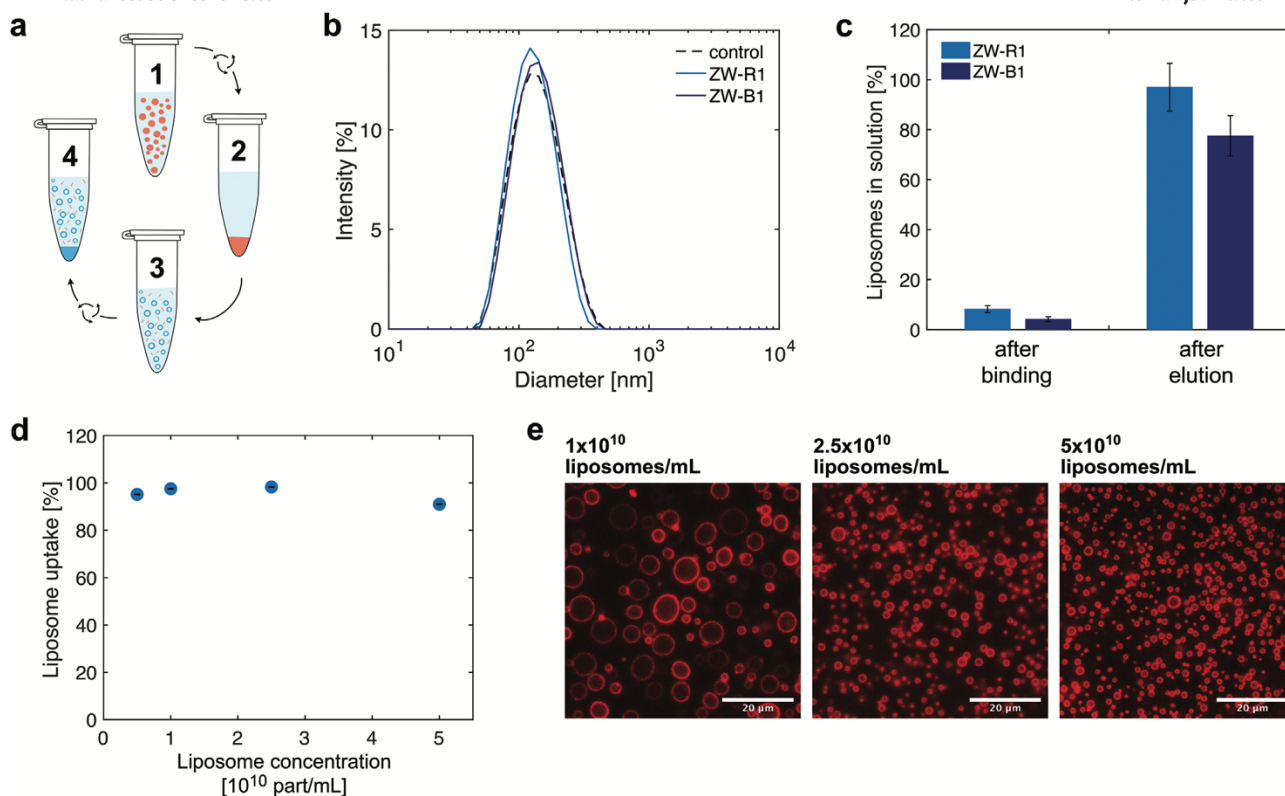
Figure 3. Liposome separation using zwitterionic coacervates. a) Schematic illustration of our process: 1) recruitment of liposomes in the ZW+ coacervates at low salt concentrations ($C_{s,binding}$), 2) separation of the ZW+ coacervates containing liposomes from the aqueous phase by centrifugation, 3) release of the liposome and dissolution of the ZW+ coacervate pellet at high salt concentration ($C_{s,elution}$), and 4) removal of the aggregates of liposomes from the final product by centrifugation. b) DLS measurements of the initial liposome samples and the liposomes recovered from the ZW+ coacervates. Most liposomes are intact after they are released from the coacervates. c) Nanoparticle tracking analysis (NTA) of the liposomes in solution after binding to the coacervates and after elution from the coacervates for random and block polymers (see Table 1). d) Coacervates can efficiently take up liposomes until a concentration of 5×10^{10} particles mL^{-1} is reached. e) Coacervate size distribution changes as a function of liposome concentration in the solution.

**ADVANCED
SCIENCE NEWS**

www.advancedsciencenews.com

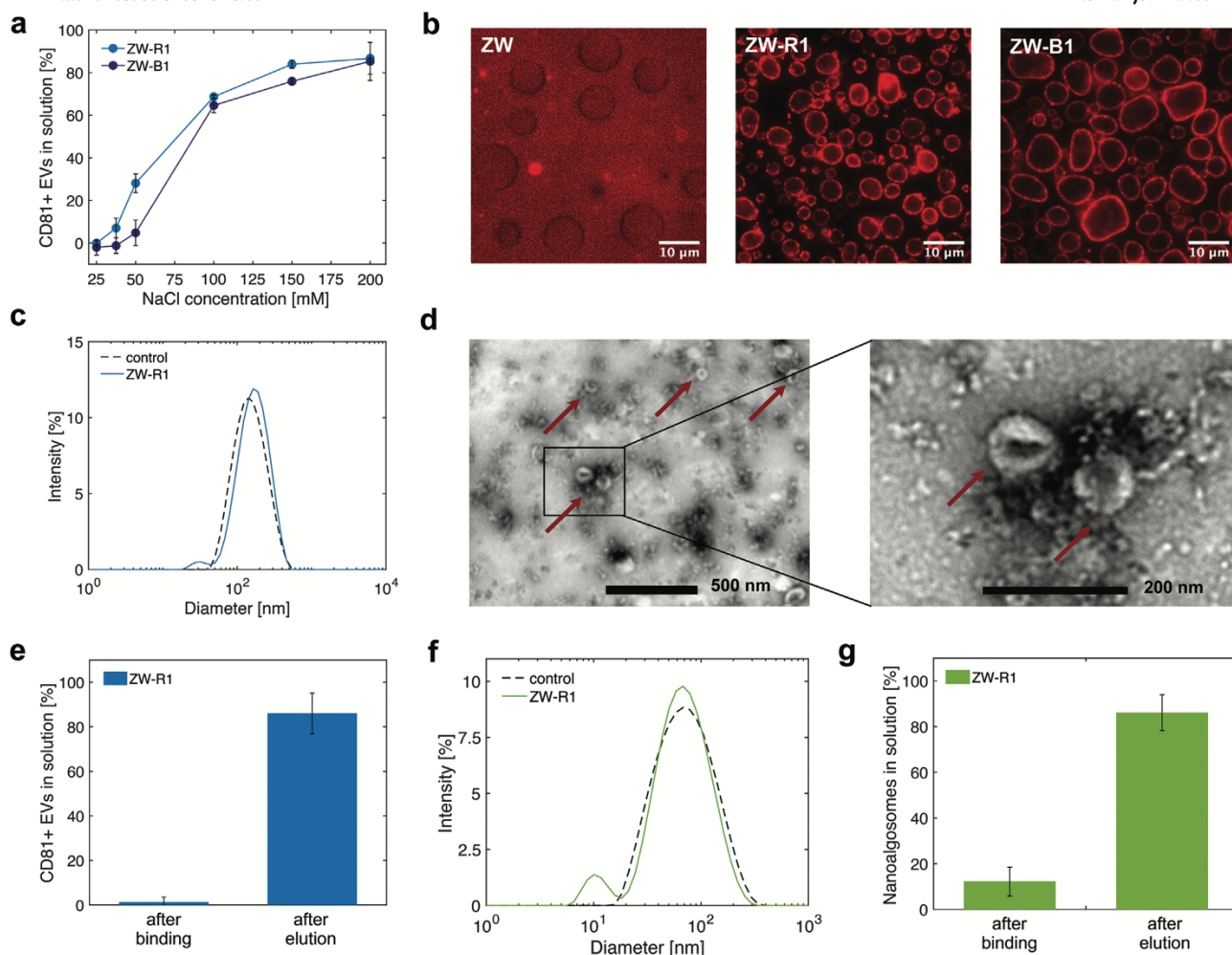NANO · MICRO

small

www.small-journal.com

Figure 4. Separation of EVs derived from HEK 293F cells and microalgae using zwitterionic coacervates. a) ELISA measurements indicated that ZW+ coacervates recruited CD81+ EVs at different salt concentrations depending on the polymer design; ZW-R1 and ZW-B1 recruited CD81+ EVs below 25 and 37.5 mm NaCl, respectively. b) Fluorescence microscopy images showed that EVs are recruited by ZW+ coacervates and excluded by control coacervates lacking positively charged monomers (ZW). EVs also localize on the rim of the ZW-R1 and ZW-B1 droplets at 25 mm NaCl. c) DLS measurements showed that the recovered EVs have a size distribution similar to the initial EVs. d) Transmission electron microscopy (TEM) images of EVs recovered from the ZW+ coacervates. The eluate contains single cup-shaped EVs (red arrows), indicating that the process did not drastically change their morphology. e) Efficiency of the separation process assessed by ELISA measurements of the CD81 in solution. Most EVs were recruited and released from the ZW-R1 coacervates. f) DLS measurements show that the ZW+ coacervates do not affect the size distribution of the nanoalgosomes. g) NTA measurements show the uptake and release efficiency of nanoalgosomes by ZW-R1 coacervates.

2.4. Purification of Extracellular Vesicles

ADVANCED
SCIENCE NEWS
www.advancedsciencenews.com

NANO · MICRO
small
www.small-journal.com

Finally, we verified the applicability of our zwitterionic coacervates for the purification of EVs from complex solutions. As EVs and most contaminants have different charges, they interact differently with ZW+ coacervates at constant salt concentrations. Similar to anion exchange resins, the recruitment of different species in the polymer coacervates could be controlled by carefully selecting a salt concentration that minimizes the interaction of impurities.

We measured the partitioning of typical medium impurities, such as DNA and proteins, in ZW-R1 coacervates. For this purpose, HEK-293F cells were cultured in a chemically defined serum-free medium, and a small amount of clarified conditioned medium was incubated with the coacervates at different salt concentrations. We observed that approximately 82% of the DNA was recruited in ZW-R1 coacervates at 100 mm NaCl, while most proteins remained in the solution (Figure 5a). Proteins were also excluded at lower NaCl concentrations, whereas purified EVs were recruited in this concentration range. Proteins typically have lower charge densities than polynucleotides and are smaller in size than EVs; thus, they have fewer binding sites than the other species in the medium. By using different discrete salt concentrations, we can sequentially recruit and eliminate proteins and then separate EVs from DNA molecules.

The purification performance of ZW-R1 on nanoalgosome solutions spiked with either rhodamine B or bovine serum albumin (BSA) was tested. The NTA measurements in Figure 5b,c show that the ZW-R1 coacervates recruited 82–95% of the nanoalgosomes and released most of them upon increasing salt concentration. In contrast, only small quantities of rhodamine B and BSA (9.1 ± 1% and 4 ± 0.1%, respectively) were observed in the eluates, and they were mostly excluded from the coacervates during the binding step. This result shows the efficiency of our purification approach to isolate EVs from impurities originating from production, functionalization, or loading.
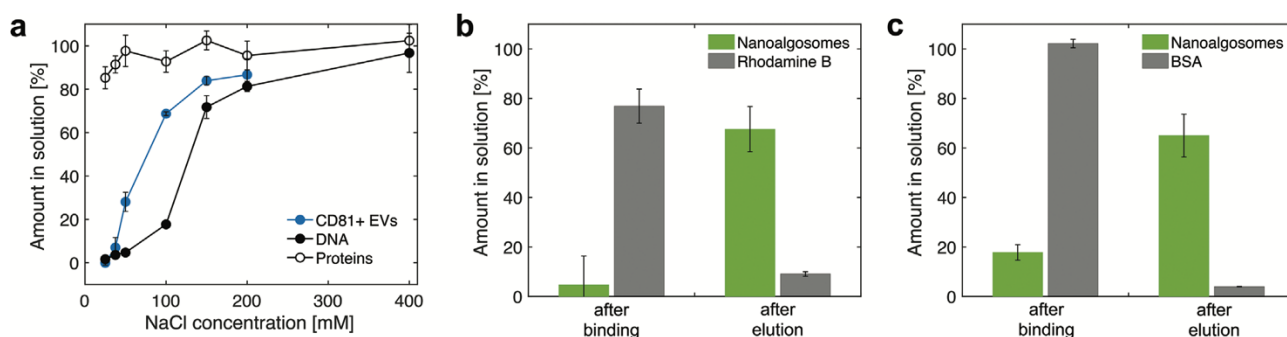
Figure 5. Separation and purification of EVs with ZW-R1 coacervates. a) Amount of protein, EVs, and DNA in solution at different salt concentrations. A low amount corresponds to a large recruitment into the coacervates. By selecting suitable salt concentrations, proteins can be removed first at low salt concentration, and EVs can be

ADVANCED
SCIENCE NEWS

www.advancedsciencenews.com

NANO · MICRO
small

www.small-journal.com

subsequently separated from DNA at higher salt concentration. Amount of nanoalgosomes in solution after binding to coacervates at low salt concentration and after elution at high salt concentration. Nanoalgosomes are recruited in ZW-R1 coacervates while b) Rhodamine B and c) BSA are preferentially excluded.

3. Discussion

Overall, our data show that our zwitterionic coacervates are promising materials for the purification of vesicles, including liposomes and human and microalgal EVs. This method combines the advantages of various purification techniques. Similar to precipitation, liquid–liquid phase separation is a scalable method that requires simple instrumentation.[32] This process is rapid and flexible with respect to the amount of product in the solution (Figure 3e) and can adjust to fluctuations of product amounts, which is a common challenge in bioprocessing.

Similar to aqueous-two-phase systems (ATPS), our purification method is based on two liquid phases. The liquidity of the coacervates makes this approach dynamic, prevents product aggregation, and facilitates resuspension. The high water content of our zwitterionic coacervates (typically 40–50%) provides a gentle environment for bioproducts.[33] Coacervates can recruit proteins at very high concentrations, without affecting their stability.[34-36] The liquidity of the coacervates also prevents the deformation of soft vesicles, which typically occurs upon binding to solid supports. The liquid phase adapts to the vesicle shape, and thus, applies lower stress on the particle membrane. One of the main limitations of ATPS for industrial applications is the limited control and understanding of partitioning. [33,37,38] Our method overcomes this limitation by combining the liquidity of ATPS and the programmability of chromatographic resins. Indeed, our zwitterionic coacervates can be easily programmed to recruit specific molecules from the surrounding medium and separate them from the impurities. The core principle of this strategy relies on the ability of our base polymer to preferentially exclude most molecules unless they are functionalized with charges, hydrophobic groups, or affinity tags. In this study, we functionalized the base material with unpaired charges to perform separation based on similar principles of anion exchange, one of the most common methods used at large scales to isolate biological particles during bioprocessing. [37,39-44] Despite the increasing application of anion exchange chromatography for EVs and virus-like particles, the recovery of particles from columns is often low. Seo et al. recently reported that only 66% of loaded EVs can be recovered from a weak anion exchanger using mild elution buffers. [41] Other studies report that the recovery of EVs from a strong anion exchange resin is slightly higher than that achieved by ultracentrifugation, which is approximately

ADVANCED
SCIENCE NEWS
www.advancedsciencenews.com

NANO · MICRO
small
www.small-journal.com

45%.[14,41,45] The reason for these low recoveries are complex and possibly include: i) the deformation and disassembly of the vesicles on the solid supports;[46] ii) high ligand densities in the columns, the resulting binding avidity between the vesicles and resins, and harsh elution conditions for recovery;[47,48] iii) nonspecific interactions of vesicle components with the base material of the resins.[49]

The above-mentioned issues of solid resins can be avoided by using our system. As the liquid droplets adapt to the vesicle shape, the deformation of vesicles can be prevented. In addition, owing to the programmability of our material, the binding interactions and binding avidity of the vesicles can be tuned by adjusting the ionic strength of the buffer and using polymer design. Indeed, we can easily modulate the type, amount, and density of the charged monomers in the polymer. Finally, the vesicles bind to the coacervates exclusively via ionic interactions. Zwitterionic baseline polymers are often applied in anti- fouling coatings, as they do not interact with any molecule unless they are functionalized with specific moieties, such as the positive charges used in this work.[50–52]

4. Conclusion

In this study, we developed programmable zwitterionic coacervates as dynamic materials for bioseparation based on anion exchange principles and demonstrated their use for the uptake and release of liposomes and EVs. Moreover, we identified key design parameters to independently control the stimulus-responsiveness and recruitment behavior of the coacervates, which can be programmed depending on specific product needs. This property of our material makes our approach very versatile. The coacervates can separate liposomes, human EVs, and nanoalgosomes from different types of impurities and release them in high yields.

Overall, this isolation approach combines the speed and simplicity of precipitation methods and the programmability of chromatography with the gentleness of a liquid-like binding phase, thereby avoiding product aggregation and degradation. This approach represents a promising alternative for low-shear, gentle, and selective purification of EVs.

5. Experimental Section

Polymer Synthesis: Polymers composed of ZB (Sulfabetaine methacrylate) and MQ ([2-(methacryloyloxy)ethyl]trimethylammonium chloride solution, 75 wt% in H2O, Sigma-Aldrich) monomers were synthesized via reversible addition-fragmentation chain-transfer (RAFT) copolymerization using ACVA (4,4′-azobis(4-

ADVANCED
SCIENCE NEWS
www.advancedsciencenews.com

NANO · MICRO
small
www.small-journal.com

cyanovalericacid, ≥98%, Sigma-Aldrich) as an initiator and CPA (4-cyano-4-(phenylcarbonothioylthio)pentanoic acid, ≥97%, Sigma-Aldrich) as a RAFT agent according to a previously published protocol.[6] ZB was synthesized according to a previously published method. The polymers were synthesized in 20/80 v/v ethanol/3 m NaCl acetic buffer (pH 4.5) at 10 wt% total monomer concentration with a CPA to ACVA molar ratio of 3:1. The monomer-to-CPA molar ratios (that is, the degree of polymerization of a single monomer i (DPi)) were varied, as shown in Table S1, Supporting Information. For example, in the case of ZW-R1 (the copolymer with DPZB = 80 and DPMQ = 20, Table S1, Supporting Information), 846 mg of ZB, 198 mg of MQ solution, 10 mg of CPA, and 3.3 mg of ACVA were dissolved in 7.6 g of acetic buffer (pH = 4.5) and 1.5 g of ethanol and poured into a septum-sealed round bottom flask. The mixture was purged with nitrogen for 10 min and then heated to 65 °C for 24 h under constant stirring. The reaction mixture was dialyzed against 2 m NaCl for 3 days using dialysis tubing (Spectra/Por, molecular weight cut-off (MWCO) = 3.5 kDa) by frequently changing the aqueous solution. The final polymer solutions were filtered using a 0.45 μm pore size nylon membrane and stored at −20 °C. ZB/MQ block copolymers (ZWB1-2 in Table 1) were synthesized via two subsequent RAFT polymerizations following the same procedure. The first MQ-based block was produced via the RAFT polymerization of MQ in the presence of ACVA and CPA. After 24 h, 846 mg of ZB and 3.3 mg of ACVA were introduced directly into the mixture to produce the second ZB-based block. The flask was purged again with nitrogen for 10 min, and the mixture was left to react for another 24 h at 65 °C and purified according to the same procedure used for random copolymers. The copolymer concentrations were evaluated using gravimetry.

NMR Spectroscopy: The conversion (*X*) and MQ molar fraction (*f*MQ,exp) of the copolymers (Table S1, Supporting Information) were evaluated via nuclear magnetic resonance (1H-NMR) spectroscopy, as described in Figure S1, Supporting Information. An aliquot of each reaction mixture was collected after the completion of the reaction and purification. The samples were dried under nitrogen, dissolved in 3 m NaCl D2O, and analyzed using a 400 MHz NMR spectrometer (Bruker).

Thermogravimetric Analysis: Thermogravimetric analysis (TGA) was performed using a Mettler Toledo TGA device to determine the polymer and salt concentrations. After purifying the polymers, approximately 1 g of dialysis water was spread on a sand-filled support to measure the salt concentration in the solution. The same procedure was followed for the polymer solutions. The actual polymer concentrations were obtained by subtracting the salt concentrations from the values measured using the polymer solution.

ADVANCED
SCIENCE NEWS
www.advancedsciencenews.com

NANO · MICRO
small
www.small-journal.com

Critical Salt Concentration: The critical salt concentrations ($C_{s,crit}$) of the polymers were evaluated using wide-field microscopy. For this purpose, 0.25 mg mL−1 polymers solutions with different NaCl concentrations were incubated overnight at room temperature in a 384- well plate with a glass bottom (Brook). The wells were covered with aluminum foil to avoid evaporation and imaged after 24 h with a Ti2-U epifluorescence inverted microscope (Nikon) in the bright-field mode.

Droplet Fusion: The fusion of droplets was evaluated using a Ti2-U epifluorescence inverted microscope (Nikon) in 384-well plates. Solutions at pH 7.4 with 20 mm Na-phosphate, 100 mm NaCl, and 0.25 mg mL−1 of either ZB polymer (DP = 200) or a copolymer of ZB and MQ (DP = 100, fZB = 0.8) were prepared. The solutions were incubated at room temperature for 1 h, and the images of the wells were acquired in the brightfield mode every 5 ms to capture droplet fusion events. The surface of the wells was treated with 100 μL of 1% BSA in Millipore water for 30 min to prevent droplet wetting in the wells. The wells were washed three times with 100 μL of Millipore water before adding the polymer solutions.

Preparation of Liposomes: 1,2-dioleoyl-*sn*-glycero-3-phospho-l- serine (DOPS, Avanti Polar Lipids) and 1,2-dimyristoyl-sn-glycero-3- phosphoethanolamine-*N*-(lissamine rhodamine B sulfonyl) ammonium salt (14:0 Liss Rhod PE, Avanti Polar Lipids) were dissolved in chloroform and mixed in a DOPS/14:0 Liss Rhod PE molar ratio of 200:1. Chloroform was evaporated first with a dry nitrogen stream for 2 h and then placed under vacuum overnight. The final lipid film was hydrated with phosphate buffer saline (PBS) and gently agitated at room temperature. The lipid suspension was then extruded through a polycarbonate membrane with a pore size of 100 nm (Whatman Nuclepore Track-Etch Membrane; Cytiva) for 15 cycles. Non-fluorescent liposomes were produced in the same manner, but without the addition of 14:0 Liss Rhod PE. All lipid vesicle suspensions were stored at 4 °C.

Production of Extracellular Vesicles: 293-F cells (Gibco) were cultured at 37 °C in CD 293 medium (Gibco) supplemented with 4 mm GlutaMAX and 250 mg L−1 Pluronic F-68. The culture was stirred at 250 rpm and maintained at pH 7.1 and a dissolved oxygen concentration of 40% in a stirred tank bioreactor (DASGIP, Eppendorf) for 166 h. Conditioned media (450 mL) was harvested from approximately 9 × 108 cells with 92% viability and clarified by two centrifugation steps, the first at 200 × g for 10 min and the second at 3000 × g for 15 min. Clarified conditioned media (50 mL) was then filtered through a 0.22 μm membrane, incubated with 25 U of Pierce Universal Nuclease (Thermo Fisher Scientific) for 2.5 h at room temperature, and concentrated 100 times with an Amicon-15 centrifugal filter (50 kDa MWCO, RC membrane, Merck Millipore). The concentrated EVs (500 μL) were loaded onto a gravity flow chromatography column packed with 10 mL Sepharose CL4B resin (Cytiva). PBS was

ADVANCED
SCIENCE NEWS
www.advancedsciencenews.com

NANO · MICRO
small
www.small-journal.com

used as the running buffer to elute the EVs. Twenty fractions (500 μL each) were collected, and the ones with the highest particle number and tetraspanin CD81 concentrations measured by ELISA were pooled together, aliquoted, and stored at −80°C. Nanoalgosomes were produced and characterized as per a procedure described in a previous work.[27]

Microscopic Analysis of Vesicle Uptake: The uptake of fluorescent liposomes and EVs in polymer droplets was analyzed in 384-well plates (MatriPLate, Glass Bottom, Brooks) with a Ti2-U inverted microscope (Nikon) equipped with an LED light source (Omicron Laserage Laserprodukte GmbH) and a camera (Zyla sCMOS 4.2P-CL10, Andor). The filter cubes DAPI HC BP Filter set F36-500, CFP ET Filter set F46- 001, EGFP ET Filter set F46-002, and Cy5 ET Filter set F46-009 (AHF Analysentechnik AG) were also used. Before adding the solutions, the wells were coated with BSA to prevent droplet wetting. Each well was incubated with 100 μL of 1% BSA in Millipore water for 30 min at room temperature and rinsed three times with Millipore water.

For liposome uptake, RhodB-DOPS liposomes of concentrations between 1×10^{10} and 5×10^{10} particles mL^{-1} were added in 100 μL solutions at pH 7.4 with 20 mm Na-phosphate, 100 mm NaCl, and 0.15 mg mL^{-1} of either ZW (DP 200), ZW-R1, or ZW-B1 (Table 1). The solutions were analyzed after incubating the samples for at least 1 h at room temperature.

For EV uptake, EVs were first labelled with photoactivatable silicon rhodamine, as previously described.[26] A 20 μm dye was added to a stock solution containing 9×10^{10} particles mL^{-1} of HEK-293F EVs, and the resultant solution was immediately photoactivated with UV light for 2 min. EVs were then introduced at 1×10^{9} particles mL^{-1} in the corresponding samples containing 0.15 mg mL^{-1} of ZW, ZW-R1, or ZW-B1 (Table 1). Images were acquired after incubating the EVs for at least 1 h at room temperature.

ELISA: Quantification of CD81 in the samples was performed using 96-well plates (TPP). Samples (50 μL per well) were diluted to obtain 100 μL solutions containing 1 m NaCl and 20 mm Na-phosphate. The pH of this solution was kept at 7.4, and the resultant solution was incubated overnight at 4 °C. The plate was then washed with high- salt buffer (20 mm Na-phosphate, 1 m NaCl, pH 7.4) and PBS and blocked with 1% BSA in PBS for 1 h at room temperature. Next, the plate was incubated with the anti-human CD81 antibody 5A6 (1:500 dilution in blocking buffer; Santa Cruz Biotechnology) for 2 h at room temperature. After extensive washing, the plate was incubated with the secondary anti-mouse HRP-conjugated antibody (1:2000 dilution in blocking buffer; m-IgGκ BP-HRP; Santa Cruz Biotechnology) for 1 h at room temperature. Finally, the plate was washed and incubated with TMB ELISA Substrate (highest sensitivity, Abcam) for 15 min at room temperature. Subsequently, 450 nm

ADVANCED
SCIENCE NEWS
www.advancedsciencenews.com

NANO · MICRO
small
www.small-journal.com

STOP Solution was added to the TMB substrate (Abcam), and the absorbance of the resultant solution was measured at 450 nm using a Clariostar Plus microplate reader (BMG Labtech). Nanoparticle Tracking Analysis (NTA) Measurements: NTA measurements of liposomes and nanoalgosomes were performed using a ZetaView instrument equipped with a CMOS camera and a 405 nm laser (Particle Metrix). The chamber was calibrated daily with polystyrene nanoparticle standards, as per the manufacturer's recommendations. Samples were diluted in a high-salt buffer (20 mm Na-phosphate, 400 mm, or 1 m NaCl, pH 7.4) to a particle concentration of 107–109 particles mL−1 and injected into the sample chamber using a 1 mL syringe until the chamber was filled. Video acquisition was performed for all samples at 11 positions with 80% scattering intensity and 100 shutter in the light scattering mode, with a trace length of 15 frames and a frame rate of 30 s−1. Data were analyzed using the ZetaView analysis software (ZetaView 8.04.02 SP2).

Quantitative Analysis of the Uptake and Release of Liposomes, EVs, and Nanoalgosomes: For these experiments, solutions were prepared in 1.5 mL microcentrifuge tubes, and the polymer was subsequently added.

The uptake of liposomes was measured at different salt concentrations. For this purpose, 300 μL solutions (pH 7.4) containing 0.25 mg mL−1 ZW-R1 or ZW-B1 (Table 1), 3×10^9 particles mL−1 liposomes, 20 mm Na-phosphate, and different NaCl concentrations (37.5, 50, 100, 150, 200, 250, and 400 mm) were prepared. These solutions were briefly vortexed and incubated for 15 min at room temperature. The tubes were then centrifuged at 10 000 × g for 15 min at 25 °C. The supernatant (270 μL) was removed, and its fluorescence intensity was measured using a ClarioStar Plus microplate reader (BMG Labtech) at excitation and emission wavelengths of 550 and 605 nm, respectively. Measurements were performed in triplicate.

The liposome uptake in ZW-R1 coacervates at different liposome concentrations (in the range of 5×10^9–1×10^{11} particles mL−1) was analyzed in a similar manner at a constant NaCl concentration of 100 mm. Solutions were centrifuged at 3000 × g for 15 min at 25 °C.

To measure the recovery of liposomes from the coacervates, solutions (300 μL, pH 7.4) containing 20 mm Na-phosphate, 100 mm NaCl, 0.25 mg mL−1 ZW-R1 or ZW-B1, and 1.3×10^{10} particles mL−1 of non-fluorescent DOPS liposomes were prepared. After polymer addition, these solutions were incubated for 1 min at room temperature and then centrifuged at 3000 × g for 5 min at 4 °C. Then, the supernatant (270 μL) was removed and replaced with high-salt buffer (270 μL) to obtain a solution (pH 7.4) containing 20 mm Na-phosphate and 400 mm NaCl. The polymer pellet was resuspended by gentle pipetting and vortexed for several seconds. The resuspended sample was centrifuged at 3000 × g for 15 min at 25 °C, and the supernatant (270 μL)

ADVANCED
SCIENCE NEWS
www.advancedsciencenews.com

NANO · MICRO
small
www.small-journal.com

was removed. All supernatants recovered during the process were analyzed using NTA to quantify the amounts of unbound and eluted liposomes. Measurements were performed in triplicate.

The uptake of HEK-293F EVs was measured by preparing solutions (150 µL, pH 7.4) containing 0.25 mg mL−1 ZW-R1 or ZW-B1, 5×10^9 particles mL−1 HEK-293F EVs, 20 mm Na-phosphate, and different NaCl concentrations (25, 37.5, 50, 100, 150, and 200 mm). Samples were mixed by gentle vortexing and incubated for 15 min at room temperature. Then, the tubes were centrifuged at 3000 × g for 15 min at 25 °C. The supernatant (125 µL) was removed and analyzed using ELISA. Measurements were performed in duplicate for two independent samples.

The recovery of HEK-293F EVs was measured by following the same procedure used for liposomes. The ZW-R1 polymer (0.25 mg mL−1) was introduced in solutions (300 µL, pH 7.4) containing 20 mm Na-phosphate, 12.5 mm NaCl, and 5×10^9 particles mL−1 of HEK-293F EVs. After adding the polymer, the solutions were incubated for 1 min at room temperature and centrifuged at 370 × g for 21 min at 4 °C. After removing the supernatant, pellets of ZW-R1 were resuspended in high-salt buffers containing 550 mm NaCl. The second centrifugation was then performed at 3000 × g for 15 min at 25 °C. All collected supernatants were analyzed using ELISA. The measurements were performed in duplicate for three independent samples. For transmission electron microscopy (TEM), the same protocol was followed for 1×10^{10} particles mL−1 of HEK-293F EVs, and the pellets were resuspended in high salt buffer (40 µL).

The recovery of the nanoalgosomes was measured by following the same procedure used for HEK-293F EVs. The number of particles in the supernatants was determined using NTA. Measurements were performed in duplicate for two independent samples. To measure the uptake of medium impurities in ZW-R1 coacervates, solutions (300 µL, pH 7.4) containing clarified conditioned medium (15 µL) from HEK-293F cultures, 0.25 mg mL−1 ZW-R1, 20 mm Na-phosphate, and different NaCl concentrations (25, 37.5, 50, 100, 150, 200, and 400 mm) were prepared. Samples were mixed by gentle vortexing and incubated for 15 min at room temperature. Subsequently, the tubes were centrifuged at 3000 × g for 15 min at 25 °C. The supernatants (270 µL) were removed and analyzed using the QuantIT dsDNA Assay Kit (highest sensitivity, Thermo Fisher Scientific) and Micro BCA Protein Assay Kit (Thermo Fisher Scientific) in duplicate.

Finally, to test the purification of nanoalgosomes from Rhodamine B and BSA, solution (300 µL, pH 7.4) were prepared using 20 mm Na-phosphate, 12.5 mm NaCl, 0.25 mg mL−1 ZW-R1, 5×10^9 particles mL−1 of nanoalgosomes, and 1.5 µm Rhodamine B or 1.5 µm BSA (Sigma-Aldrich) labelled with Rhodamine B. The

ADVANCED
SCIENCE NEWS
www.advancedsciencenews.com

NANO · MICRO
small
www.small-journal.com

samples were incubated for 1 min at room temperature and centrifuged at 3000 × g for 5 min at 4 °C. After removing the supernatant, the samples were resuspended in high-salt buffer with 550 mm NaCl and 20 mm Na-phosphate at pH 7.4. The second centrifugation was then performed at 3000 × g for 15 min at 25 °C. The number of particles in the supernatants was measured in duplicates by NTA, and their fluorescence intensities were analyzed in triplicate at excitation and emission wavelengths of 550 and 605 nm, respectively, using a Clariostar Plus microplate reader (BMG Labtech).

Dynamic Light Scattering (DLS) Measurements: The size distributions of the non-fluorescent liposomes, HEK-293F EVs, and the nanoalgosomes were measured using a Zetasizer Nano ZSP DLS system (Malvern) in backscattering mode at 173° and 20°C.

Transmission Electron Microscopy: Five microliters of sample was placed on glow discharged (negatively at 25 mA for 30 s in an Emitech K100X glow discharge system, Quorum Technologies Ltd.) carbon-coated grids (Plano GmbH) and allowed to adsorb for 60 s. Subsequently, the excess liquid was drained with a filter paper, and the samples were subjected to negative staining with 2% uranyl acetate (w/v) by two successive incubations of 1 and 15 s. The grids were air-dried and imaged using a JEM-1400Flash electron microscope (JOEL) in the bright-field mode operated at 100 kV.

Fluorescence-Based Microfluidic Diffusion Sizing (fluoMDS) Measurements: FluoMDS analysis was performed as described in a previous study. [26] For lipid staining, HEK-293F EVs were mixed with 20 μm photoactivatable silicon rhodamine[30] and photoactivated with UV light for 2 min. For labeling the tetraspanins, HEK-293F EVs were blocked for 1 h at room temperature with 0.1% BSA in PBS and incubated with APC-conjugated anti-CD81 antibodies (1D6, 1:500 dilution in blocking buffer, Invitrogen) and PE-conjugated anti-CD63 antibodies (H5C6, 1:500 dilution in blocking buffer, Invitrogen). All samples had a final particle concentration of 1.5×10^{11} particles mL−1. Five microliters of sample were then loaded in the fluoMDS device, which was run at 60 μL h−1 using blocking buffer as the running buffer. After image acquisition with a Ti2-U inverted microscope (Nikon), the diffusion profiles were fitted, and the average particles sizes were computed as previously reports.[26]

EV Track: All relevant data from these experiments were submitted to the EV-TRACK knowledgebase (EV-TRACK ID: EV220295).[54]

Statistical Analysis: The number of particles in the solution [%] was referred to as the control sample without the polymer. All data were presented as mean ± standard deviation.

Supporting Information

Supporting Information is available from the Wiley Online Library or from the author.

Conflict of Interest
The authors declare no conflict of interest.

Data Availability Statement
The data that support the findings of this study are available from the corresponding author upon reasonable request.

References

[1] S. F. Banani, H. O. Lee, A. A. Hyman, M. K. Rosen, Nat. Rev. Mol. Cell Biol. 2017, 18, 285.
[2] B. G. O'Flynn, T. Mittag, Curr. Opin. Cell Biol. 2021, 69, 70.
[3] S. Boeynaems, S. Alberti, N. L. Fawzi, T. Mittag, M. Polymenidou, F. Rousseau, J. Schymkowitz, J. Shorter, B. Wolozin, L. Van Den Bosch, P. Tompa, M. Fuxreiter, Trends Cell Biol. 2018, 28, 420.
[4] E. Gomes, J. Shorter, J. Biol. Chem. 2019, 294, 7115.
[5] H. Zhao, E. Ibarboure, V. Ibrahimova, Y. Xiao, E. Garanger,

S. Lecommandoux, Adv. Sci. 2021, 8, 2102508.

[6] U. Capasso Palmiero, C. Paganini, M. R. G. Kopp, M. Linsenmeier, A. M. Küffner, P. Arosio, Adv. Mater. 2022, 34, 2104837.

[7] A. M. Rumyantsev, N. E. Jackson, J. J. De Pablo, Annu. Rev. Condens. Matter Phys. 2021, 12, 155.

[8] C. E. Sing, S. L. Perry, Soft Matter 2020, 16, 2885.

[9] C. Paganini, U. Capasso Palmiero, G. Pocsfalvi, N. Touzet, A. Bongiovanni, P. Arosio, Biotechnol. J. 2019, 14, 1800528.

[10] J. Chen, P. Li, T. Zhang, Z. Xu, X. Huang, R. Wang, L. Du, Front. Bioeng. Biotechnol. 2022, 9, 811971.

[11] T. Liangsupree, E. Multia, M. L. Riekkola, J. Chromatogr. A 2021, 1636, 461773.

[12] I. K. Herrmann, M. J. A. Wood, G. Fuhrmann, Nat. Nanotechnol. 2021, 16, 748.

[13] C. Gardiner, D. Di Vizio, S. Sahoo, C. Théry, K. W. Witwer, M. Wauben, A. F. Hill, J. Extracell. Vesicles 2016, 5, 32945.

[14] N. Heath, L. Grant, T. M. De Oliveira, R. Rowlinson, X. Osteikoetxea, N. Dekker, R. Overman, Sci. Rep. 2018, 8, 5730.

[15] I. L. Colao, R. Corteling, D. Bracewell, I. Wall, Trends Mol. Med. 2018, 24, 242.

[16] B. Barnes, T. Caws, S. Thomas, A. P. Shephard, R. Corteling, P. Hole, D. G. Bracewell, J. Chromatogr. A 2022, 1670, 462987.

[17] M. Y. Konoshenko, E. A. Lekchnov, A. V. Vlassov, P. P. Laktionov, Biomed. Res. Int. 2018, 8545347.

[18] G. Adamo, M. E. Barone, D. Fierli, A. Aranyos, D. P. Romancino, S. Picciotto, M. Gai, R. Carrotta, S. Morsbach, S. Raccosta, C. Stanly, C. Paganini, A. Cusimano, V. Martorana, R. Noto, F. Librizzi, L. Randazzo, R. Parkes, E. Rao, A. Paterna, P. Santonicola, A. Kisslinger, V. Kralj-iglič, U. C. Palmiero, L. Corcuera, E. Di Schiavi, G. L. Liguori, K. Landfester, P. Arosio, G. Pocsfalvi, et al., J. Extracell. Vesicles 2021, 10, e12081.

[19] S. Picciotto, M. E. Barone, D. Fierli, A. Aranyos, G. Adamo, D. Božič, D. P. Romancino, C. Stanly, R. Parkes, S. Morsbach, S. Raccosta, C. Paganini, A. Cusimano, V. Martorana, R. Noto, R. Carrotta, F. Librizzi, U. Capasso Palmiero, P. Santonicola, A. Iglič, M. Gai, L. Corcuera, A. Kisslinger, E. Di Schiavi, K. Landfester, G. L. Liguori, V. Kralj-Iglič, P. Arosio, G. Pocsfalvi, M. Manno, et al., Biomater. Sci. 2021, 9, 2917.

[20] Y. Xu, M. Mazzawi, K. Chen, L. Sun, P. L. Dubin, Biomacromolecules 2011, 12, 1512.

[21] J. D. Delgado, J. B. Schlenoff, Macromolecules 2017, 50, 4454.

[22] R. Upadhya, L. N. Madhu, S. Attaluri, D. L. G. Gitaí, M. R. Pinson, M. Kodali, G. Shetty, G. Zanirati, S. Kumar, B. Shuai, S. T. Weintraub, A. K. Shetty, J. Extracell. Vesicles 2020, 9, 1809064.

[23] V. Luga, L. Zhang, A. M. Viloria-Petit, A. A. Ogunjimi, M. R. Inanlou, E. Chiu, M. Buchanan, A. N. Hosein, M. Basik, J. L. Wrana, Cell 2012, 151, 1542.

[24] T. Lu, K. K. Nakashima, E. Spruijt, J. Phys. Chem. B 2021, 125, 3080.

[25] L. W. Chang, T. K. Lytle, M. Radhakrishna, J. J. Madinya, J. Vélez, C. E. Sing, S. L. Perry, Nat. Commun. 2017, 8, 1273.

[26] C. Paganini, B. Hettich, M. R. G. Kopp, A. Eördögh, U. Capasso Palmiero, G. Adamo, N. Touzet, M. Manno, A. Bongiovanni, P. Rivera-Fuentes, J. C. Leroux, P. Arosio, Adv. Healthcare Mater. 2021, 11, 2100021.

[27] A. Paterna, E. Rao, G. Adamo, S. Raccosta, S. Picciotto, D. Romancino, R. Noto, N. Touzet, A. Bongiovanni, M. Manno, Front. Bioeng. Biotechnol. 2022, 10, 836747.

[28] J. Kowal, G. Arras, M. Colombo, M. Jouve, J. P. Morath, B. Primdal-Bengtson, F. Dingli, D. Loew, M. Tkach, C. Théry, Proc. Natl. Acad. Sci. U. S. A. 2016, 113, E968.

[29] D. K. Jeppesen, A. M. Fenix, J. L. Franklin, J. N. Higginbotham, Q. Zhang, L. J. Zimmerman, D. C. Liebler, J. Ping, Q. Liu, R. Evans, W. H. Fissell, J. G. Patton, L. H. Rome, D. T. Burnette, R. J. Coffey, Cell 2019, 177, 428.

[30] A. Eördögh, C. Paganini, D. Pinotsi, P. Arosio, P. Rivera-Fuentes, ACS Chem. Biol. 2020, 15, 2597.

[31] N. Hammerschmidt, S. Hobiger, A. Jungbauer, Process Biochem. 2016, 51, 325.

[32] M. Martinez, M. Spitali, E. L. Norrant, D. G. Bracewell, Trends Biotechnol. 2019, 37, 237.

[33] M. Iqbal, Y. Tao, S. Xie, Y. Zhu, D. Chen, X. Wang, L. Huang, D. Peng, A. Sattar, M. A. B. Shabbir, H. I. Hussain, S. Ahmed, Z. Yuan, Biol. Proced. Online 2016, 18, 18.

[34] W. C. Blocher McTigue, S. L. Perry, Soft Matter 2019, 15, 3089.

[35] L. Zhou, H. Shi, Z. Li, C. He, Macromol. Rapid Commun. 2020, 41, 1. [36] W. C. Blocher McTigue, S. L. Perry, Small 2020, 16, 1907671.

[37] P. Nestola, C. Peixoto, R. R. J. S. Silva, P. M. Alves, J. P. B. Mota, M. J. T. Carrondo, Biotechnol. Bioeng. 2015, 112, 843.

[38] H. O. Johansson, J. Persson, F. Tjerneld, Biotechnol. Bioeng. 1999, 66, 247.

[39] S. B. Carvalho, C. Peixoto, M. J. Manuel, R. J. Ricardo, Biotechnol. Bioeng. 2021, 118, 2845.

[40] M. G. Moleirinho, R. J. S. Silva, P. M. Alves, M. J. T. Carrondo, C. Peixoto, Expert Opin. Biol. Ther. 2020, 20, 451.

[41] N. Seo, J. Nakamura, T. Kaneda, H. Tateno, A. Shimoda, T. Ichiki, K. Furukawa, J. Hirabayashi, K. Akiyoshi, H. Shiku, J. Extracell. Vesicles 2022, 11, e12205.

[42] S. Fedosyuk, T. Merritt, M. P. Peralta-Alvarez, S. J. Morris,

ADVANCED
SCIENCE NEWS
www.advancedsciencenews.com

NANO · MICRO
small
www.small-journal.com

A. Lam, N. Laroudie, A. Kangokar, D. Wright, G. M. Warimwe, P. Angell-Manning, A. J. Ritchie, S. C. Gilbert, A. Xenopoulos, A. Boumlic, A. D. Douglas, Vaccine 2019, 37, 6951.

[43] M. Kosanovic, B. Milutinovic, S. Goc, N. Mitic, M. Jankovic, BioTechniques 2017, 63, 65.

[44] J. Ruscic, C. Perry, T. Mukhopadhyay, Y. Takeuchi, D. G. Bracewell, Mol. Ther. Methods Clin. Dev. 2019, 15, 52.

[45] D.-K. Kim, H. Nishida, S. Y. An, A. K. Shetty, T. J. Bartosh, D. J. Prockop, Proc. Natl. Acad. Sci. U. S. A. 2016, 113, 170.

[46] M. Yu, Y. Li, S. Zhang, X. Li, Y. Yang, Y. Chen, G. Ma, Z. Su, J. Chromatogr. A 2014, 1331, 69.

[47] T. Vicente, R. Fáber, P. M. Alves, M. J. T. Carrondo, J. P. B. Mota, Biotechnol. Bioeng. 2011, 108, 1347.

[48] H. Park, T. N. Sut, B. K. Yoon, V. P. Zhdanov, N. J. Cho, J. A. Jackman, J. Phys. Chem. Lett. 2021, 12, 6722.

[49] E. Lerer, Z. Oren, Y. Kafri, Y. Adar, E. Toister, L. Cherry, E. Lupu, A. Monash, R. Levy, E. Dor, E. Epstein, L. Levin, M. Girshengorn, N. Natan, R. Zichel, A. Makovitzki, BioTech 2021, 10, 22.

[50] J. Ladd, Z. Zhang, S. Chen, J. C. Hower, S. Jiang, Biomacromolecules 2008, 9, 1357.

[51] L. D. Blackman, P. A. Gunatillake, P. Cass, K. E. S. Locock, Chem. Soc. Rev. 2019, 48, 757.

[52] N. Y. Kostina, S. Sharifi, A. De Los Santos Pereira, J. Michálek, D. W. Grijpma, C. Rodriguez-Emmenegger, J. Mater. Chem. B 2013, 1, 5644.

[53] M. Sponchioni, P. Rodrigues Bassam, D. Moscatelli, P. Arosio, U. C. Palmiero, Nanoscale 2019, 11, 16582.

[54] J. van Deun, P. Mestdagh, P. Agostinis, Ö. Akay, S. Anand, J. Anckaert, Z. A. Martinez, T. Baetens, E. Beghein, L. Bertier, G. Berx, J. Boere, S. Boukouris, M. Bremer, D. Buschmann, J. B. Byrd, C. Casert, L. Cheng, A. Cmoch, D. Daveloose, E. De Smedt, S. Demirsoy, V. Depoorter, B. Dhondt, T. A. P. Driedonks, A. Dudek, A. Elsharawy, I. Floris, A. D. Foers, K. Gärtner, et al., Nat. Methods 2017, 14, 228.

Chapter 8

General discussion and Future prospects

8.1 General discussion

EVs obtained from mammalian cells, such as mesenchymal stem cells (MSCs), have been studied for their therapeutic benefits in various diseases, but their production is limited by technical challenges[1]. Microalgae were found to produce EVs in the culture medium, and six strains were selected for further analysis (Chapter 3)[2]. The EVs from these strains had attributes expected of small EVs (sEVs) in terms of morphology, size distribution and protein content. The freshwater glaucophyte *Cyanophora paradoxa*, in particular, produced a yield of ~2 μg of total sEV-protein per ml of microalgal conditioned media (Chapter 3)[2]. The yield was comparable to that of plant-derived vesicles and GMP-grade MSC-derived exosomes, indicating the potential of microalgal EVs as a sustainable source for tailor-made bio-products (Chapter 3)[2]. The use of microalgae as a natural source for EVs offers advantages, including high growth rates, controlled environmental conditions in large-scale photobioreactors, and a natural and sustainable origin (Chapter 4)[3]. The use of TFF-derived culture facilitates the cyclical production of nanoalgosomes, and highlights the competitive advantages of nanoalgosomes over EVs derived from other sources, including renewability (Chapter 5)[4].

In addition, the characterization of the surface properties of isolated microalgal EVs, showed their hydrophilic nature and ability to interact with biological membranes. It has been shown that nanoalgosomes can be internalized by different cell types, including cancer cells. This makes them potentially useful for drug delivery applications (Chapter 4 & Chapter 6)[3,5]. Furthermore, to showcase the potential use of nanoalgosomes as a drug delivery mechanism, the study employed the *C. elegans* biological system as a model to investigate their uptake and biodistribution. Three different administration routes were evaluated, and a specific signal was detected in the cytoplasm of intestinal cells, with only slight variations among the three methods. The results highlighted the potency of *C. elegans* as a model system for examining the absorption, persistence, and distribution of exogenous EVs (Chapter 6)[5].

Finally, a new method was developed for the purification of vesicles, such as liposomes human and EV/microalgal, using zwitterionic coacervate (Chapter 7)[6]. This method combines the advantages of various purification techniques and can adapt to fluctuations in product quantities, making it a scalable and flexible method for bioprocessing. The coacervates provide a delicate bioproducts environment, preventing the aggregation of the product and facilitating its re-suspension. They prevent the deformation of vesicles and their programmability allows you to regulate interactions and bonding greed. Vesicles bind exclusively through ion interactions, modulated by the regulation of the type, quantity and density of charged monomers in the polymer. The results suggest that zwitterion coacervates offer a promising new

approach for the purification of vesicles derived from human and microalgae and the development of bioprocessing strategies.

8.2 Future prospects

Microalgae will be further exploited as a sustainable and renewable biological resource for the production of the nanoalgosome, with the advantages over other sources of extracellular vesicles. Also, nanoalgosomes will be further developed as bioactive effectors and as drug delivery system for cosmetics and pharmaceutic applications. For that, several aspects will support the development of nanoalgome-based studies:

1) Extracellular vesicles enclose or expose on their surface a large number of biomolecules including RNA, lipids, proteins, and possibly DNA. Further studies on the highly conserved PM H+-ATPase in nanoalgosome membranes will certainly allow for a better definition and a possible application of PM H+-ATPase as a biomarker for nanoalgosomes. In the future, the discovery of H+-ATPase will provide important insights into the mechanisms of nanoalgosome-mediated cellular uptake and also will be key for the development of important tool for microalgal-derived EV analyses (i.e., cytofluorimetric studies). Nanoalgosome will continue to play a crucial role in cellular communication by delivering their payload to target cells. Preliminary results indicate the successful characterization of the presence of H+ATPase on the surface of nanoalgosomes using two in-silico systems, as shown in Figure 1(a). The immunoassay performed using flow cytometry showed that H+ATPase protein was present on nanoalgosomes (figure 1b). The shift in the median fluorescence intensity of the samples stained for H+ATPase was significantly larger compared to controls (data not shown). The use of magnetic beads with H+ATPase-nanoalgosome staining was found to be effective in capturing and quantifying sEVs. In addition, the co-localization analysis of f-nanoalgosome and nanoalgosome with H+ATPase was performed using uptake based on Zwitterionic Droplets. Bead-based flow cytometry analysis and uptake based on Zwitterionic Droplets confirmed the presence of H+ATPase on both f-nanoalgosomes and nanoalgosomes. Further analysis of the production and properties of H+ATPase-nanoalgosome using a new system for the characterization and purification of EVs showed promising results.
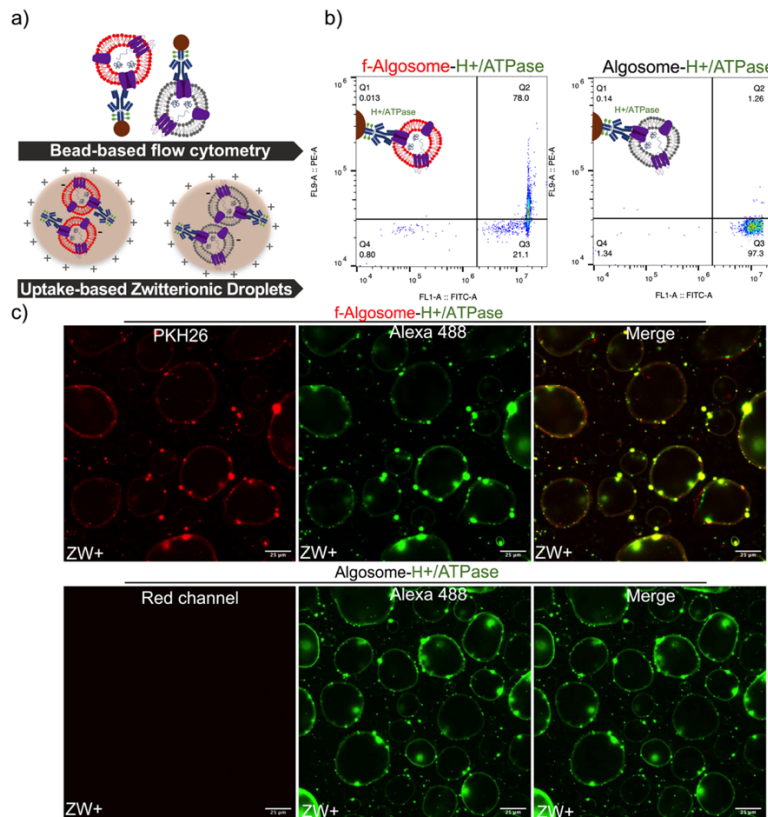
Figure 1. **In silico analysis of nanoalgosomes Plasma Membrane H+-ATPase**. (a) Representative scheme of f-algosome & algosome - H+ATPase co-localization analysis using two different systems: Bead-based flow cytometry analysis and uptake based on Zwitterionic Droplets; (b) Bead-based flow cytometry analysis of f-algosome (red) -H+/ATPase (green) and algosome-H+/ATPase (green). Controls (beads with algosome unlabeled and beads with PBS-Alexa 488) were used to prove the absence of nonspecific binding of the antibodies to the beads (data no shown) (c) Using a Zwitterionic Droplets (ZW+), the merge of representative fluorescence microscopy images show the co-localization of red-algosome with the protein green-H+/ATPase with a Pearson's_Rr = 0.8 (f-Algosome- H+/ATPase). Below is the uptake of the algosome in ZW+ that have only undergone immunostaing and not red-dye labeling as control (Algosome-/H+/ATPase). The other controls, red algosome, PBS-PKH26-Alexa 488 (data no shown) (Magnification 60X). Scale bar 25 μm.

Moreover, the uptake of f-nanoalgosomes and nanoalgosomes in MDA-MB 231 cell lines showed the co-localization of nanoalgosomes with H+/ATPase, indicating the successful internalization of the sEVs. Further analysis using confocal microscopy showed the colocalization of f-nanoalgosomes and H+/ATPase in MDA-MB231cells, suggesting the potential use of these sEVs as drug delivery systems. However, more research is required to fully understand the properties and potential applications of these sEVs. In vitro studies will continue to investigate the possible effects of EV-mediated cell uptake on membrane reorganization.
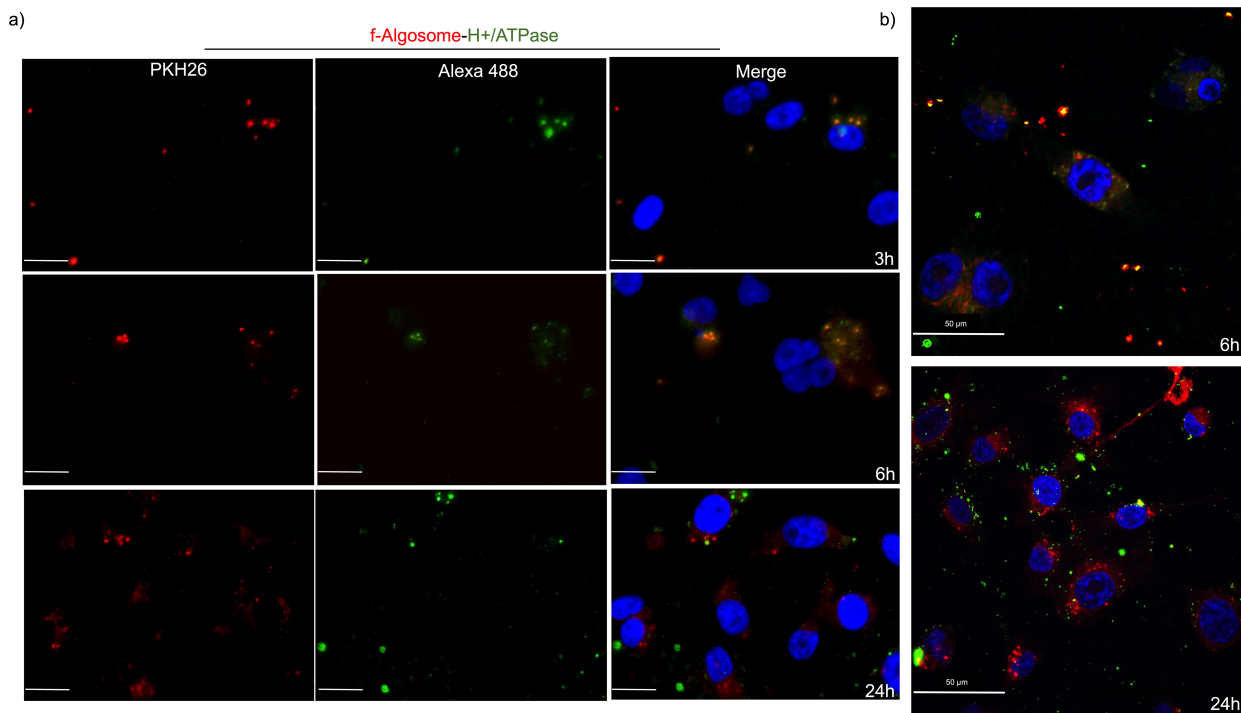
Figure 2. (a) Representative fluorescence microscopy images showing the cellular uptake of f-algosome (red) - H+/ATPase (green) in MDA-MB 231 cell lines (nuclei in blue), incubated with 2 μg/ml of f-algosome-H+/ATPase at 37◦C for 3, 6 and 24 h and the co-localization of algosome with H+/ATPase only at 3 and 6h. PBS+free dye and Alexa 488 are used as negative controls (data no shown). Magnification 40X. (b) Confocal microscopy analysis of 2 μg/ml f-algosome (red) - H+/ATPase (green) internalization in MDA-MB231cells (nuclei stained with DAPI in blue), at 37◦C for 6 and 24 h Scale bar 50 μm.

2) Several small drugs have been effectively loaded into extracellular vesicles (EVs) as cargo, demonstrating improved potency, increased accumulation in target cells, and enhanced drug stability. The use of small drugs as cargo for extracellular vesicles (EVs) will continue to improve, leading to increased potency, enhanced drug stability, and greater accumulation in target cells. Nanolgosomes, could be become a widely used drug delivery system. Preliminary results indicate that doxorubicin, a commonly used chemotherapeutic, can be successfully loaded into nanoalgosomes using various strategies (figure 3). Passive incubation was found to be the most effective method for loading compere to freeze/thaw resulted. To determine loading efficiency, nanoalgosome-Dox samples were lysed and the fluorescence signal was detected, with passive incubation resulting in the highest loading efficiency (figure 3b). These results suggest that nanoalgosomes may be a promising carrier for the delivery of hydrophobic small molecules, such as doxorubicin, to target cells.

In an MTS assay conducted on tumor and normal cells (MDA MB 231 and 1-7 HB2, respectively), nanoalgosome-Dox was compared to free doxorubicin at the same concentration (0.5 μM) after 24, 48, and 72 hours of treatment (figure 3c,d). The data indicates that doxorubicin loaded-nanoalgosomes induced a faster cytotoxic effect in tumor cells compared to normal cells (figure 3c,d). These findings are consistent with previous studies showing rapid internalization of fluorescent nanoalgosomes in tumor cells compared to normal cells. These preliminary results suggest that doxorubicin loaded-nanoalgosomes have potential as a more effective cancer treatment than free doxorubicin. Further studies are necessary to confirm these findings.
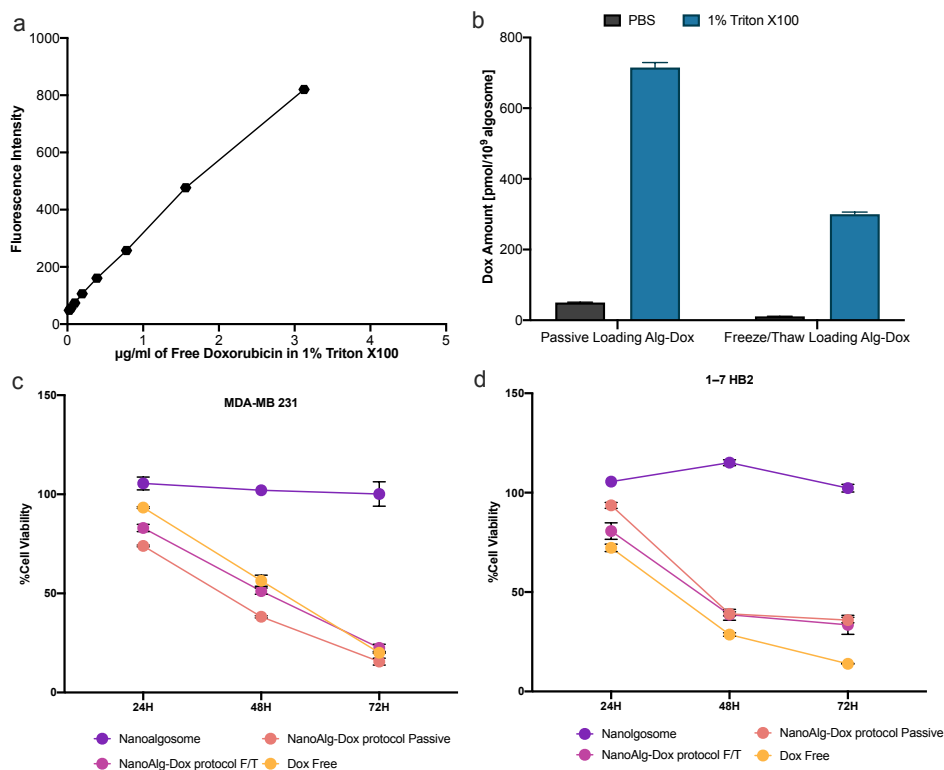
Figure 3. a) Calibration curve of free Doxorubin in 1% Triton X100; b) Loading efficient of Doxorubicin in nanoalgosome sample, expressed as amount pmol/10^9 algosome, using two different methos: passive loading and Freeze/Thaw. Cytotoxicity effect of Doxorubicin-loaded nanoalgosomes in c) tumoral and d) normal cell line.

8.3 References

1. Manzoor, T., Saleem, A., Farooq, N. et al. Extracellular vesicles derived from mesenchymal stem cells — a novel therapeutic tool in infectious diseases. Inflamm Regener 43, 17 (2023). https://doi.org/10.1186/s41232-023-00266-6.

2. Picciotto S, Barone ME, Fierli D, Aranyos A, Adamo G, BoŽič D, Romancino DP, Stanly C, Parkes R, Morsbach S, Raccosta S, Paganini C, Cusimano A, Martorana V, Noto R, Carrotta R, Librizzi F, Capasso Palmiero U, Santonicola P, Iglič A, Gai M, Corcuera L, Kisslinger A, Di Schiavi E, Landfester K, Liguori GL, Kralj-Iglič V, Arosio P, Pocsfalvi G, Manno M, Touzet N, Bongiovanni A. Isolation of extracellular vesicles from microalgae: towards the production of sustainable and natural nanocarriers of bioactive compounds. Biomater Sci. 2021 Apr 21;9(8):2917-2930. doi: 10.1039/d0bm01696a. Epub 2021 Feb 23. PMID: 33620041. Impact Factor: 7.59

3. Adamo G, Fierli D, Romancino DP, Picciotto S, Barone ME, Aranyos A, Božič D, Morsbach S, Raccosta S, Stanly C, Paganini C, Gai M, Cusimano A, Martorana V, Noto R, Carrotta R, Librizzi F, Randazzo L, Parkes R, Capasso Palmiero U, Rao E, Paterna A, Santonicola P, Iglič A, Corcuera L, Kisslinger A, Di Schiavi E, Liguori GL, Landfester K, Kralj-Iglič V, Arosio P, Pocsfalvi G, Touzet N, Manno M, Bongiovanni A. Nanoalgosomes: Introducing extracellular vesicles produced by microalgae. J Extracell Vesicles. 2021 Apr;10(6):e12081. doi: 10.1002/jev2.12081. Epub 2021 Apr 27. PMID: 33936568; PMCID: PMC8077145. Co-first Author. Impact Factor: 25.84

4. Paterna A, Rao E, Adamo G, Raccosta S, Picciotto S, Romancino D, Noto R, Touzet N, Bongiovanni A, Manno M. Isolation of Extracellular Vesicles From Microalgae: A Renewable and Scalable Bioprocess. Front Bioeng Biotechnol. 2022 Mar 14;10:836747. doi: 10.3389/fbioe.2022.836747. PMID: 35360396; PMCID: PMC8963918. Impact Factor: 6.064

5. Picciotto S, Santonicola P, Paterna A, Rao E, Raccosta S, Romancino DP, Noto R, Touzet N, Manno M, Di Schiavi E, Bongiovanni A, Adamo G. Extracellular Vesicles From Microalgae: Uptake Studies in Human Cells and Caenorhabditis elegans. Front Bioeng Biotechnol. 2022 Mar 24;10:830189. doi: 10.3389/fbioe.2022.830189. PMID: 35402397; PMCID: PMC898791. Impact Factor: 6.064

6. C. Paganini, U. Capasso Palmiero, S. Picciotto, A. Molinelli, I. Porello, G. Adamo, M. Manno, A. Bongiovanni, P. Arosio. High-Yield Separation of Extracellular Vesicles Using Programmable Zwitterionic Coacervates. Small 2022, 2204736. https://doi.org/10.1002/smll.202204736. Impact Factor: 15.153

Conclusion

Microalgae are increasingly being recognized as a promising source for the production of extracellular vesicles (EVs) due to their ability to grow rapidly in controlled environmental conditions and their natural and sustainable origin. Studies have shown that microalgal EVs, particularly those from the freshwater glaucophyte *Cyanophora paradoxa* and *Tetraselmis chuii*, can produce yields that are comparable to plant-derived vesicles and GMP-grade MSC-derived exosomes. These EVs possess hydrophilic properties, allowing them to interact with biological membranes, and can be internalized by various cell types, including cancer cells, making them a valuable tool as bioactive effectors and in drug delivery applications.

In addition, a new method for the purification of vesicles has been developed using zwitterionic coacervate, which is both scalable and flexible for bioprocessing. This new approach can be applied to various types of vesicles, including liposomes, human EVs, and microalgal EVs, making it an important advancement in the field of extracellular vesicle research. Moreover, the study has identified the H+-ATPase protein as a biomarker for nanoalgosomes, and its presence on the surface of nanoalgosomes has been successfully characterized.

In conclusion, these findings have demonstrated the potential for using nanoalgosomes as bioactive effectors and as a drug delivery system. However, further research is required to gain a better understanding of their properties and potential applications.

Overall, these recent advancements in the production and purification of microalgal EVs represent exciting developments in the field of drug delivery and hold promise for future therapeutic applications.

Curriculum Vitae

Personal Information

Name: **Sabrina Picciotto**
Date of birth: **April 14,1992**
Place of birth: **Palermo, Italy**

CONTACT

Via Castelfidardo, 7, 91025, Marsala (TP), Italy

sabrina.picciotto@irib.cnr.it;
sabrina.picciotto@unipa.it;
sabrina.picciotto92@gmail.com.

Education and training

20/03/2023-20/03/2024
Post Doctoral Position. Institute for Biomedical Research and Innovation (IRIB - CNR) Palermo, (Italy). Scientific director: Dr. Antonella Bongiovanni.

18/12/2019-18/03/2023 Palermo, Italy:
PhD in Technology and Science for Human Healt. University of Palermo (Palermo, Italy)/Institute for Biomedical Research and Innovation (IRIB - CNR) Palermo, (Italy). Thesis: Extracellular Vesicles from a renewable natural source: development of new biomaterial. Scientific director: Dr. Antonella Bongiovanni.

25/01/2022 – 31/05/2022 Zurich, Swizzerland:
Internship-Eidgenössische Technische Hochschule (ETH). Visiting PHD Student at the laboratory of Prof. Paolo Arosio.

25/07/2019 – 24/10/2019 Palermo (Italy):
Collaboration Assignment. Institute for Biomedical Research and Innovation (IRIB - CNR) Palermo, (Italy). Scientific director: Dr. Antonella Bongiovanni.

01/10/2017 – 15/03/2019 Palermo (Italy):
Master's Degree in Medical Biotechnology and Molecular Medicine. University of Palermo (Palermo, Italy).
Thesis: Crosstalk between S-palmitolation and Alix ubiquitination in skeletal muscle cells. Scientific director: Dr. Antonella Bongiovanni.

16/01/2018 -31/01/2019 Palermo (Italy):

Internship. Institute for Biomedical Research and Innovation (IRIB - CNR) Palermo, (Italy). Scientific director: Dr. Antonella Bongiovanni.

24/05/2017- 22/12/2017 Palermo (Italy):

Internship. Institute for Biomedical Research and Innovation (IRIB - CNR) Palermo, (Italy). Scientific director: Dr Giovanni Duro.

23/03/2016 Palermo (Italy):

Bachelor's degree in Biological Sciences. University of Palermo (Palermo, Italy). Thesis: Morphological characteristics of human spermatozoa of patients with suspected infertility

10/10/2015-1/03/2016- Palermo (Italy)

Internship. University of Palermo (Palermo, Italy). Scientific director: Pr. M.C. Roccheri.

Publication

Buffa V, Adamo G, **Picciotto S**, Bongiovanni A, Romancino DP. A Simple, Semi-Quantitative Acyl Biotin Exchange-Based Method to Detect Protein S-Palmitoylation Levels. Membranes (Basel). 2023 Mar 21;13(3):361. doi: 10.3390/membranes13030361. PMID: 36984748. **Impact Factor: 4.562**

C. Paganini, U. Capasso Palmiero, **S. Picciotto**, A. Molinelli, I. Porello, G. Adamo, M. Manno, A. Bongiovanni, P. Arosio. High-Yield Separation of Extracellular Vesicles Using Programmable Zwitterionic Coacervates. Small 2022, 2204736. https://doi.org/10.1002/smll.202204736. **Impact Factor: 15.153**

Paterna A, Rao E, Adamo G, Raccosta S, **Picciotto S**, Romancino D, Noto R, Touzet N, Bongiovanni A, Manno M. Isolation of Extracellular Vesicles From Microalgae: A Renewable and Scalable Bioprocess. Front Bioeng Biotechnol. 2022 Mar 14;10:836747. doi: 10.3389/fbioe.2022.836747. PMID: 35360396; PMCID: PMC8963918. **Impact Factor: 6.064**

Picciotto S, Santonicola P, Paterna A, Rao E, Raccosta S, Romancino DP, Noto R, Touzet N, Manno M, Di Schiavi E, Bongiovanni A, Adamo G. Extracellular Vesicles From Microalgae: Uptake Studies in Human Cells and Caenorhabditis elegans. Front Bioeng Biotechnol. 2022 Mar 24;10:830189. doi: 10.3389/fbioe.2022.830189. PMID: 35402397; PMCID: PMC8987914. **Co-first Author; Impact Factor: 6.064**

Longo V, Longo A, Adamo G, Fiannaca A, **Picciotto S**, La Paglia L, Romancino D, La Rosa M, Urso A, Cibella F, Bongiovanni A, Colombo P. 2,2'4,4'-Tetrabromodiphenyl Ether (PBDE-47) Modulates the Intracellular miRNA Profile, sEV Biogenesis and Their miRNA Cargo Exacerbating the LPS-Induced Pro-Inflammatory Response in THP-1 Macrophages. Front Immunol. 2021 May 7;12:664534. doi: 10.3389/fimmu.2021.664534. PMID: 34025666; PMCID: PMC8138315. **Impact Factor: 8.787**

Adamo G, Fierli D, Romancino DP, **Picciotto S**, Barone ME, Aranyos A, Bo žič D, Morsbach S, Raccosta S, Stanly C, Paganini C, Gai M, Cusimano A, Martorana V, Noto R, Carrotta R, Librizzi F, Randazzo L, Parkes R, Capasso Palmiero U, Rao E, Paterna A, Santonicola P, Iglič A, Corcuera L, Kisslinger A, Di Schiavi E, Liguori GL, Landfester K, Kralj-Iglič V, Arosio P, Pocsfalvi G, Touzet N, Manno M, Bongiovanni A. Nanoalgosomes: Introducing extracellular vesicles produced by microalgae. J Extracell Vesicles. 2021 Apr;10(6):e12081. doi: 10.1002/jev2.12081. Epub 2021 Apr 27. PMID: 33936568; PMCID: PMC8077145. **Co-first Author; Impact Factor: 25.84**

Picciotto S, Barone ME, Fierli D, Aranyos A, Adamo G, BoŽič D, Romancino DP, Stanly C, Parkes R, Morsbach S, Raccosta S, Paganini C, Cusimano A, Martorana V, Noto R, Carrotta R, Librizzi F, Capasso Palmiero U, Santonicola P, Iglič A, Gai M, Corcuera L, Kisslinger A, Di Schiavi E, Landfester K, Liguori GL, Kralj-Iglič V, Arosio P, Pocsfalvi G, Manno M, Touzet N, Bongiovanni A. Isolation of extracellular vesicles from microalgae: towards the production of sustainable and natural nanocarriers of bioactive compounds. Biomater Sci. 2021 Apr 21;9(8):2917-2930. doi: 10.1039/d0bm01696a. Epub 2021 Feb 23. PMID: 33620041. **Co-first Author; Impact Factor: 7.59**

Chapter Book

Mario Allegra, Antonella Bongiovanni, Giuseppe Città, Antonella Cusimano, Valentina Dal Grande, Manuel Gentile, Annamaria Kisslinger, Dario La Guardia, Giovanna Liguori, Fabrizio Lo Presti, Salvatore Perna, **Sabrina Picciotto**, Simona Ottaviano, Carla Sala & Alessandro Signa (2021). The Role of Metaphor in Serious Games Design: the BubbleMumble Case Study. In: de Rosa, F., Marfisi Schottman, I., Baalsrud Hauge, J., Bellotti, F., Dondio, P., Romero, M. (eds) Games and Learning

Alliance. GALA 2021. Lecture Notes in Computer Science, vol 13134. Springer, Cham. https://doi.org/10.1007/978-3-030-92182-8_19. **Chapter Book**

Sabrina Picciotto; Daniele P. Romancino Valentina Buffa Antonella Cusimano Antonella Bongiovanni Giorgia Adamo. "Chapter Four - Post-translational lipidation in extracellular vesicles: chemical mechanisms, biological functions and applications". Advances in Biomembranes and Lipid Self-Assembly, Volume 32 ISSN 2451-9634.

Honours and Awards

"Young Investigator Award"- Best Oral Communication "Young Investigator Award"- Rilasciato da 93° Congresso Nazionale della SIBS-1925 · apr 2021Rilasciato da 93° Congresso Nazionale della SIBS-1925 · apr 2021. Vincita del premio per la migliore comunicazione orale conseguita nel contesto dei lavori del 93° Congresso Nazionale della SIBS-1925. Titolo della Presentazione: EXPLORATION OF MICROALGAE-DERIVED EXTRACELLULAR VESICLES: CELLULAR UPTAKE OF NANOALGOSOMES

Oral Comunication

10/2022
"Nanoalgosome Quality control" in BOW project – Biogenic Organotropic Wetsuits, CONSORTIUM MEETIN.

09/2022
Retreat IRIB 2023, Institute for Biomedical Research and Innovation (IRIB - CNR)

09/2022
"Standardization of EV production, handling and characterization" in Second BOW Young Researcher Meeting. BOW project – Biogenic Organotropic Wetsuit

06/2022
"Novel tool to analyse algosome membrane topology/integrity" in BOW project – Biogenic Organotropic Wetsuits Bimonthly Technical meeting

11/2021
"Validation of Nanoalgosome staining using different Lipid dyes" in First BOW Young Researcher Meeting. BOW project – Biogenic Organotropic Wetsuit

04/2021
"Exploration of microalgae-derived extracellular vesicles: cellular uptake of nanoalgosomes" 93° Congresso Nazionale della SIBS**.**

Poster Presentation

6-10/02/2023
Sabrina Picciotto, Giorgia Adamo, Paola Gargano, Daniele Romancino, Angela Paterna, Estella Rao, Monica Salamone, Samuele Raccosta, Antonella Cusimano, Rosina Noto, Nicolas Touzet, Mauro Manno and Antonella Bongiovanni.
"**Microalgae-derived extracellular vesicles as a green biotechnology for therapeutic and cosmetic application**". **XXVII SCHOOL OF PURE AND APPLIED BIOPHYSICS**: Extracellular vesicles: from biophysical to translational challenges. Venice, Italy.

09/2022
Samuele Raccosta, Angela Paterna, Estella Rao, Giorgia Adamo, **Sabrina Picciotto**, Paola Gargano, Daniele Romancino, Rosina Noto, Antonella Bongiovanni and Mauro Manno. "**Biochimical sorting and biomechanical properties of extracellular vescicles**." SIBPA XXVI Congresso Nazionale.

05/2022
Giorgia Adamo, **Sabrina Picciotto**, Paola Gargano, Daniele Romancino, Angela Paterna, Estella Rao, Monica Salamone, Samuele Raccosta, Antonella Cusimano, Rosina Noto, Nicolas Touzet, Mauro Manno and Antonella Bongiovanni. **"Microalgal Extracellular Vesicles as nature designed delivery platforms for therapeutic and cosmetic applications". ISEV 2022.** Lion, France

05/2021
Giorgia Adamo, Pamela Santonicola, Daniele Romancino, **Sabrina Picciot**to, Samuele Raccosta, Antonella Cusimano, Rosina Noto, Estella Rao, Angela Paterna, Nicolas Touzet, Mauro Manno, Elia di Schiavi, and Antonella Bongiovanni**. "Nanoalgosomes: "microalgal-derived extracellular vesicles in *in vitro e in vivo* cellular uptake studies. ISEV 2021.** Virtual**.**

2020
Sabrina Picciotto, Giorgia Adamo, Daniele Romancino, Estella Rao, Angela Paterna, Samuele Raccosta, Rosina Noto, Rita Carrotta, Nicolas Touzet, Mauro Manno, Antonella Bongiovanni. **"Nanoalgosomes: analyses of the cellular uptake".** University of Ljubljana, Socratic Symposium. Virtual.

04/2019
Nicolas Touzet, Daniele Romancino, Giorgia Adamo, Mauro Manno, Antonella Cusimano, **Sabrina Picciotto**, Samuele Raccosta, Vincenzo Martorana, Rosina Noto, Rita Carrotta, Elia Di Schiavi, Giovanna L. Liguori, Annamaria Kisslinger, Katharina Landfester, Blanca Rodriguez, Svenja Morsbach, Ales Iglic, Veronika Iglic, Laura Corcuera, Paolo Arosio, Gabriella Pocsfalvi, and Antonella Bongiovanni. **"VES4US:**

**Extracellular vesicles from a natural source for tailor-made nanomaterials".
ISEV 2019.** Kyoto, Japan.

Courses

6-10/02/2023
XXVII SCHOOL OF PURE AND APPLIED BIOPHYSICS: Extracellular
vesicles: from biophysical to translational challenges. Venice, Italy.

02/2021
**Analysis of samples in solution by PUMP/PROBE spectroscopy at
FEMTOSECONDO**. Dr Alice Sciortino and Prof. Fabrizio Messina. University of
Palermo, Palermo (Italy)

02/2021
An R tutorial for Beginners. Dr Anna Maria Cardullo." University of Palermo,
Palermo (Italy)

10/2020
Confocal Training: Microscopia a fluorescenza Confocale. Dr Giuseppe Sancataldo
and Prof. Valeria Vetri. University of Palermo, Palermo (Italy)

10/2020
Microraman microscopia raman. Dr. Angelo Armano, Dr. Luigi Tranchina, Prof.
Simonpietro Agnello. University of Palermo, Palermo (Italy).

12/2018
Recognition of distress, pain and suffering of Rodents, organized by the Department
of Biopathology and Medical Biotechnology of the University of Palermo.

05/2018
Good practice and safety in research laboratories, organized by the Institute of
Molecular Biomedicine and Immunology National Research Council (IRIB-CNR) and
University of Palermo, held in Palermo (Italy).

Works published on congress

09/2022
Pamela Santonicola, Giorgia Adamo, **Sabrina Picciotto**, Andrea Zendrini, Daniele P.
Romancino, Angela Paterna, Estella Rao, Samuele Raccosta, Stella Frabetti, Rosina
Noto, Olivia Candini, Nicolas Touzet, Mauro Manno, Paolo Bergese, Antonella
Bongiovanni and Elia Di Schiavi. "characterization of EV toxicity and biodistribution
in vivo in the model system C. elegans". Workshop EV Connect: fostering
collaboration.

09/2022
Giorgia Adamo; **Sabrina Picciotto**; Paola Gargano; Monica Salamone; Aldo Nicosia; Antonella Cusimano; Daniele Romancino; Angela Paterna, Estella Rao, Rosetta Noto, Samuele Raccosta, Mauro Manno and Antonella Bongiovanni. "CELL-TECH HUB: Cell-based technologies and bioactives for research and innovation". Workshop EV Connect: fostering collaboration.

09/2022
Estella Rao, Angela Paterna, Valeria Longo, Noemi Aloi, Giorgia Adamo, Alessandra Longo, Rosina Noto, Rita Carrotta, **Sabrina Picciotto**, Paola Gargano, Samuele Raccosta, Daniele Romancino, Valeria Vetri, Paolo Colombo, Antonella Bongiovanni and Mauro Manno. "Comouflage of allergens for specific immunotherapy: loading proteins into microalgal extracellular vescicles." SIBPA XXVI Congresso Nazionale.

05/22
Estella Rao; Angela Paterna; Valeria Longo; Noemi Aloi; Giorgia Adamo; Alessandra Longo; Vincenzo Martorana; Rosina Noto; **Sabrina Picciotto**; Samuele Raccosta; Daniele Romancino; Valeria Vetri; Paolo Colombo; Antonella Bongiovanni; Mauro Manno. "Loading proteins into microalgal extracellular vesicles to camouflage allergens for specific immunotherapy. ISEV2022 Abstract Book. DOI: 10.1002/jev2.12224.

09/2021
Giorgia Adamo, **Sabrina Picciotto**, Daniele Romancino, Angela Paterna, Estella Rao, Samuele Raccosta, Antonella Cusimano, Rosina Noto, Rita Carrotta, Nicolas Touzet, Mauro Manno and Antonella Bongiovanni. Extracellular vesicles from microalgae: anti-oxidant bioactivity and cellular uptake studies. 2st EVIta Symposium.

09/2021
Pamela Santonicola, Giorgia Adamo, **Sabrina Picciotto**, Daniele P. Romancino, Angela Paterna, Estella Rao, Samuele Raccosta, Rosina Noto, Nicolas Touzet, Mauro Manno, Antonella Bongiovanni and Elia Di Schiavi. Caenorhabditis elegans as model system to study EV bioactivity and biodistribution in vivo. 2st EVIta Symposium

09/2021
Samuele Raccosta, Angela Paterna1, Estella Rao, Giorgia Adamo, **Sabrina Picciotto**, Daniele P. Romancino, Antonella Cusimano, Rosina Noto, Rita Carrotta, Vincenzo Martorana, Fabio Librizzi1,2, Nicolas Touzet, Antonella Bongiovanni, and Mauro Manno. Extracellular vesicles from microalgae: biophysical/biomechanical characterisation. 2st EVIta Symposium

11/2019

Sabrina Picciotto, Giorgia Adamo, Daniele Romancino, Valentina Cigna, Aurelio Maggio, Antonino Giambona, Antonella Bongiovanni and Francesco Picciotto. "Isolation and characterization of extracellular vesicles (EVs) derived from human coelomic fluid" Abstract pubblicato su atti del congresso: 1st EVIta Symposium" organizzato dalla Società Italiana delle vescicole extracellulari, svoltosi a Palermo (Italia).

11/2019

S. Raccosta, R. Carrotta, F. Librizzi, V. Martorana,R. Noto,G. Adamo,A. Cusimano,**S. Picciotto**,D. Romancino, C. Stanly, E.Di Schiavi,G. L. Liguori,A.Kisslinger, K.Landfester, S. Morsbach, A. Iglic,V. Iglic,L. Corcuera, P. Arosio,G.Pocsfalvi, N. Touzet, A. Bongiovanni, M. Manno. "VES4US, a Horizon 2020 Future and Emerging Technology project: Biophysical experimental tools for EVs structural characterisation" .1st EVIta Symposium, 6-8 Novermber 2019, Palermo.

11/2019

C. Stanly, R. Bokka, M. Moubarak, A. P. Ramos Juare, G. Antonucci, I. Fiume, A. Cusimano, G. Adamo, D. Romancino, **S. Picciotto**, S. Raccosta, V. Martorana, R. Noto, R. Carrotta, P. Santonicola, E. Di Schiavi, G. L. Liguori, R. Parkes, D. Fierli, A. Aranyos, M. E. Barone, A. Kisslinger, K. Landfester, B. Rodriguez, S. Morsbach, D. Božič, A. Iglic, V. Iglic, L. Corcuera, P. Arosio, M. Manno, N. Touzet, and A. Bongiovanni, A. Bhattacharya, L. Ehrdardt and G. Pocsfalvi." Preparative and Analytical ultracentrifugation of EVs". 1st EVIta Symposium, 6-8 Novermber 2019, Palermo.

Technical skills

Diverse skill set in the field of nanotechnology, molecular and cellular biology, and applied biochemistry. Here's a summary of the skills you mentioned:

- Isolation and characterization of extracellular vesicles from different biological sources, particularly from microalgae
- Techniques for isolating extracellular vesicles from cells using differential ultracentrifugation and Tangential Flow Filtration
- Nanoparticle tracking analysis using light-scattering and fluorescence
- Growth, manipulation, and cryopreservation of different species of microalgae
- Cell biology techniques, including cell culture growth and manipulation, cryopreservation, cell counting, cell growth curves, cytotoxicity and genotoxicity tests
- Characterization, staining, functionalization, and loading of nanoparticles (extracellular vesicles), as well as chemical conjugation techniques with biomolecules such as proteins, monoclonal antibodies, fluorescent probes, nucleic acids, siRNA, and chemotherapeutic drugs

- Biochemistry techniques, including protein analysis, total protein extraction, dialysis, SDS-page electrophoresis, Western-Blotting, densitometric analysis, and enzyme-linked immunosorbent assays (ELISA)
- Immunohistochemistry techniques, including slide preparation, staining of cells and tissues, and immunofluorescence using fluorescence and confocal microscopy
- UV-VIS spectrophotometry and spectrofluorometry
- Cytofluorimetric analysis
- Molecular biology techniques, including extraction and purification of genomic DNA, PCR, electrophoresis on agarose gel, and enzymatic analysis using spectrofluorimetric assays
- Seminal fluid analysis, including initial macroscopic and microscopic analysis of samples, sample preparation techniques, cell staining tests, indirect immunofluorescence assays, and Tunel assay for the evaluation of DNA fragmentation.

Acknowledgments

I would like to express my heartfelt gratitude to all the individuals who have made significant contributions to the completion of this PhD thesis, providing me with unwavering support, invaluable inspiration, and constant encouragement throughout the journey. Without their exceptional dedication and valuable contributions, this remarkable achievement would not have been possible.

First and foremost, I would like to express my heartfelt gratitude to my supervisor, **Dr. Antonella Bongiovanni**. Her exceptional guidance, wisdom, and unwavering support have profoundly influenced my research journey. Her dedication, passion for teaching, and unwavering belief in my abilities have played a pivotal role in shaping my growth. The constructive critiques she offered and the invaluable advice she provided elevated the quality of my work. I am immensely thankful for her boundless patience and the time she generously devoted to discussing my ideas, encouraging me to overcome the challenges encountered along the way. Thank you for inspiring me to become a better researcher and for providing me with a solid foundation for my future career.

Would like to express my heartfelt gratitude to my colleague, **Giorgia Adamo**, who has been a consistent presence and guide throughout my entire doctoral studies. Her collaboration, expertise, and willingness to share knowledge and experiences have profoundly enriched my research journey. I am deeply thankful for her valuable suggestions, stimulating discussions, and the mutual support we have provided to each other. I am truly grateful for our collaboration and everything I have learned from her during this remarkable doctoral journey.

I would like to extend a special thanks **to Prof. Paolo Arosio** for kindly hosting me in his ETHZ laboratory. His generosity and passion for science have made my time in his lab an incredibly rewarding and stimulating experience. I am grateful for the opportunity he gave me to collaborate closely with his research team, especially with my now dear friend, **Carolina Paganini and Karl Normak**. Thank you for your constant support, encouragement, and our countless scientific discussions.

I would like to extend my sincere gratitude to the faculty members, specifically **Prof. Giulio Ghersi, Prof. Maurizio Leone and Prof. Vincenzo Cavalieri**, and members of the evaluation committee, **Prof. Dr. Markus Rehberg** and **Prof. Antonio Marcilla** for their valuable contribution and the time they devoted to reading and evaluating this

thesis. Their insightful observations and invaluable suggestions have played a significant role in refining my work and making it more robust and meaningful.

Finally, I want to thank all those who have participated in my research, including my laboratory colleagues **Mauro** Manno, **Daniele** Romancino, **Paola** Gargano, **Angela** Paterna, **Samuele** Raccosta, **Estella** Rao, **Rosina** Noto, **Monica** Salamone, **Antonella** Cusimano, the study participants, the entire **Ves4Us** and **Bow Project** teams. Your collaboration and willingness have made the completion of this thesis possible. I am grateful for your valuable contributions and the sharing of your experiences, which have enriched my work and broadened my perspective.

I cannot conclude this PhD thesis without expressing my deepest and sincerest gratitude to **my parents**, **my sister**, **my family**, and **my friends** for their unconditional love, support, and constant encouragement. Their presence in my life has been an immeasurable blessing. They have been my unwavering source of inspiration, providing unwavering support and being my anchor during challenging times. Their belief in me has fueled my determination, and their unwavering faith in my abilities has given me the strength to overcome obstacles along the way. I am infinitely grateful for their constant presence and unconditional support they have given me throughout this journey. Without them, this journey would not have been as profoundly meaningful and rewarding.

Thank you all.

Ringraziamenti

Desidero esprimere la mia sincera gratitudine a tutte le persone che hanno dato un contributo significativo al completamento di questa tesi di dottorato, fornendomi un sostegno incrollabile, un'ispirazione inestimabile e un incoraggiamento costante per tutto il viaggio. Senza la loro eccezionale dedizione e i loro preziosi contributi, questo straordinario risultato non sarebbe stato possibile.

Innanzitutto vorrei esprimere la mia sincera gratitudine alla mia supervisore, **la Dott.ssa Antonella Bongiovanni**. La sua guida eccezionale, la sua saggezza e il suo sostegno incrollabile hanno profondamente influenzato il mio percorso di ricerca. La sua dedizione incrollabile, la passione per l'insegnamento, e fiducia nelle mie capacità hanno svolto un ruolo fondamentale per la mia crescita. Le critiche costruttive che ha offerto e i preziosi consigli che ha fornito hanno elevato la qualità del mio lavoro. Sono immensamente grato per la sua pazienza senza limiti e per il tempo che ha dedicato generosamente a discutere le mie idee, incoraggiandomi a superare le sfide incontrate lungo il cammino. Grazie per avermi ispirato a diventare una ricercatrice migliore e per avermi fornito una solida base per la mia futura carriera.

Vorrei esprimere la mia sincera gratitudine alla mia collega**, Giorgia Adamo**, che è stata una presenza costante e guida durante tutti i miei studi di dottorato. La sua collaborazione, competenza e disponibilità a condividere conoscenze ed esperienze hanno profondamente arricchito il mio percorso di ricerca. Sono profondamente grato per i suoi preziosi suggerimenti, stimolando le discussioni e il reciproco sostegno che ci siamo dati. Sono davvero grato per la nostra collaborazione e tutto ciò che ho imparato da lei durante questo straordinario viaggio di dottorato.

Un ringraziamento speciale va al **Prof. Paolo Arosio** per avermi gentilmente ospitato nel suo laboratorio ETHZ durante il mio percorso di ricerca. La sua generosità e passione per la scienza hanno reso il mio tempo nel suo laboratorio un'esperienza incredibilmente gratificante e stimolante. Sono grato per l'opportunità che mi ha dato di collaborare a stretto contatto con il suo team di ricerca, soprattutto con la mia ormai cara amica, **Carolina Paganini e con Karl Normak**. Grazie per il vostro costante sostegno, incoraggiamento, e le nostre innumerevoli discussioni scientifiche.

Desidero estendere la mia sincera gratitudine ai docenti, in particolare il **Prof. Giulio Ghersi**, il **Prof. Maurizio Leone** e il **Prof. Vincenzo Cavalieri**, e ai membri del comitato di valutazione, **Prof. Dr. Markus Rehberg** e **Prof. Antonio Marcilla** per il loro prezioso contributo e il tempo dedicato alla lettura e alla valutazione di questa tesi. Le loro osservazioni perspicaci e preziosi suggerimenti hanno svolto un ruolo significativo nel perfezionare il mio lavoro e renderlo più robusto e significativo.

Infine, voglio ringraziare tutti coloro che hanno partecipato alla mia ricerca, compresi i miei colleghi di laboratorio **Mauro Manno**, **Daniele Romancino**, **Paola Gargano**,